LUT
Lappeenranta
University of Technology

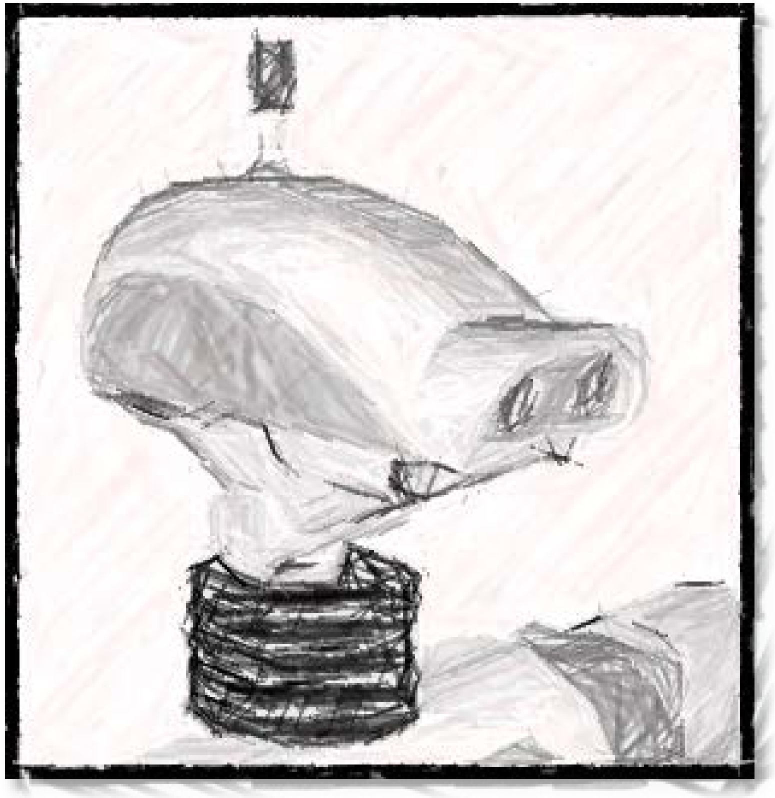

TIERA

Mobile Assembly and Repair Robot

For Hazardous Areas

DSc. Tech. Eng. Hamid Roozbahani

Laboratory of Intelligent Machines

Lappeenranta University of Technology

Lappeenranta University of Technology

Lappeenranta University of Technology (LUT) is an international university established in 1969 in Lappeenranta on the shore of Saimaa Lake in Finland. In 2015, the university counts 894 staff members and around 4900 undergraduate and postgraduate students. As all Finnish universities, it is state funded – it received 48.9 million euros from the Ministry of Education in 2015. The university provides numerous areas of study and research such as business management, mechanical engineering and energy.

LUT Sustainable Development Policy

Lappeenranta University of Technology is committed to recognizing its environmental responsibility in all its actions. LUT is the only Finnish university to meet the ISO 14001 standard and environmental is part of the way of thinking and operating of the university. LUT has an environment policy since September 4th, 2013, meaning that the environment responsibility is taken into account in every university's activities such as scientific research, academic education, societal interaction or support services. The environmental policy sets goals for the university and commits it to maintain and develop its management of environmental issues and to educate its staff about it.

Laboratory of Intelligent Machines

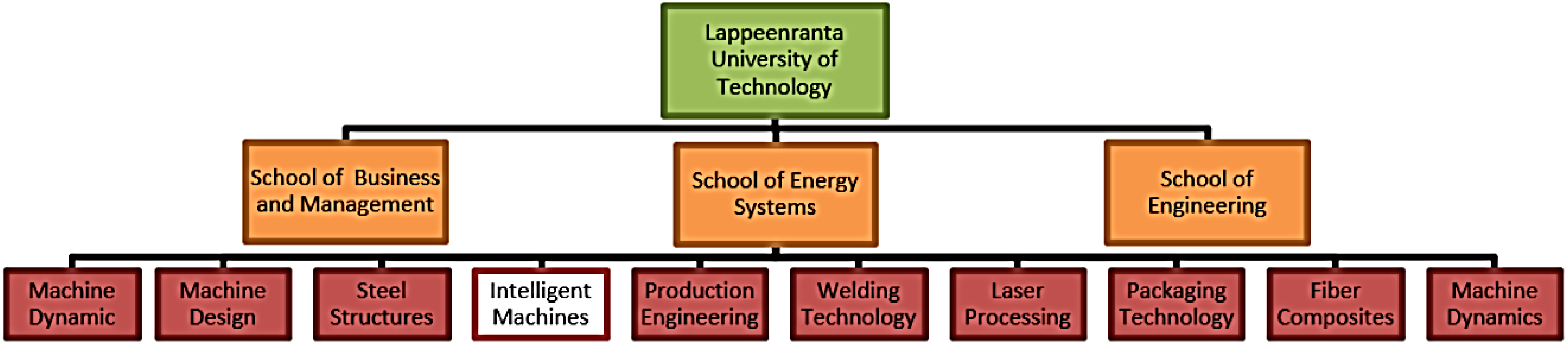

How it all started . . .

HERO 50

Fukushima Daiichi nuclear disaster - 11 March 2011

Hazardous Environment

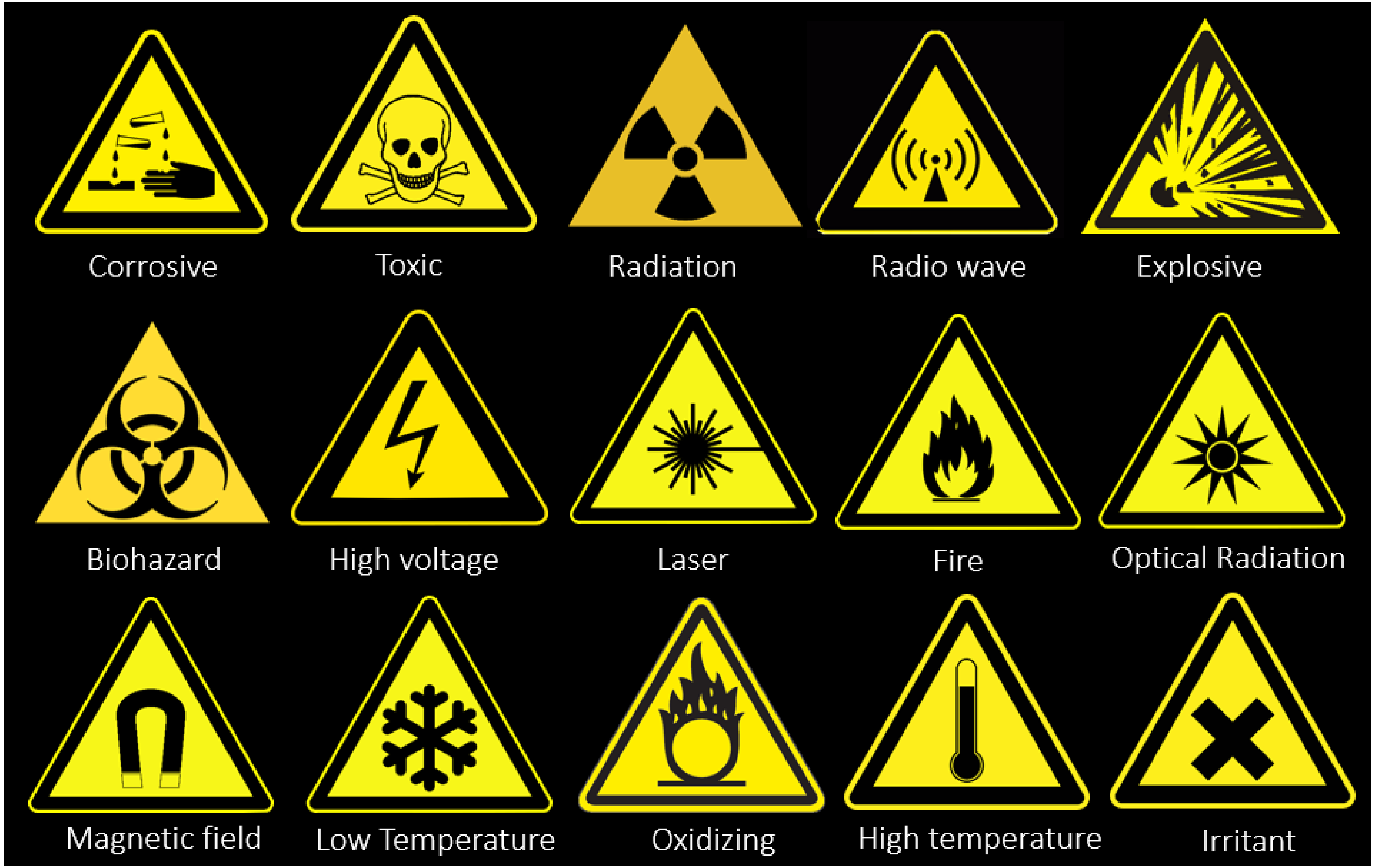

Statistics

	Accidents at work involving at least four calendar days of absence from work			Fatal accidents at work		
	Total	Male	Female	Total	Male	Female
EU-28	*2 487 794*	*1 953 554*	*533 984*	3 515	3 362	153
Belgium	49 546	40 451	9 093	46	46	0
Bulgaria	1 768	1 353	415	90	82	8
Czech Republic	36 013	26 820	9 193	104	102	2
Denmark	34 245	26 825	7 292	43	42	1
Germany	709 940	578 076	131 794	473	452	21
Estonia	4 993	3 065	1 928	11	10	1
Ireland	9 794	6 828	2 921	42	42	0
Greece	11 926	9 446	2 480	37	34	3
Spain	281 045	212 968	68 077	273	266	7
France	461 376	353 980	107 396	524	494	30
Croatia	8 844	6 766	2 078	50	50	0
Italy	274 040	219 282	54 758	469	450	19
Cyprus	1 511	1 127	384	7	7	0
Latvia	1 213	875	338	33	30	3
Lithuania	2 303	1 698	605	55	54	1
Luxembourg	6 299	5 378	921	13	13	0
Hungary	16 717	11 879	4 838	60	58	2
Malta	2 190	1 978	212	7	7	0
Netherlands	116 029	89 307	26 722	31	31	0
Austria	56 299	46 731	9 568	137	128	9
Poland	67 472	50 290	17 182	303	284	19
Portugal	109 511	82 685	26 826	162	157	5
Romania	2 889	2 308	581	257	245	12
Slovenia	11 505	9 318	2 187	21	21	0
Slovakia	7 469	5 405	2 064	49	49	0
Finland	34 821	28 042	6 779	32	30	2
Sweden	24 864	18 674	6 189	37	34	3
United Kingdom	143 171	111 998	31 162	149	144	5
Norway (²)	14 855	12 335	2 520	34	32	2
Switzerland	72 106	60 352	11 754	60	57	3

(¹) NACE Rev. 2 Section A and Sections C to N. Non-fatal accidents reported in the framework of ESAW are accidents that imply at least four full calendar days of absence from work (serious accidents).
(²) 2011.
Source: Eurostat (online data code: hsw_mi01)

Further Eurostat information Publications

- European social statistics — 2013 edition
- Health and safety at work in Europe (1999–2007)
- Statistics in focus — 8.6% of workers in the EU experienced work-related health problems

Statistics

Fatal accidents at work, 2011 and 2012 ([1]) (standardized incidence rates per 100 000 persons employed)

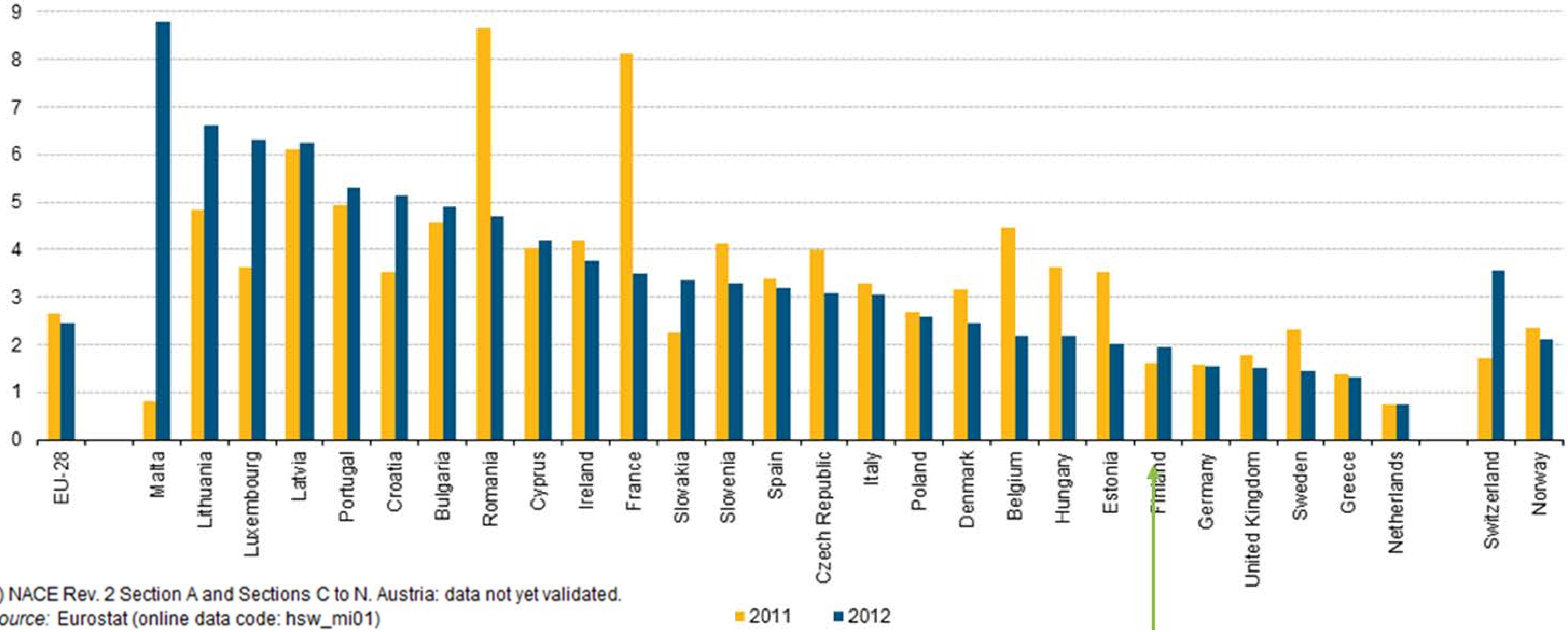

([1]) NACE Rev. 2 Section A and Sections C to N. Austria: data not yet validated.
Source: Eurostat (online data code: hsw_mi01)

Further Eurostat information Publications

- European social statistics — 2013 edition
- Health and safety at work in Europe (1999–2007)
- Statistics in focus — 8.6% of workers in the EU experienced work-related health problems

What Market Needs . . .

A reliable product

To Replace Humans

In Hazardous Environments

- A reliable product to replace Humans in places that humans can not perform

Our Motivation & Market Need

Our motivation:

- To practice the cutting edge technology available in the field
- To provide a proper base to transfer our knowledge and experience
- To develop a powerful marketing tool which shows our power in the field

Our First target:

- A mobile robot which is capable of applying assembly and repair

- *Robot Manipulators*
- *Mobile Robots*
  - *Ground Robots*
    - *Wheeled Robots*
    - *Legged Robots*
  - *Submarine Robots*
  - *Aerial Robots*

(Kelly, Santibáñez & Loría, 2005, p 3).

Telepresence concept.

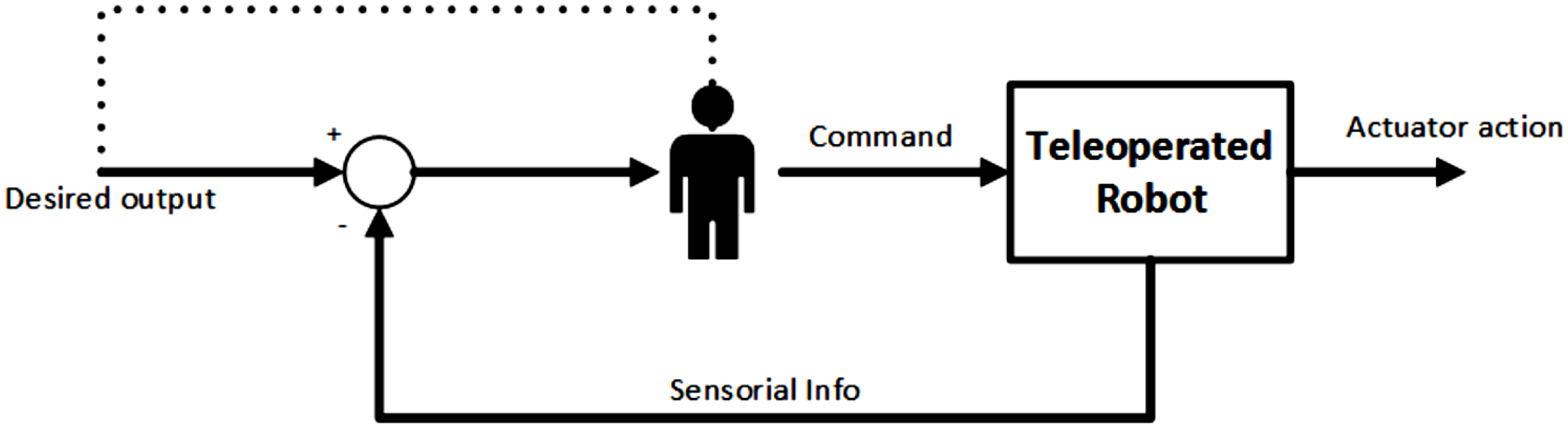

Primary Potential Applications

- **Repair and Assembly**

Other Potential Applications

- Inspection and maintenance
- Cleaning
- Security & Defense
- Logistic system
- Agriculture
- Urban transport
- Entertainment
- Oil and Gas

Major Competitors

KUKA MOBILE ROBOTICS QUANTEC

Systems

- Teleoperated mobile robot (Up to 2 Km distance from control station)
- Two UR10 robotic hands equipped with force feedback 3 finger grippers
- Full HD camera system: 3D, on hands
- Sound recognition via human ear models recovers with voice direction capacity
- Voice command capabilities
- Quadcopter station on the back of the robot, HD real-time video for extra vision access
- LiDAR, Gyro, GPS
- Haptic capabilities

The robot main application: performing assembly and repair tasks in different workspaces; special hazardous environments.

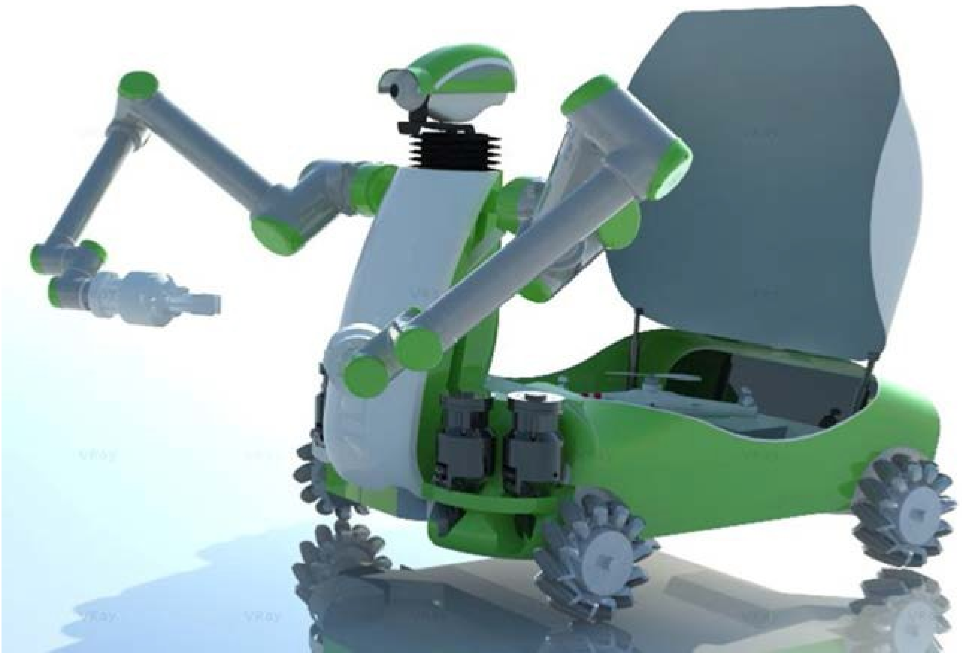

Design

Design

Design

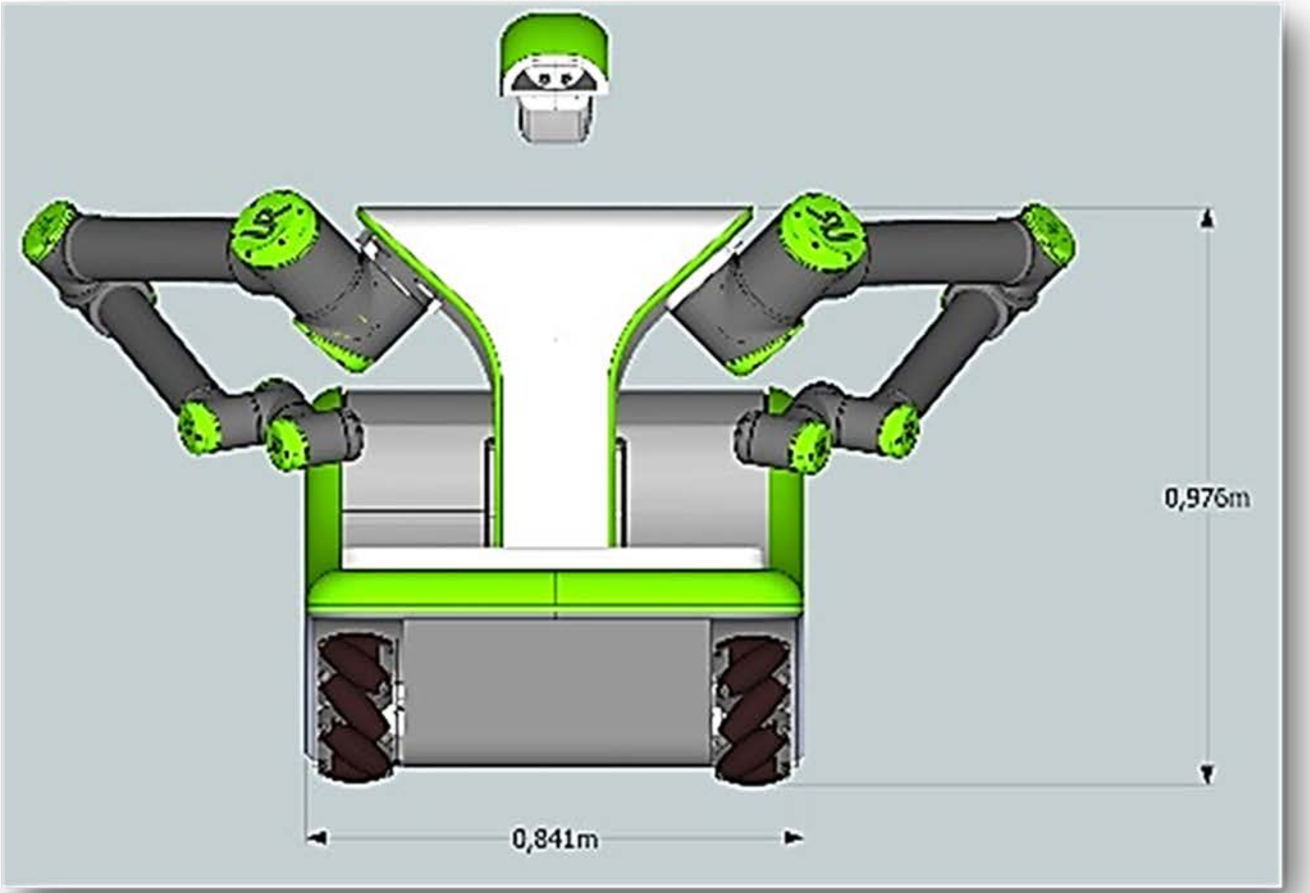

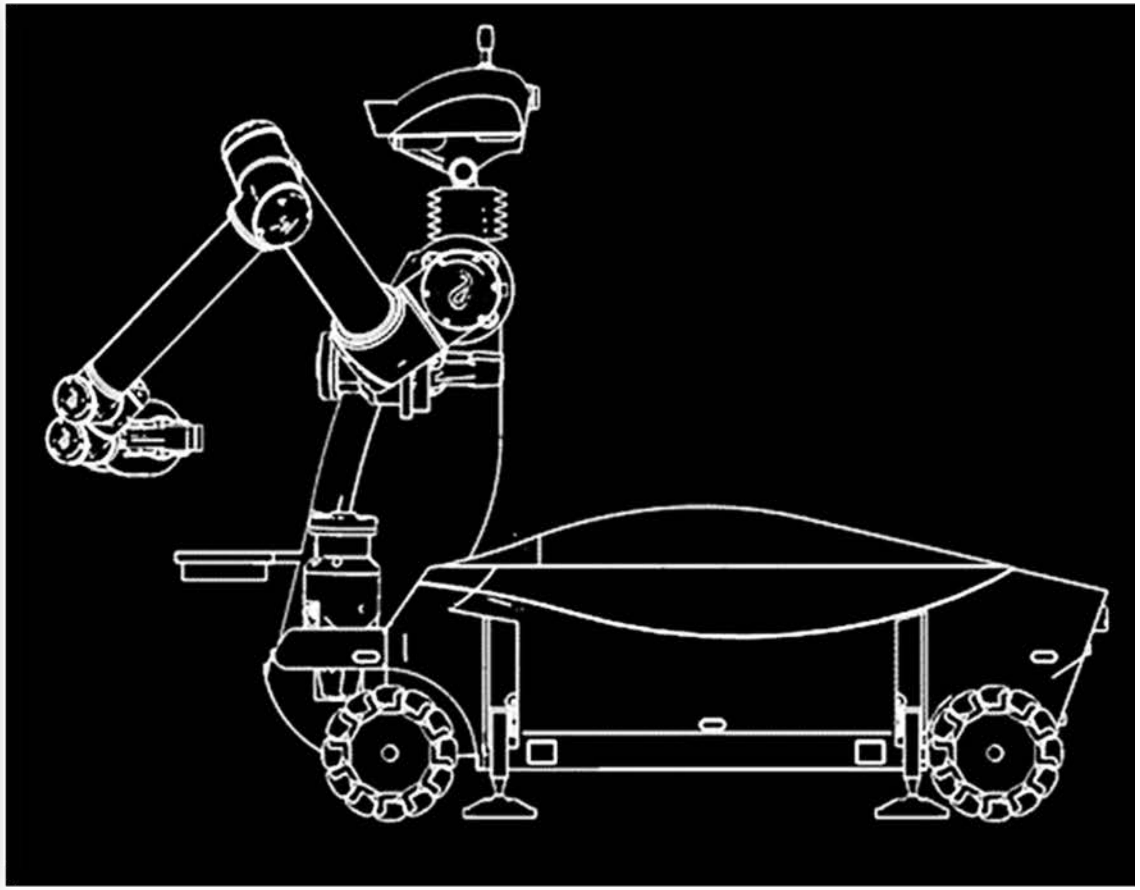

Design

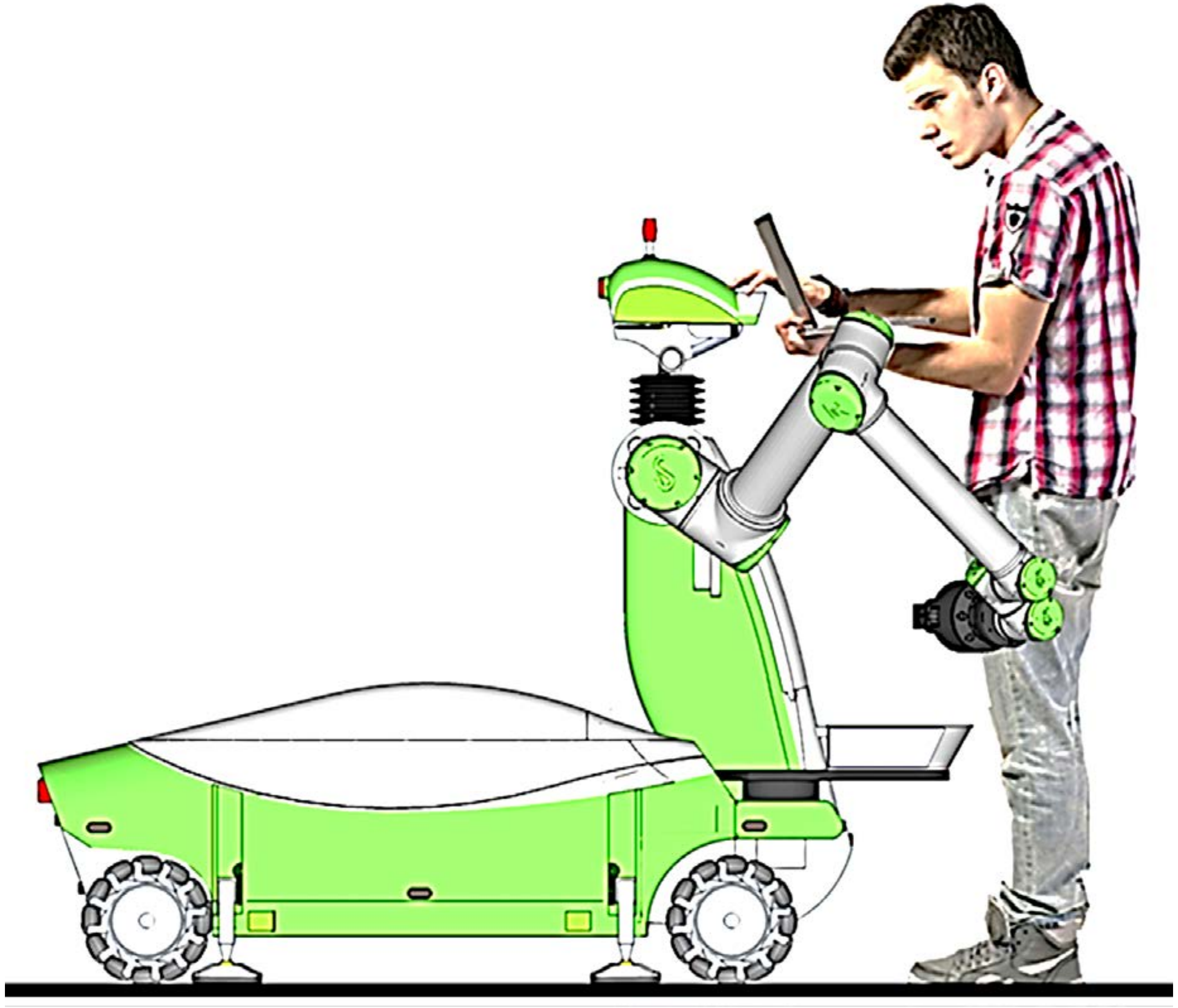

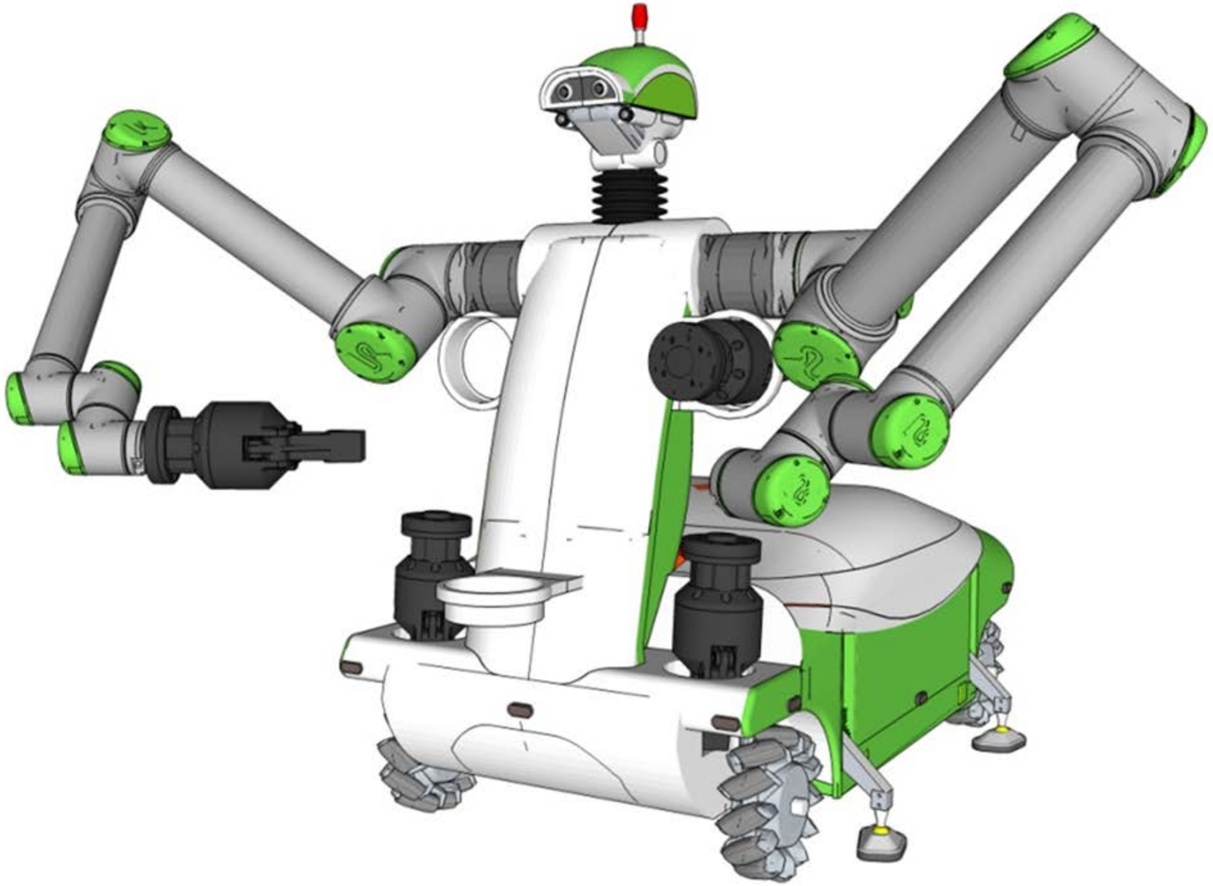

State-of-the-art

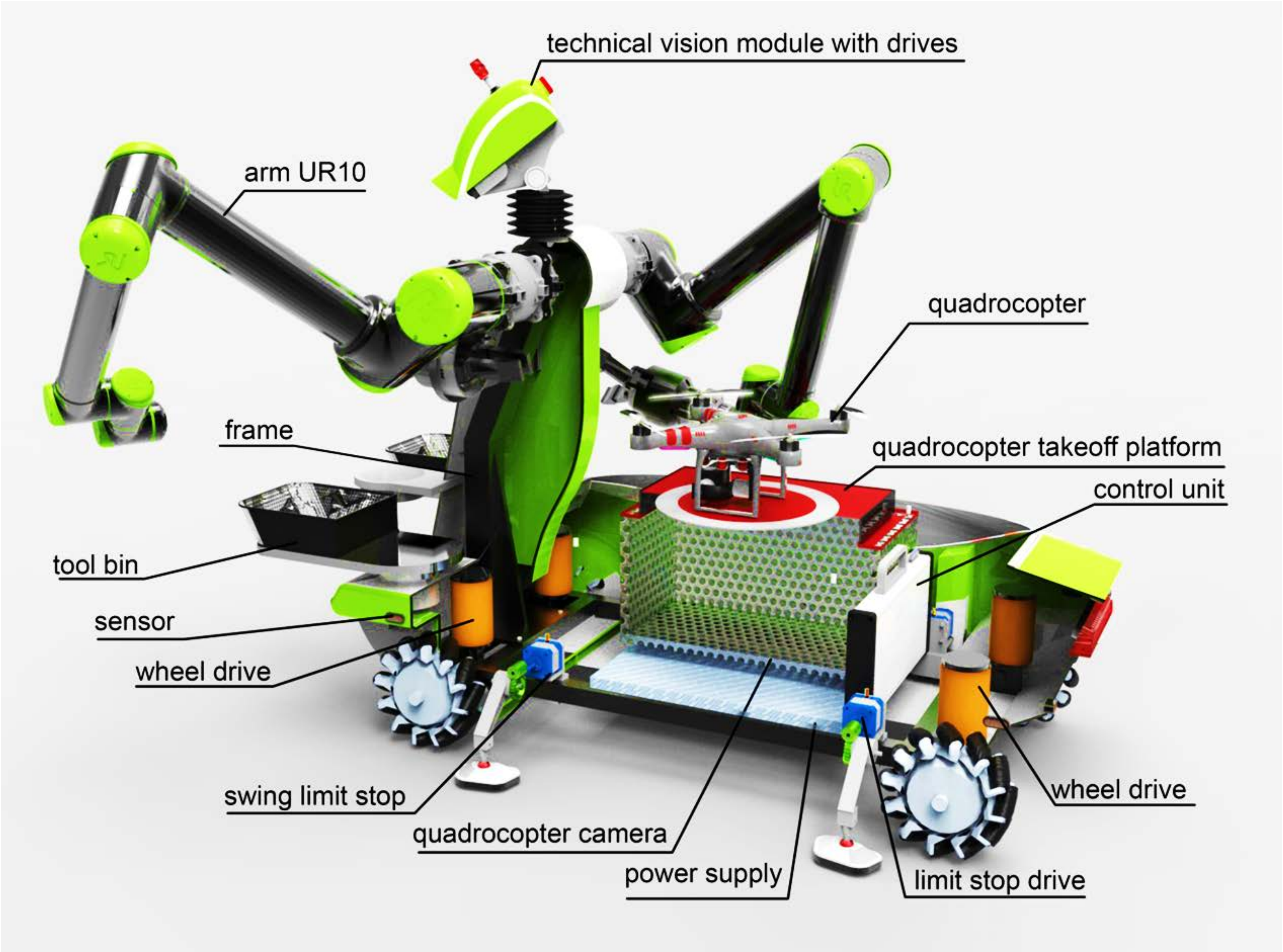

State-of-the-art

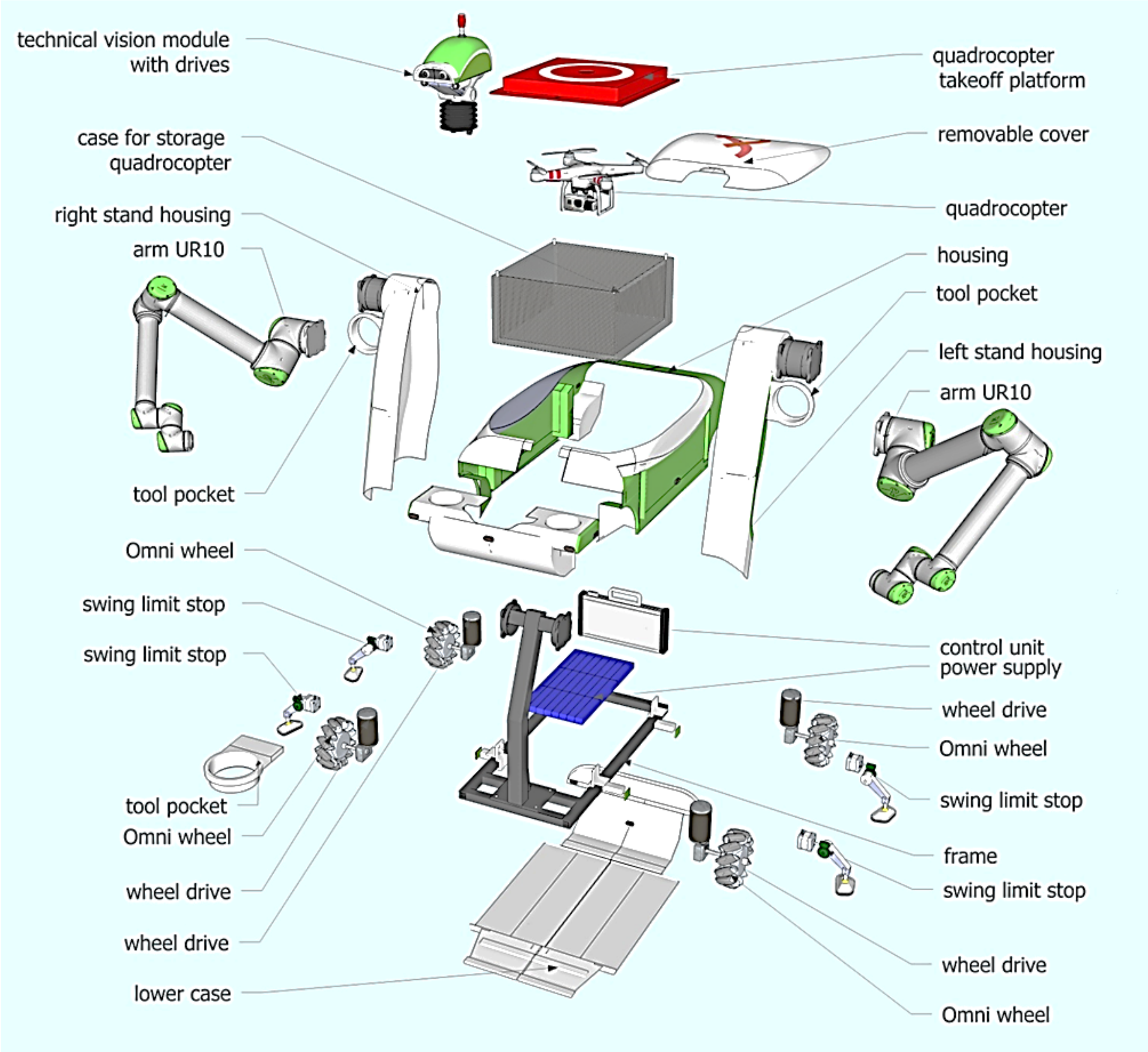

Chassis

Chassis

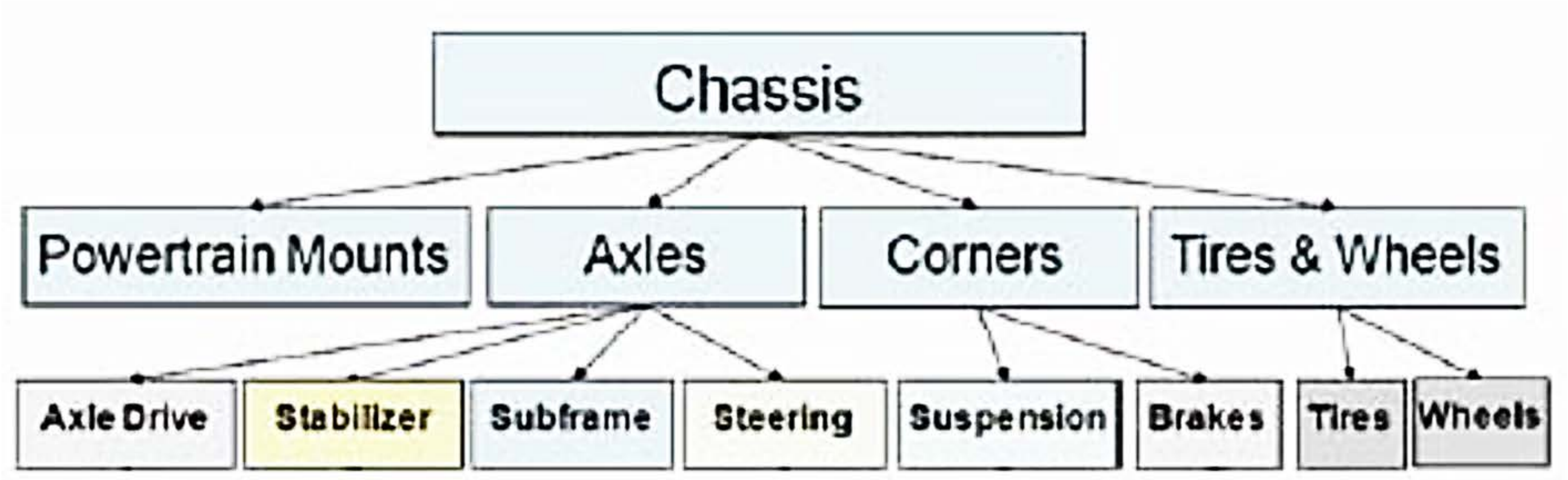

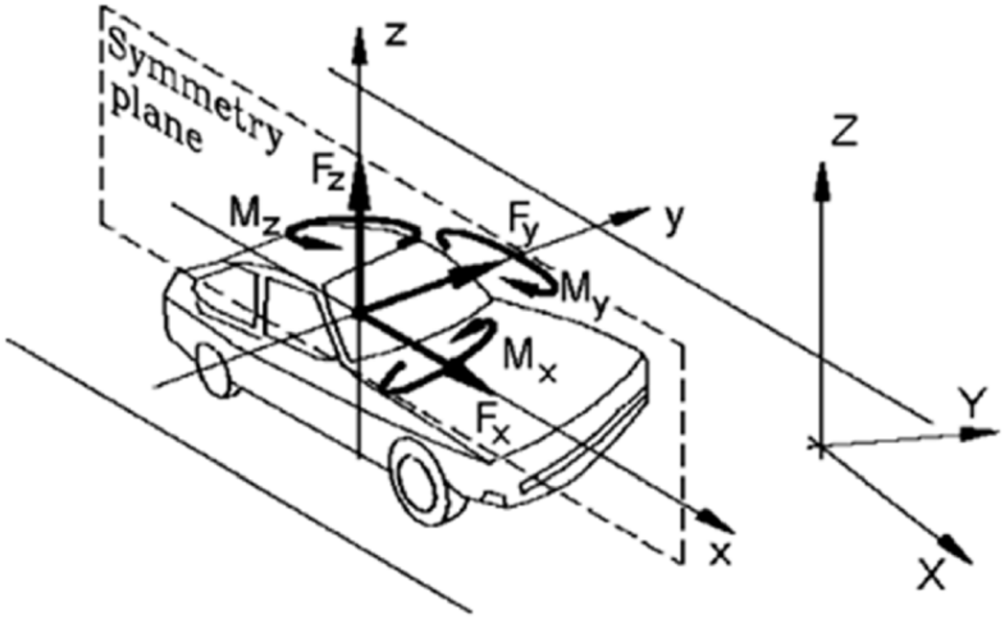

Reference frame, force and moment in dynamic study of the vehicles

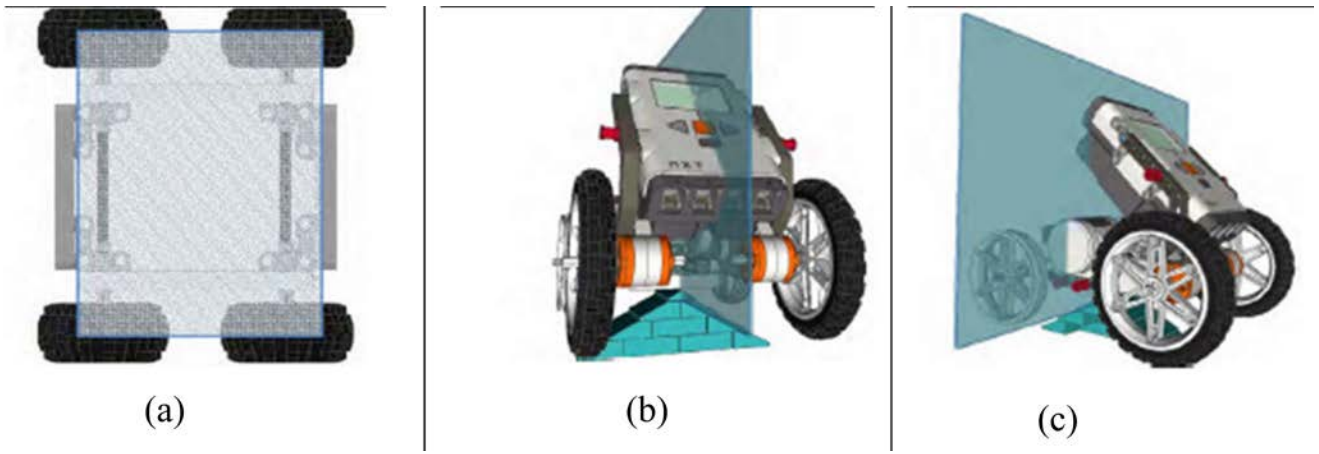

(a) Wheel base of four-wheel (b) longitudinal balance plane (c) lateral balance plane

Chassis

Corgi lotus elan back bone chassis

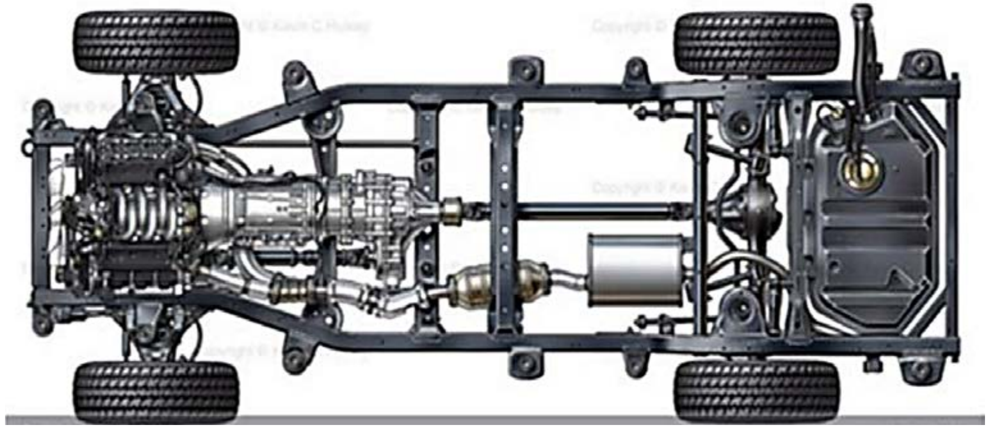

Ladder frame chassis

Jaguar XE monocoque chassis frame

Space frame chassis

Categories for design consideration

Traditional Considerations

1. Materials
2. Geometry
3. Operating conditions
4. Cost
5. Availability
6. Producibility
7. Component life

Modern Considerations

1. Safety
2. Ecology
3. Quality of life

Miscellaneous Considerations

1. Reliability and maintainability
2. Ergonomics and aesthetics
3. Assembly and disassembly
4. Analysis

Chassis

Part and other parameter specifications defined in the project plan

Chassis Constrain	System parts	Parameters
Two UR 10 robotic arm to be connected similar to human shoulder	UR10 robotic arm	The weight of each UR10 arm weighing 30 kg
		Shoulder height should not be less than 800mm
		They should be placed in front of the robot.
		Each robot arm has pay load of 10 kg.
Provide two robot arm with controller in the mounted space	UR 10 controller	10Kg weight of each arm controller mounted with chassis frame.
Mounted with chassis frame	Battery	16 piece of battery.
		Each battery weighing 2.3kg
		They should compact as a 1 piece.

Part and other parameter specifications defined in the project plan

Chassis Constrain	System parts	Parameters
Provide landing space at the top of the chassis frame	Quadcopter	4kg
		Dimension 438*451*301mm
Electronic parts	Advantech, DC/DC converter, arm controller etc.	Provide the space in such a way that they can access any situation
		Space for wiring and extra component that can be required in the future
Frame should be connected with the bearing point provided by modular system designer	Electronic part ,Drive modular system	Chassis frame should be mounted on bearing mounting position.
		Modular system should be inside the chassis frame.
Manufactured by conventional method	Chassis frame	Should not be more than 80kg.
		Length and width should be within 1600*800mm.
		Manufacturing process may be laser cutting, CNC milling, welding or other available process
		Low cost
Mass of overall robot		Should not exceed more than 300Kg

Weight Calculation

Weight from drive traction system

Part name	Mass per part* number of parts	Total mass(kg)	Weight (N)
Gearhead	3*4	12	117.6
Motor	2.4*4	9.6	94.08
Controller	0.33*4	1.32	12.936
Brake	0.18*4	0.72	7.056
Coupler	0.92*2	1.82	17.836
	1..08*2	2.16	21.168
Gear box	4.5*4	18	176.4
TimkenTapered bearing	3.2*4	12.8	125.44
Mechanum wheel	7.2*	28.8	282.24
Others		3.2	31.36
Total		90.42	886.116

Weight and dimension of robot arm, controller and DC/DC converter.

Name	mass* number of parts	Total mass(Kg)	Dimension in mm
UR 10 robotic arm	30*2	60	1300 length and base diameter 170
UR 10 arm controller	10*2	20	426*196*194
Advantech computer	4*1	4	220*210*196
Battery	2.3*16	36.8	203*114*61
DC/DC converter(48V)	1.94 *4	7.76	295*127*41
DC/DC converter (12V)	0.48*3	1.44	159*98*38
Inspire 1	2.935*1	2.935	438*451*301
Total		135.935	

Chassis

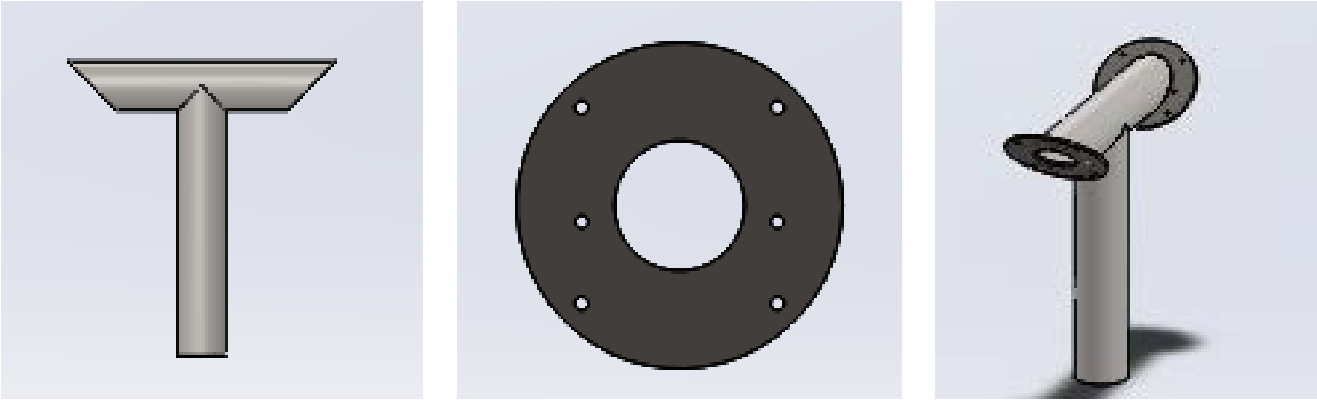

3D-CAD model of (a) tubular joint (b) UR 10 robot mounting point (c) Assembly of T-joint with UR 10mounting part

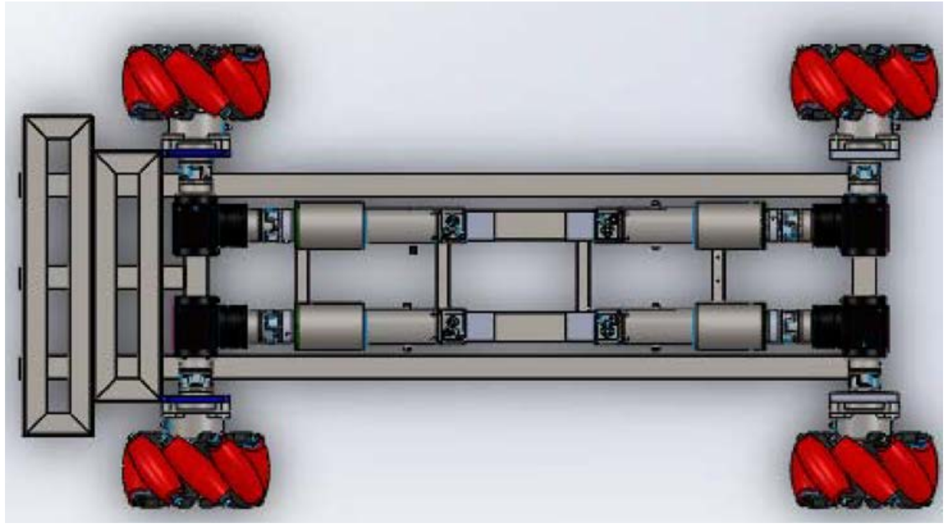

Ladder chassis frame for robot

Battery place in chassis frame

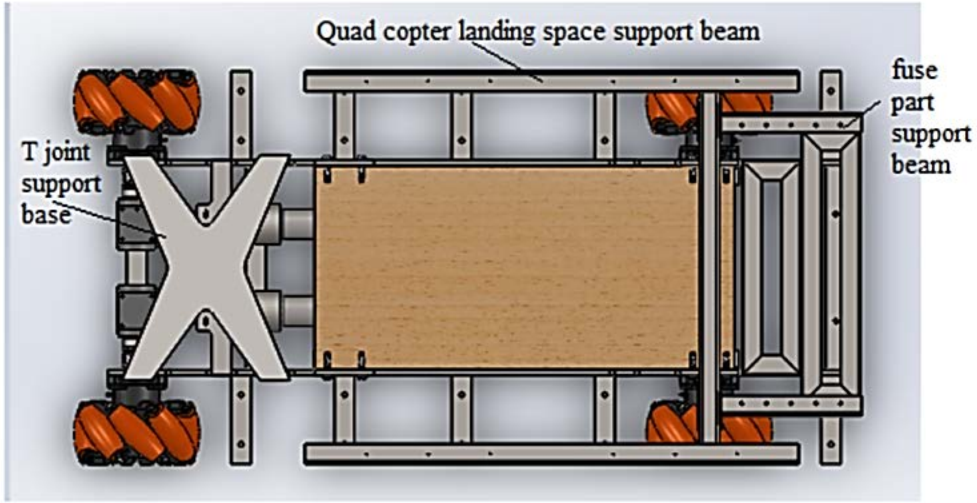

Chassis frame extended with landing space for quadcopter and T-joint

Chassis

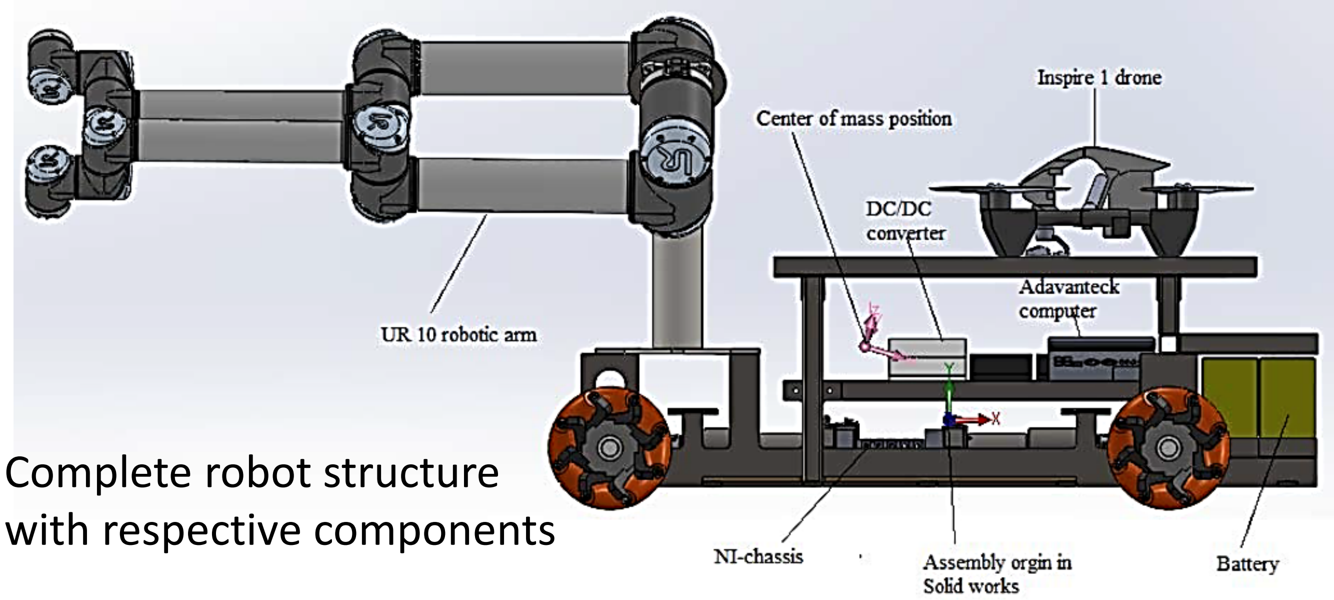

Complete robot structure with respective components

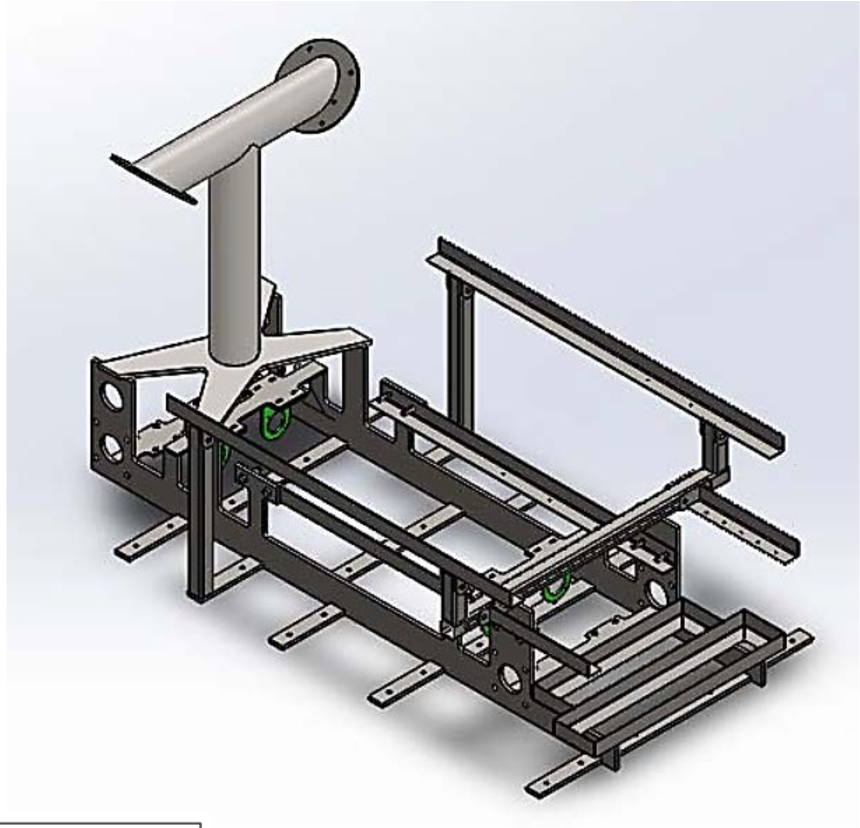

General result for chassis frame design

Speciation	Result and process
Position of center of mass	528mm back from front wheel center, 345 mm toward center from front right wheel, 338mm from ground level.
Total chassis frame mass	Around 80.50Kg from Solid-works mass calculation.
Overall robot dimension	1597 length and 800 mm width and 950mm height.
Manufacturing and joining process	Welding, machining and cutting
Overall robot weight	Around 300Kg

ANALYSIS OF A CHASSIS FRAME

Material property define in FEMAP

Stiffness and density	FEMAP input	SI unit value
Young modulus,(E)	210000 MPa	$200*10^9$ pa
Shear Modulus,(G)	76000 MPa	$76*10^9$ pa
Poisson ratio,	0.3 (unit less)	0.3 (unit less)
Mass density	$8.65*10^{-9}$ Tones/mm^3	7850 Kg/m^3

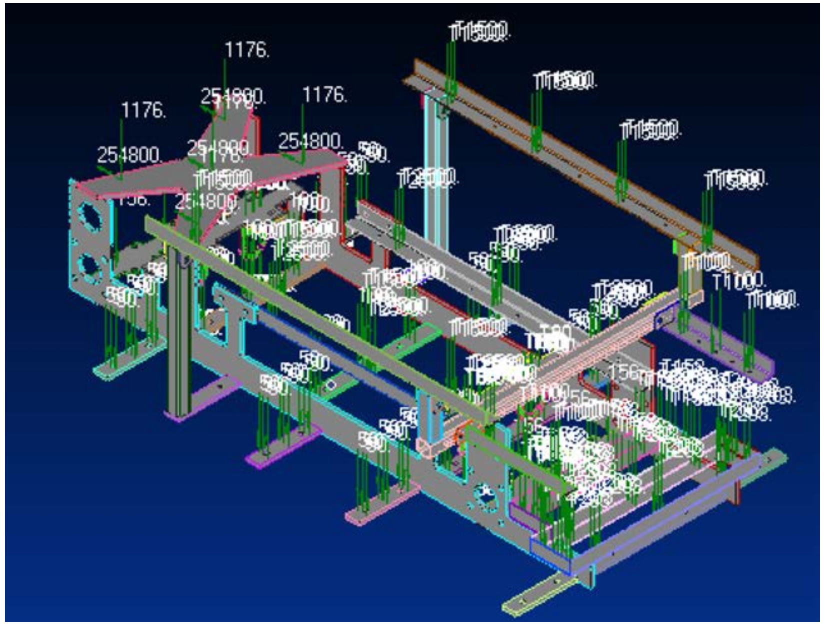

Loading on the chassis frame.

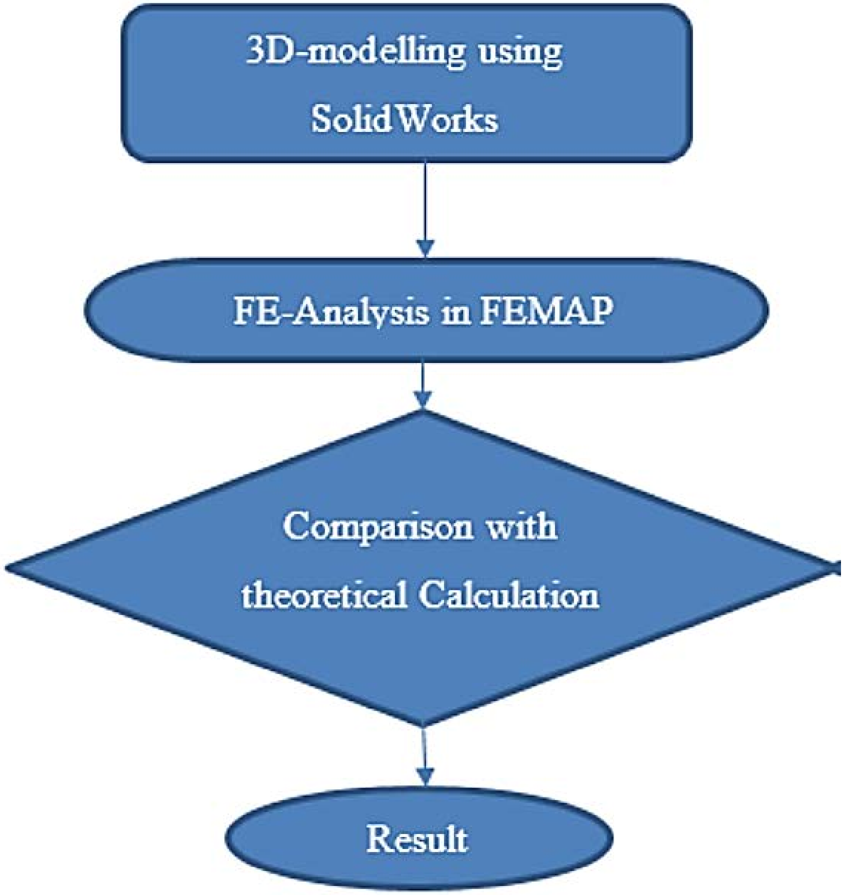

Flow chart for analysis process.

ANALYSIS OF A CHASSIS FRAME

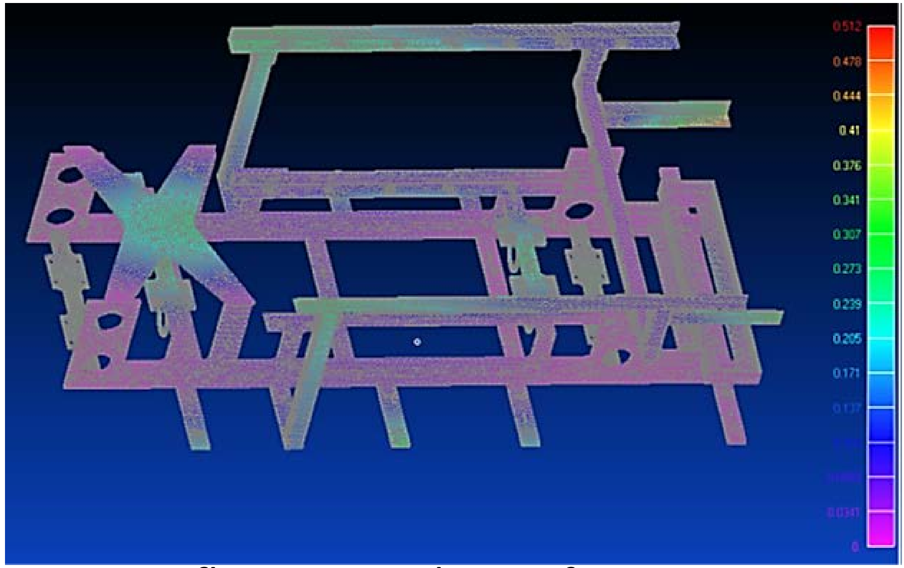

Deflection on chassis frame

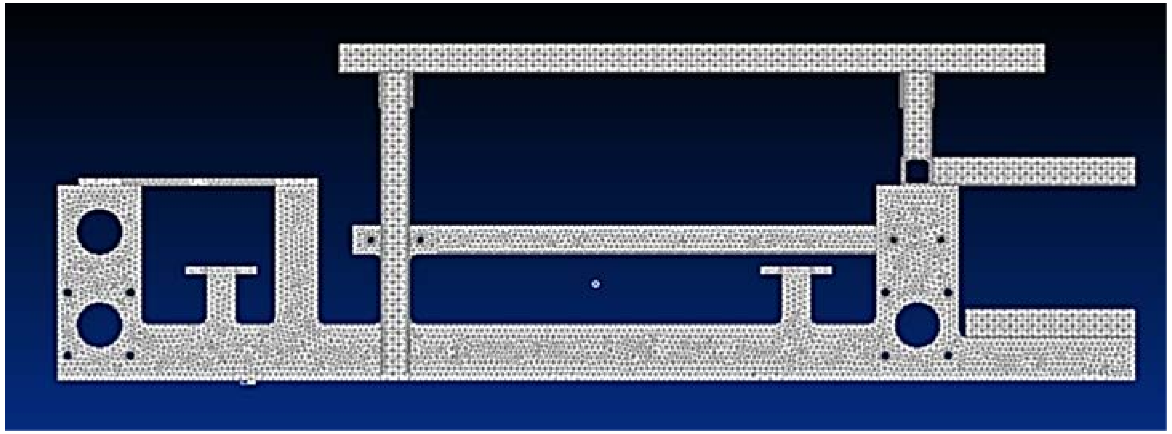

Linear tetrahedral (solid) element meshing in chassis frame.

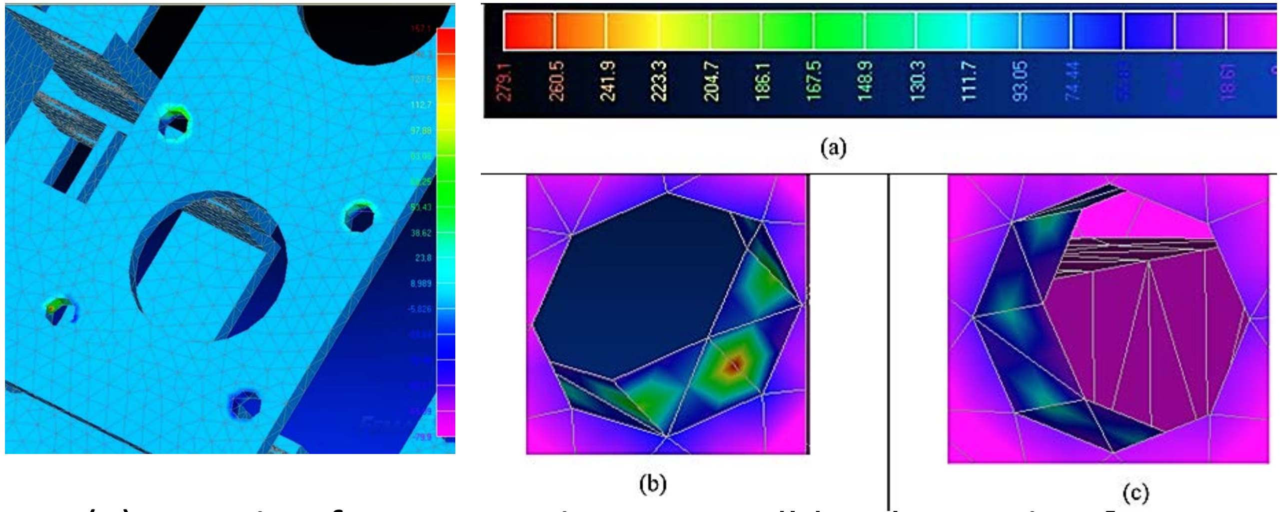

(a) Reaction force range in Newton (b) Bolt reaction force range in front hole (c) Rear bolt reaction force in rear hole.

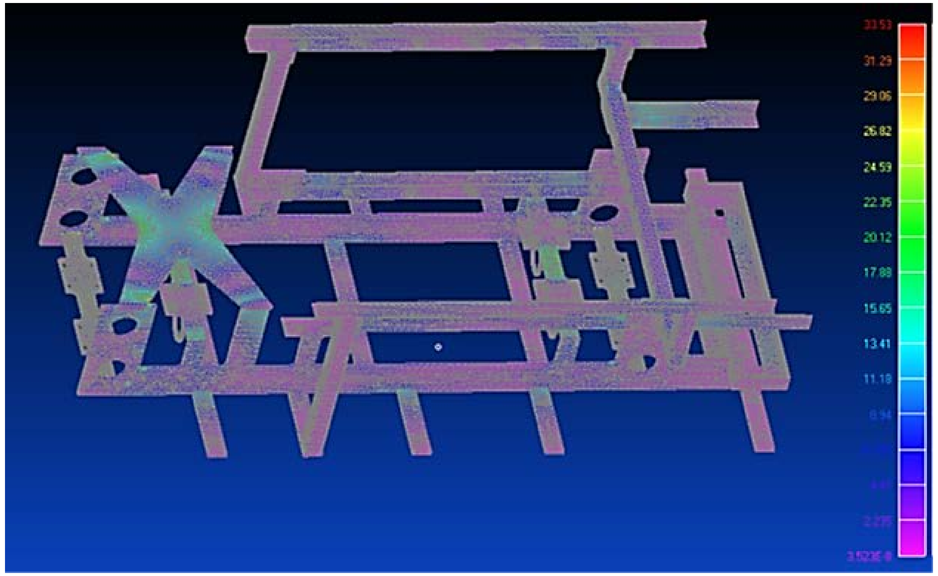

Von misses stress result from FEMAP.

ANALYSIS OF A CHASSIS FRAME

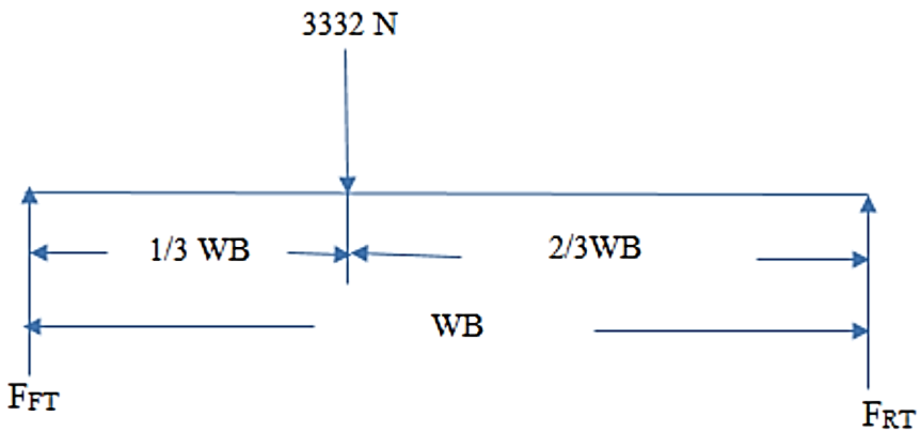

Numerical representation with free body diagram for robot

Robot weight table for analytical analysis.

Total weight of the robot and payload		
	kg	**N**
Pay load	40	392
Net robot weight	300	2940
Gross robot weight (GRW)	340	3332

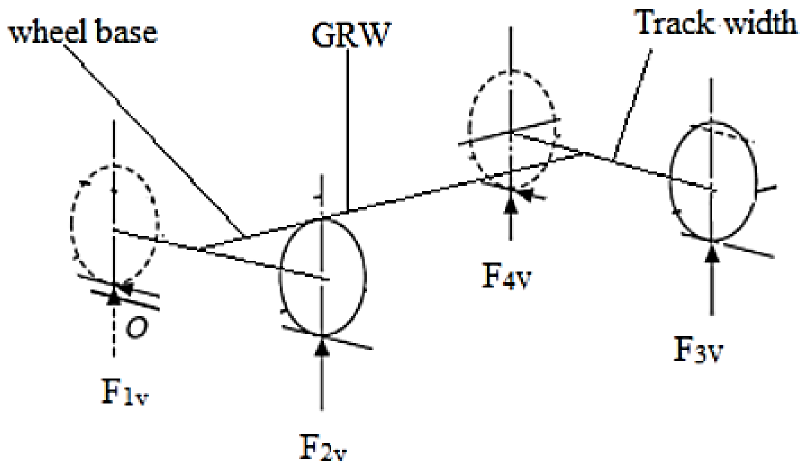

Combining bending and torsion load.

Comparison of analytical result and FEMAP.

Name	**FEMAP result**	**Analytical result**
Reaction force in front mounting hole	279.1 MPa	277.66N
Reaction force in rear mounting hole	130.3MPa	138.835N
Bending stress	33.53MPa (Von misses stress)	34.30MPa
Deflection	0.518 (it on fuse support part)	0.28 (it on plate beam)

ANALYSIS OF A CHASSIS FRAME

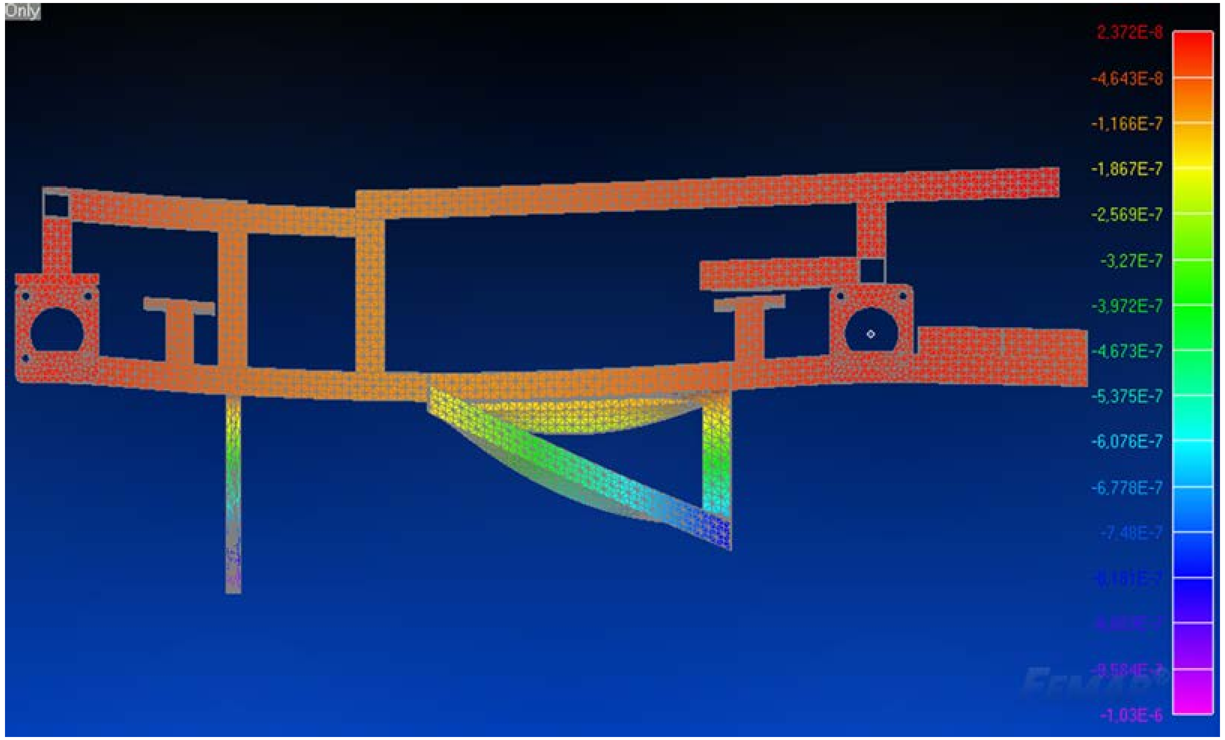

Deflection from simulating result

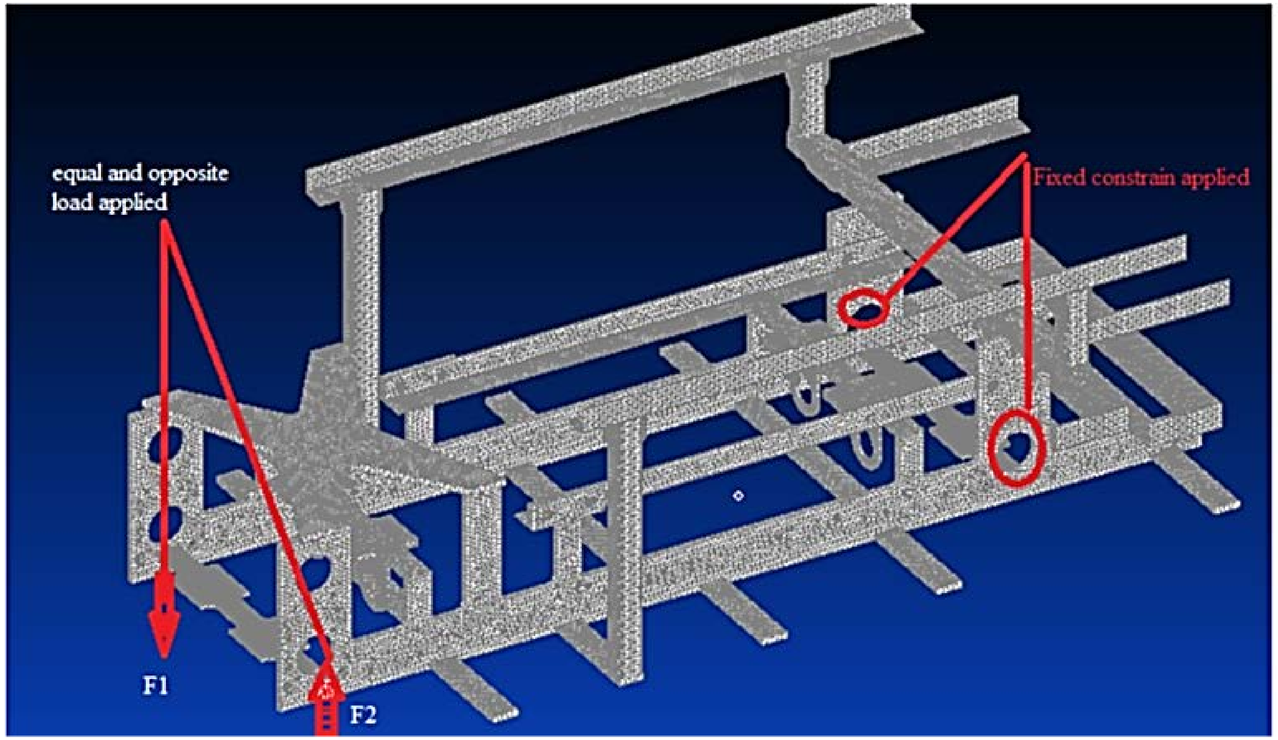

Applied force and constrain in torsional stiffness.

ANALYSIS OF A CHASSIS FRAME

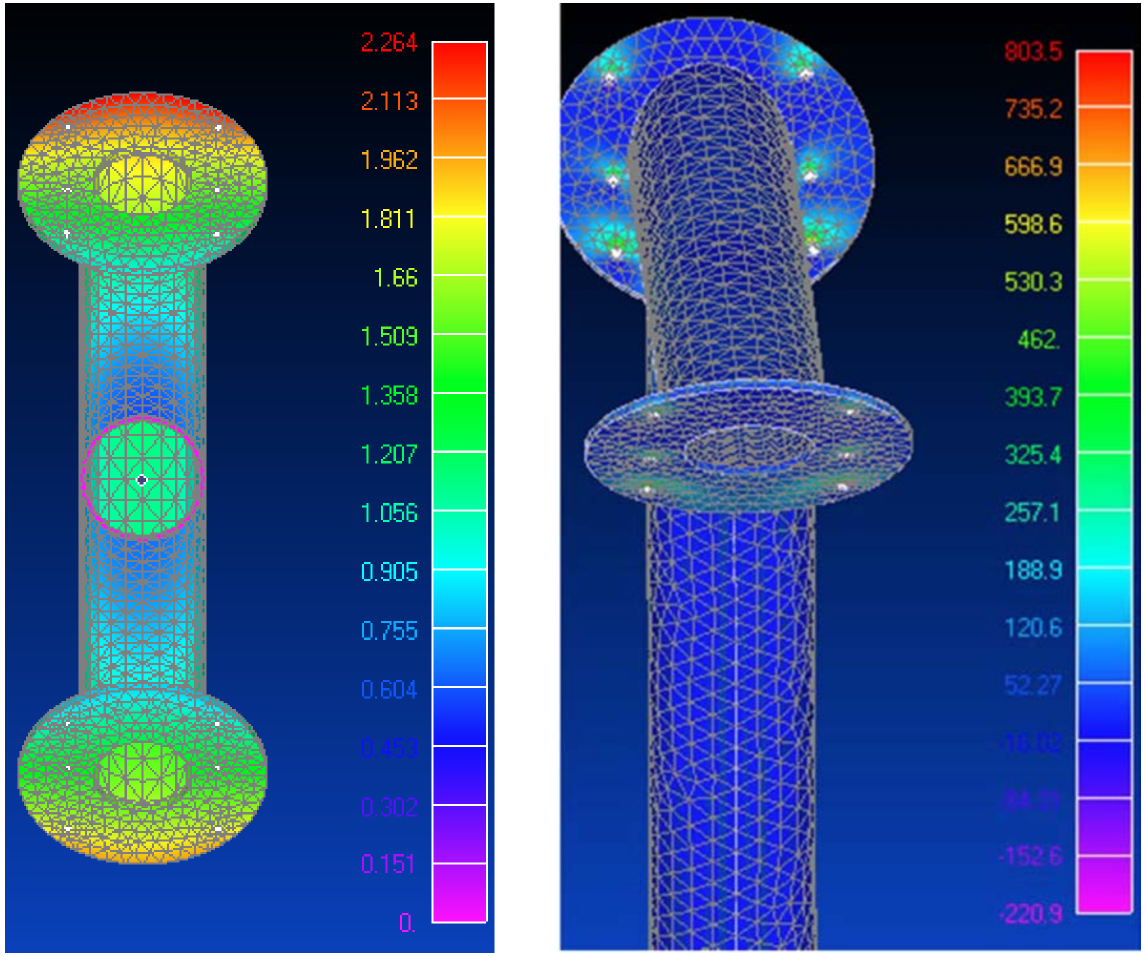

Analysis result for T-joint with 6mm plate
(a) Deflection result (b) Maximum principle stress.

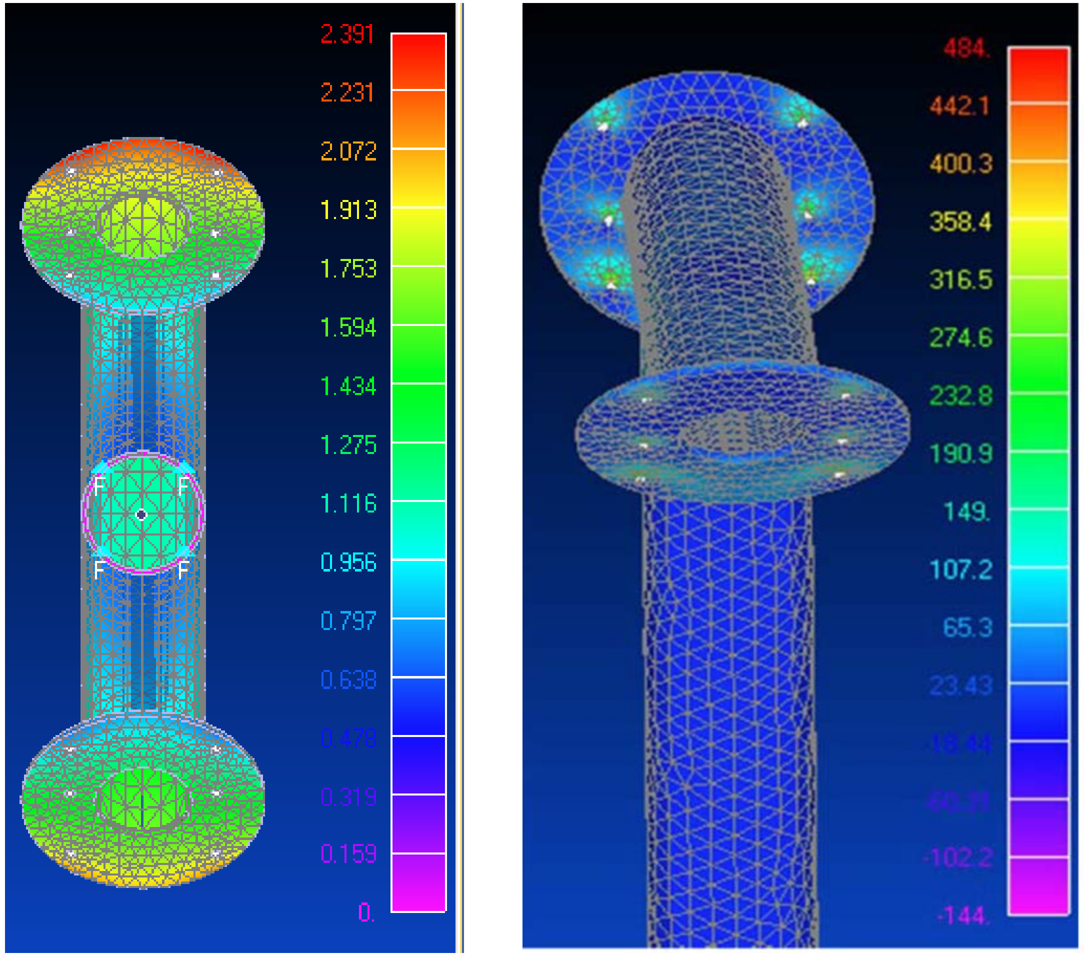

Analysis result for T-joint with 8 mm plate (a) Deflection result (b) Maximum principle stress.

Summary of the result.

Constrain	Parameters
Overall chassis dimension	1597*800*950
Chassis mass	80.50Kg
Overall robot center of position (all component included)	528mm back from front wheel center, 345 mm toward center from front right wheel, 338mm from ground level.
Maximum deflection chassis frame	0.512mm
Bending stiffness of plate beam	11823.56N/mm.
Maximum stress in bending case	33.53MPa
Maximum deflection torsional case	1.941mm
Torsional stiffness	3382484.848Nmm/degree
Maximum principle stress in combined load case	255.8MPa
Constrain	**Parameters**
Dynamic factor for robot frame	2.35
Maximum stress in T-joint	484MPa
Maximum deflection on T-joint	2.264mm

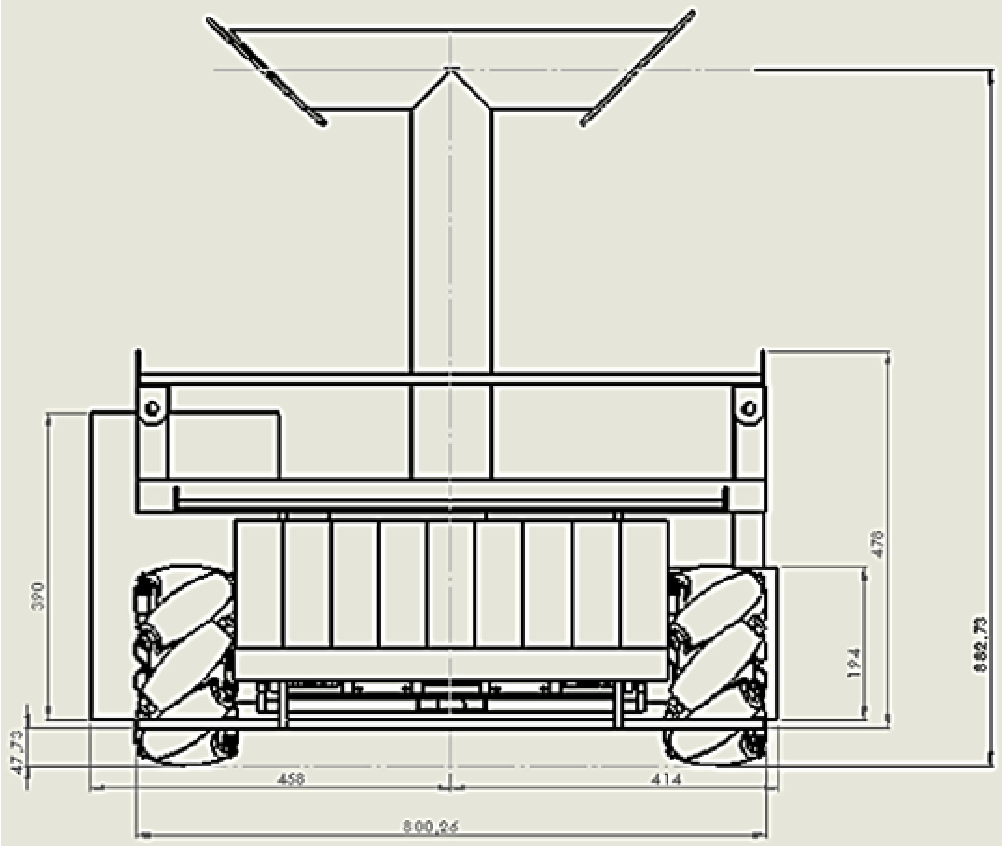

Chassis

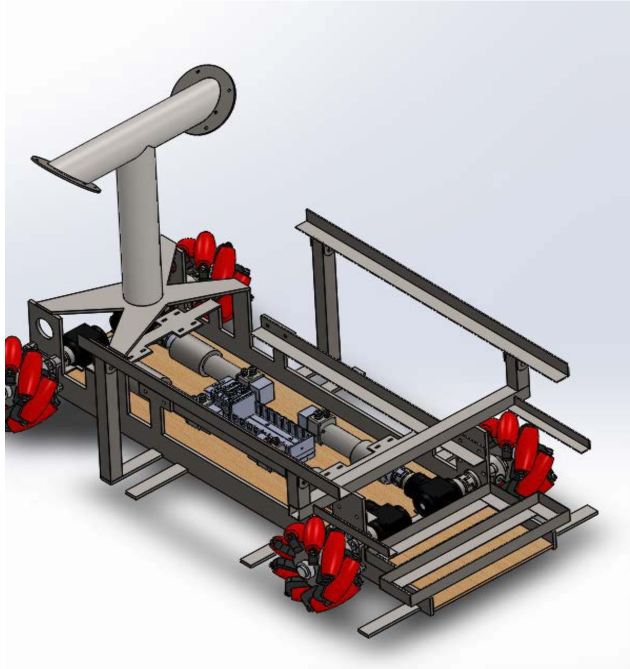

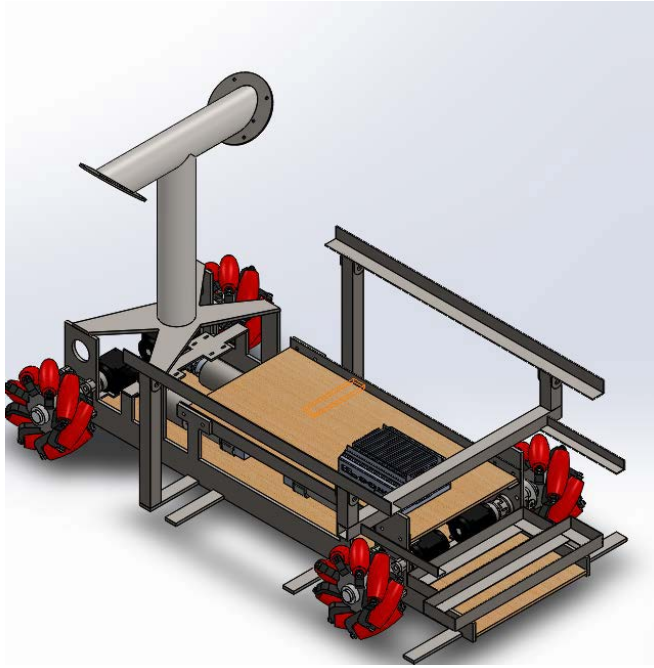

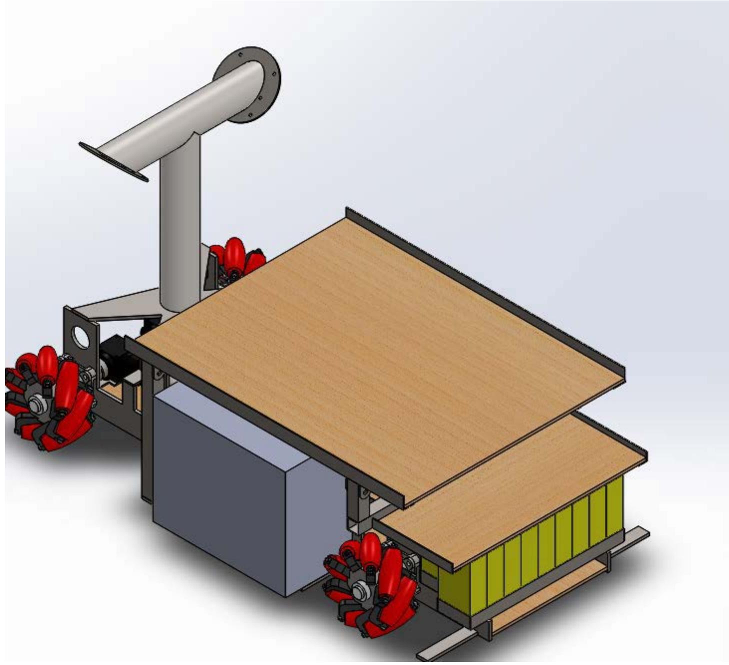

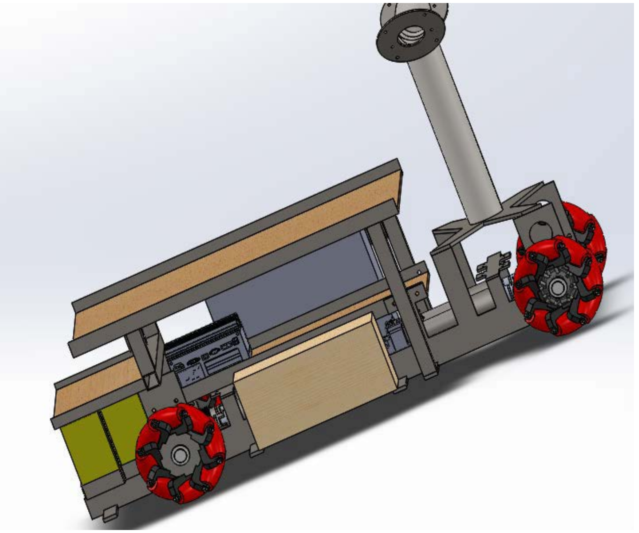

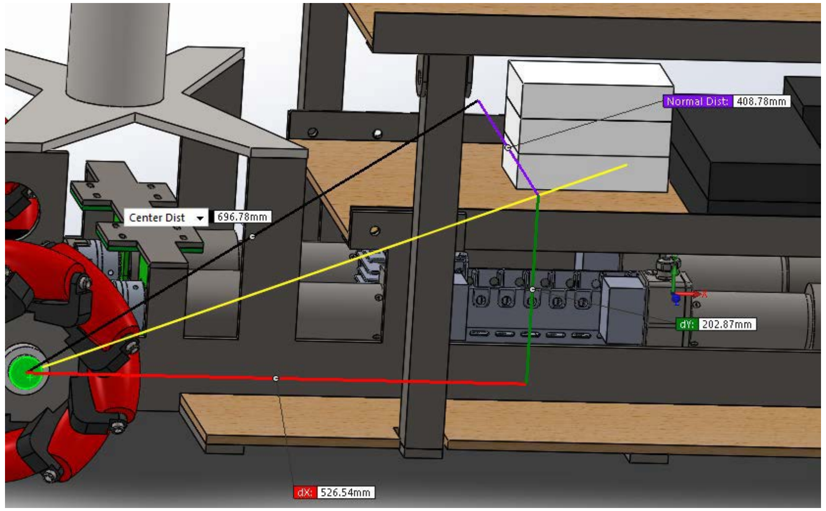
Normal Dist: 408.78mm
Center Dist
696.78mm
dY: 202.87mm
dX: 526.54mm

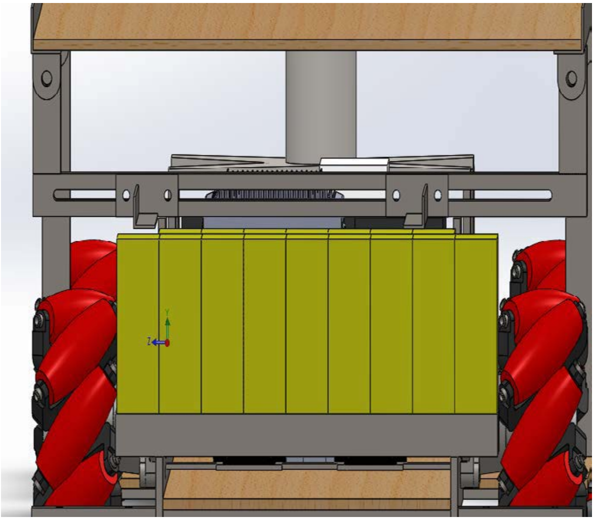

Chassis

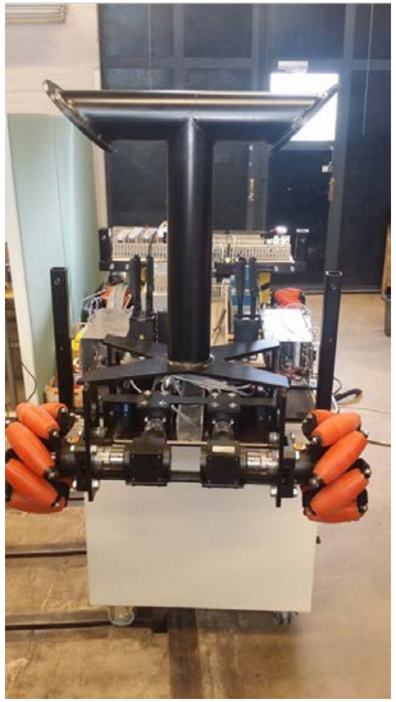

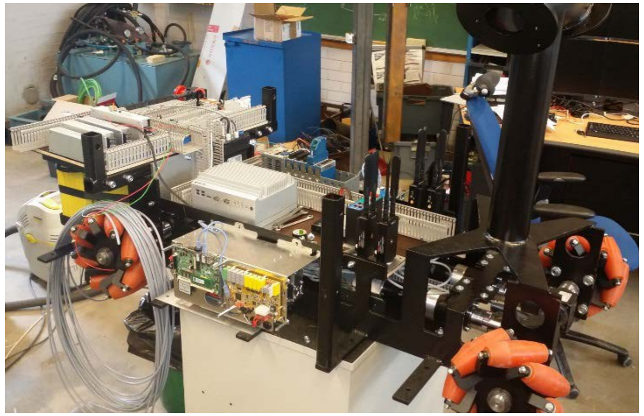

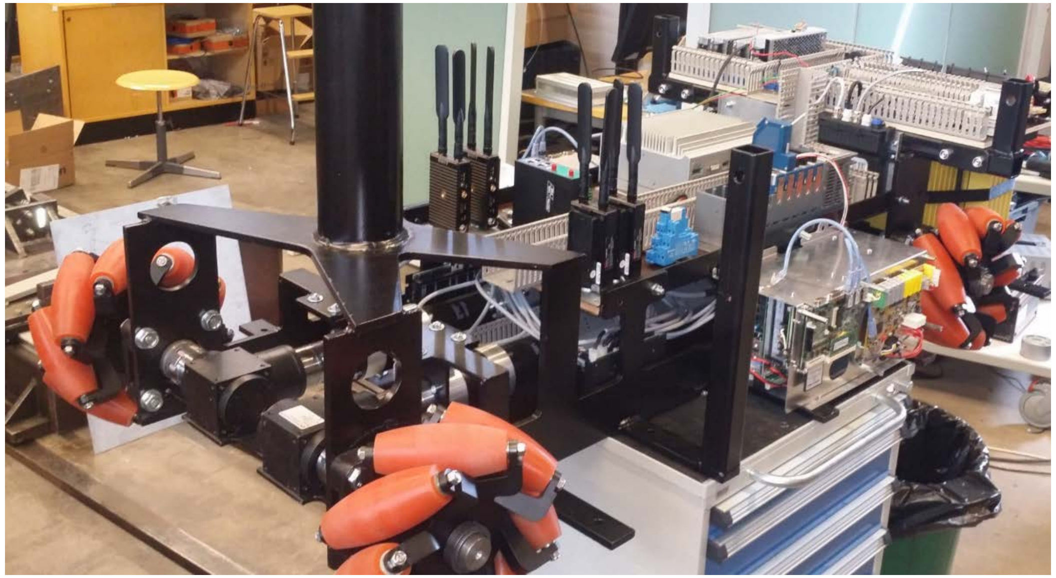

Traction

OMNI Traction

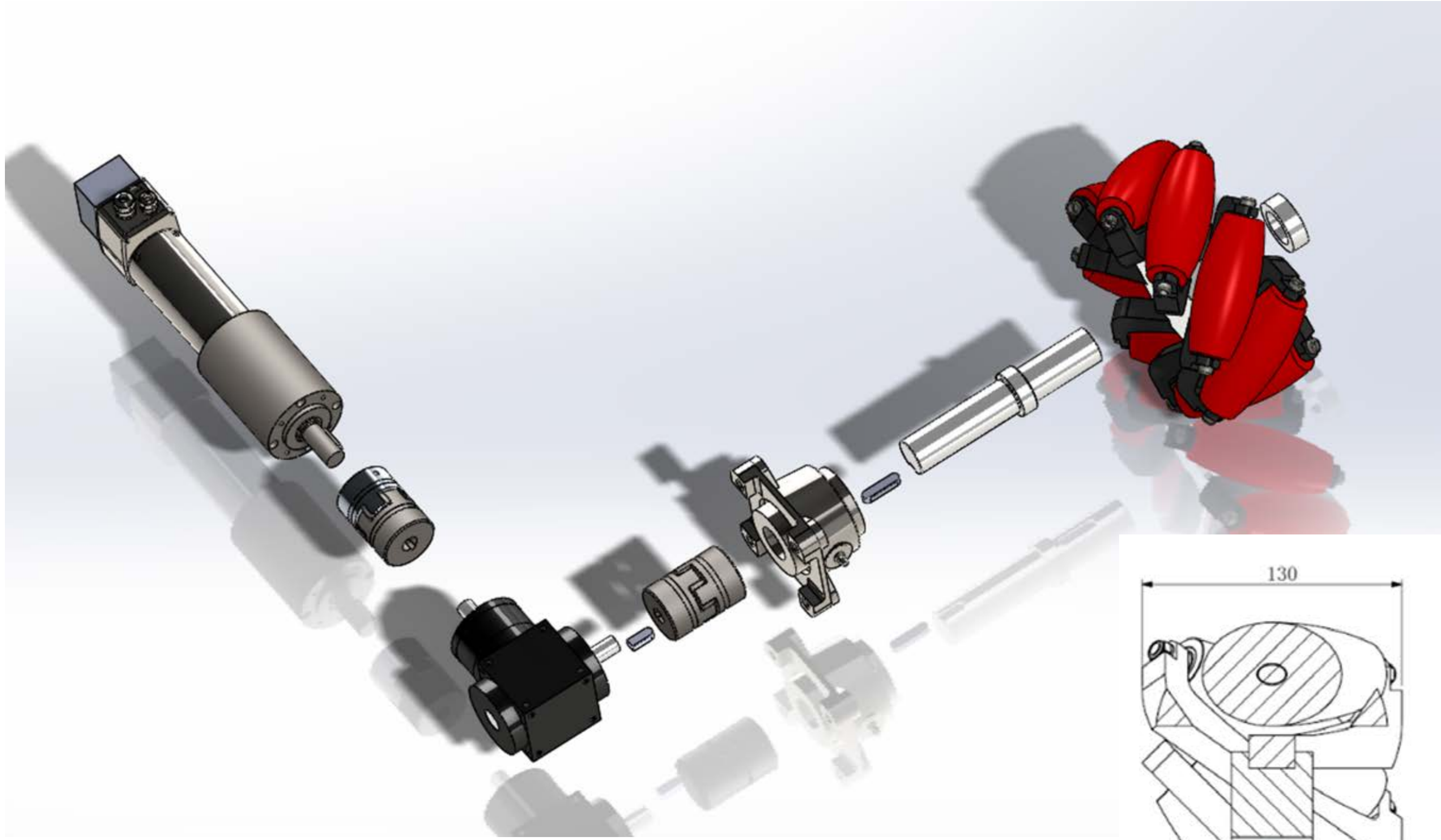

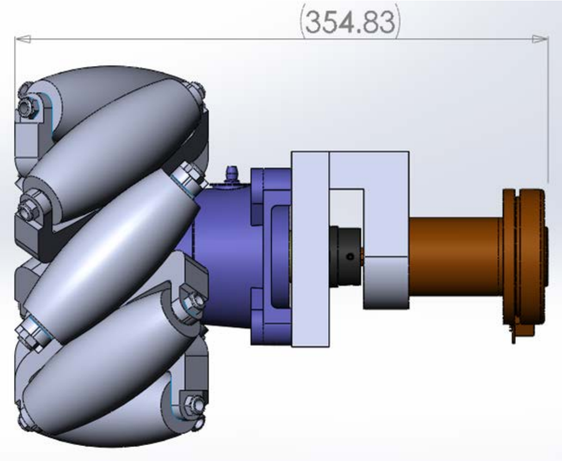

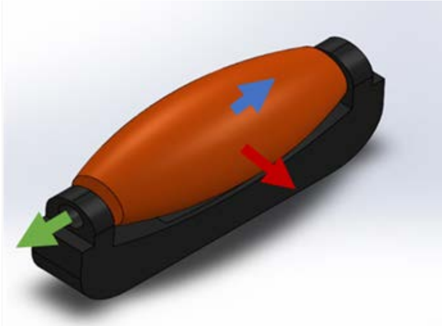

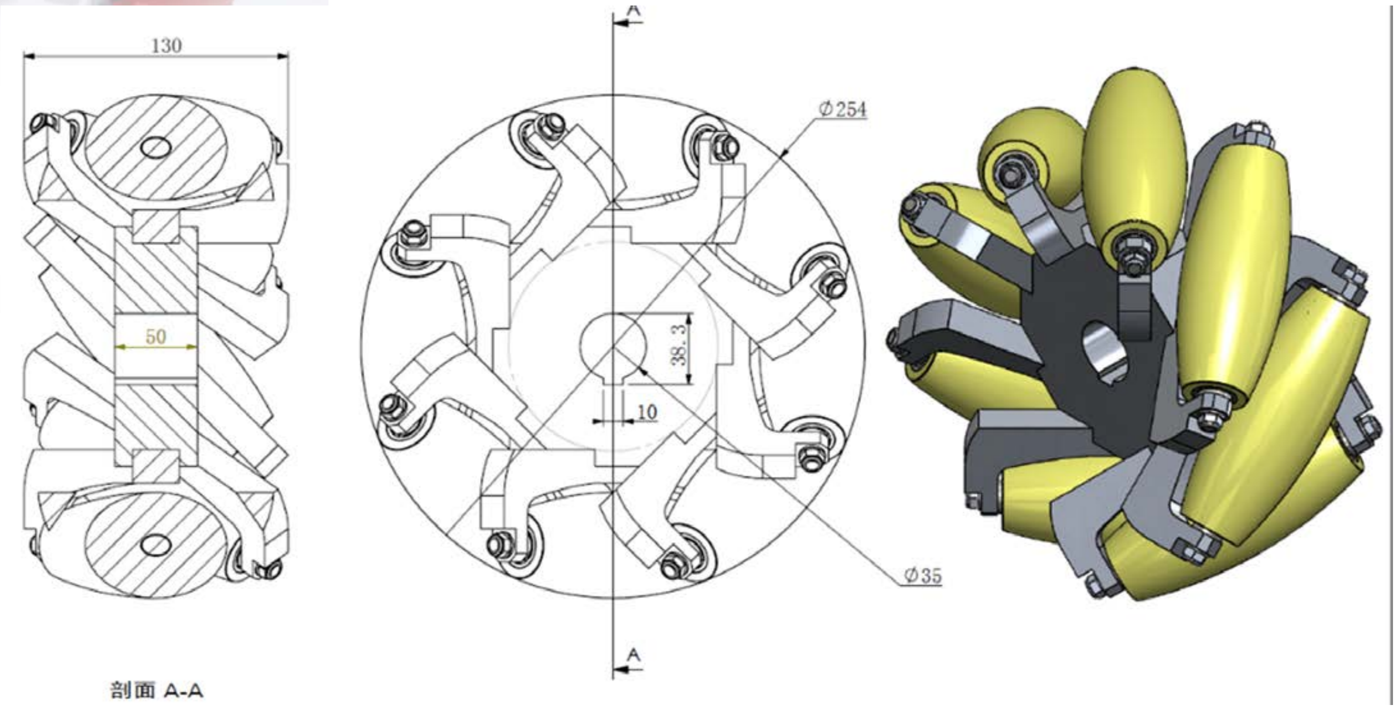

Items in the traction system

Maxon EC60 400W	Reference number: 167132 Brushless motors	X4
Epos 2 70/10 Drives	Motor drives for maxon motors.	X4
Mecanum wheel		X4

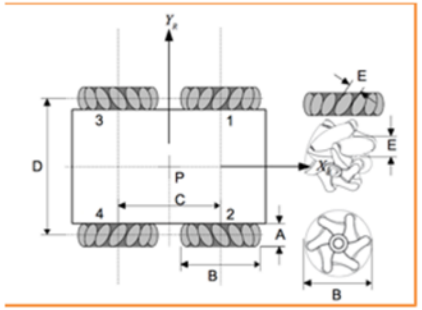

	A	B	C	D	E
Tiera	130 mm	254 mm	1400 mm	560mm	38,2 mm

CANOPEN cables	For serial communication of all motors	X4
RS232 cable	For serial communication of master drive with Advantech	X1
Advantech	Industrial computer	X1

Planetary gearhead GP 81 A	Reference number: 110410 Reduction rate: 25:1	X4

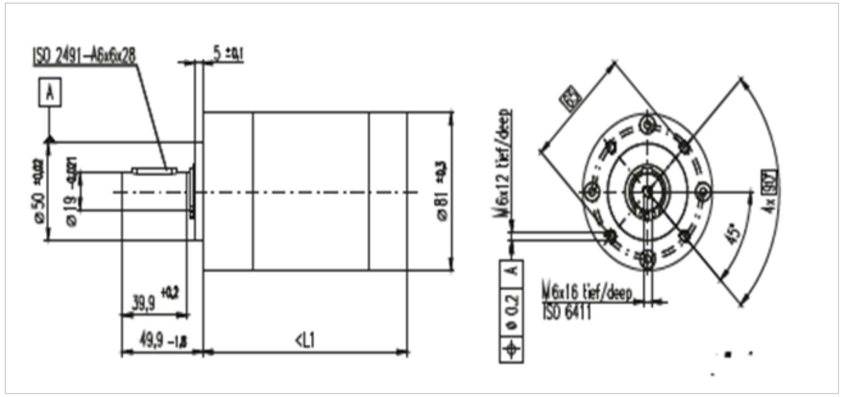

Torsionally flexible jaw-type couplings	Company: KTR Reference number: No. 001 Shaft coupling Coupler material: T-PUR (95/98 Shore-A) Size: 24	X8

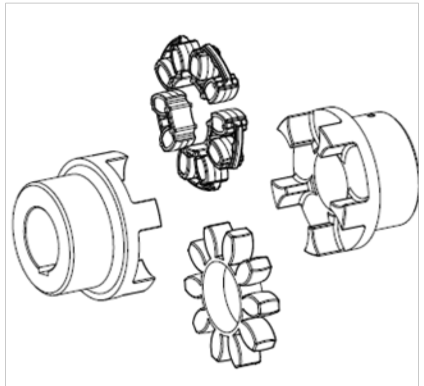

Type No. 001 – shaft coupling

Items in the traction system

L transmission	Company: MS-Graessner Item: PowerGear P75L 1:1 Art. No. 21075P000003 Perpendicular transmission from axle to wheel shaft.  	X4

Xbox controller	Windows base xbox controller for manual control, USB connection.	X1

Tapered roller bearing	Company: Timken Type: E-4BF-TRB 1 3/8 Tapered roller bearing type E housed, flange, 4-blot, cast iron, bore size 1 and 3/8 inches 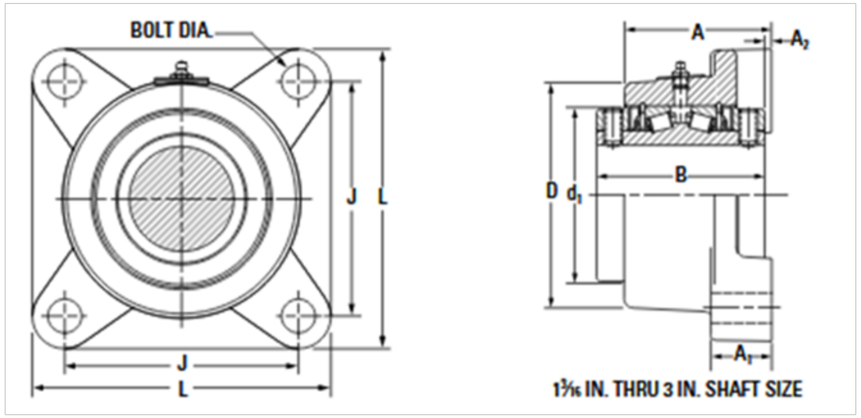 	X4

Shaft Dia.	Part No.	B	L	A	J	A_2	Bolt Dia.	A_1	D	d_1	Approx. Wt.
in. mm		in.	in.	in.	in.	in.	in.	in.	in.	in.	lbs.
1 3/8 1 7/16	E-4BF-TRB-1 3/8 E-4BF-TRB-1 7/16	3	4 5/8	2 19/32	3 1/2	1/16	1/2	1 1/16	3 1/2	2 3/4	7

Motor and Drive

	Motor Data		167132
	Values at nominal voltage		
1	Nominal voltage	V	48
2	No load speed	rpm	5370
3	No load current	mA	733
4	Nominal speed	rpm	4960
5	Nominal torque (max. continuous torque)	mNm	747
6	Nominal current (max. continuous current)	A	9.38
7	Stall torque	mNm	11800
8	Stall current	A	139
9	Max. efficiency	%	86
	Characteristics		
10	Terminal resistance phase to phase	Ω	0.345
11	Terminal inductance phase to phase	mH	0.273
12	Torque constant	mNm/A	84.9
13	Speed constant	rpm/V	113
14	Speed/torque gradient	rpm/mNm	0.457
15	Mechanical time constant	ms	3.98
16	Rotor inertia	gcm^2	831

EPOS2 70/10
- DC and EC motors up to 700 W
- Point to point control unit (1 axis)
- Interpolated Position Mode (PVT)
- Combination of several drives via CAN Bus
- CANopen
- 10 digital inputs
- 5 digital outputs
- 2 analog inputs
- Robust design

Details pages 384–387

Slave version (online commanding) using CAN Master (EPOS2 P, PC, PLC, SoftPLC, etc.) or PC via USB or RS232 interface

Typical applications:
- Production equipment
- System automation tasks
- Plant construction

Structure of the Traction Control

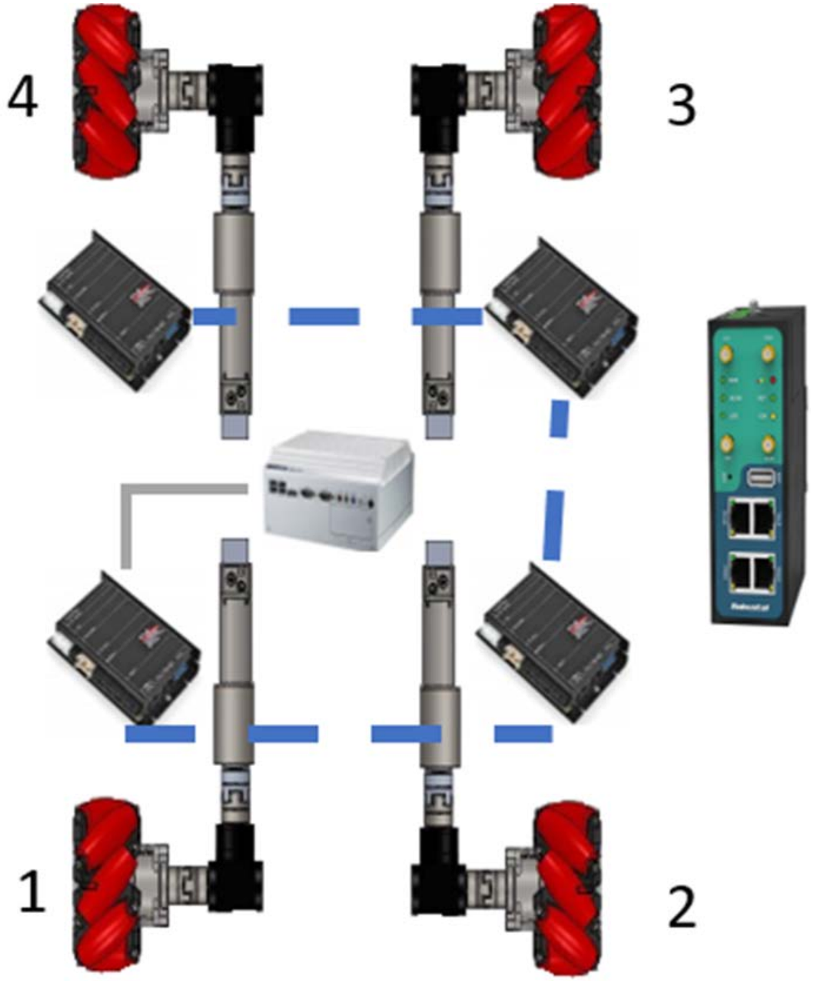

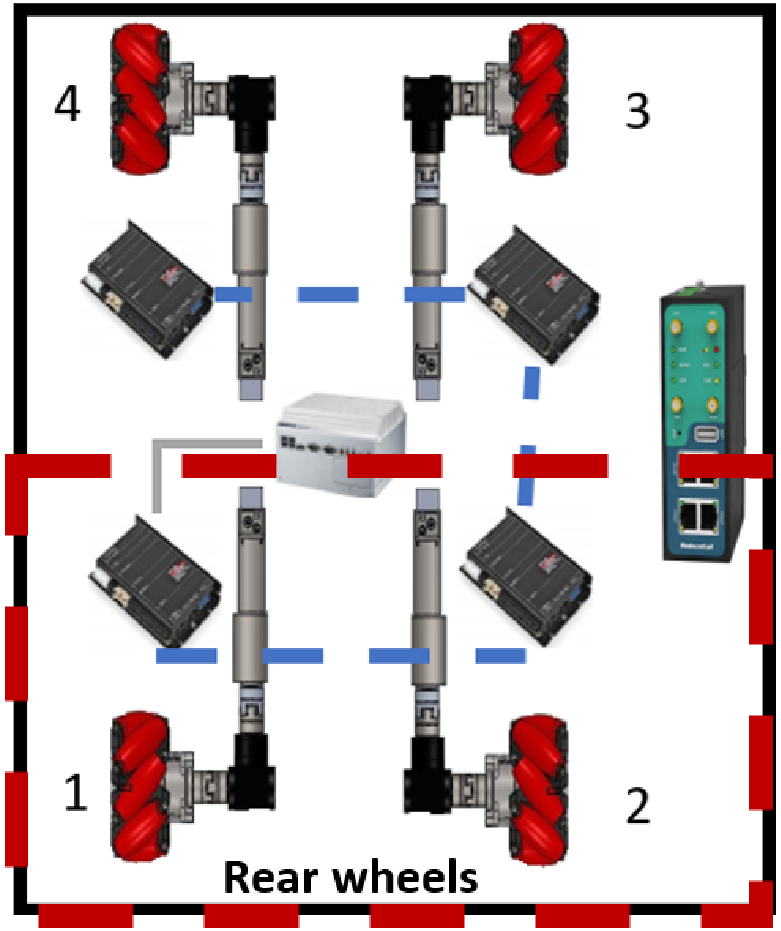

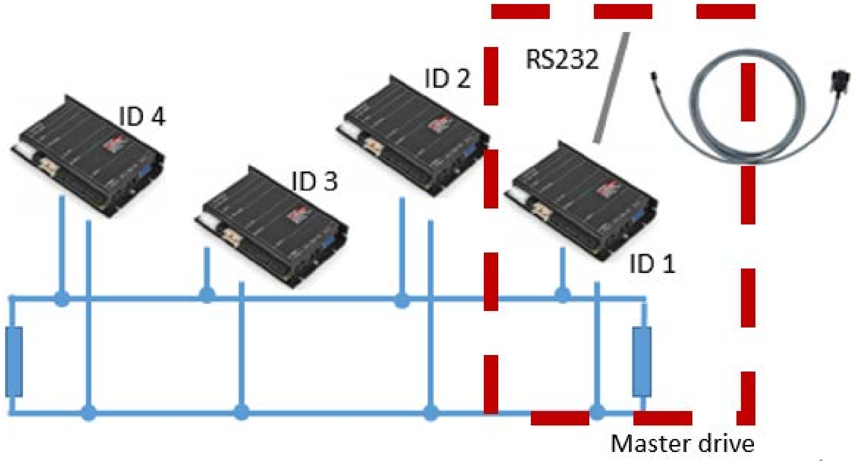

Motor ID	Location
1	Rear-Left (Start-End, Master)
2	Rear-Right
3	Front-Right
4	Front-Left (Start-End)

Driving system layout

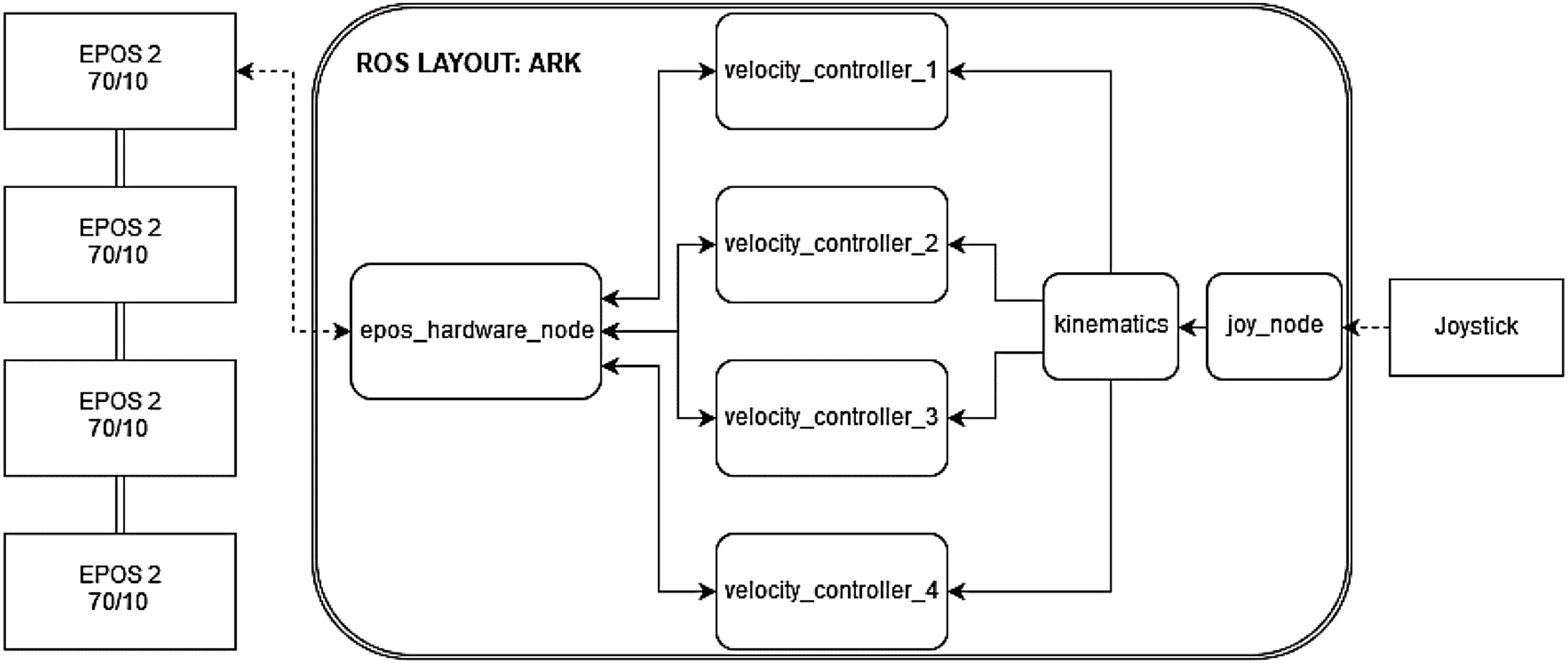

Traction Calculation

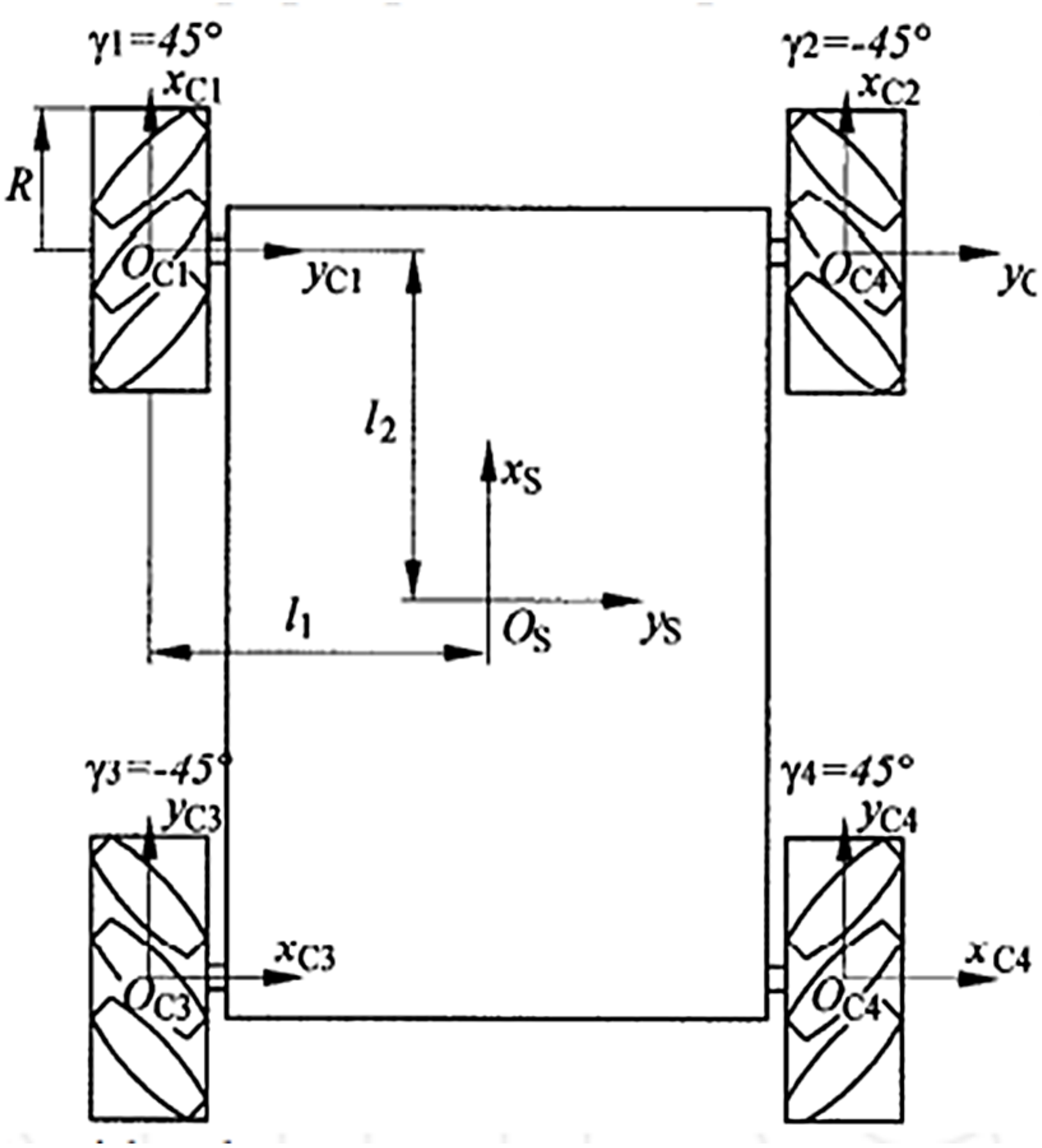

Velocity analysis for wheel:

$$V_{iX} = V_{iw} + V_{ir} cos45°$$

$$V_{iY} = V_{ir} sin45°$$

Velocity analysis for robot:

$$V_{iX} = v_X - l\omega_Z$$

$$V_{iY} = v_Y + L\omega_Z$$

$$V_{1w} = v_X - v_Y - (L + l)\omega_Z$$

$$V_{2w} = v_X + v_Y + (L + l)\omega_Z$$

$$V_{3w} = v_X + v_Y - (L + l)\omega_Z$$

$$V_{4w} = v_X - v_Y + (L + l)\omega_Z$$

$$\begin{bmatrix} v_X \\ v_Y \\ \omega_Z \end{bmatrix} = \frac{1}{4} \cdot \begin{bmatrix} 1 & 1 & 1 & 1 \\ -1 & 1 & 1 & -1 \\ -\frac{1}{(l+L)} & \frac{1}{(l+L)} & -\frac{1}{(l+L)} & \frac{1}{(l+L)} \end{bmatrix} \cdot \begin{bmatrix} R_w \dot{\omega}_1 \\ R_w \dot{\omega}_2 \\ R_w \dot{\omega}_3 \\ R_w \dot{\omega}_4 \end{bmatrix}$$

Robot's tracking parameters

$$\begin{bmatrix} v_x \\ v_y \\ \omega_z \end{bmatrix} = \frac{1}{4} \begin{bmatrix} 1 & 1 & 1 & 1 \\ -1 & 1 & 1 & -1 \\ -\frac{1}{L+w} & \frac{1}{L+w} & -\frac{1}{L+w} & \frac{1}{L+w} \end{bmatrix} \begin{bmatrix} R_w\dot{\phi}_1 \\ R_w\dot{\phi}_2 \\ R_w\dot{\phi}_3 \\ R_w\dot{\phi}_4 \end{bmatrix}$$

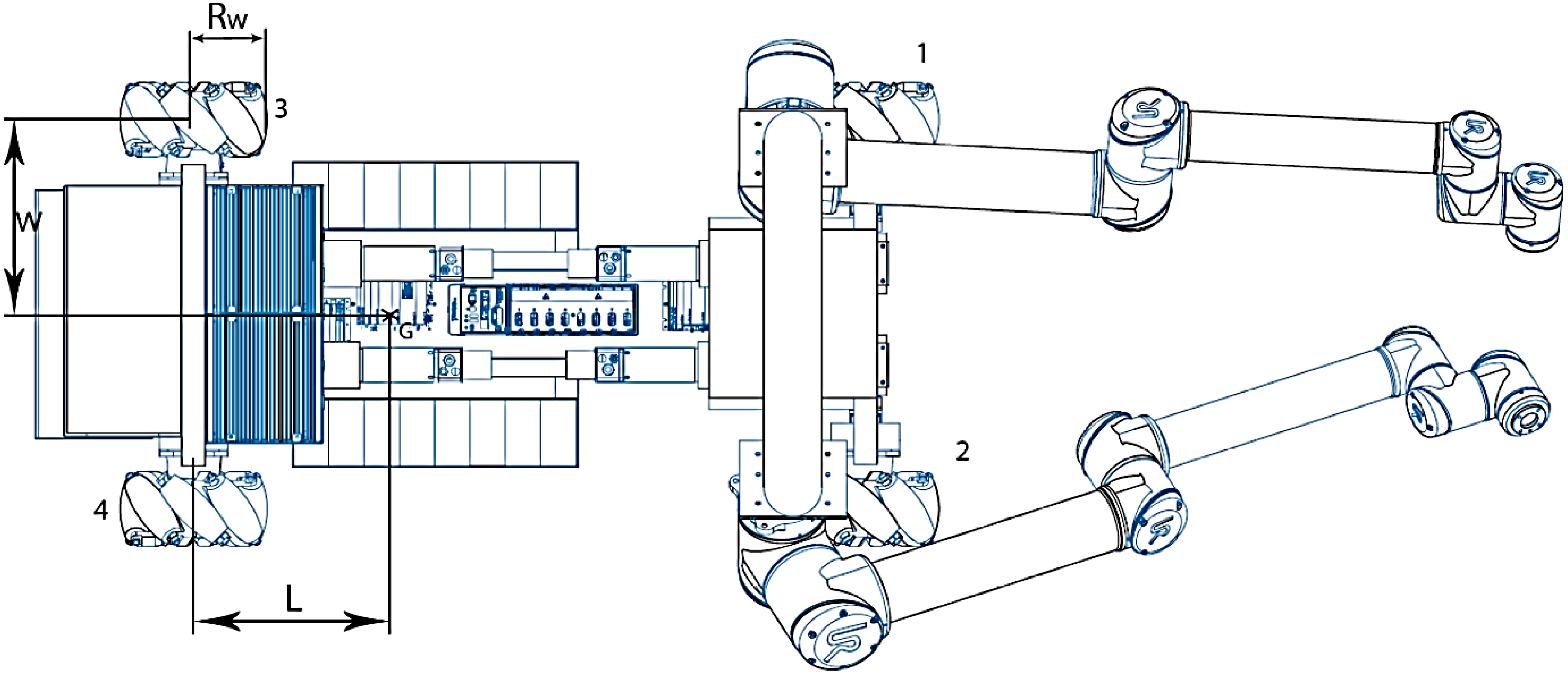

Traction Programming

Kinematics code

```
// #include "MecanumDrive.h"

#include <math.h>

// measurements in units of millimeters


void Mecanum(float vx, float vy, float omega)

{
const float width =    ;           // half distance between left right wheels center
const float length =    ;           // half distance between front back wheels center
const float wheelRadius = 127;       // radius of mecanum wheel


////////////////////////////////////////
//
//                1\\\       ///2
//
//
//
//
//
//
//                3///       \\\4
//
////////////////////////////////////////



// Inverse Kinematics for mecanum wheel drive robot

// w1-w4 are wheel rotation speed

// vx, vy represent the desired translational and rotational velocity of the robot at an instant in , omega is positive anticlockwise


vx =   ;
vy =   ;
omega =   ;

float w[];

w1 = 1/wheelRadius*(vx+vy+(width+length)*omega);

w2 = 1/wheelRadius*(vx-vy+(width+length)*omega);

w3 = 1/wheelRadius*(vx-vy-(width+length)*omega);

w4 = 1/wheelRadius*(vx+vy-(width+length)*omega);

}
```

```
// Checks on parameters
if (autorepeat_rate_ > 1 / coalesce_interval_)
  ROS_WARN("joy_node: autorepeat_rate (%f Hz) > 1/coalesce_interval (%f Hz) does not make sense. Tim

if (deadzone_ >= 1)
{
  ROS_WARN("joy_node: deadzone greater than 1 was requested. The semantics of deadzone have changed.
  deadzone_ /= 32767;
}

if (deadzone_ > 0.9)
{
  ROS_WARN("joy_node: deadzone (%f) greater than 0.9, setting it to 0.9", deadzone_);
  deadzone_ = 0.9;
}

if (deadzone_ < 0)
{
  ROS_WARN("joy_node: deadzone_ (%f) less than 0, setting to 0.", deadzone_);
  deadzone_ = 0;
}

if (autorepeat_rate_ < 0)
{
  ROS_WARN("joy_node: autorepeat_rate (%f) less than 0, setting to 0.", autorepeat_rate_);
  autorepeat_rate_ = 0;
}

if (coalesce_interval_ < 0)
{
  ROS_WARN("joy_node: coalesce_interval (%f) less than 0, setting to 0.", coalesce_interval_);
  coalesce_interval_ = 0;
}
```

ROS

Joystick basic code

```
void joy()
{
    int threhold=  ;                       // threhold: adjust it to increase or decrease deadzone to get rid of unintentional minor movements

    while (1 == 1)                         // loop forever
    {
      // Remote control commands
      Frontleft = Ch3+Ch1+Ch4;                       // Ch3 represents left joystick forward & back, Ch4 represents left joystick left & right
      Frontright = Ch3-Ch1-Ch4;                      // Ch1 represents right joystick ratotaion
      Rearleft = Ch3+Ch1-Ch4;
      Rearright = Ch3-Ch1+Ch4;
      motor[Frontleft] = abs(Frontleft) > threshold ? Frontleft : 0;
      motor[Frontright] = abs(Frontright) > threshold ? Frontright : 0;
      motor[Rearleft] = abs(Rearleft) > threshold ? Rearleft : 0;
      motor[Rearright] = abs(Rearright) > threshold ? Rearright : 0;
```

Moving Algorithm

	N1	N2	N3	N4	
Forward	+N	-N	-N	+N	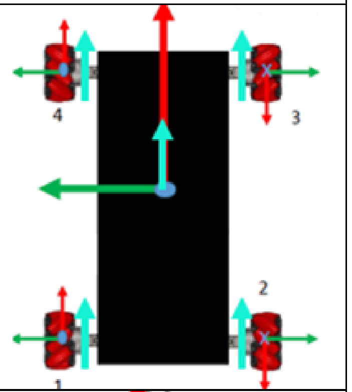
Backward	-N	+N	+N	-N	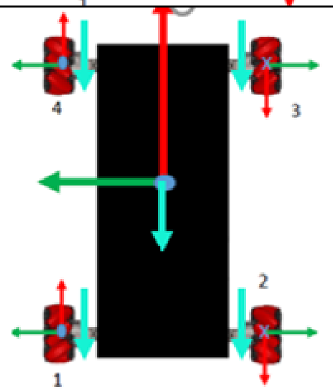
Left	N	N	-N	-N	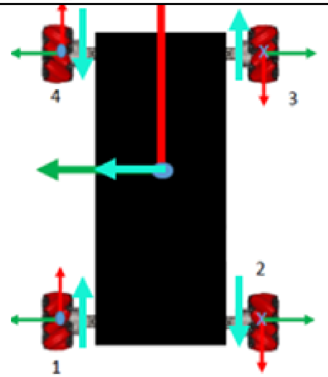

	N1	N2	N3	N4	
Right	-N	-N	N	N	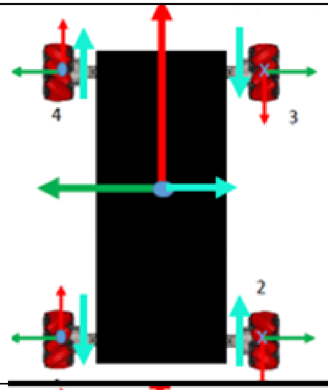
Left twist	-N	-N	-N	-N	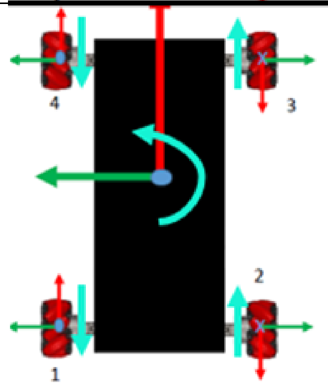
Right twist	N	N	N	N	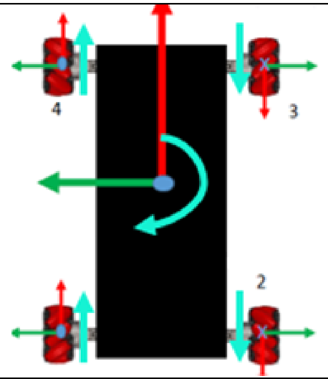

	N1	N2	N3	N4	
Forward-Left	Na	-Nb	-Na	Nb	Na>>Nb 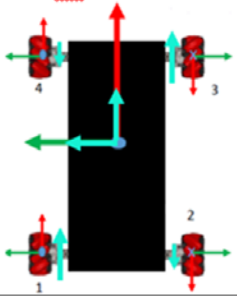
Forward-Right	Na	-Nb	-Na	Nb	Na<<Nb 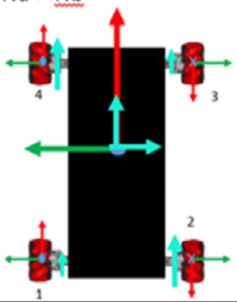

	N1	N2	N3	N4	
Backward-left	Na	Nb	-Na	-Nb	Na<<Nb 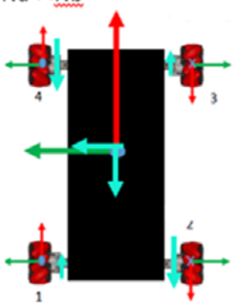
Backward-Right	-Na	Nb	Na	-Nb	Na>>Nb 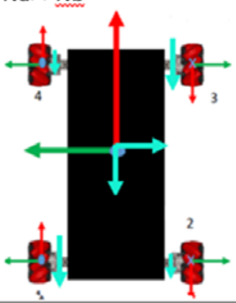

Simulation in ROS

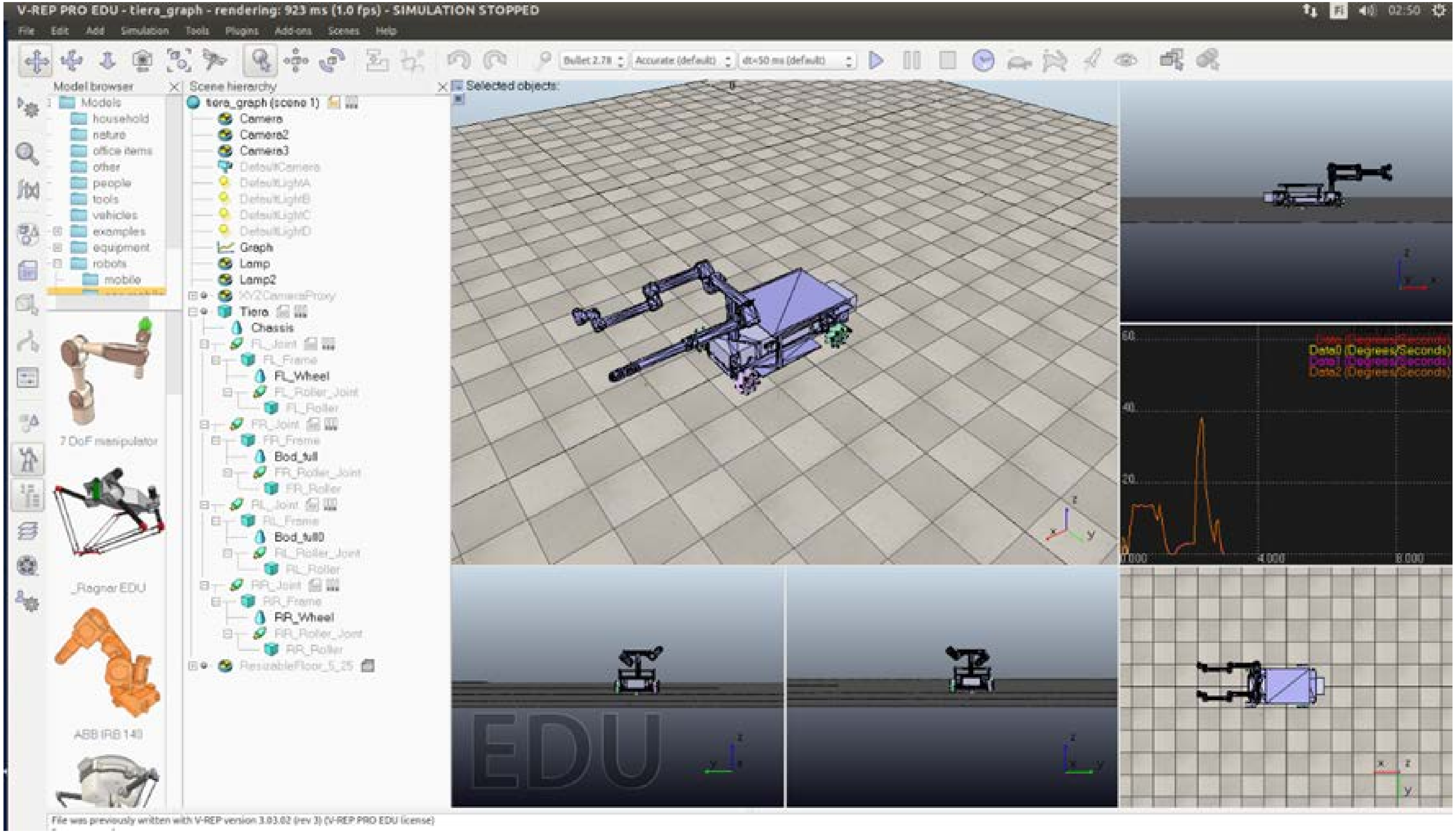

Robot Simulation – Balance test

Resulting 3D model in Gazebo.

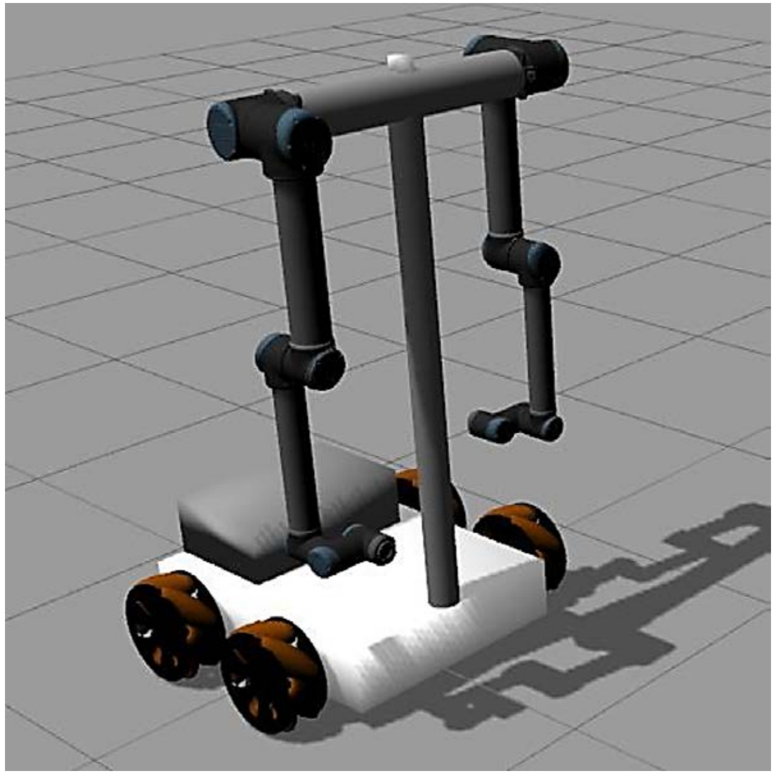

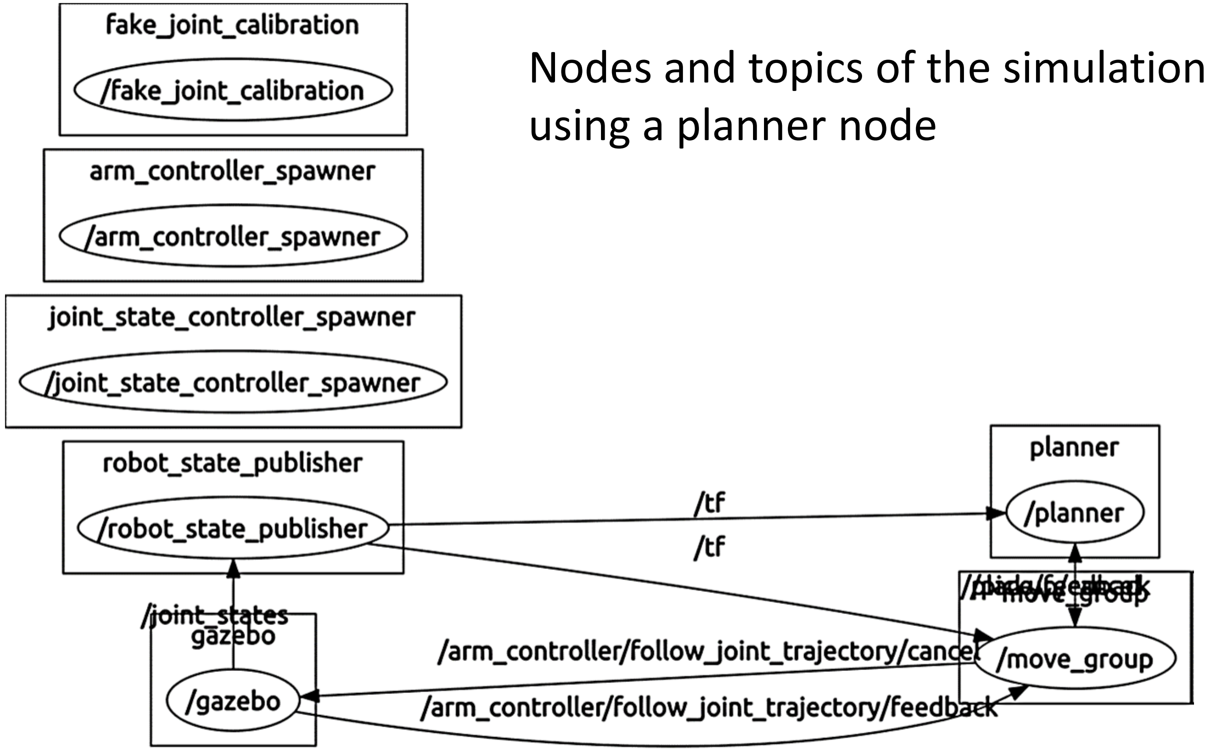

Nodes and topics of the simulation using a planner node

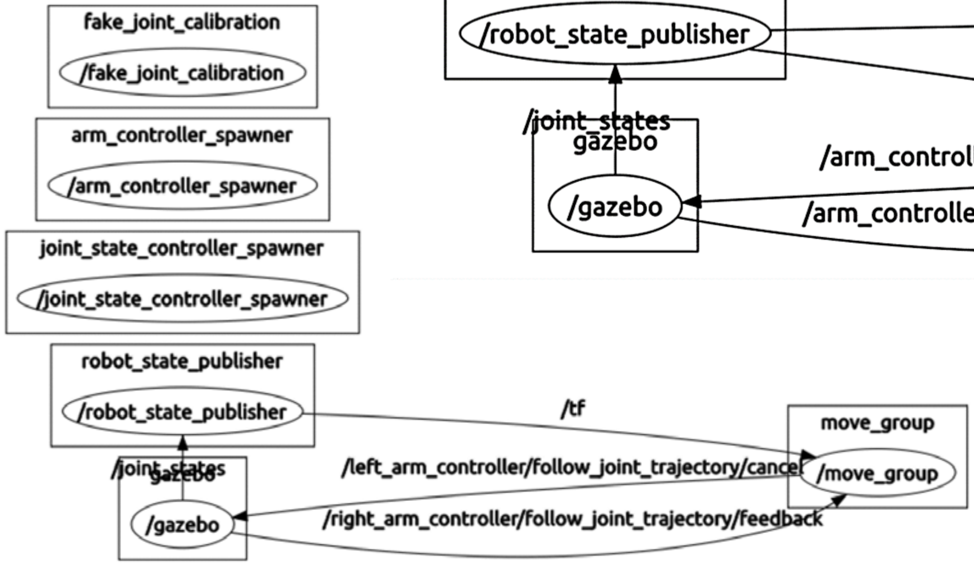

Nodes and topics of the simulation

Rviz planning: first arm.

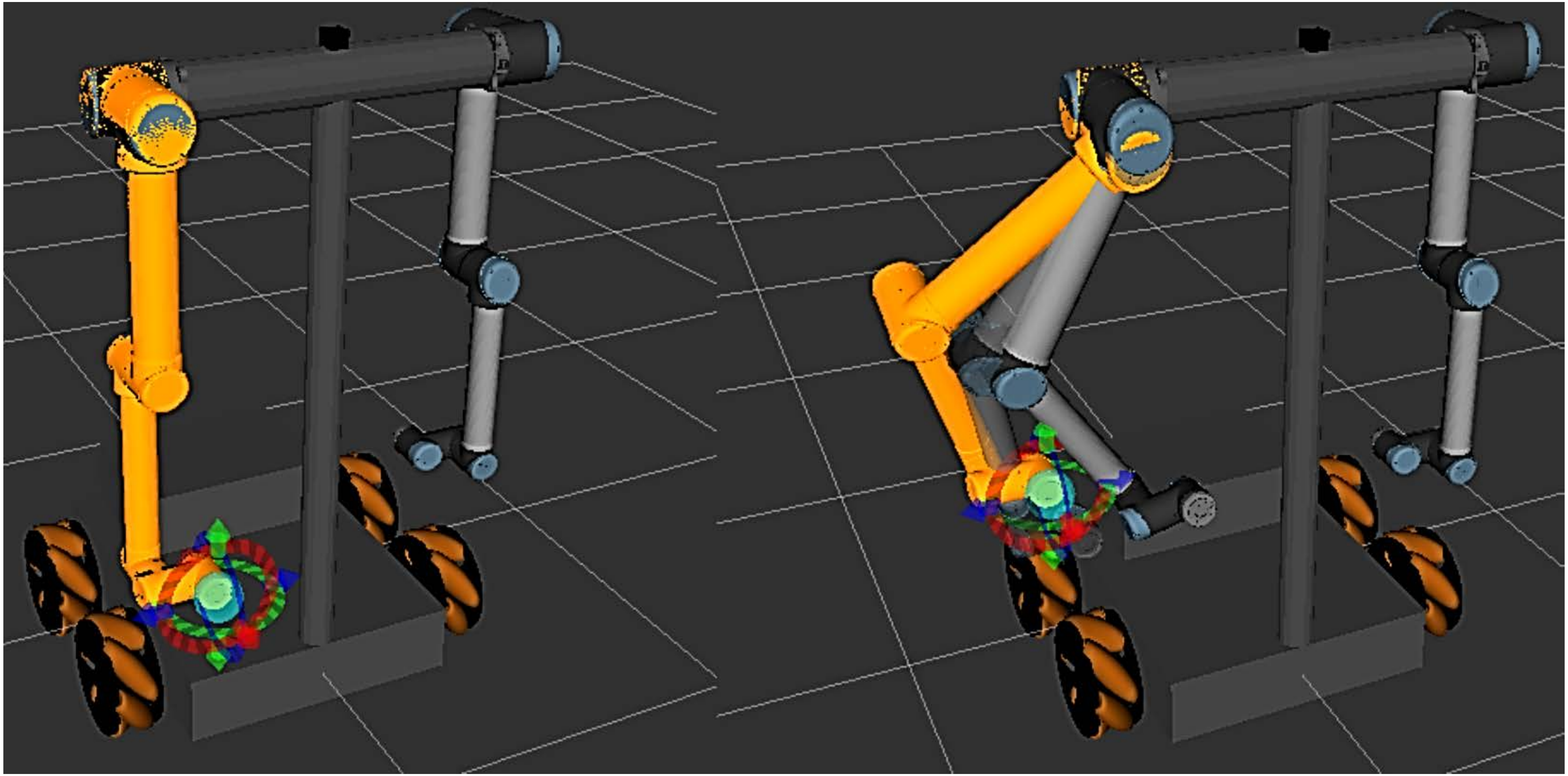

Gazebo Simulation: moving first arm.

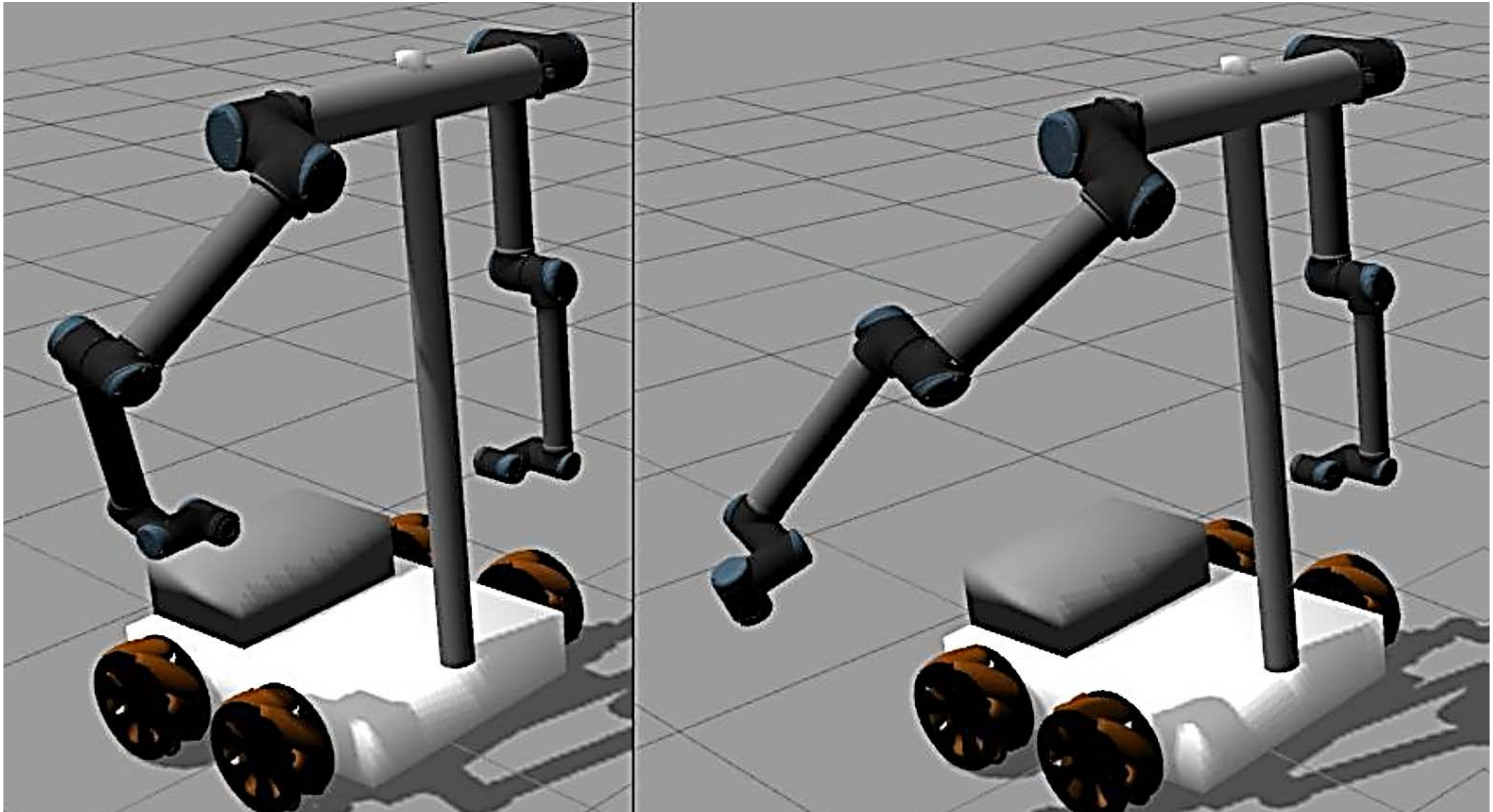

Rviz planning: collision detection.

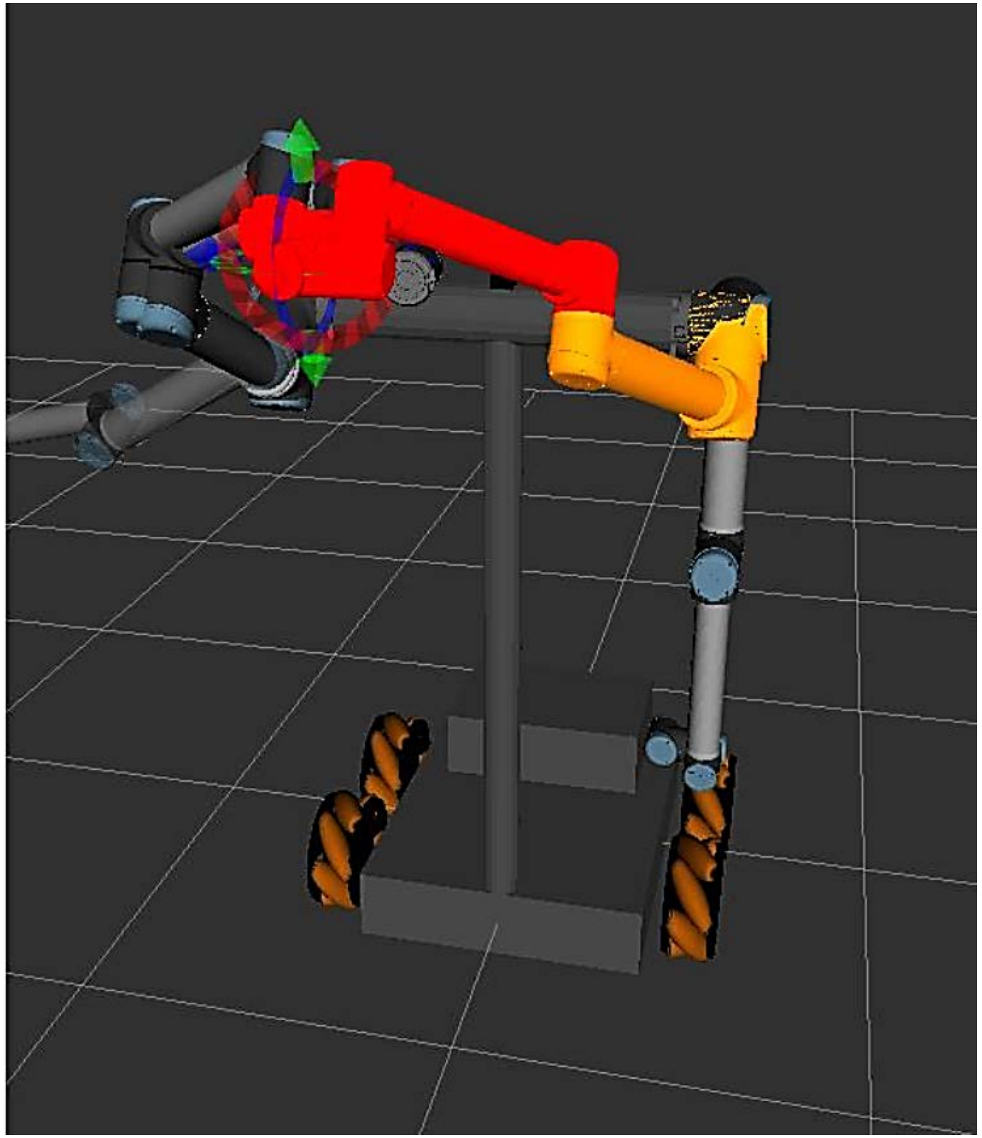

PID controller and Simulation results

	K_p	K_i	K_d	$i_{clamping}$
Shoulder_pan_joint	600	500	100	100
Shoulder_lift_joint	1500	500	100	100
Elbow_joint	1500	500	100	100
Wrist_1_joint	100	0	0	0
Wrist_2_joint	100	0	0	0
Wrist_2_joint	100	0	0	0

	$K_p = 600$	$K_p = 900$	$K_p = 1500$
	$t_r\ (s)$		
Shoulder_pan_joint	3.5	4.7	5
Shoulder_lift_joint	5.5	5.7	3.5
Elbow_joint	5.6	5.9	3.5

$$\lambda_{Max}\{K_i\} \geq \lambda_{Min}\{K_i\} > 0$$

$$\lambda_{Max}\{K_p\} \geq \lambda_{Min}\{K_p\} > k_g$$

$$\lambda_{Max}\{K_v\} \geq \lambda_{Min}\{K_v\} > \frac{\lambda_{Max}\{K_i\}}{\lambda_{Min}\{K_p\} - kg} \cdot \frac{\lambda^2_{Max}\{M\}}{\lambda_{Min}\{M\}}$$

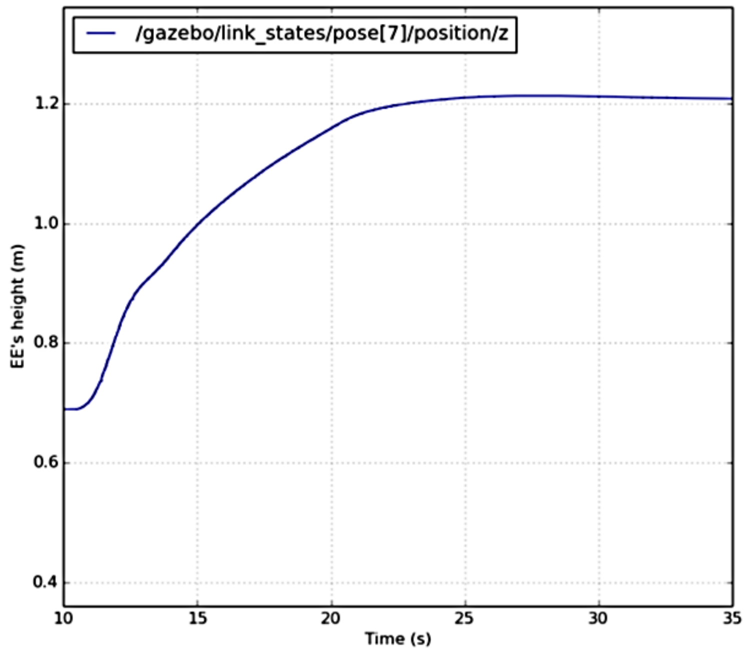

$$\begin{cases} \lambda_{Max}\{K_i\} = 500 \\ \lambda_{Min}\{K_i\} = 0 \end{cases} \rightarrow 500 \geq 0 \geq 0$$

$$\begin{cases} \lambda_{Max}\{K_p\} = 1500 \\ \lambda_{Min}\{K_p\} = 100 \end{cases} \rightarrow 500 \geq 100 > kg = 0$$

$$\begin{cases} \lambda_{Max}\{K_v\} = 100 \\ \lambda_{Min}\{K_v\} = 0 \\ \lambda_{Max}\{M\} = 3.84 \\ \lambda_{Min}\{M\} = -0.05 \end{cases} \rightarrow 100 \geq 0 > \frac{500}{100} \cdot \frac{3.84^2}{-0.05}$$

Arms

Teleoperation method

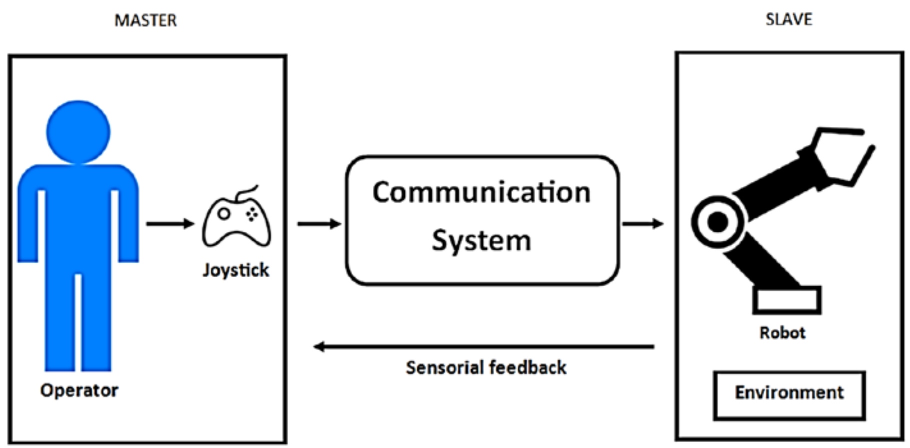

Teleoperation method

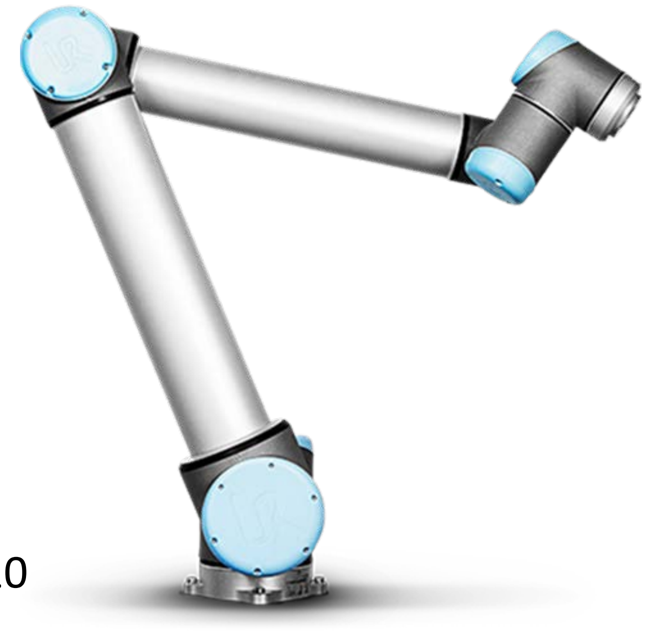

UR10

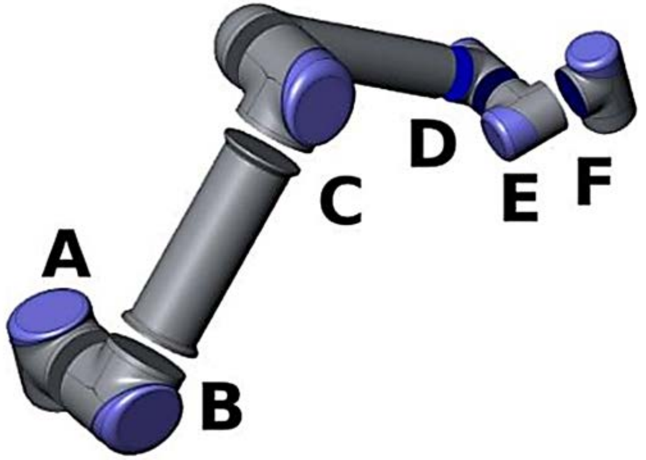

Joints.:

A: Base

B: Shoulder

C: Elbow

D: Wrist1

E: Wrist2

F: Wrist3

Stability Margin Index

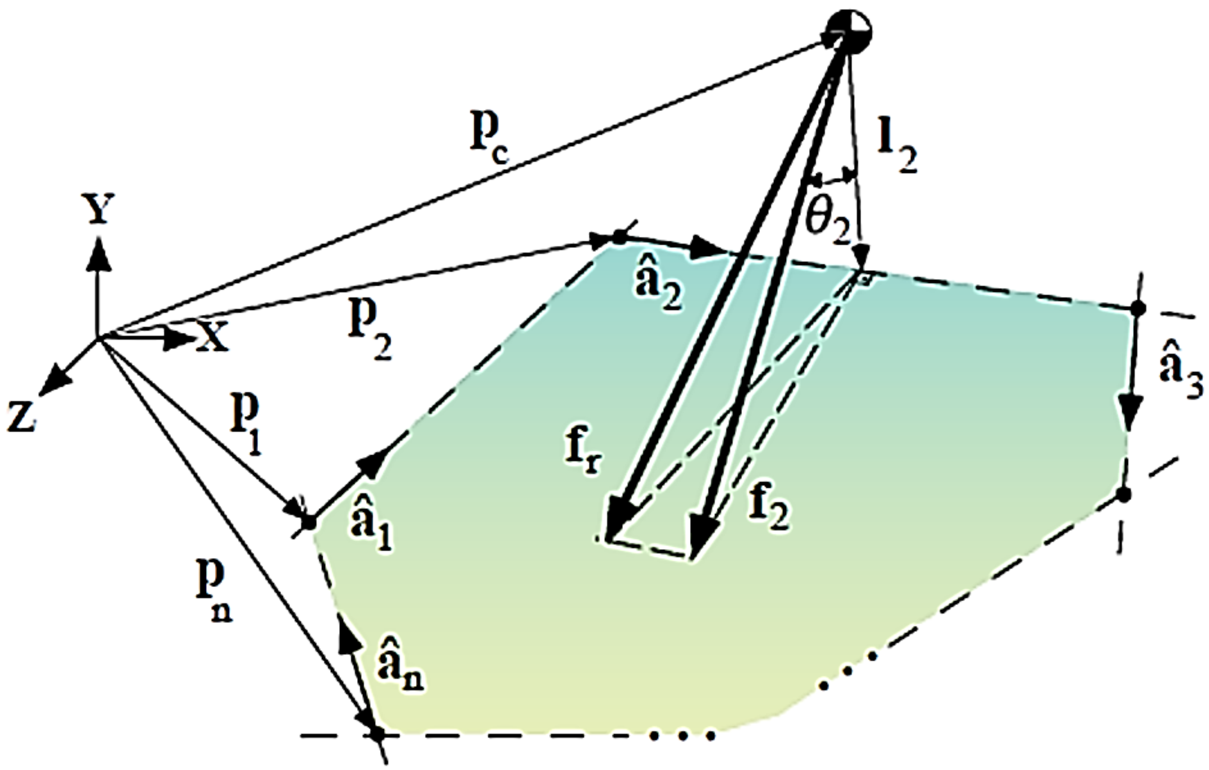

$$\hat{a}_i = \frac{p_{i+1} - p_i}{|p_{i+1} - p_i|} \qquad i = \{1, \ldots, n-1\}$$

$$\boldsymbol{I_i} = (\mathbf{1} - \hat{a}_{\boldsymbol{i}}\hat{a}_{\boldsymbol{i}}^{\boldsymbol{T}})(\boldsymbol{p_{i+1}} - \boldsymbol{p_c})$$

$$\boldsymbol{f_i} = (\mathbf{1} - \hat{a}_{\boldsymbol{i}}\hat{a}_{\boldsymbol{i}}^{\boldsymbol{T}})\boldsymbol{f_r}$$

$$n_i = (\hat{a}_i\hat{a}_i^T)n_r$$

$$f_i^* = f_i + \frac{\hat{I}_i \times n_i}{|I_i|}$$

$$\theta_i = \sigma_i \cos^{-1}(\hat{f}_i^* \cdot \hat{I}_i)$$

$$\sigma_i = \begin{cases} +1 & if\ (\hat{I}_i \times \hat{f}_i^*) \cdot \hat{a}_i < 0 \\ -1 & else \end{cases}$$

$$\alpha_i = \theta_i |f_r|$$

Which angels?

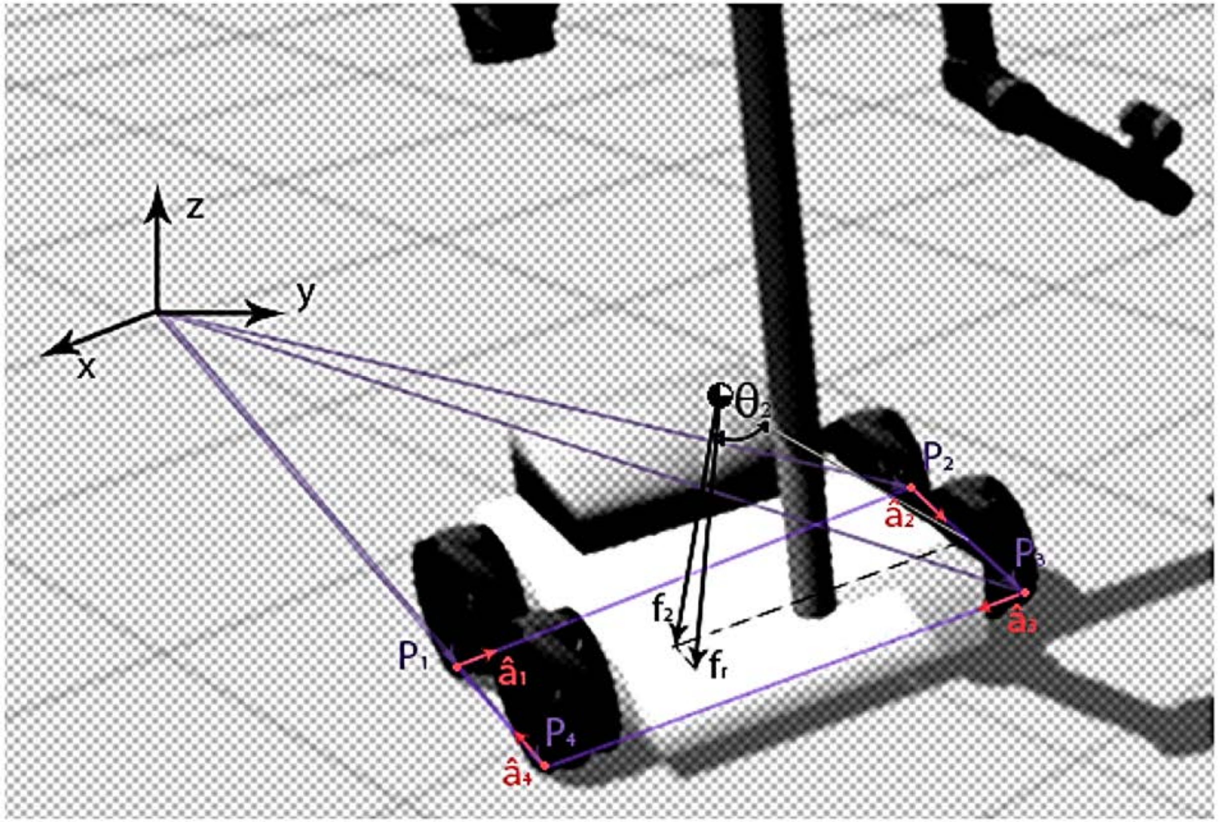

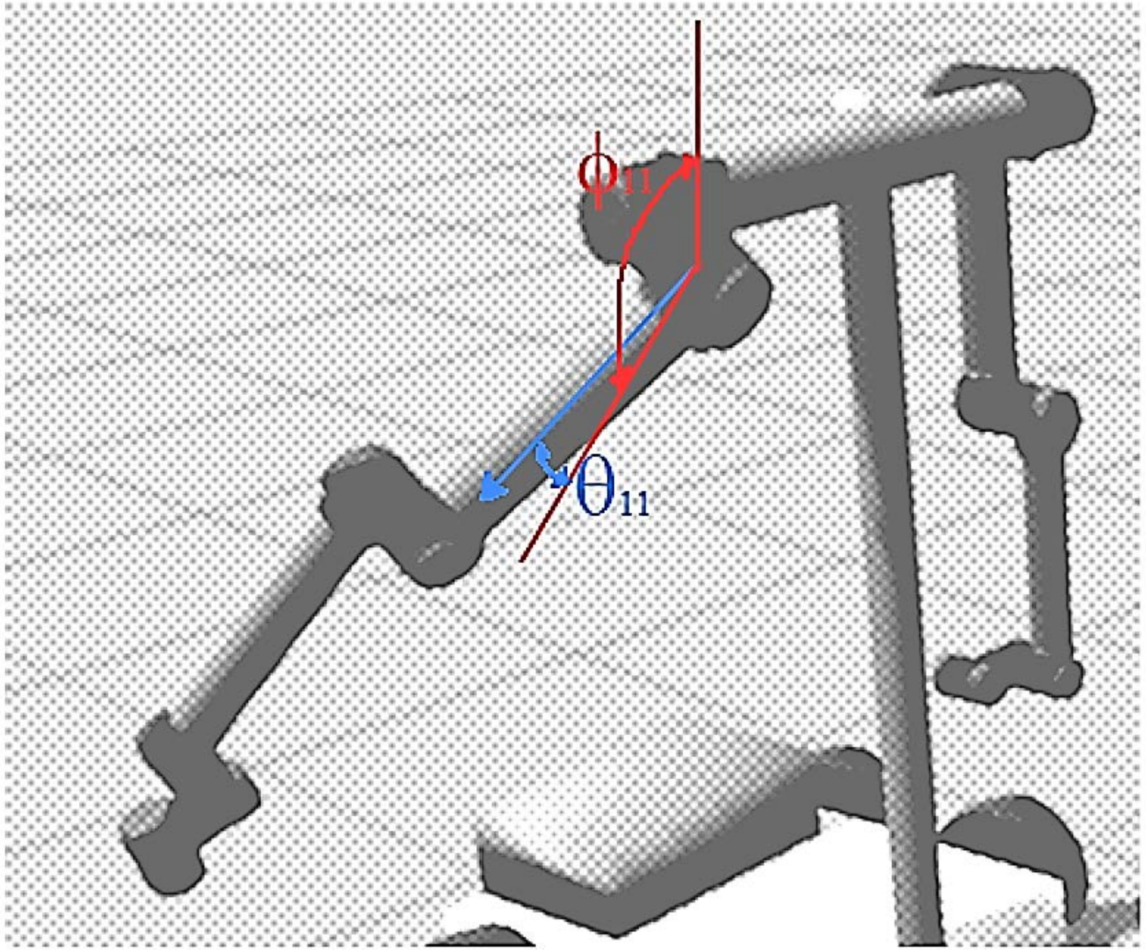

Which angels? Which height? How fast?

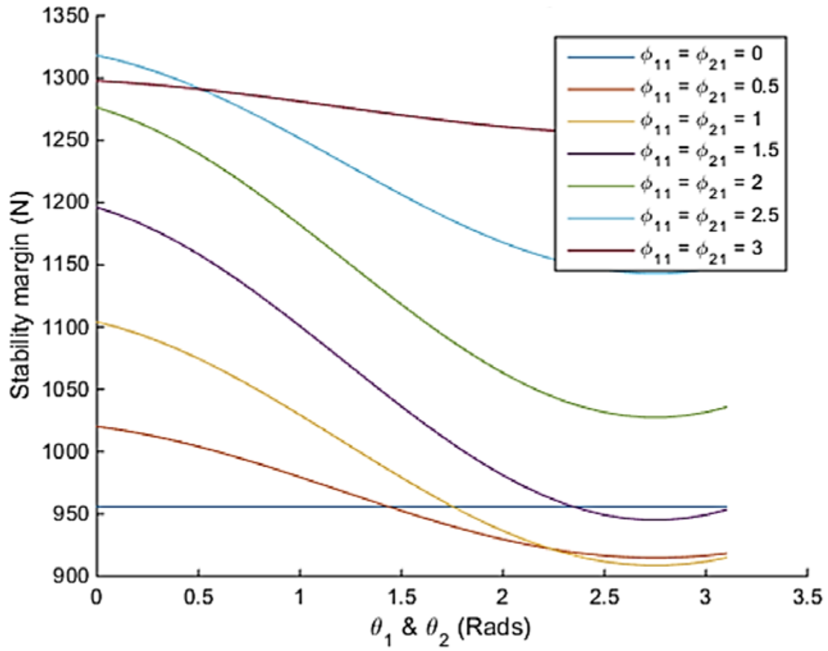

Effect of the first angles

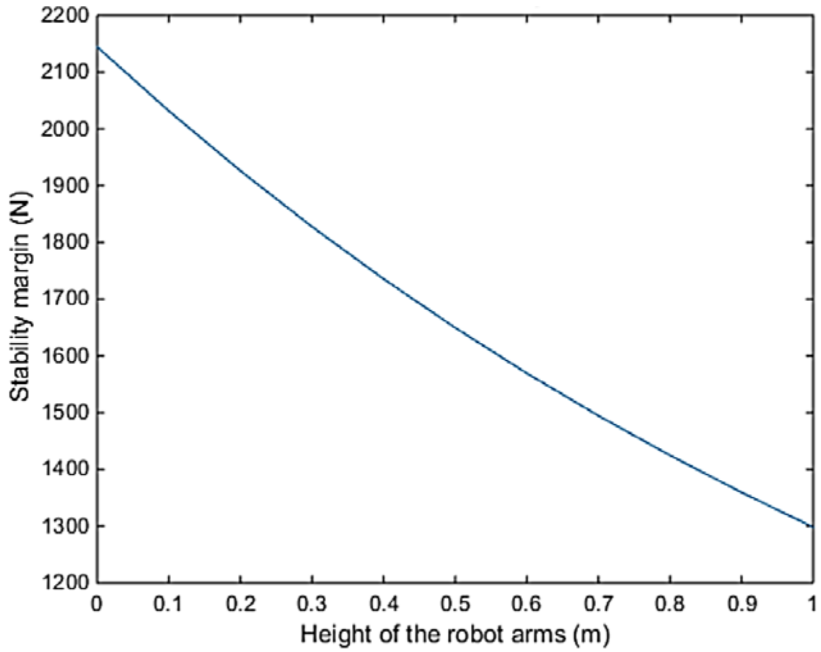

Effect of the arm's height

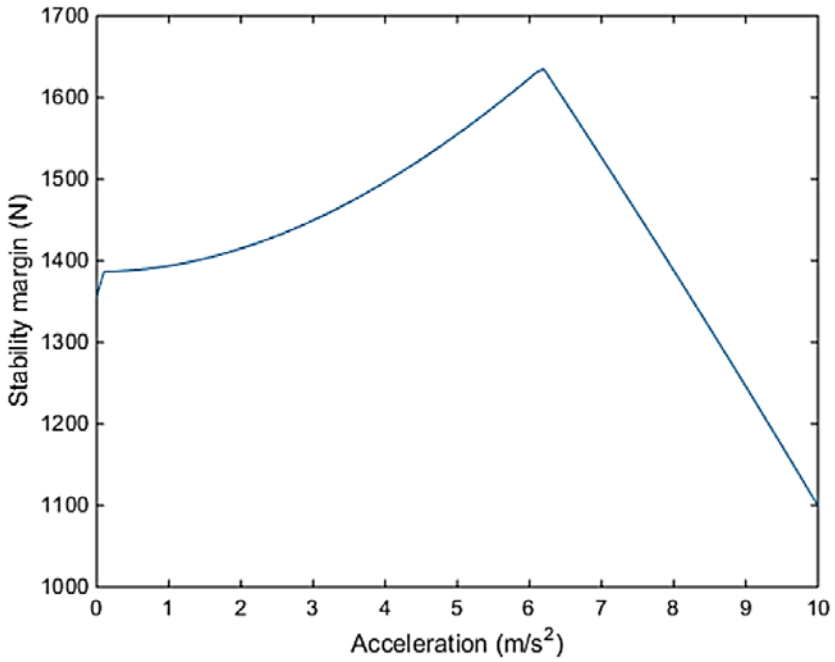

Effect of the arm's acceleration

Arms

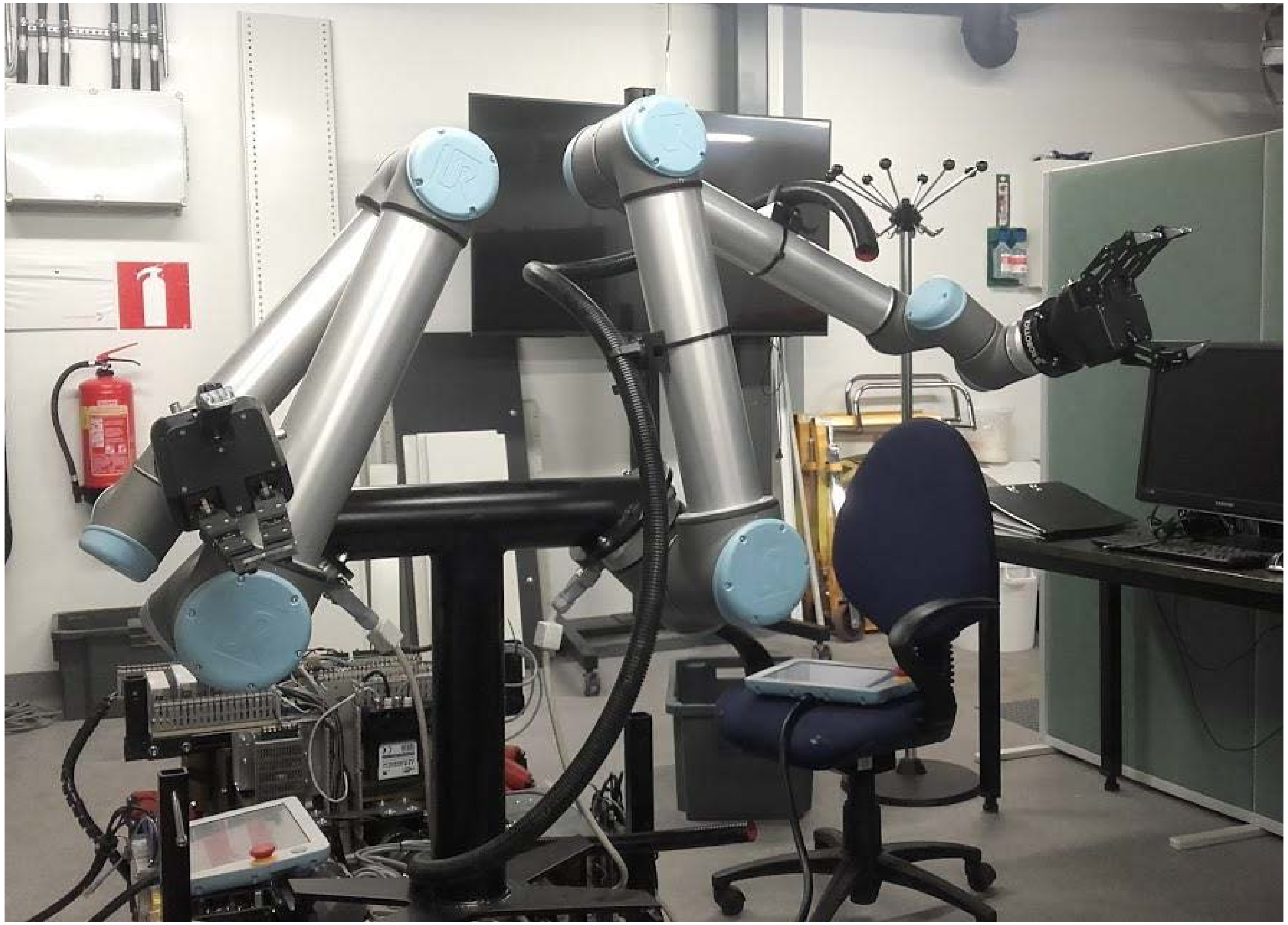

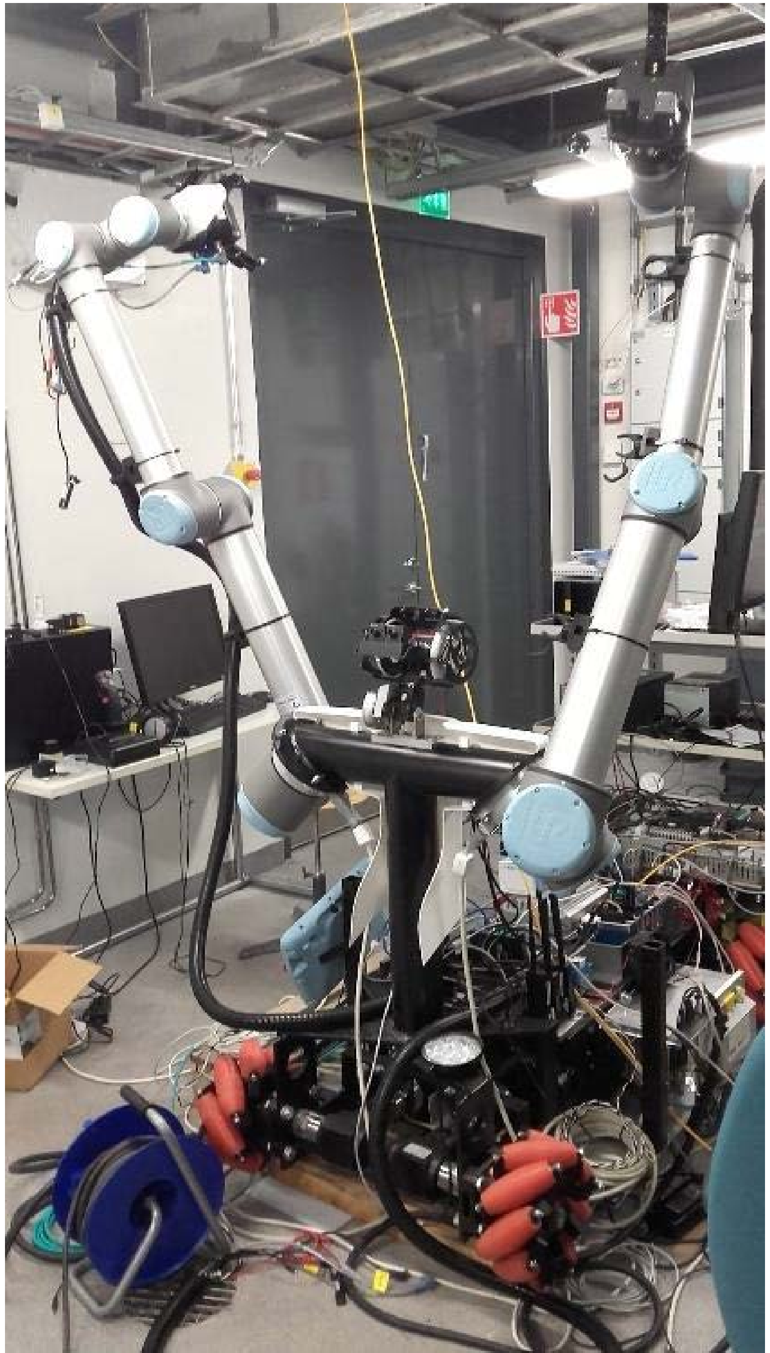

Arms

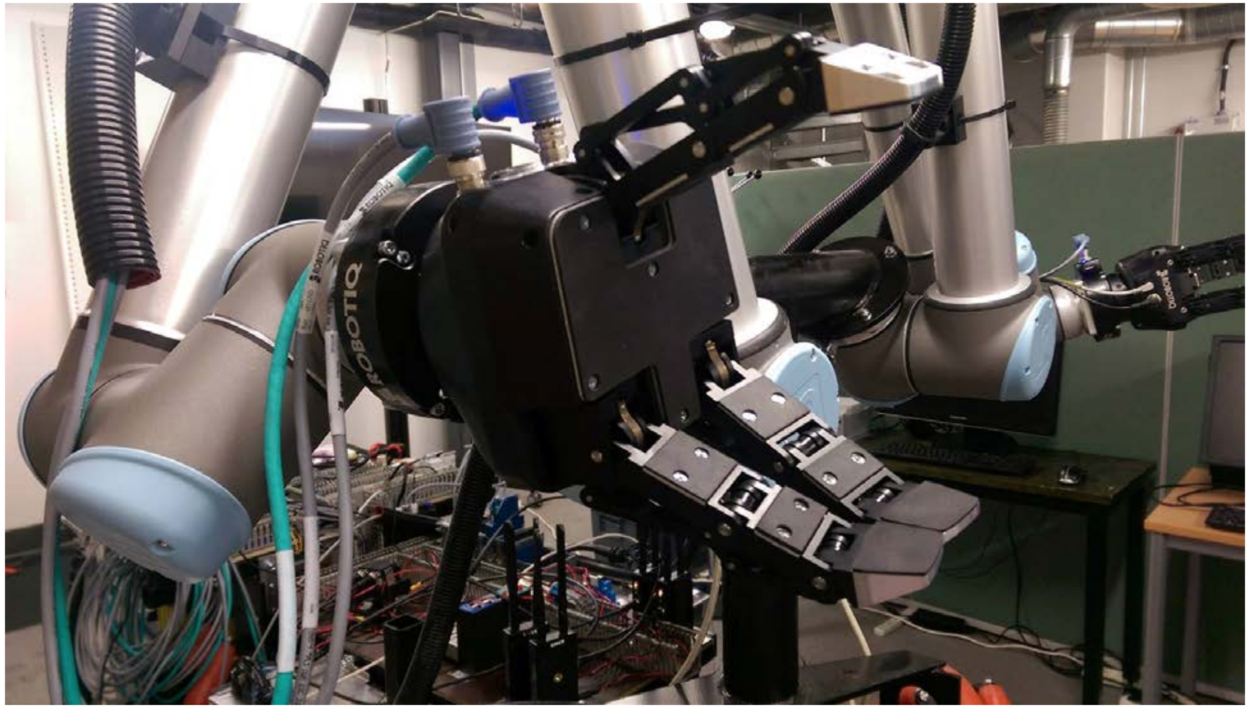

Arms Anti Collision System

COLLISION AWARE TELEOPERATION OF ROBOTIC ARM

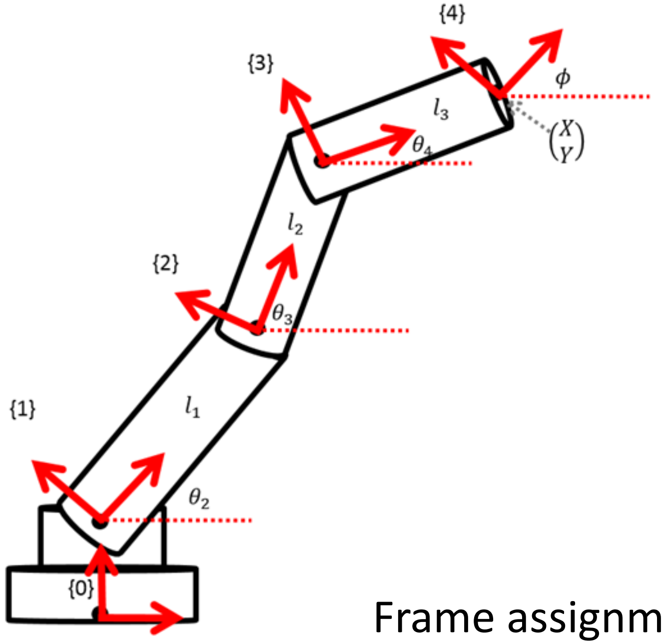

Frame assignment for UR10 based on D-H Convention

$$X = l_1 \cos\theta_2 + l_2 \cos(\theta_2 + \theta_3) + l_3 \cos(l_1 + l_2 + l_3)$$

$$Y = l_1 \sin\theta_{21} + l_2 \sin(\theta_2 + \theta_3) + l_3 \sin(\theta_2 + \theta_3 + \theta_4)$$

$$\phi = \theta_2 + \theta_3 + \theta_4$$

$$T_{AB} = \begin{bmatrix} R_{AB} & p_{AB} \\ 0_{1\times3} & 1 \end{bmatrix}$$

Planar serial link robotic arm with three revolute joints

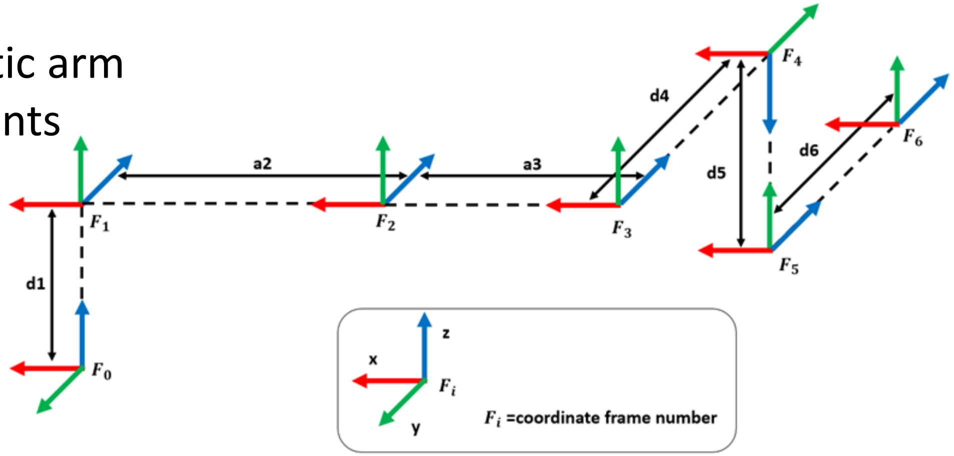

COLLISION AWARE TELEOPERATION OF ROBOTIC ARM

Transformation	Link length (a_i)	Link twist (α_i)	Joint offset (d_i)	Joint angle (θ_i)	offset
T_{01}	0	π/2	0.1273	q1	0
T_{12}	-6.12	0	0	q2	-π/2
T_{23}	-5723	0	0	q3	0
T_{34}	0	π/2	0.163941	q4	-π/2
T_{45}	0	-π/2	0.1157	q5	0
T_{56}	0	0	0.0922	q6	0

$$T_{06} = T_{01} \times T_{12} \times T_{23} \times T_{34} \times T_{45} \times T_{56}$$

$$T_{i,i-1} = \begin{bmatrix} \cos\theta_i & -\cos\alpha_i \sin\theta_i & \sin\alpha_i \sin\theta_i & a_i \cos\theta_i \\ \cos\theta_i & \cos\alpha_i \cos\theta_i & -\sin\theta_i \cos\theta_i & a_i \sin\theta_i \\ 0 & \sin\alpha_i & \cos\alpha_i & d_i \\ 0 & 0 & 0 & 1 \end{bmatrix}$$

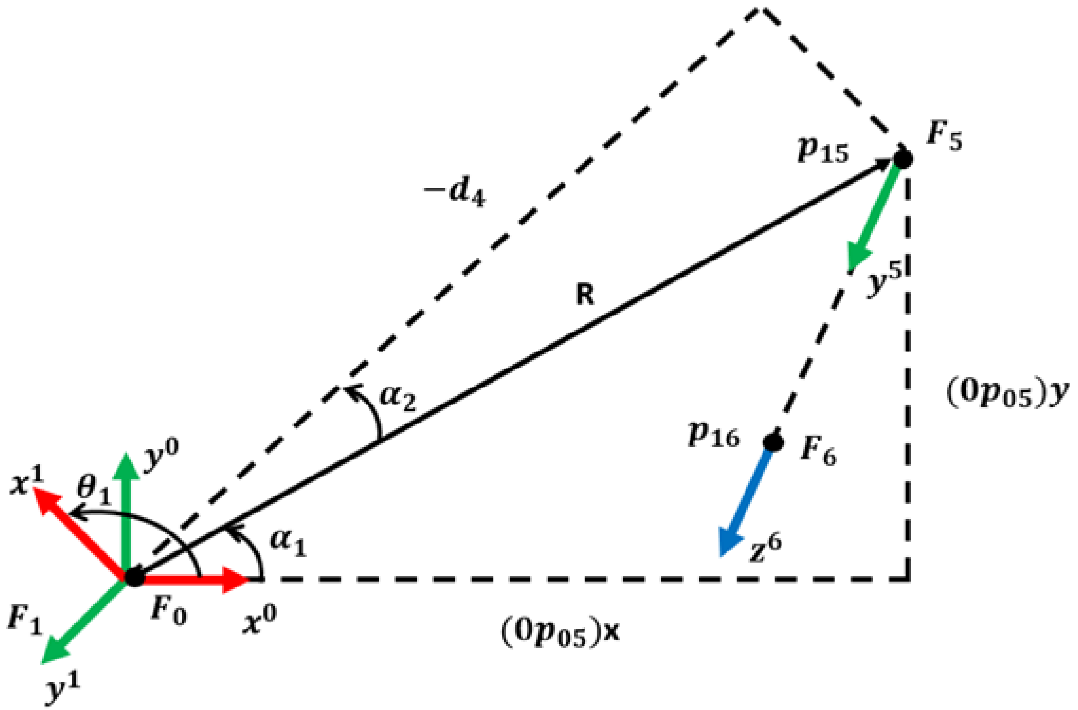

Overhead head view of UR10 in X-Y plane for finding theta θ_1

$$\theta_1 = \text{atan2}((0p_{05})y, (0p_{05})x) \pm \cos^{-1}\frac{d_4}{R} + {}^{\pi}/_{2}$$

COLLISION AWARE TELEOPERATION OF ROBOTIC ARM

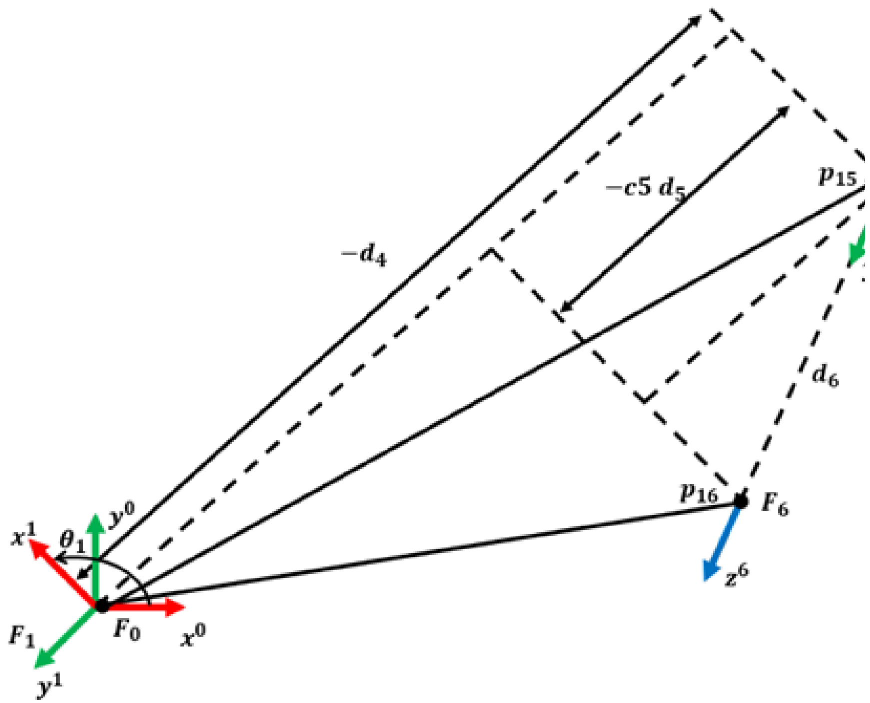

Overhead head view of UR10 in X-Y plane for finding theta θ_5

$$\theta_5 = \pm \cos^{-1} \frac{p_x s_1 - p_y C_1 - d_4}{d_6}$$

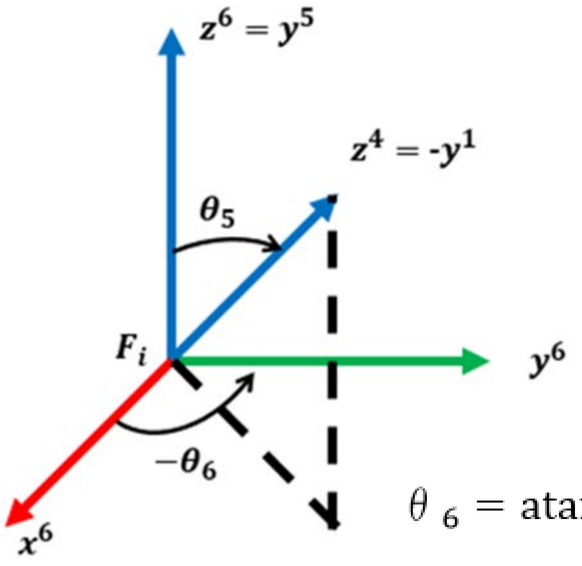

$$\theta_6 = \operatorname{atan2}\left(\frac{-y_x s_1 + y_y c_1}{s_5}, \quad \frac{-(-x_x s_1 + x_y c_1)}{s_5}\right)$$

Overhead head view of UR10.

$$\theta_3 = \operatorname{atan2}(\sin\theta_3, \cos\theta_3)$$

$$\theta_2 = \operatorname{atan2}((k_1 Y_n - k_2 Y_n), (k_1 X_n - k_2 X_n))$$

$$\theta_4 = \phi - (\theta_2 + \theta_3)$$

Where, $k_1 = l_1 + l_2 \cos\theta_3$, $k_2 = l_2 \sin\theta_3$,

$$\cos\theta_3 = \frac{(X^2 + Y^2 - l_1^2 + l_2^2)}{2 l_1 l_2}, \ \sin\theta_3 = \sqrt{\pm(1 - \cos^2\theta_3)},$$

$$X_n = X - l_3 \cos\phi \text{ and } Y_n = Y - l_3 \sin\phi$$

Workspace of dual UR10 with fixed torso

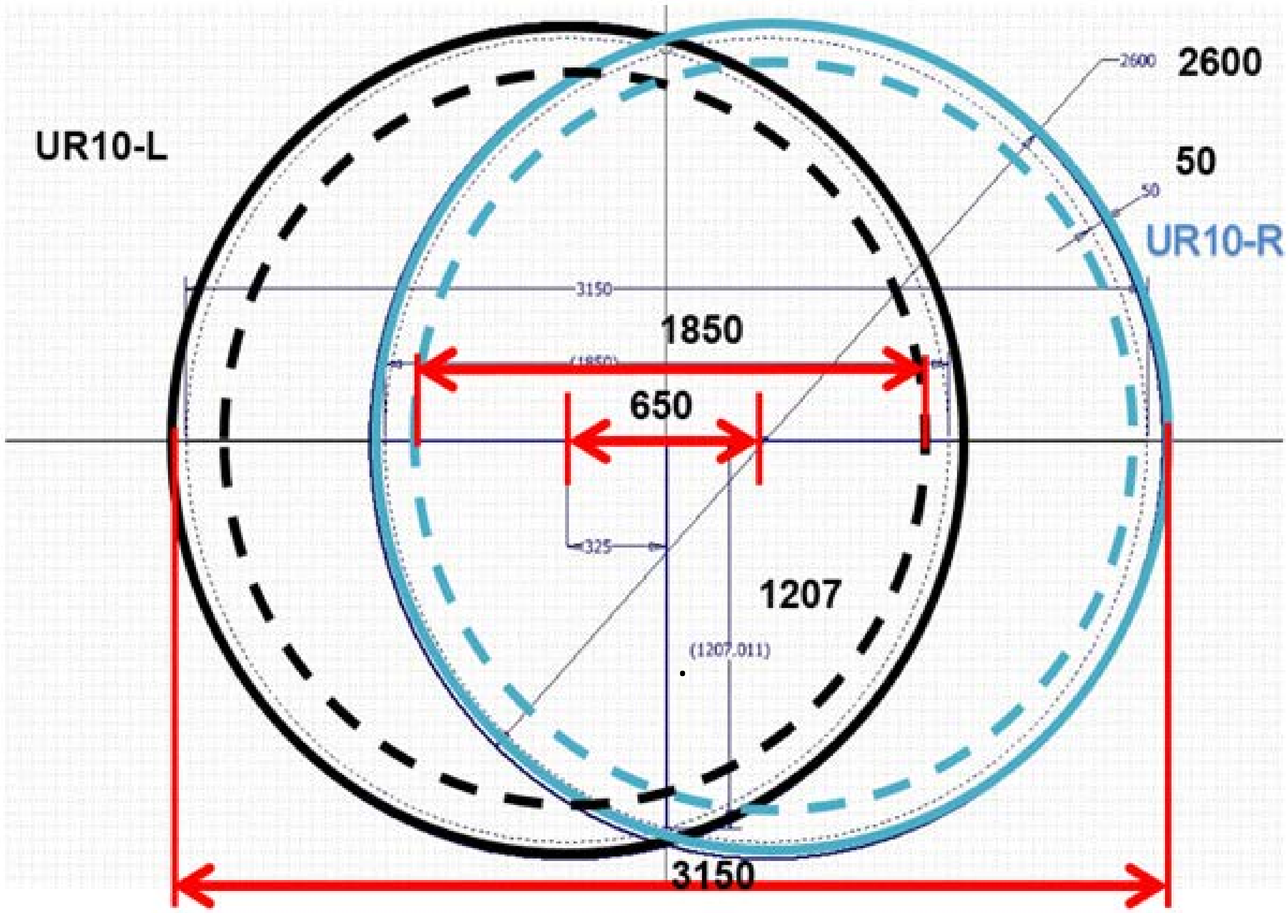

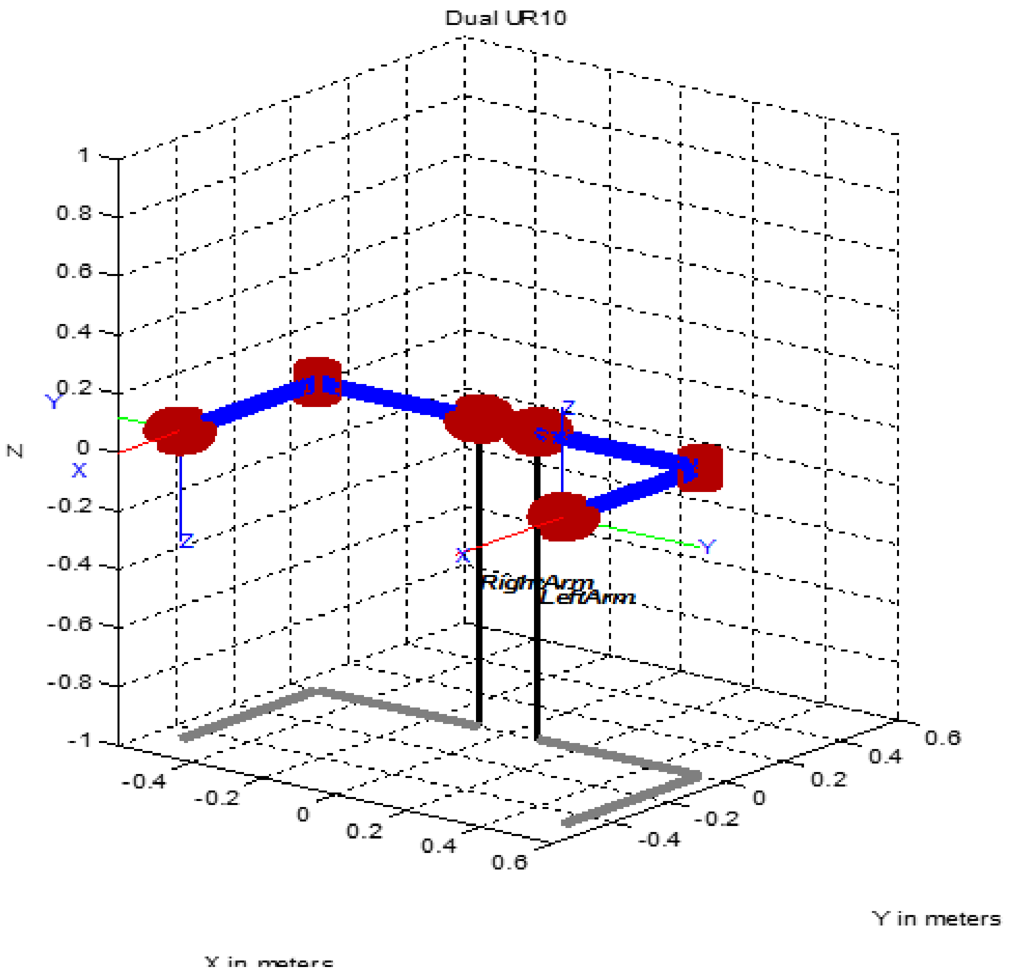

ANFIS procedure and model

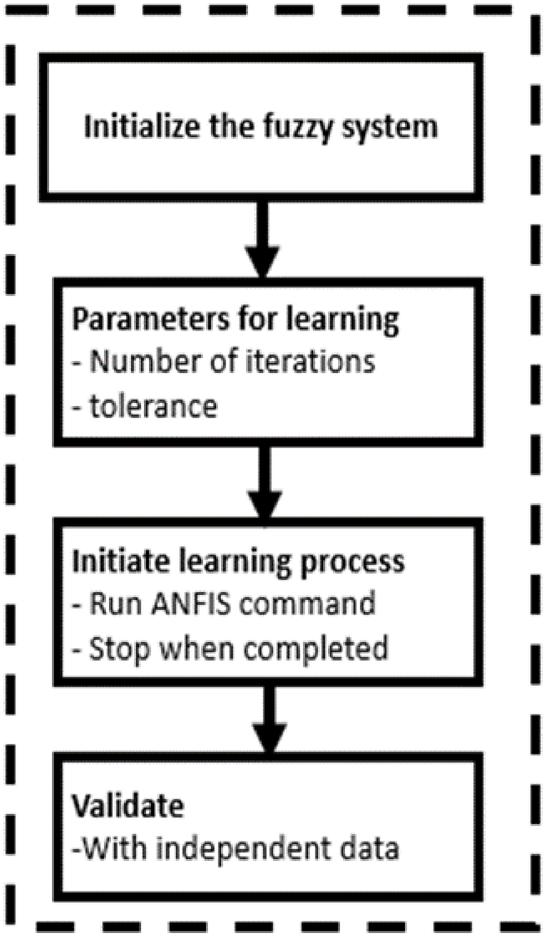

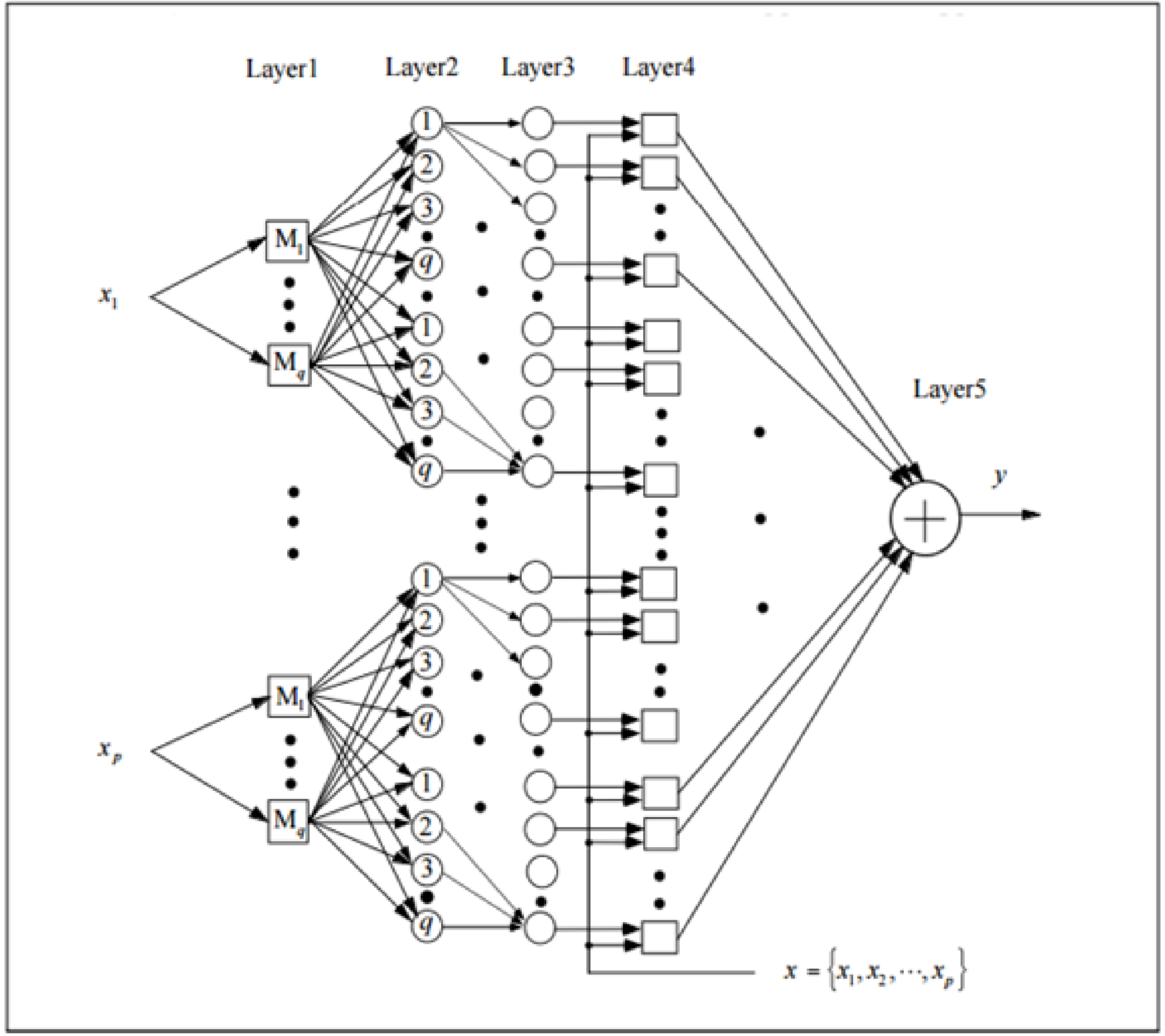

Reachable workspace of UR10

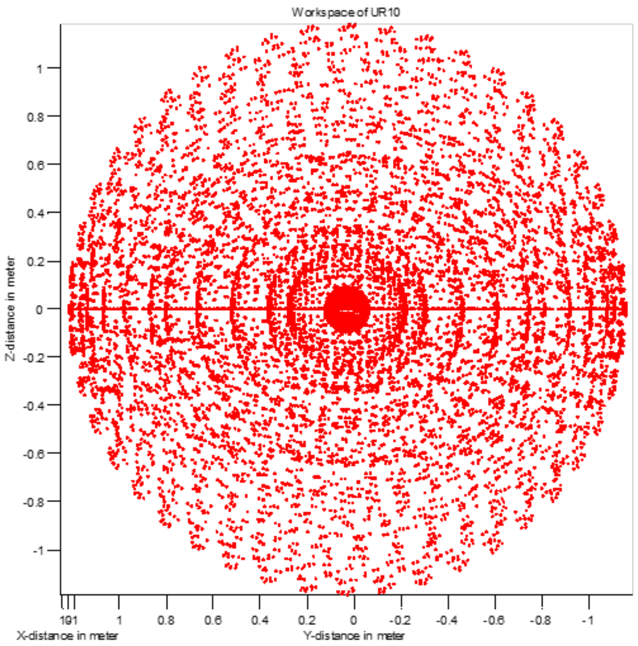

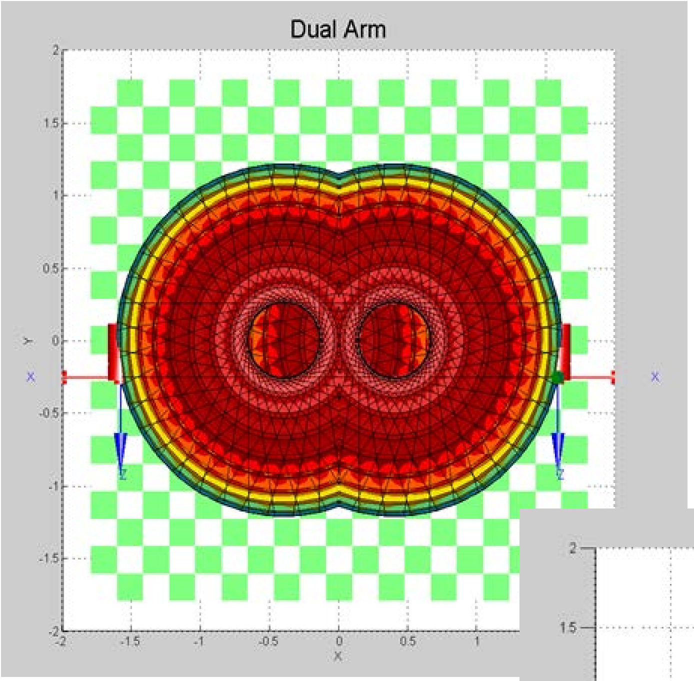

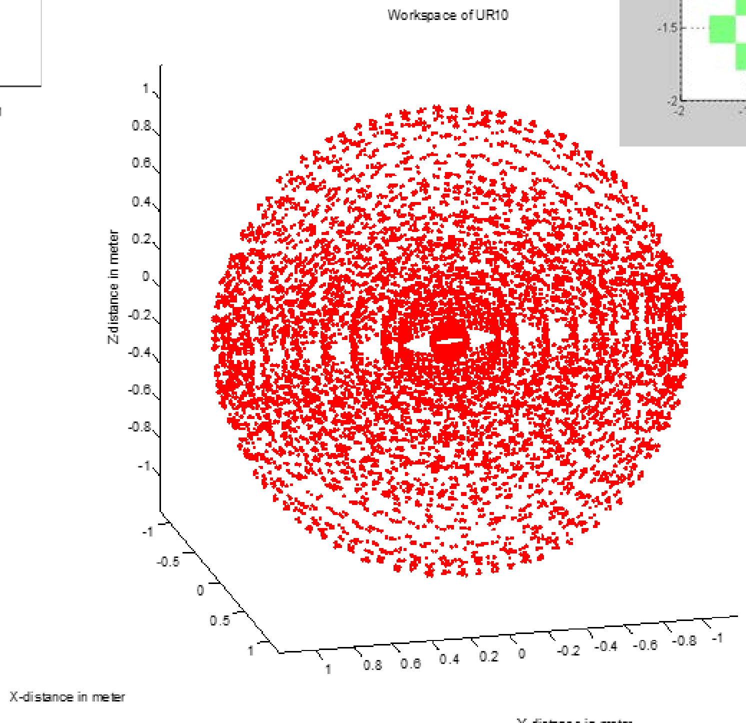

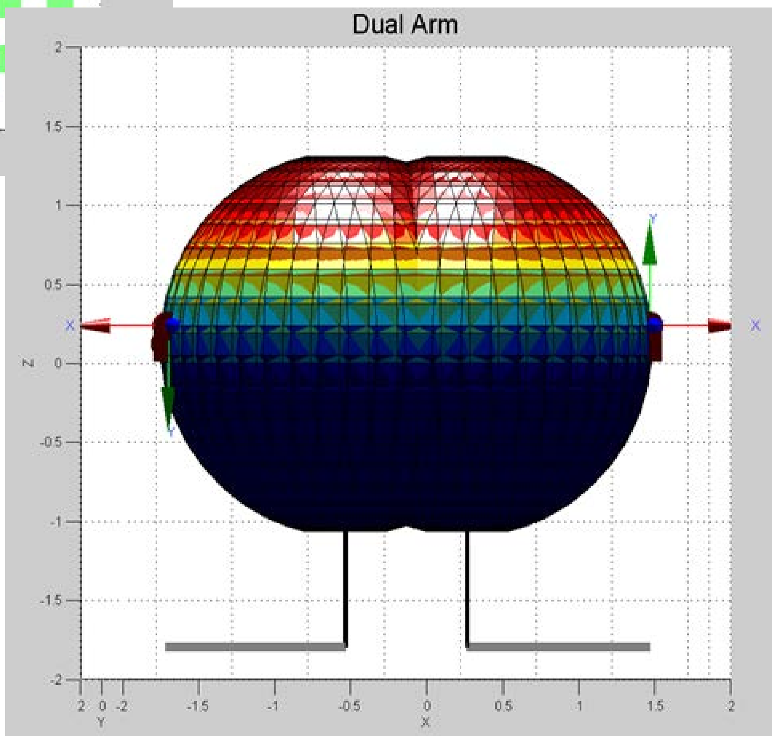

Reachable workspace of Geomagic Touch

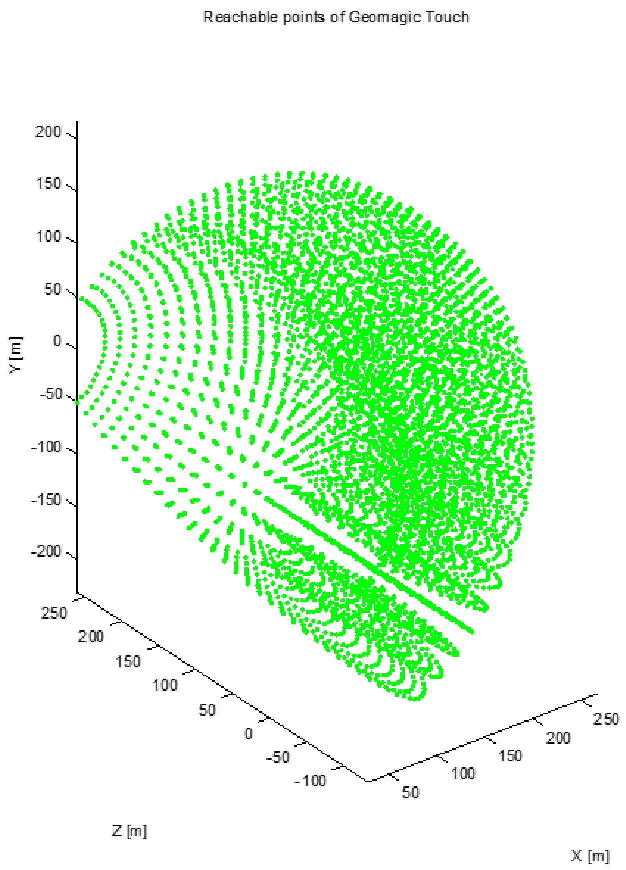

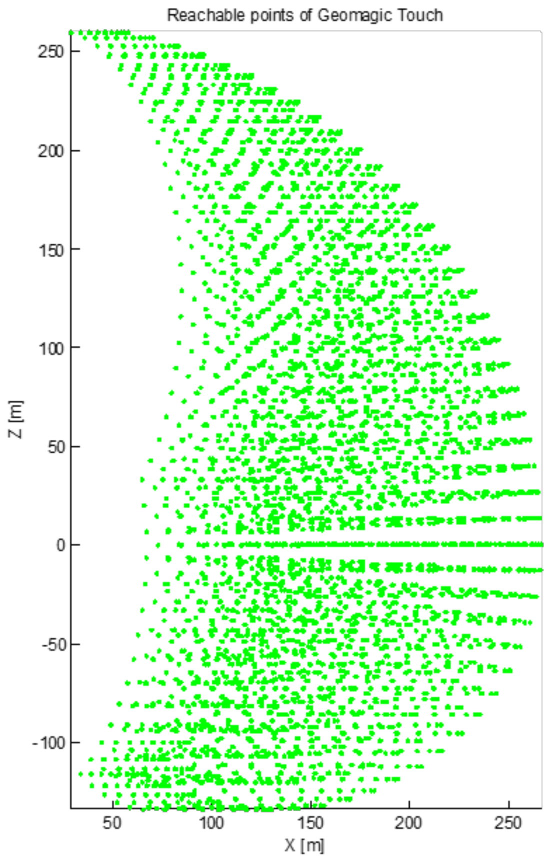

Reachable workspace of Geomagic Touch

Geomagic touch haptic device

Reachable workspace of Geomagic Touch

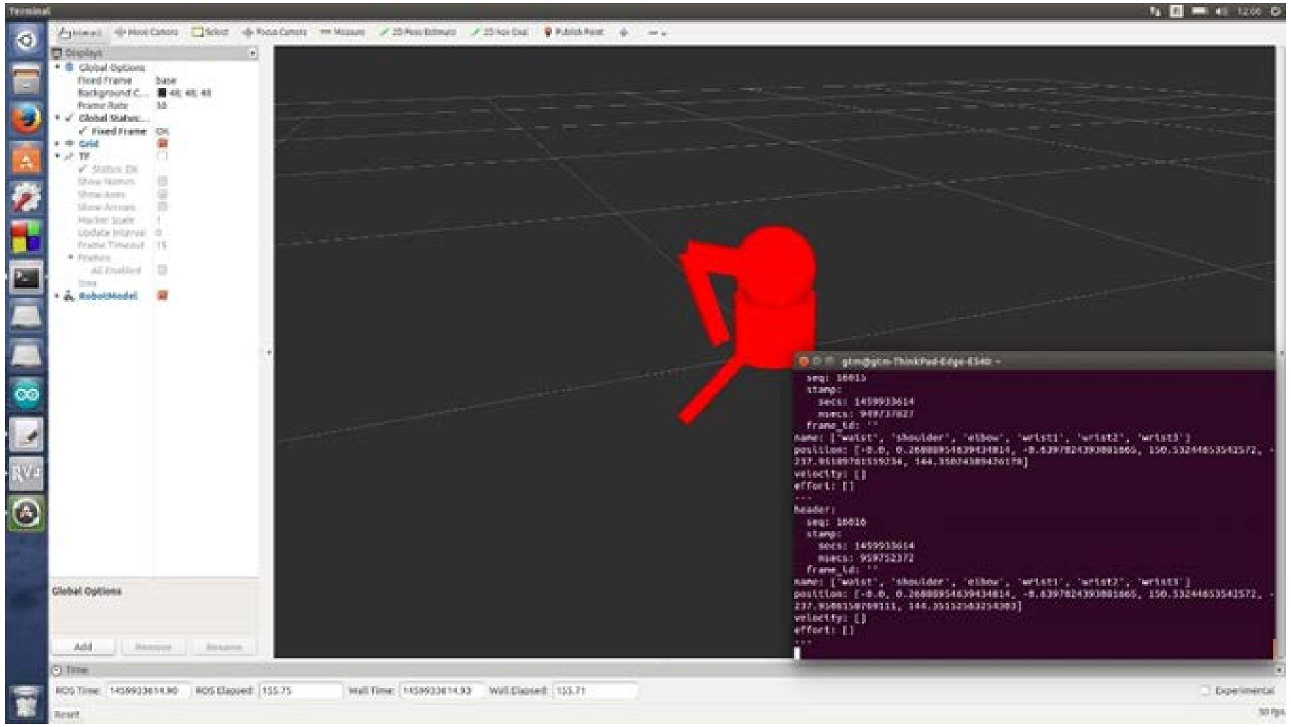

Geomagic touch haptic device

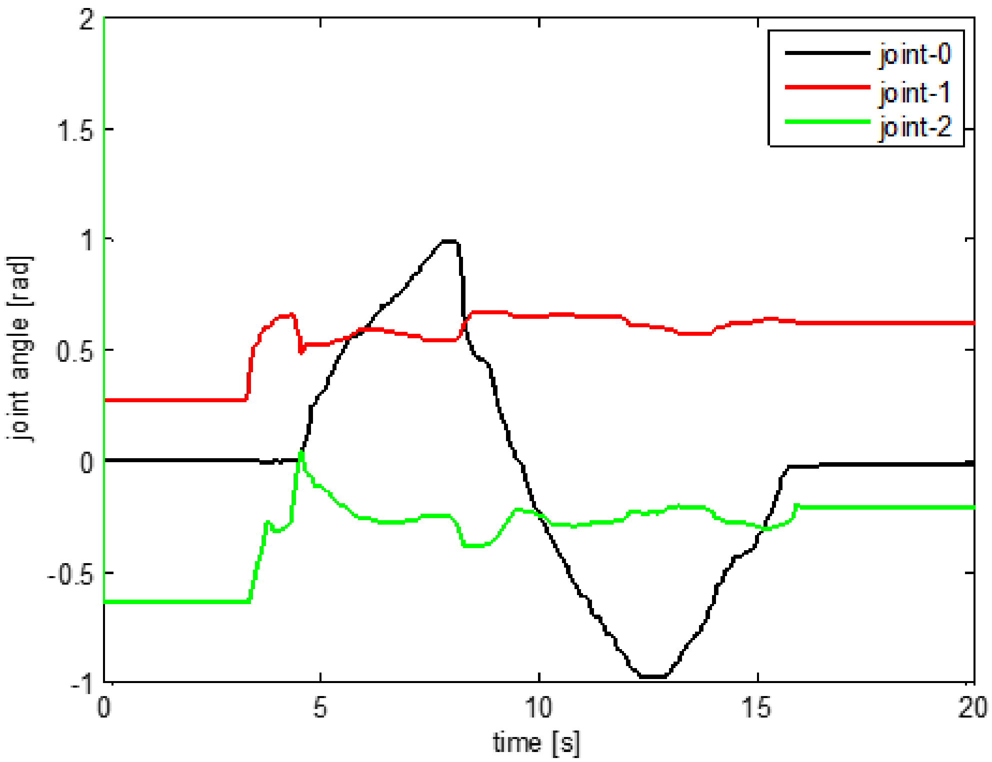

Joint values from Geomagic touch device.

Robot model for collision detection using joint torque or motor current

$$M(q)\ddot{q} + C(q,\dot{q})\dot{q} + g(q) = \tau + \tau_K = \tau_{tot}$$

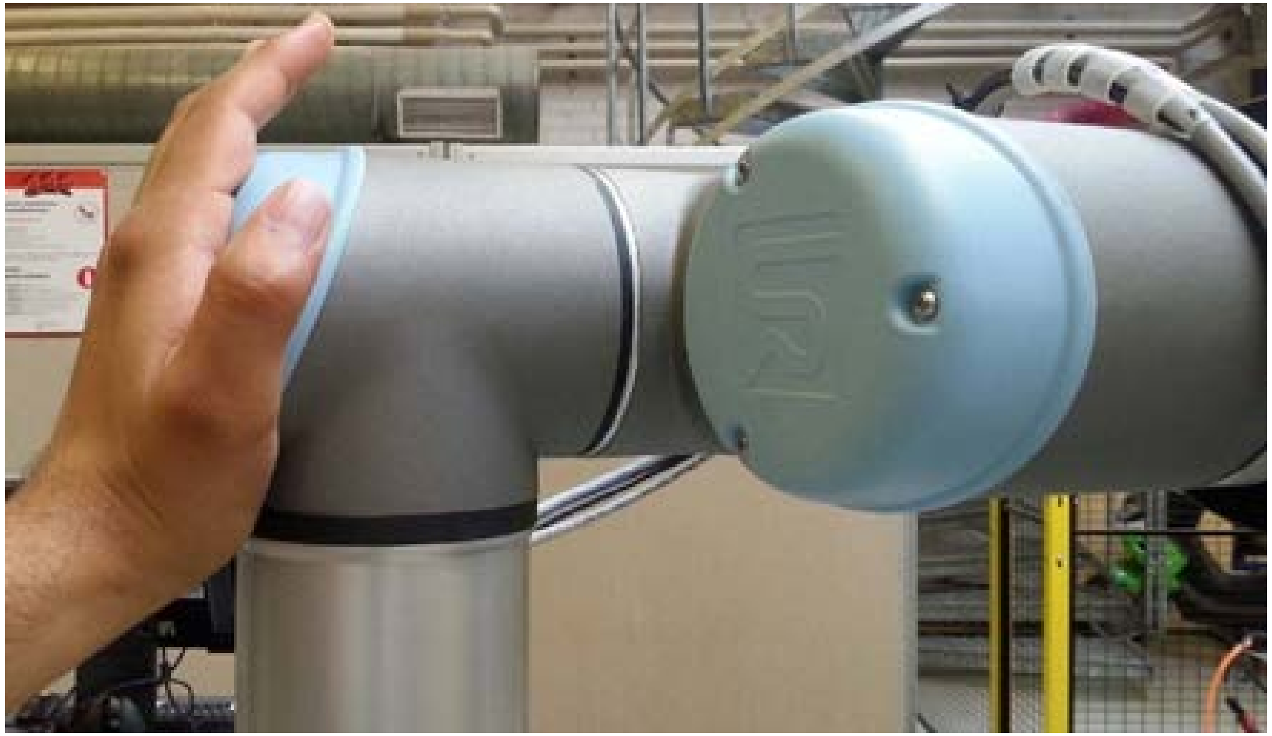

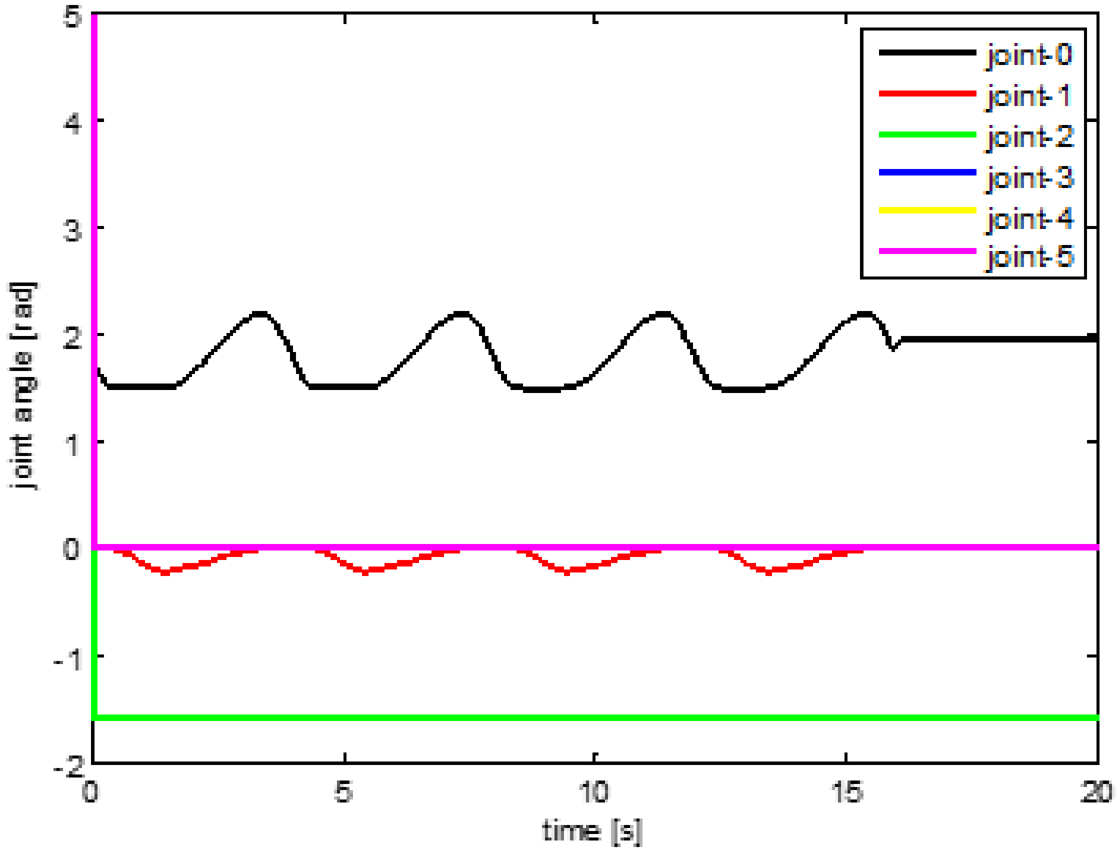

Robot in collision (a) and joint angle (b)

Collision detection in neighboring link

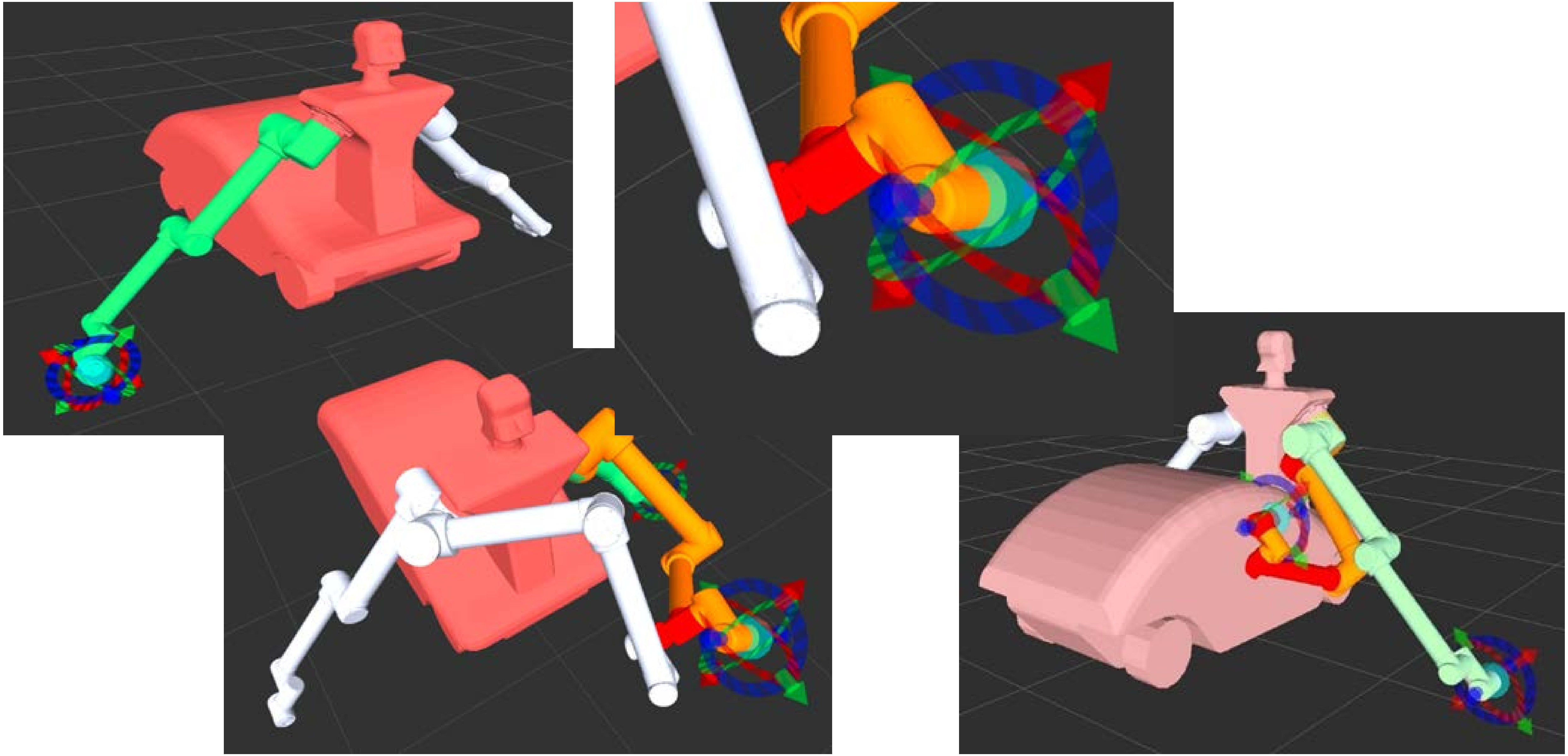

Grippers

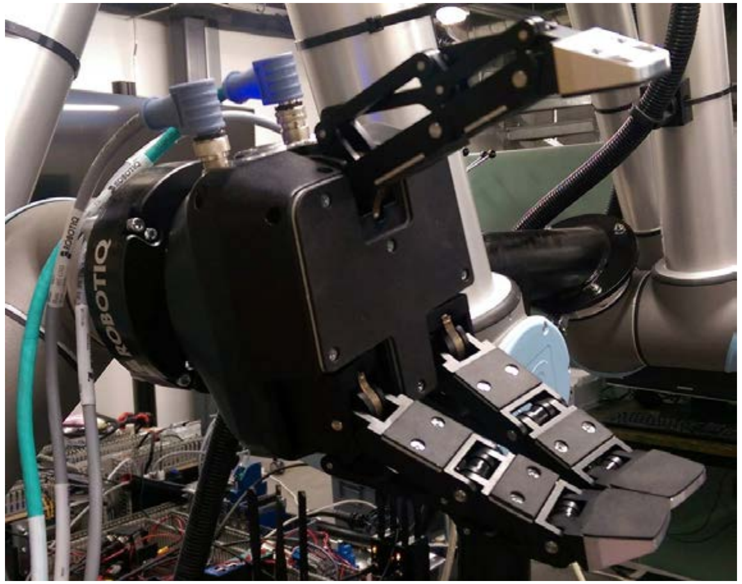

BASIC MODE

WIDE MODE

ENCOMPASSING GRIP

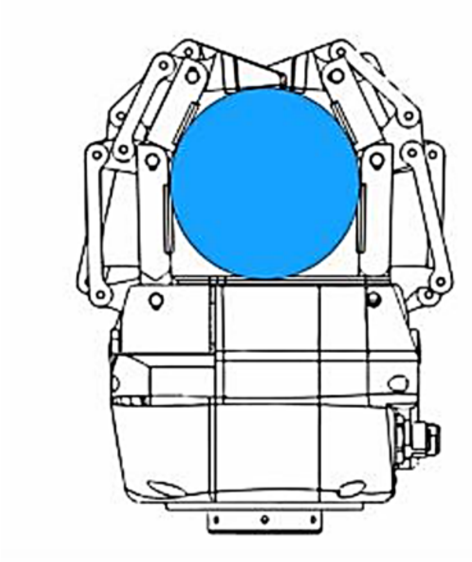

PINCH MODE

SCISSOR MODE

FINGERTIP GRIP

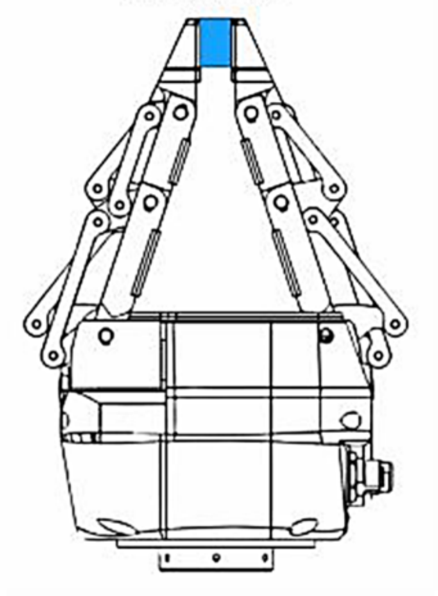

COLLISION AVOIDANCE IN END-EFFECTOR

Grasping

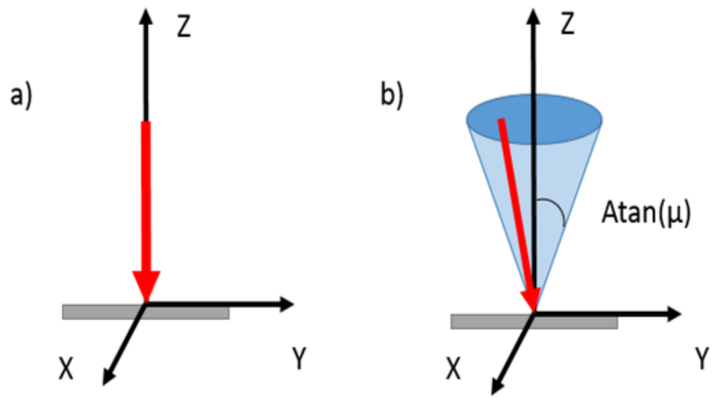

Contact model: point contact without friction (left) and point contact with friction.

Robotiq 3-finger adaptive gripper with three different grab modes

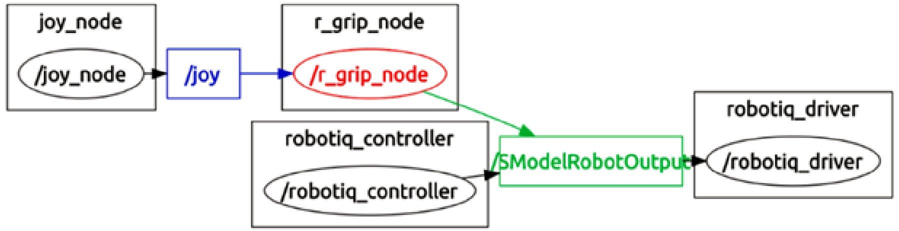

Active nodes for teleoperation of gripper using joystick.

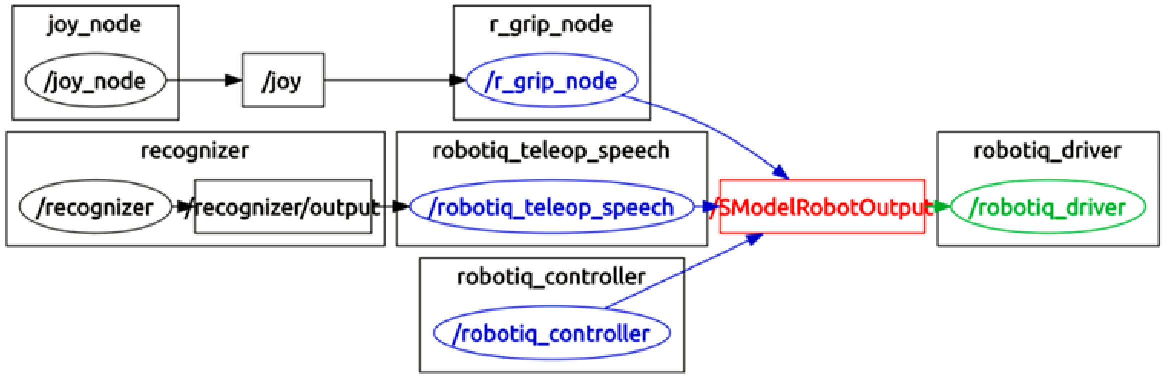

Active nodes for teleoperation of gripper

COLLISION AVOIDANCE IN END-EFFECTOR

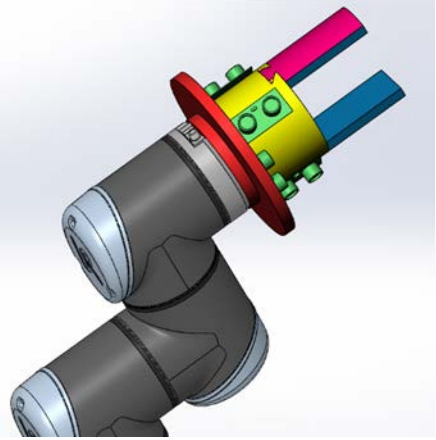

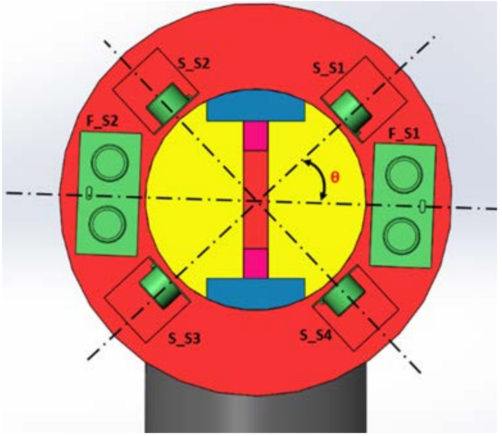

Sonar Sensor array on end-effector.

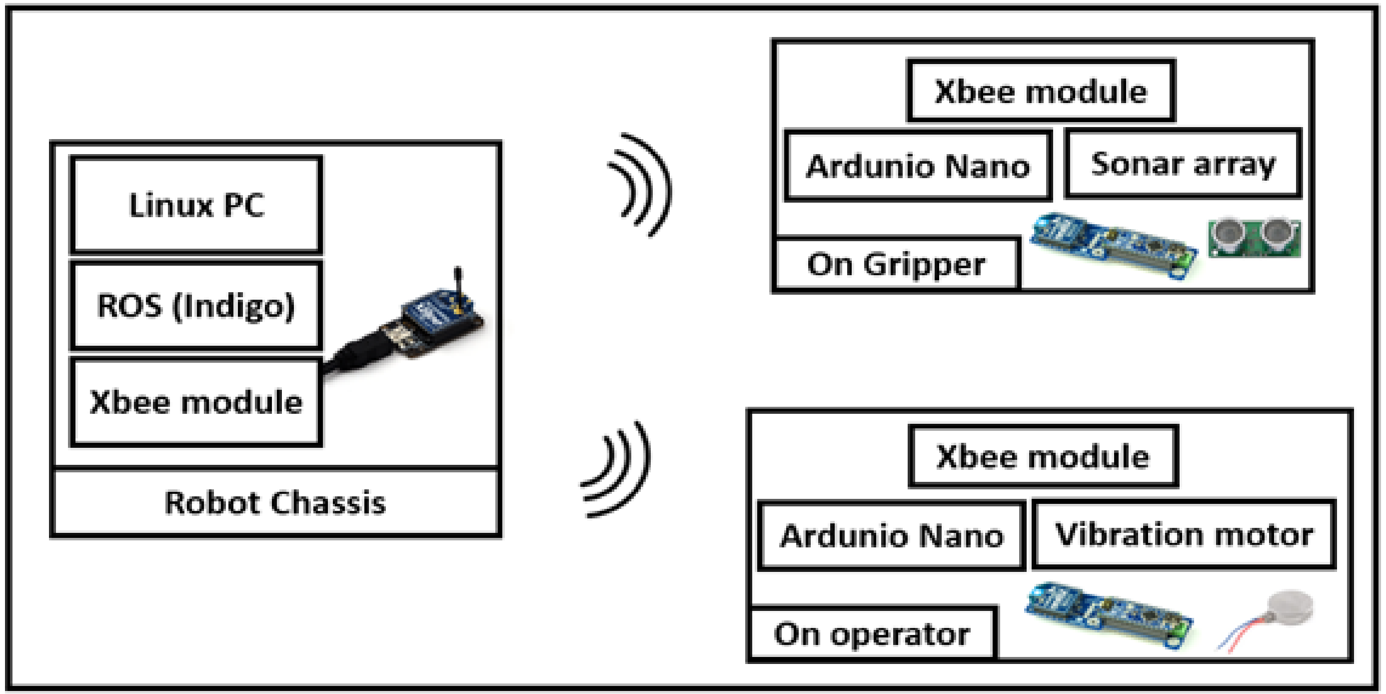

Hardware for haptic wrist band.

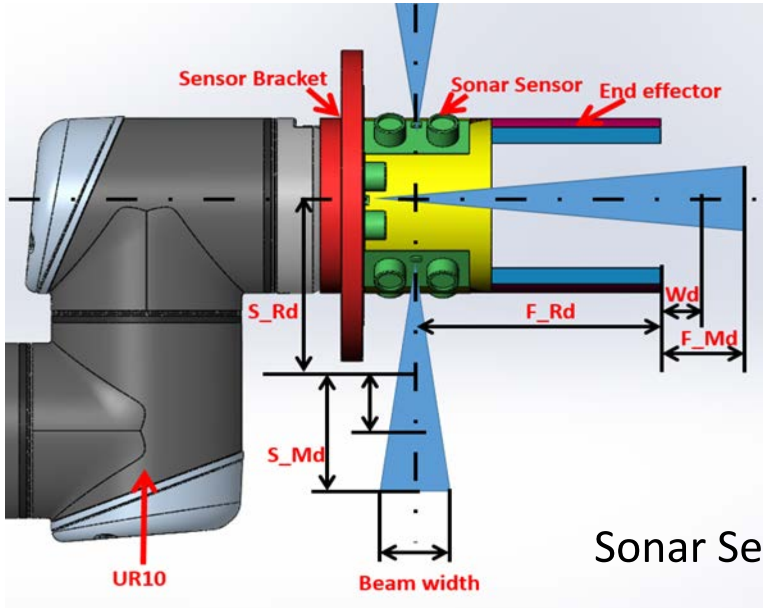

Sonar Sensor array

Robot grippers' layout.

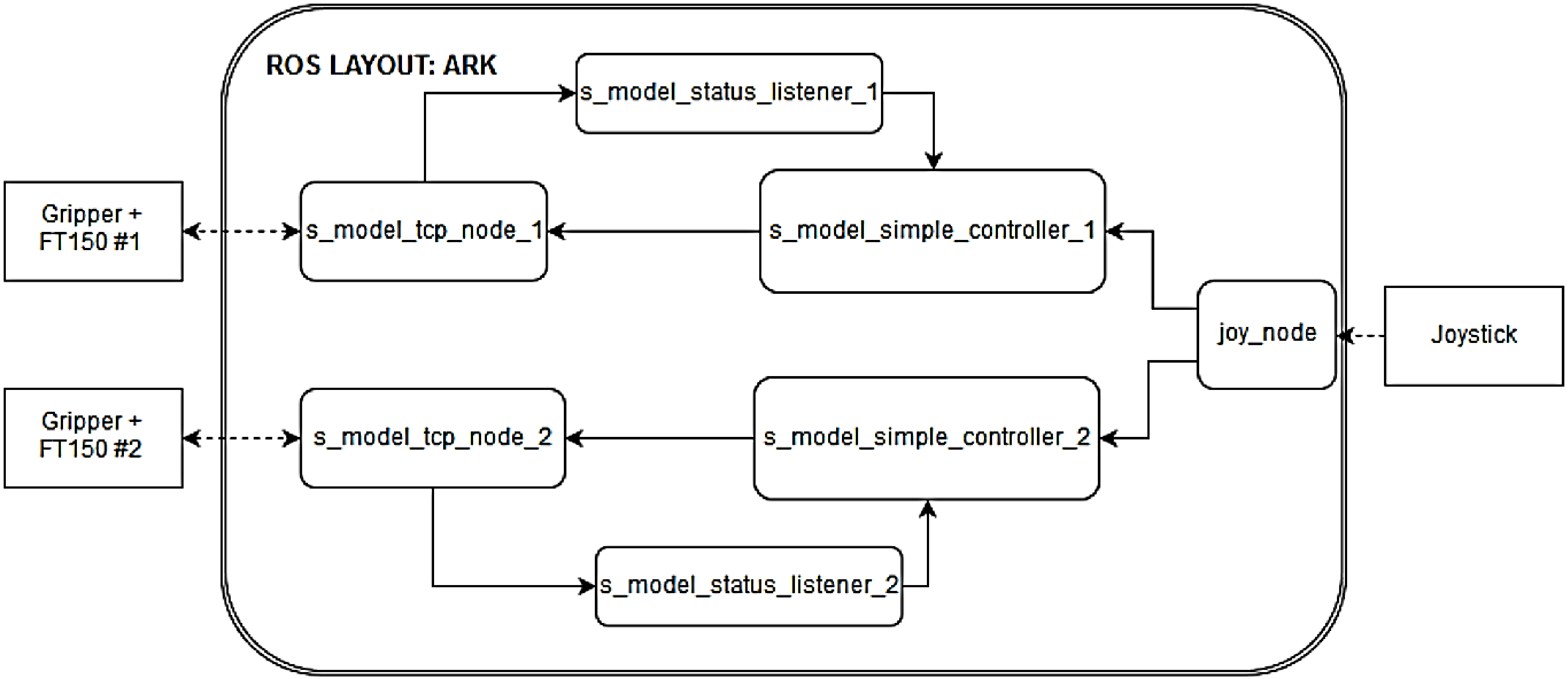

Collision detection in end-effector.

Condition	Nature of alert	Action for arm controller	remarks
Distance > set-point	No action	No action	No obstacles
Distance < set-point1 (<20->10)	Enable vibration motor (corresponding to sonar sensor) for 0.25s in every 1 second interval as long the condition is true.	No action	Obstacles are present. Move arm with caution.
Distance < set-point2 (<10)	Enable vibration motor (corresponding to sonar sensor) as long the condition is true	Pause motion of robot for 1 second.	When the controller resume after delayed time. Move robot opposite to the direction of collision.

Alert type

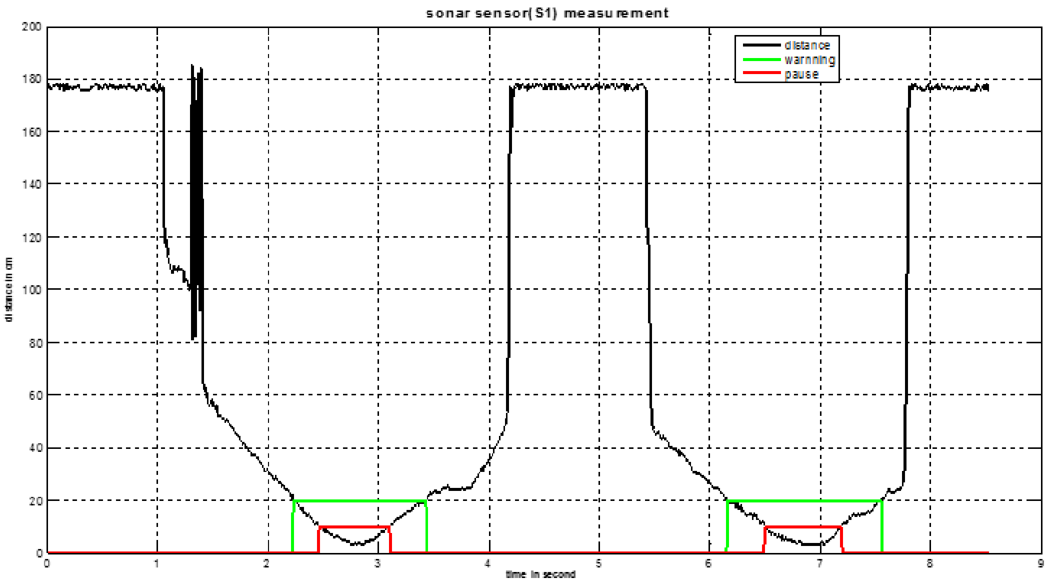

Distance measurement from the S_S1 sensor and collision detection

Main Control System

Control and Communication

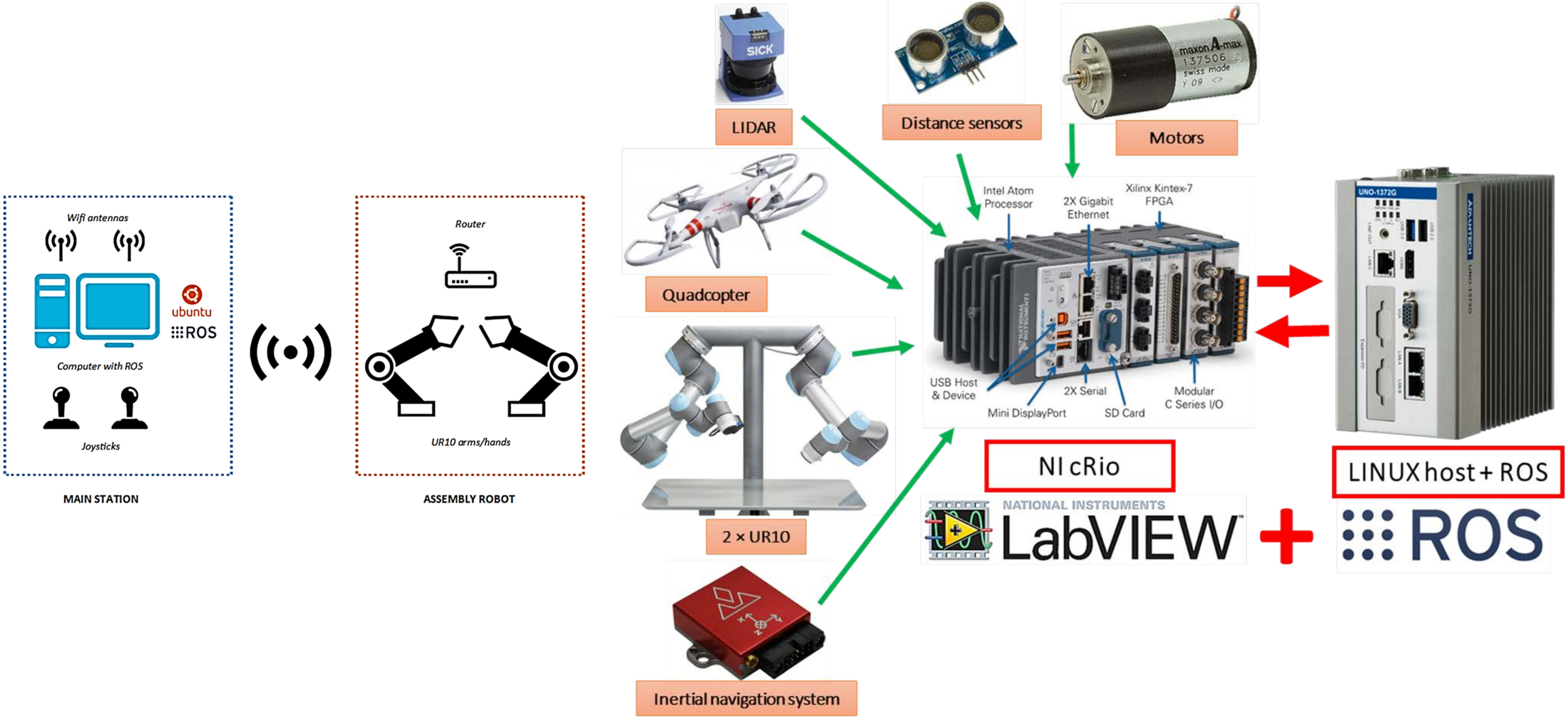

ROS

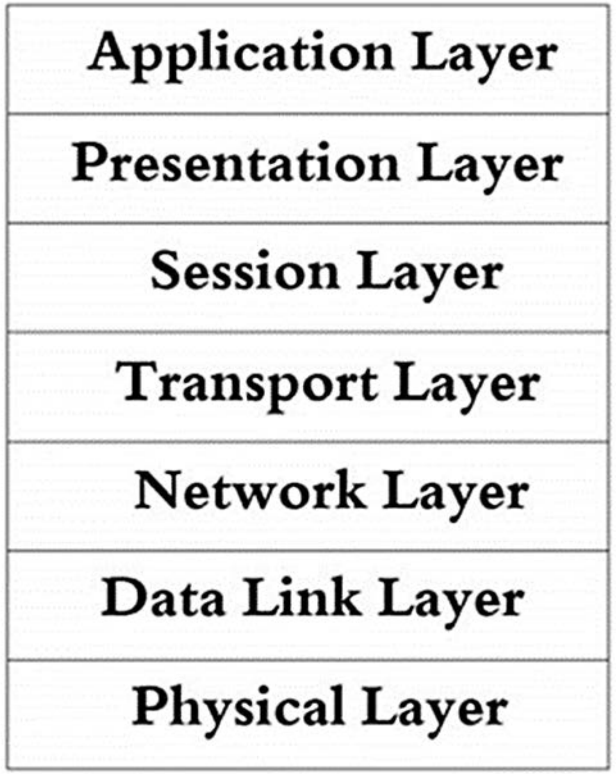

Seven layers of the ISO OSI model

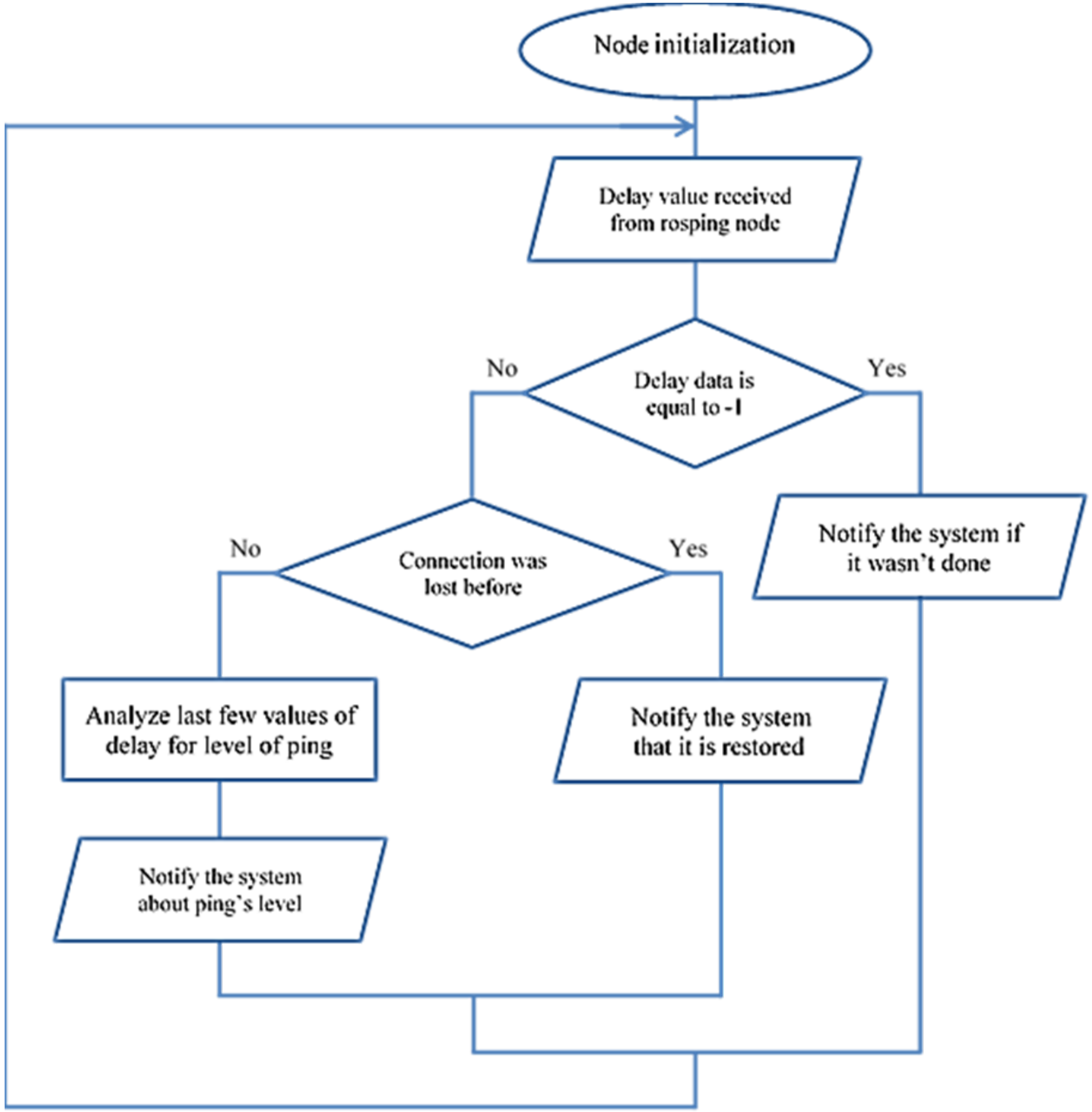

Simplified block diagram of connection state analysis algorithm

ROS Control for Arms

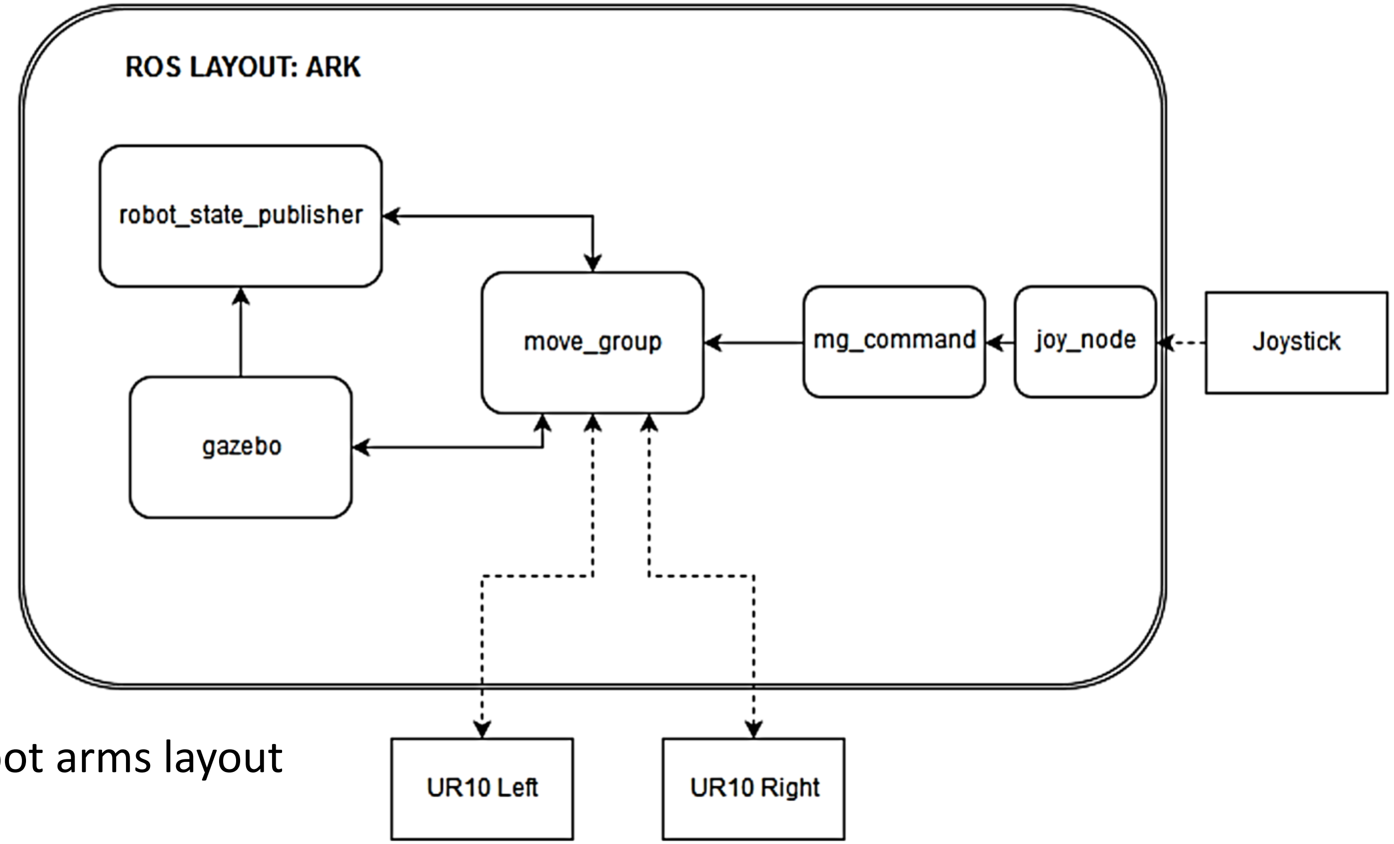

Robot arms layout

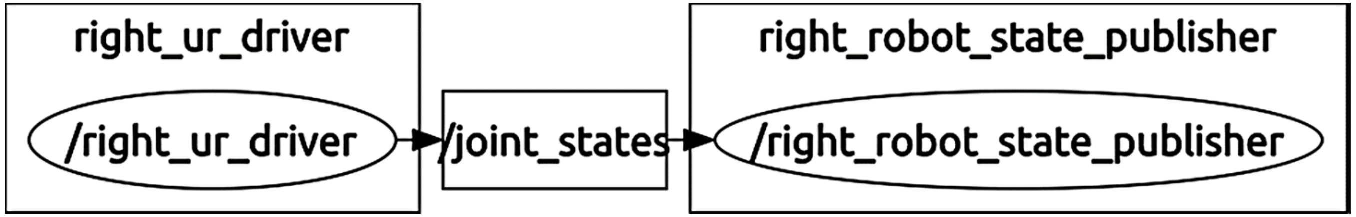

Rqt_graph of the right arm.

Graphic representation of the robot's URDF file.

ROS concept for Image transffer

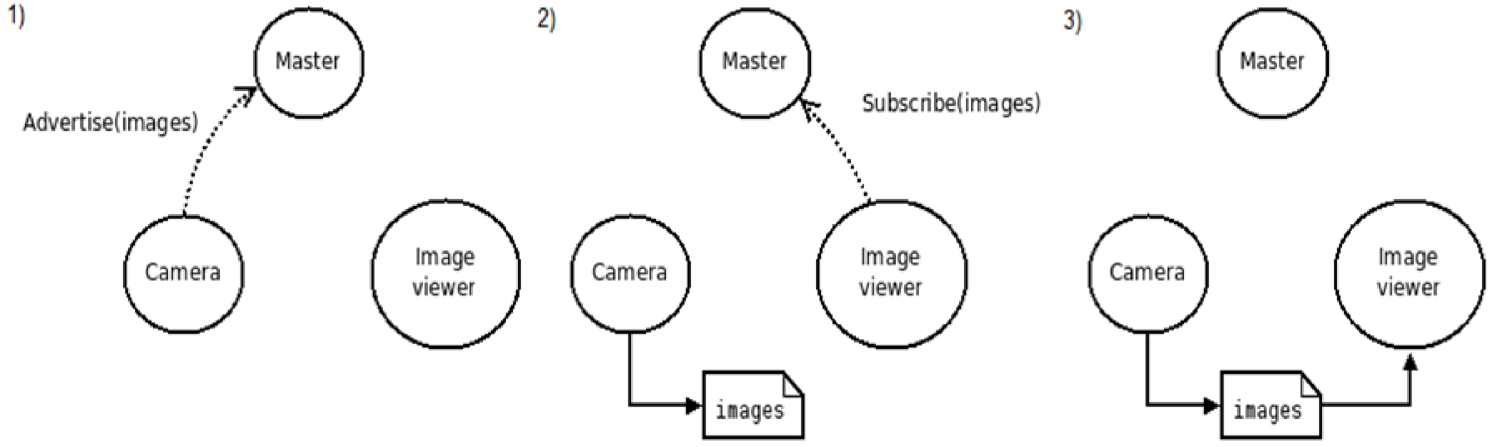

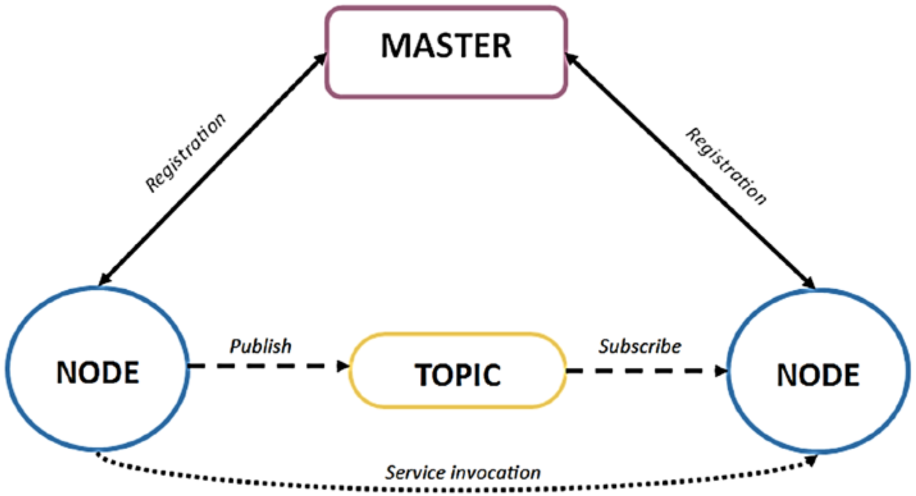

Steps of establishing peer-to-peer communication over a topic between two nodes

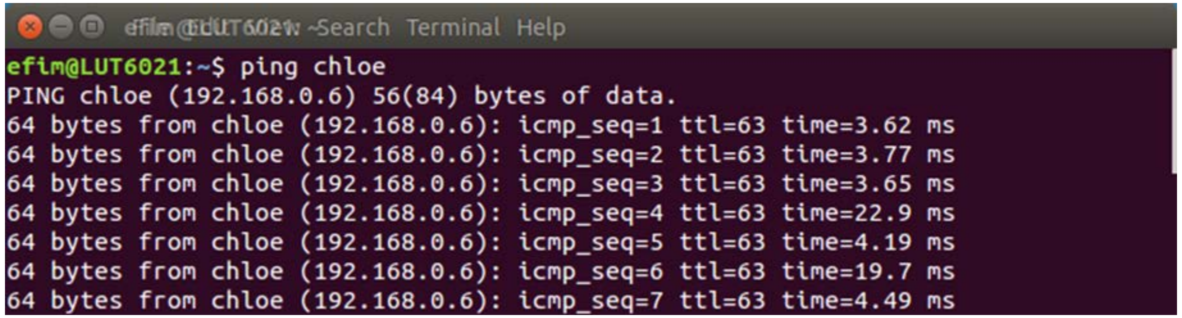

Simple test with Connectivity with ping

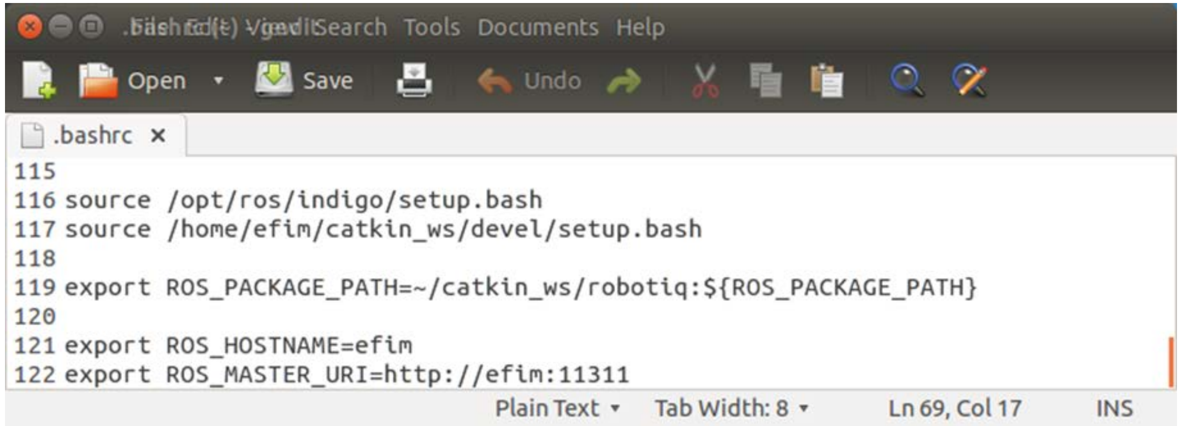

Adding ROS environment variables to the .bashrc script.

ROS node-topic structure (ROS, 2015b).

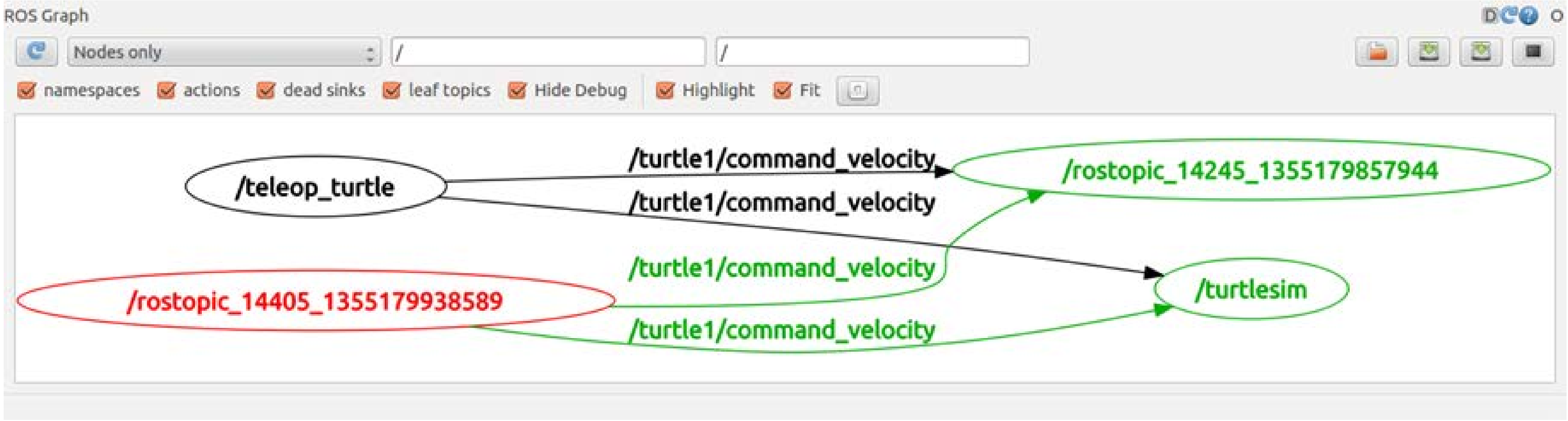

Graph representing dependencies of nodes and topics of turtlesim package

ROS graph work of both UR10 arms

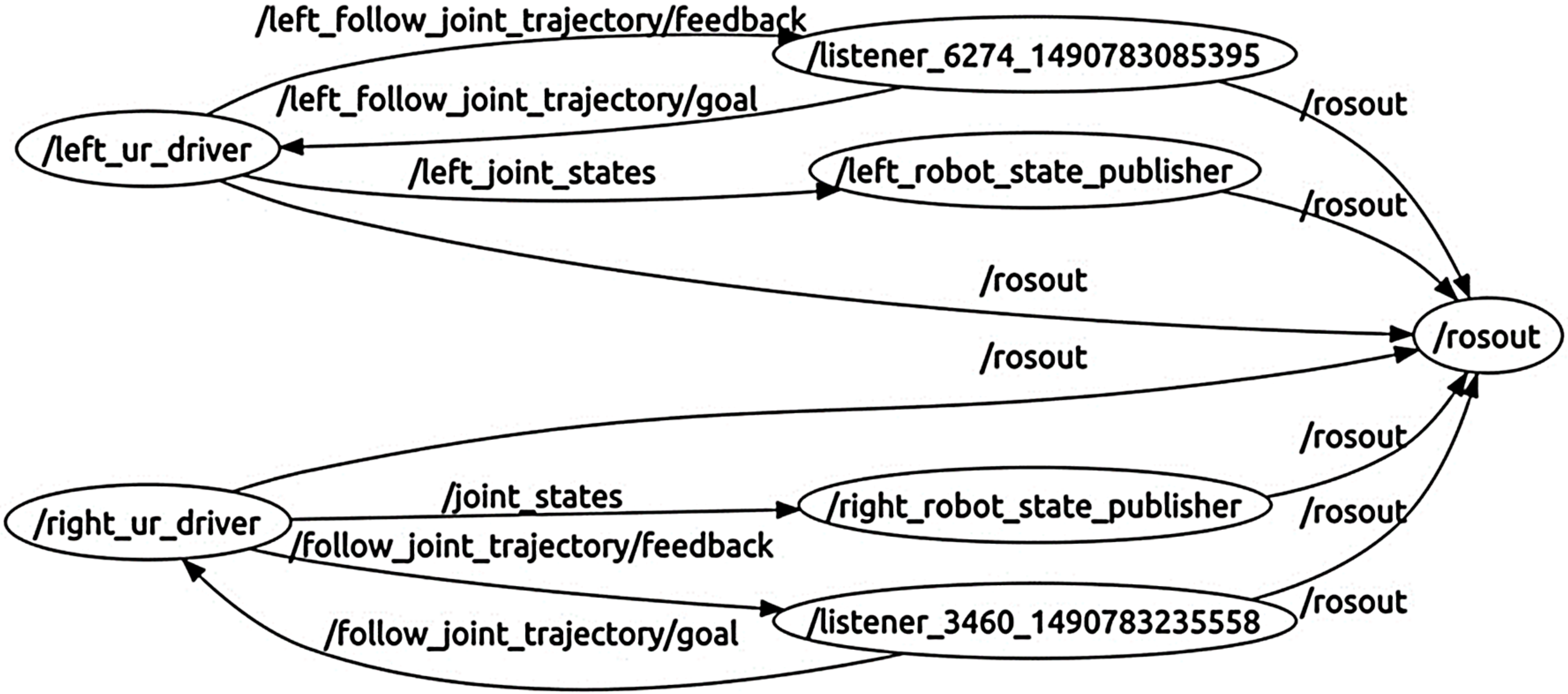

Arms, Grippers and Joysticks

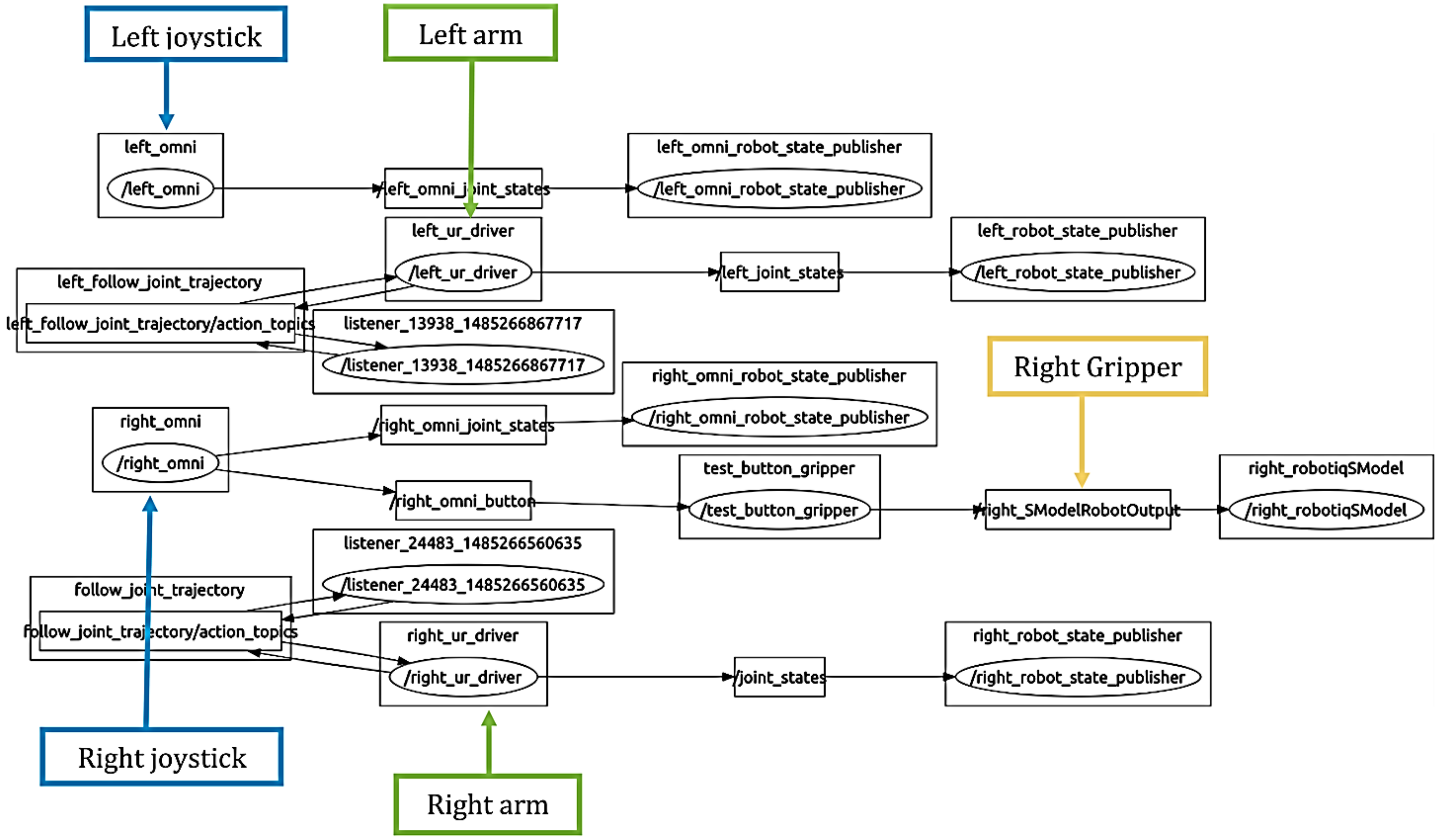

Delay and Latency

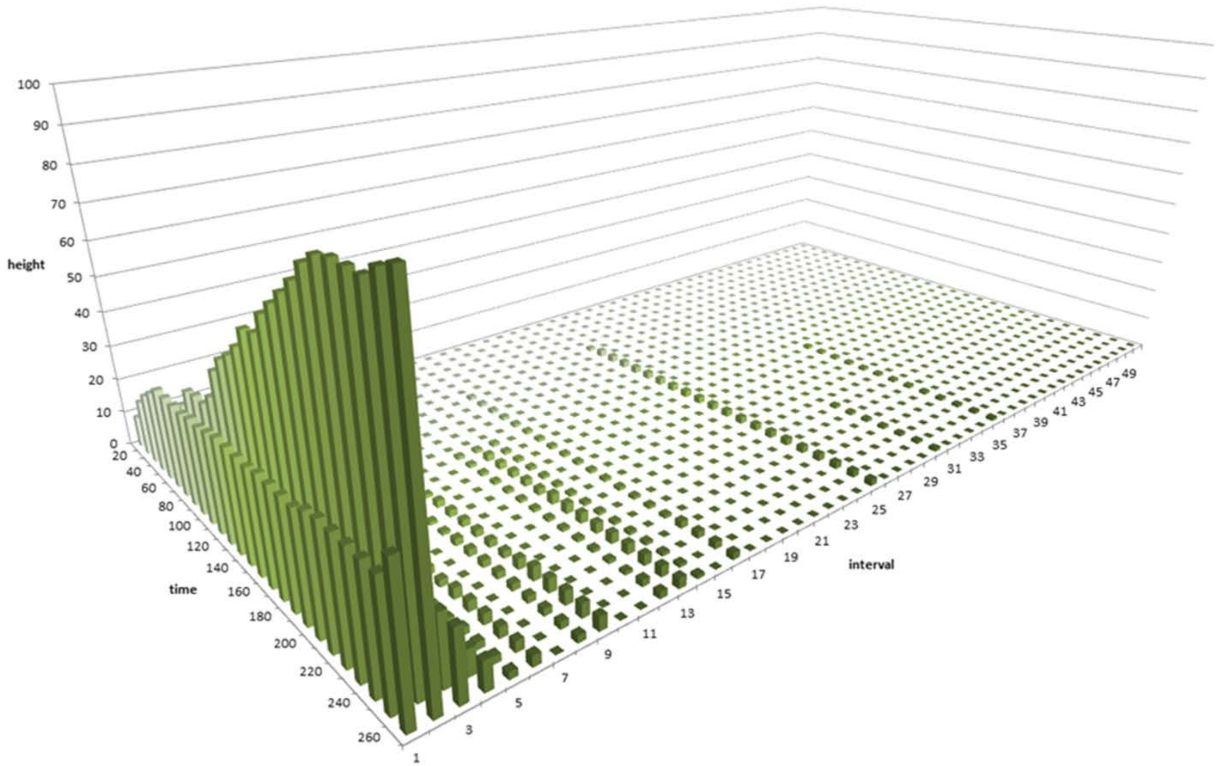

Dynamic of frequency histogram change over time

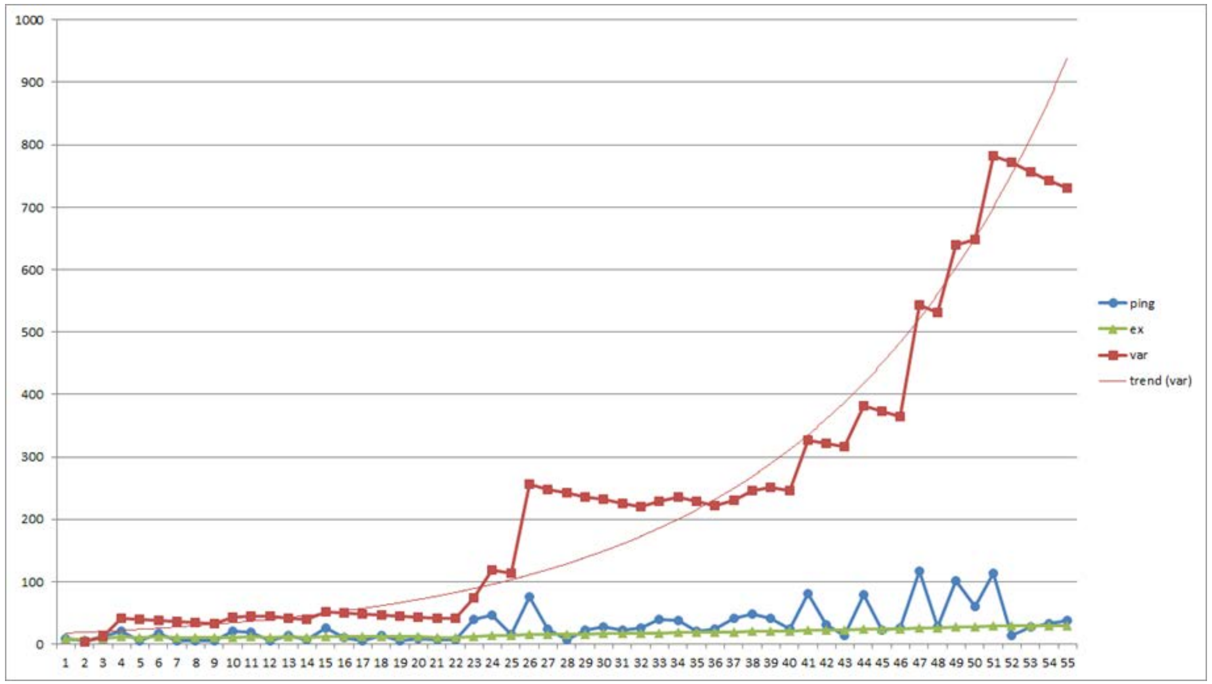

Delay, expectation, variance and trend for variance before the first connection drop based on experiment № 2 data

TIERA network

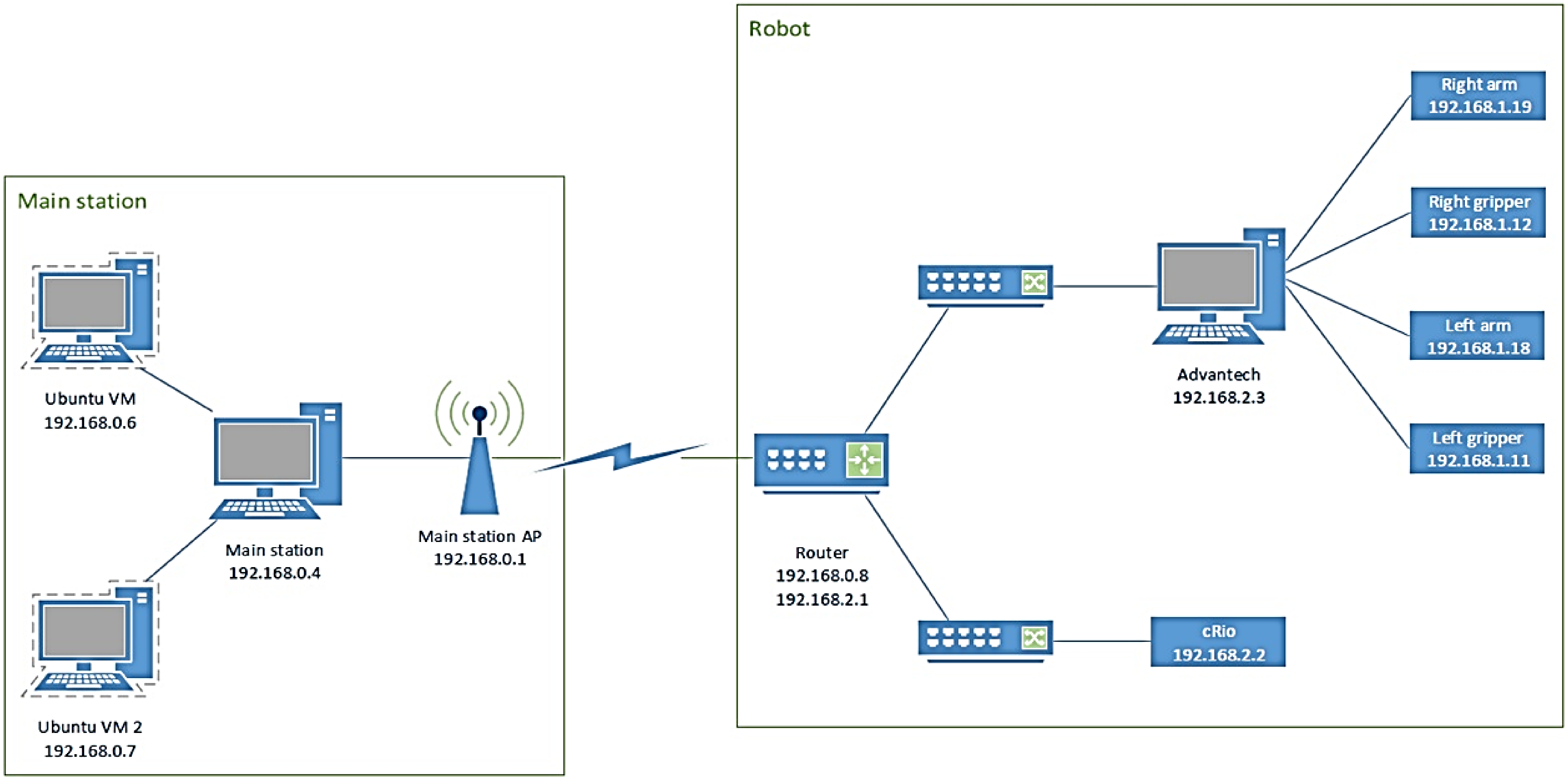

Robot Control Sections

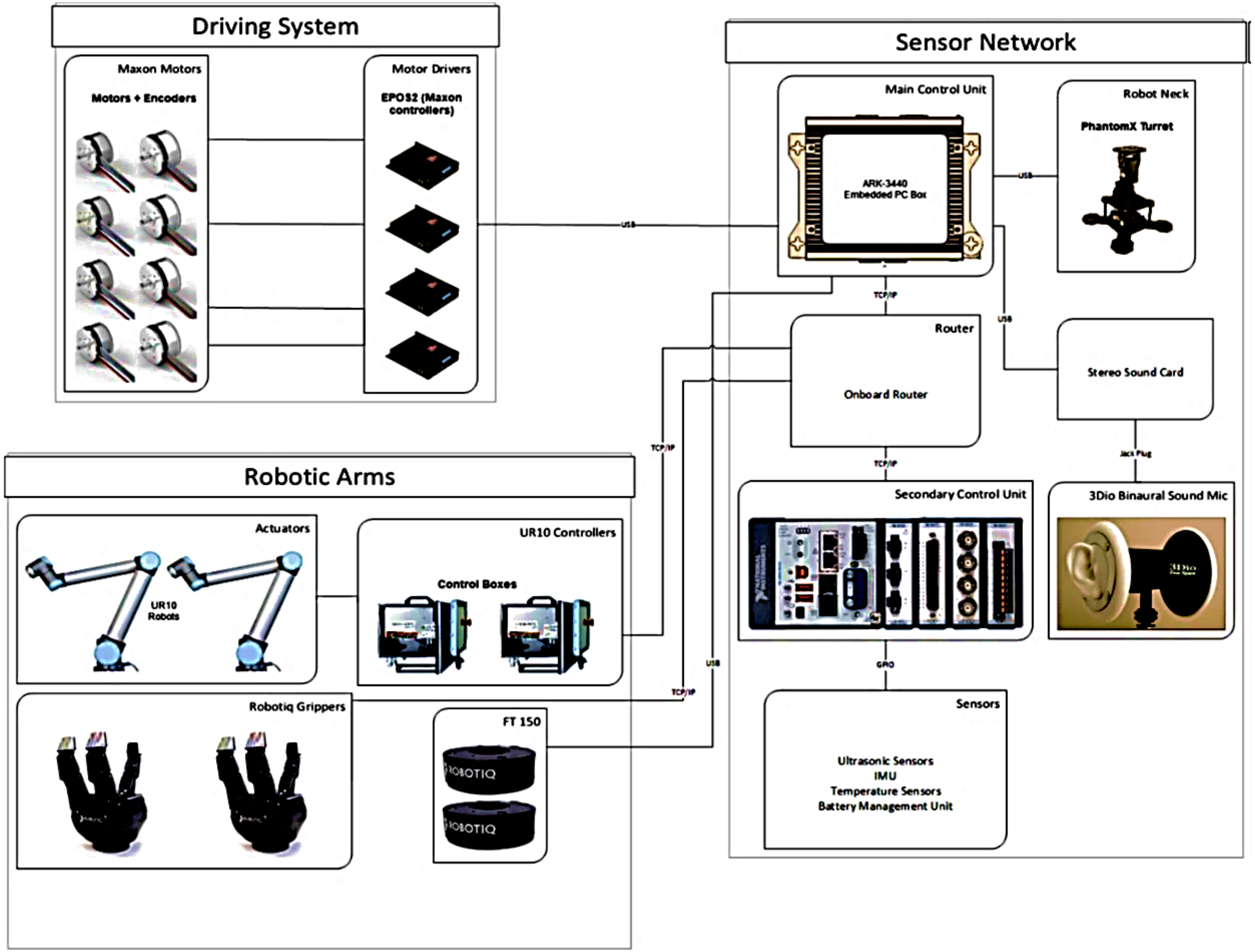

Movegroup conceptual diagram

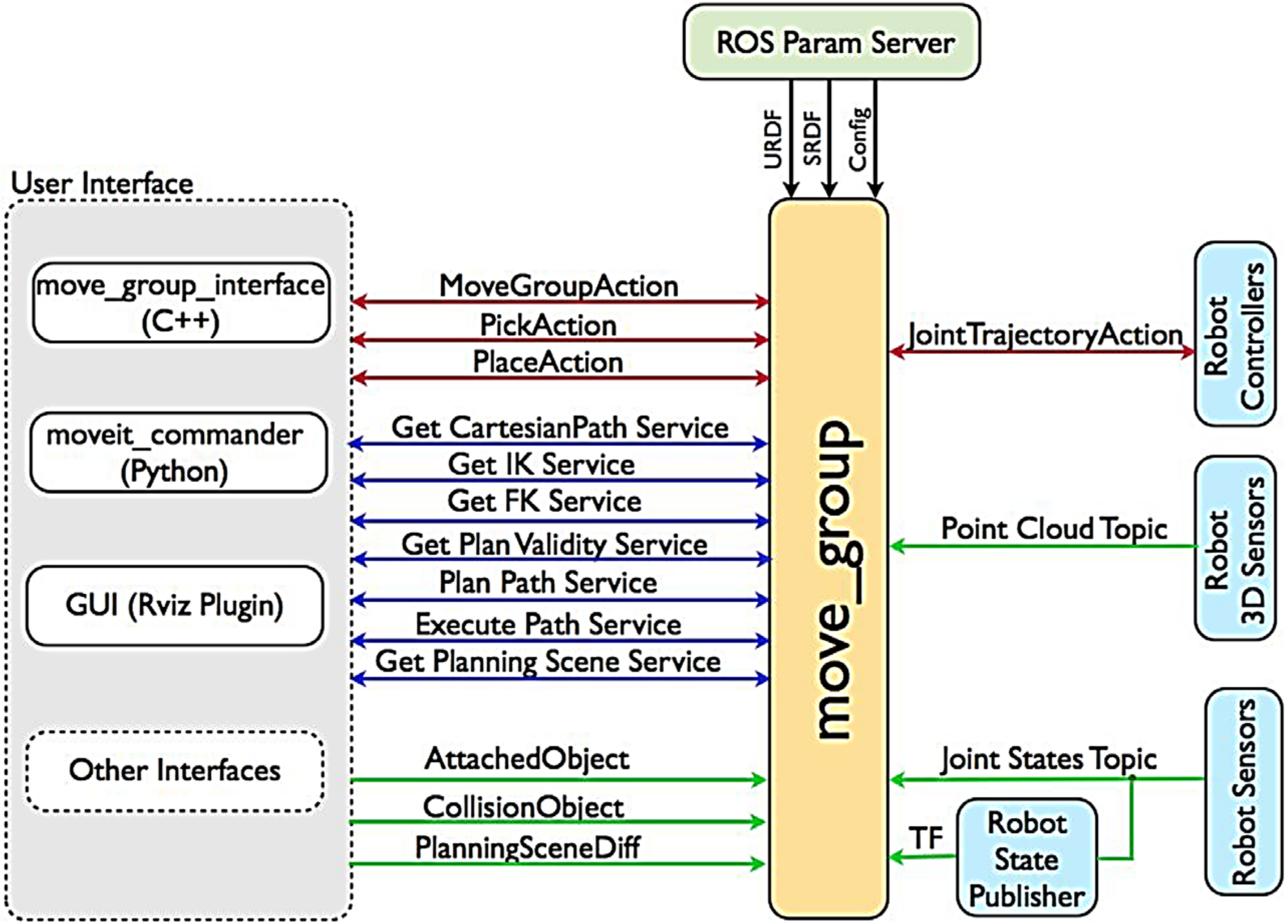

Movegroup conceptual diagram

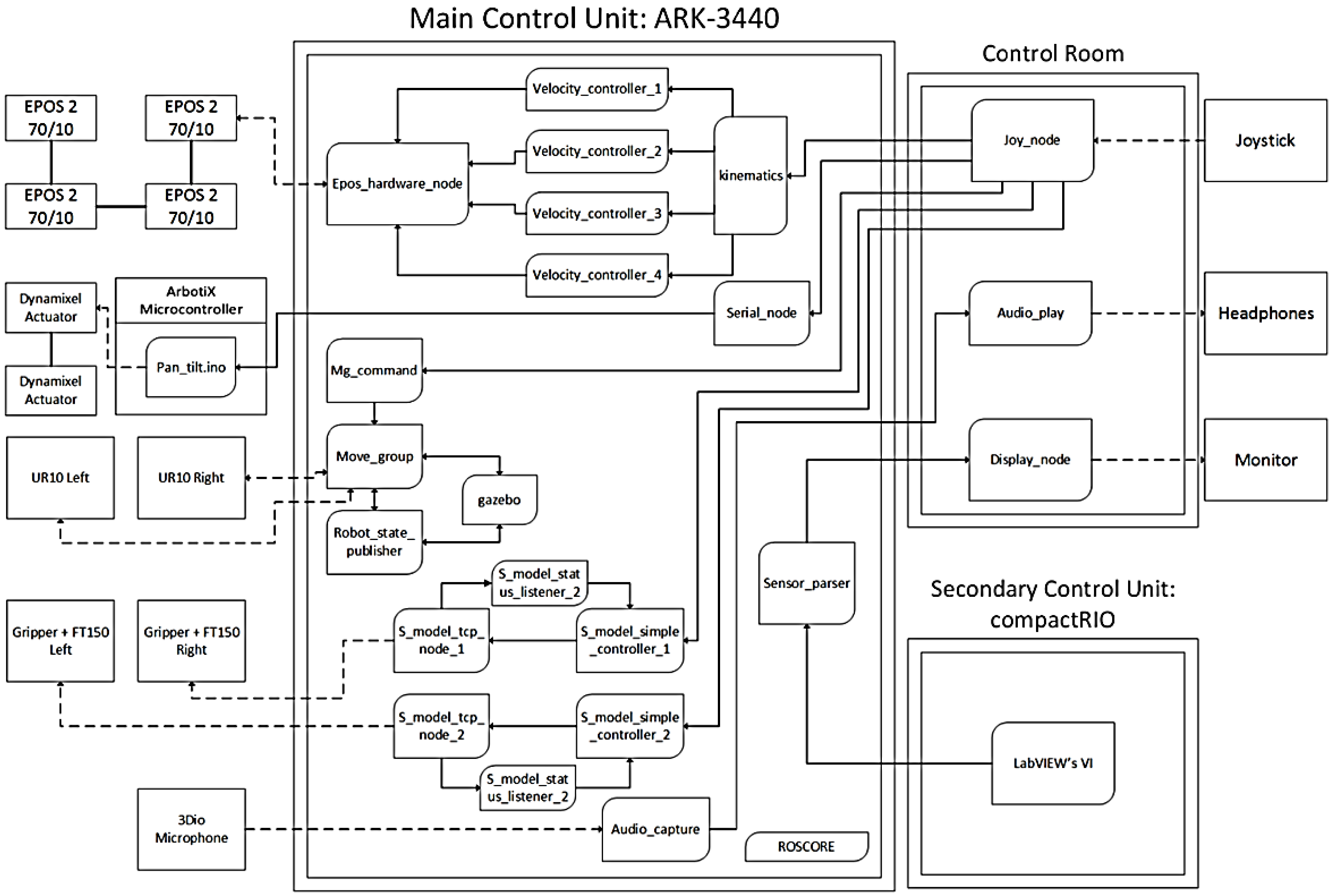

Diagram of virtual private network for the LUT Mobile Assembly Robot

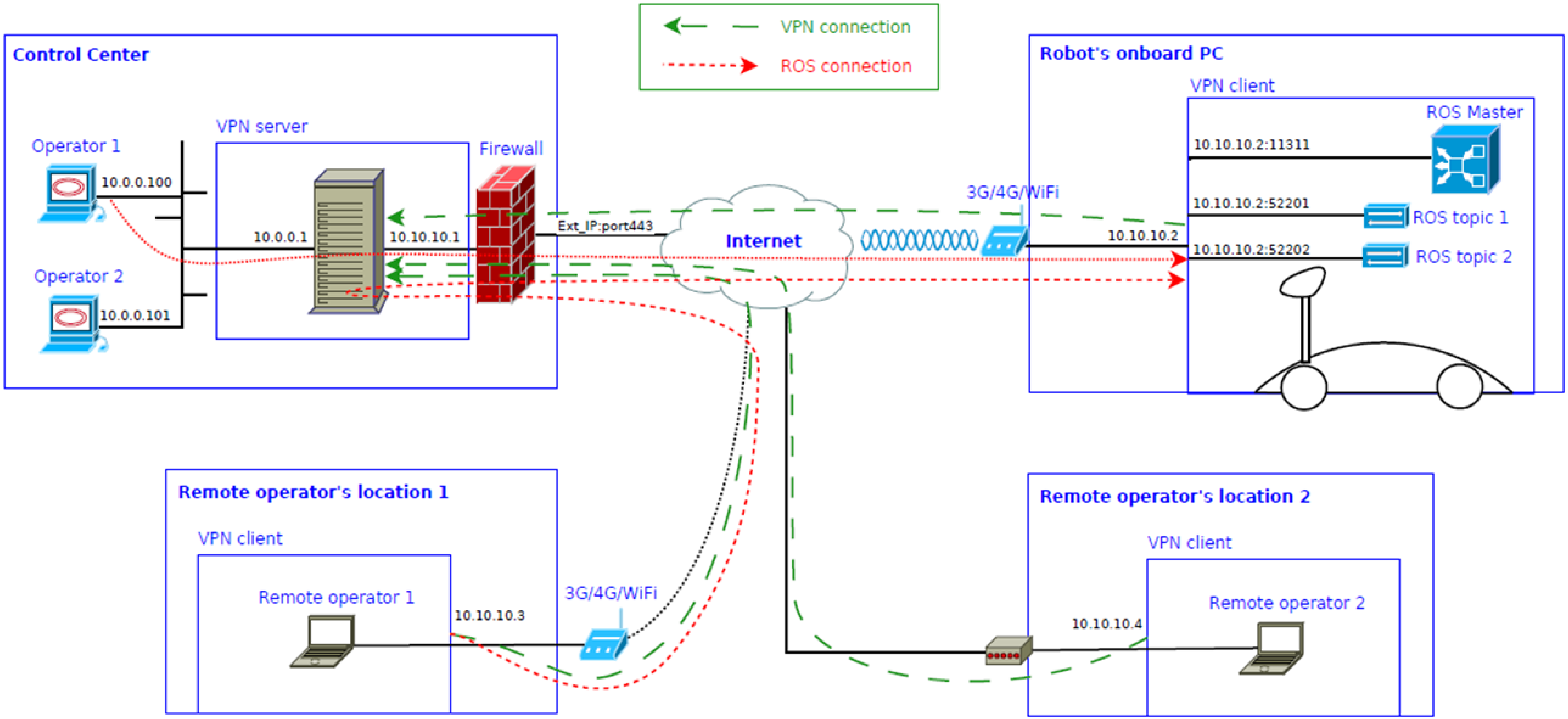

Low level Control System

National Instruments cRIO industrial controller + ROS

Implementation of publishing mechanism in ROS for LabVIEW tool

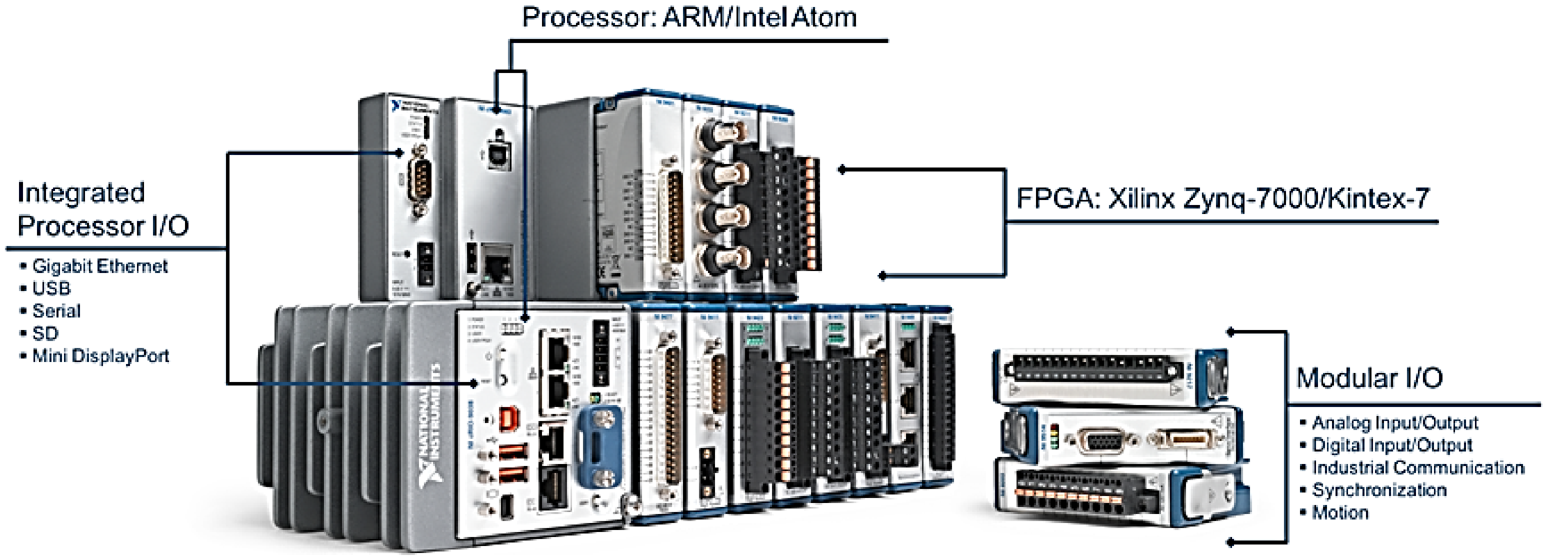

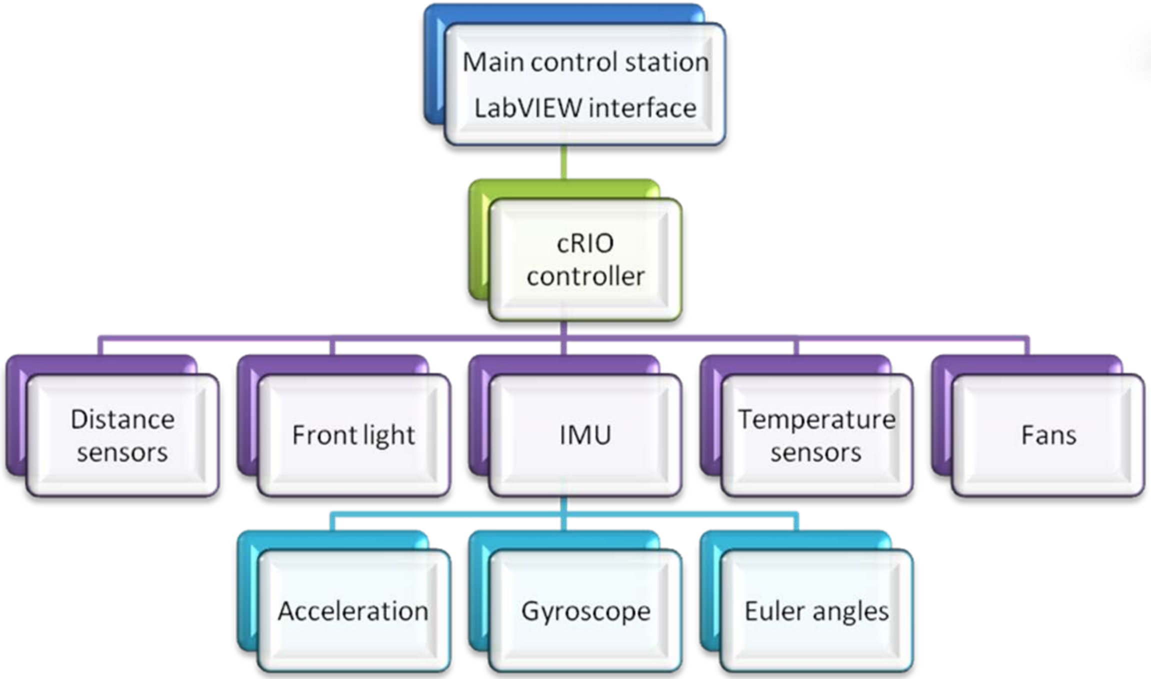

Communication diagram of the lower level subsystem

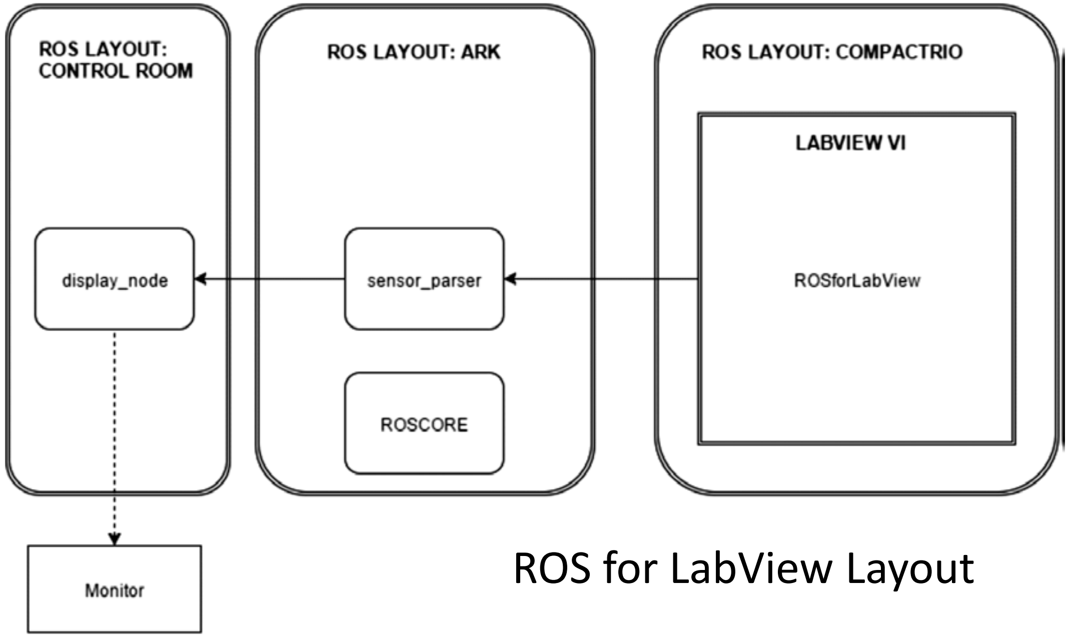

ROS for LabView Layout

Temp Control

Thermometer with a platinum wire

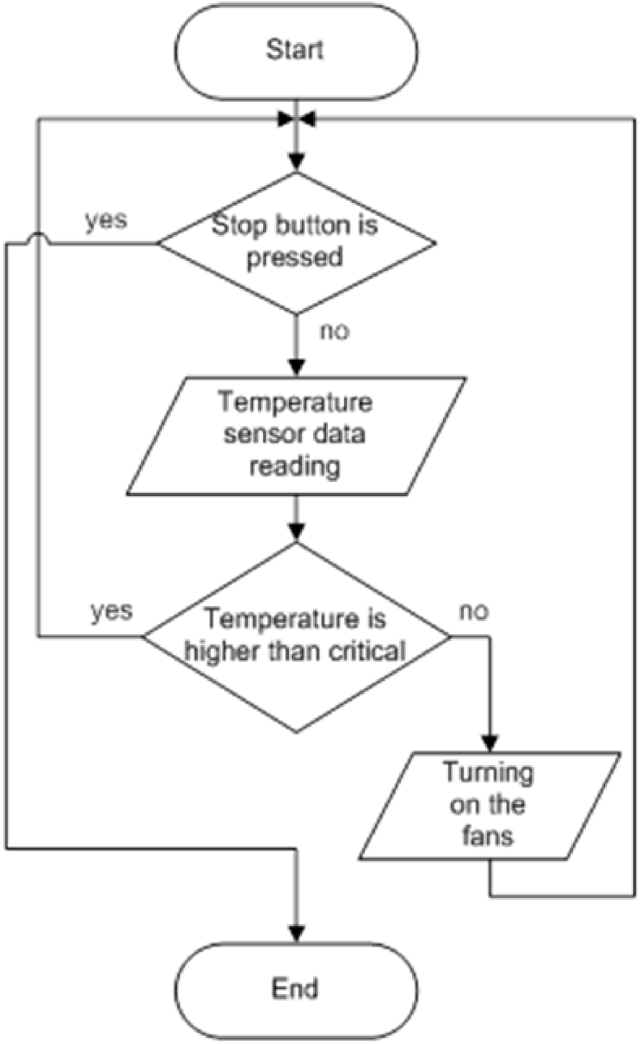

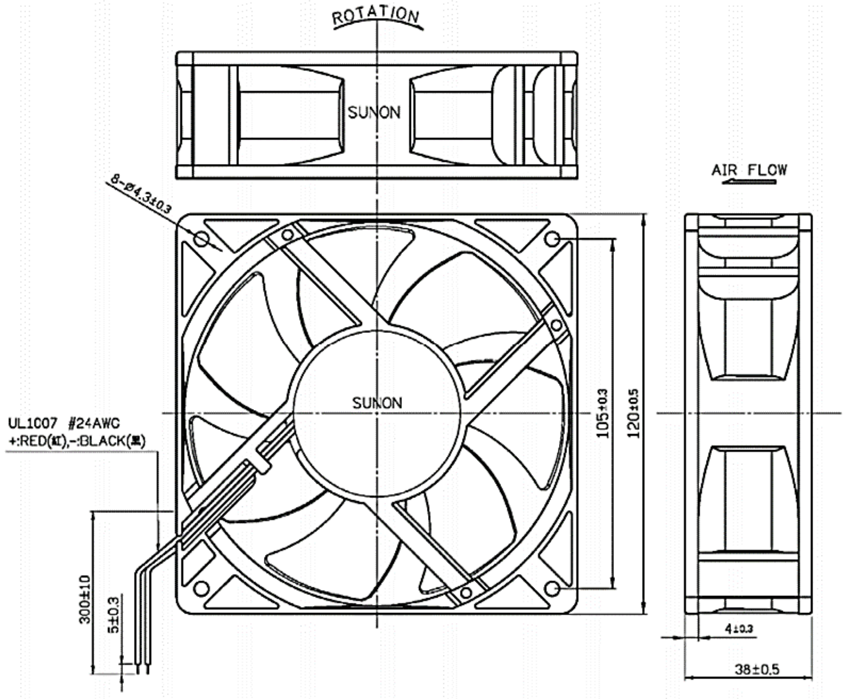

SUNON PMD2412PMB1-A fan

Logic of the transceiver operation

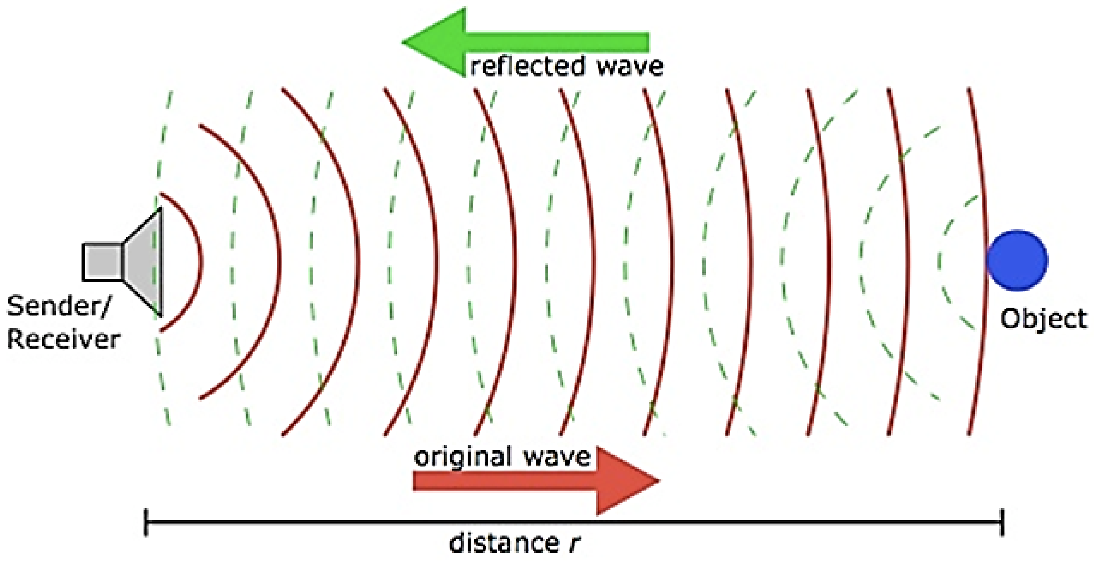

Ultrasonic distance sensor SRF06

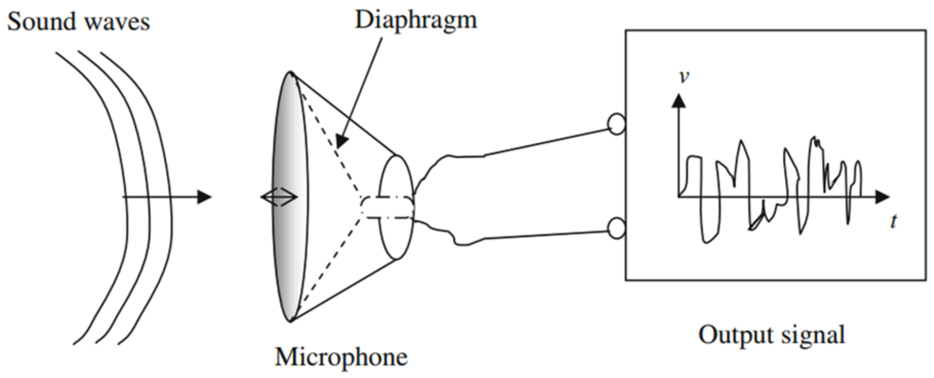

Inertial Sensor

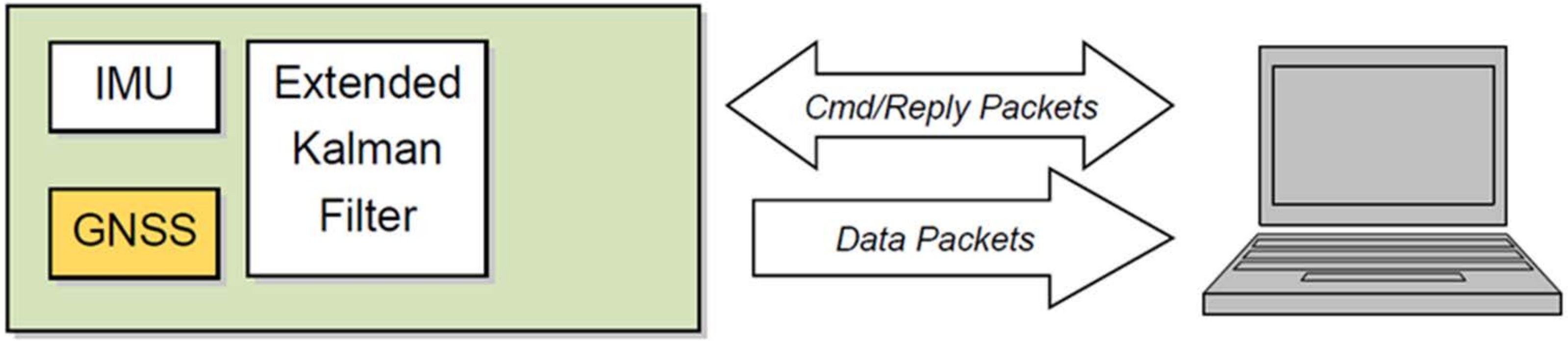

Communication data flow between the inertial sensor and the computer

Header				Packet Payload			Checksum	
SYNC1 "u"	*SYNC2 "e"*	*Descriptor Set byte*	*Payload Length byte*	*Field Length byte*	*Field Descriptor byte*	*Field Data*	*MSB*	*LSB*
0x75	**0x65**	**0x01**	**0x02**	**0x02**	**0x01**	*N/A*	**0xE0**	**0xC6**

Packet of "Ping" command

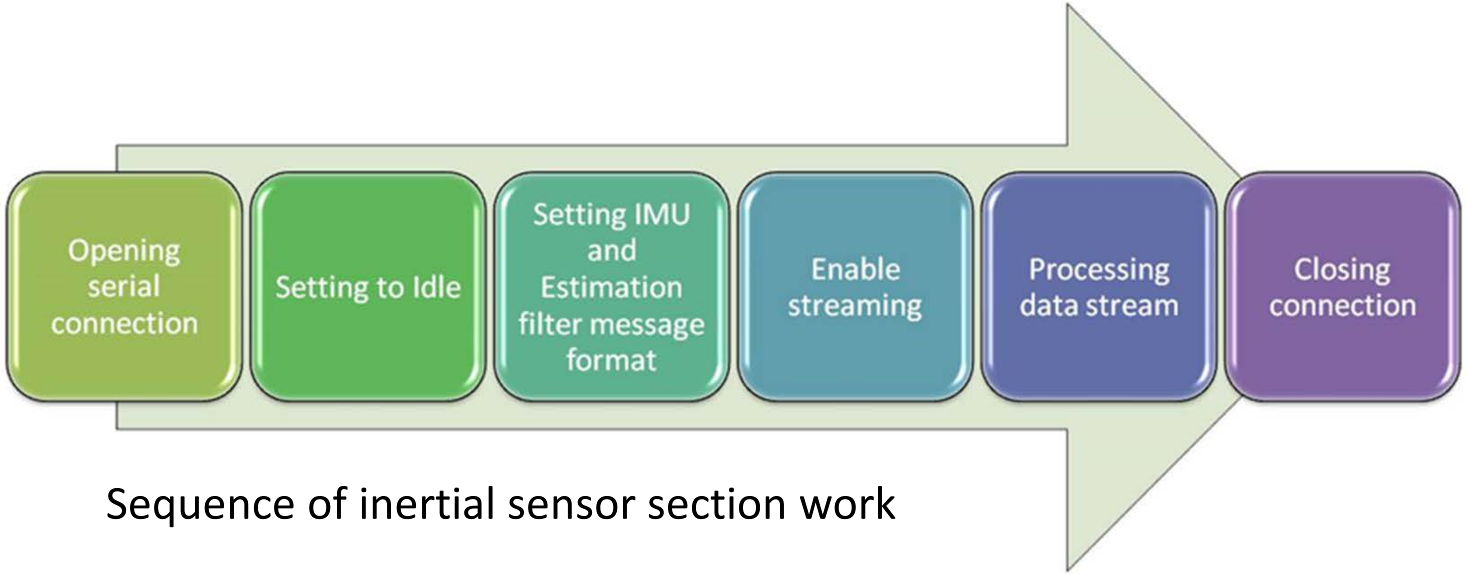

Sequence of inertial sensor section work

Packet generator for inertial sensor

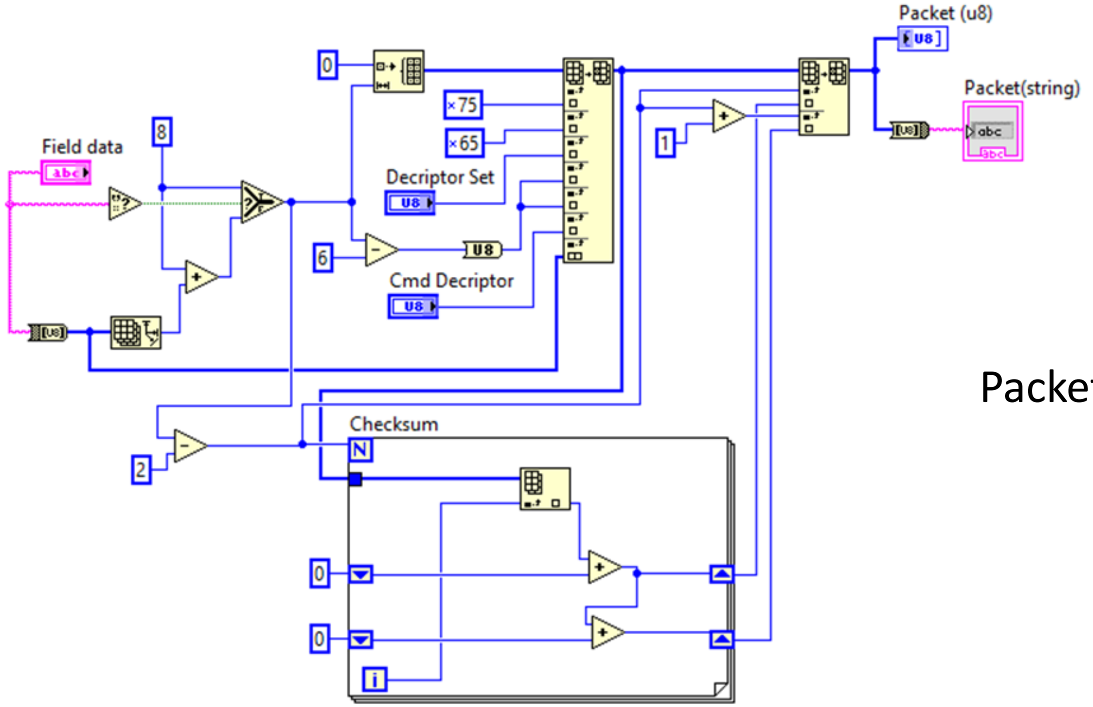

Packet generator for inertial sensor

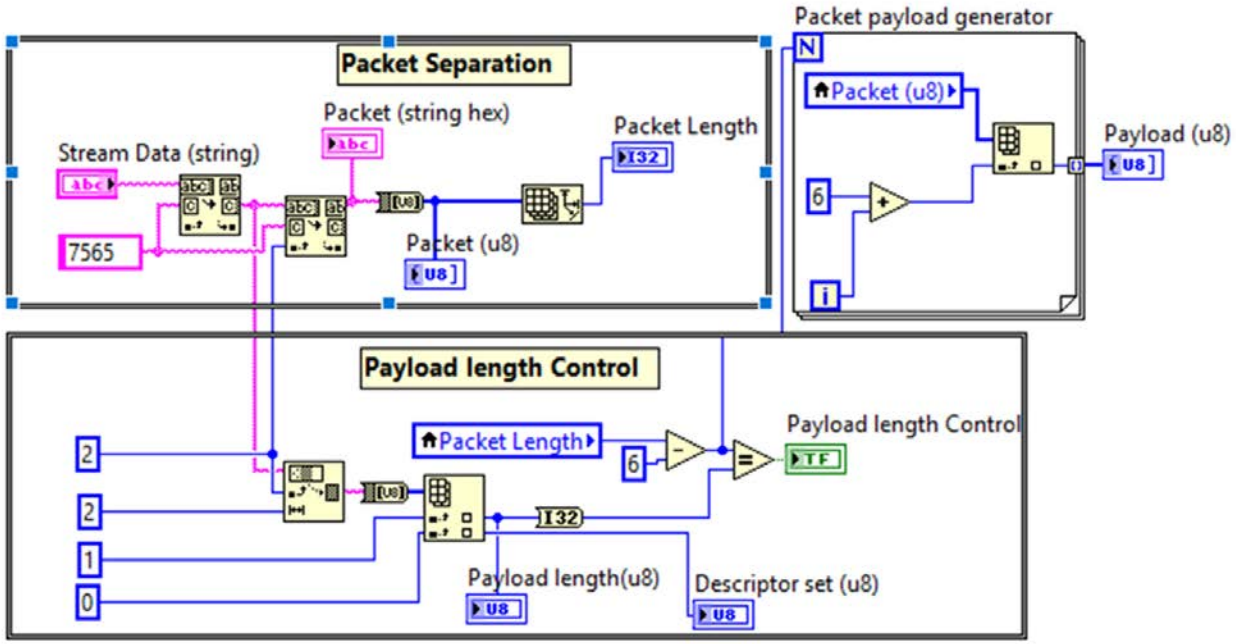

Packet parser for the inertial sensor Part 1

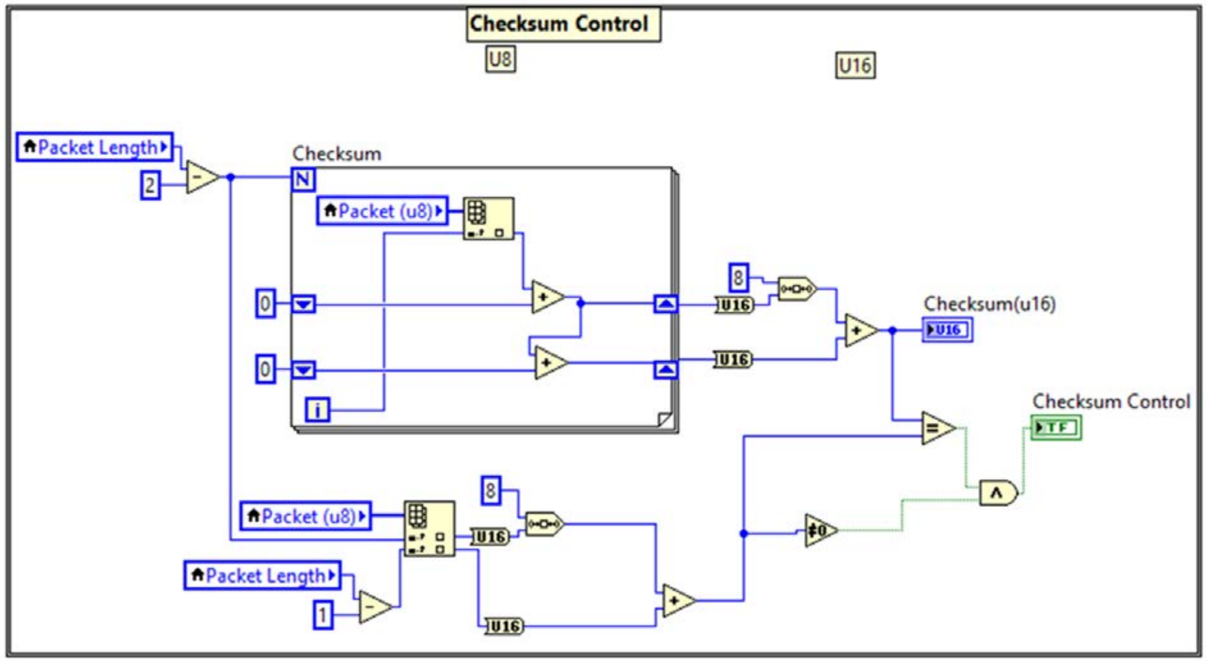

Packet parser for the inertial sensor Part 2

Data stream analysis.

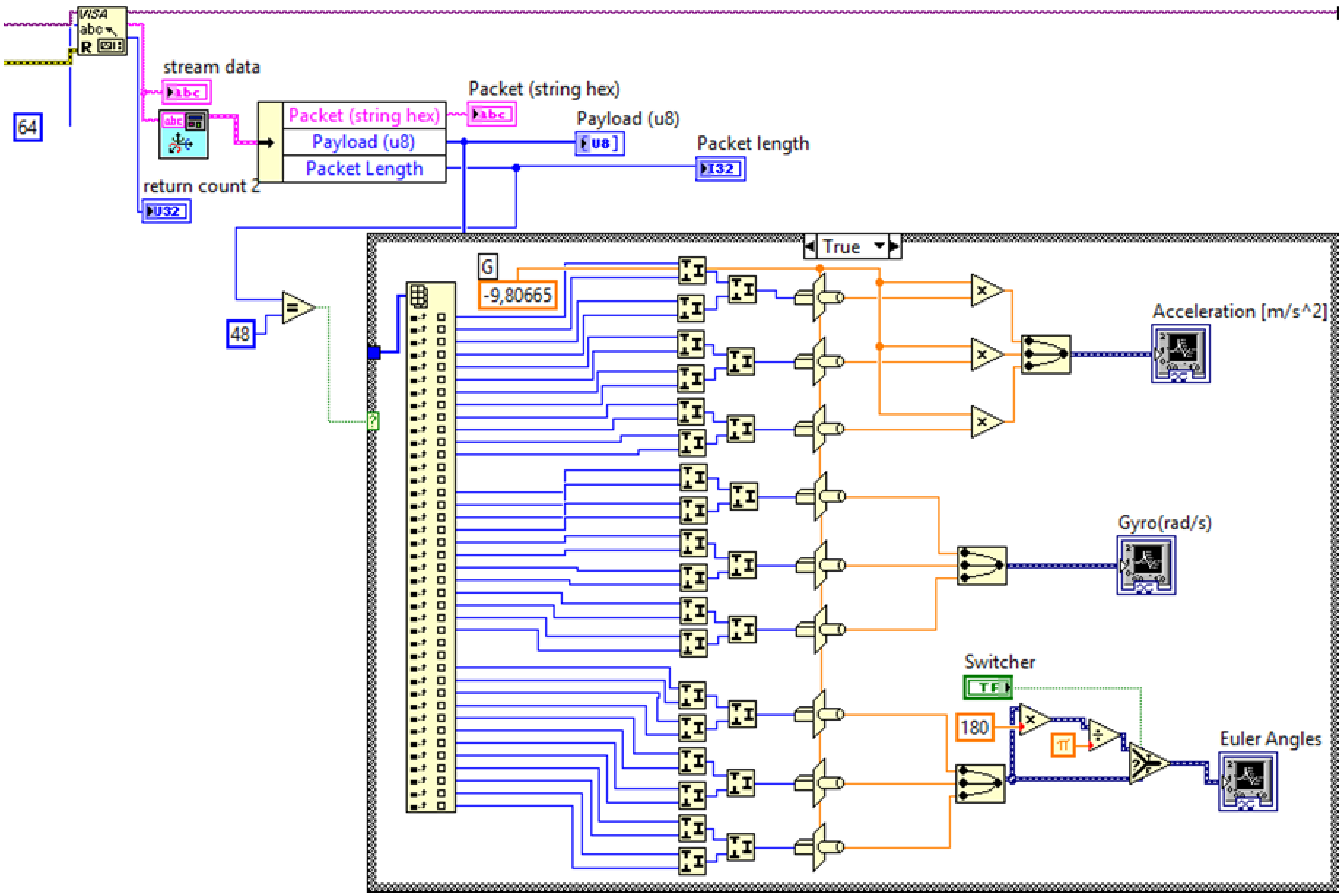

Developed platform interface in LabVIEW.

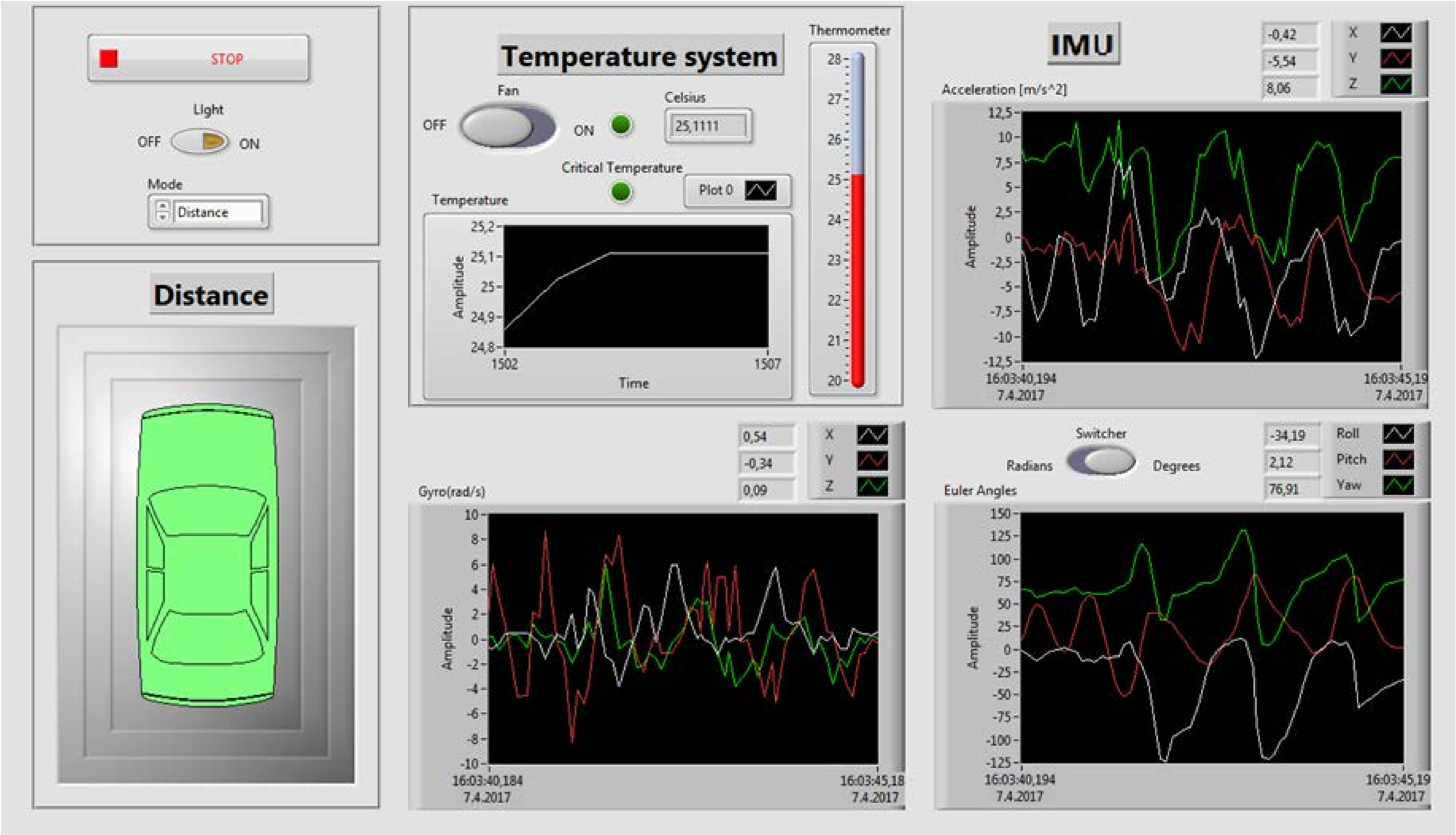

Haptics & Joystick

Geomagic Touch Joysticks and

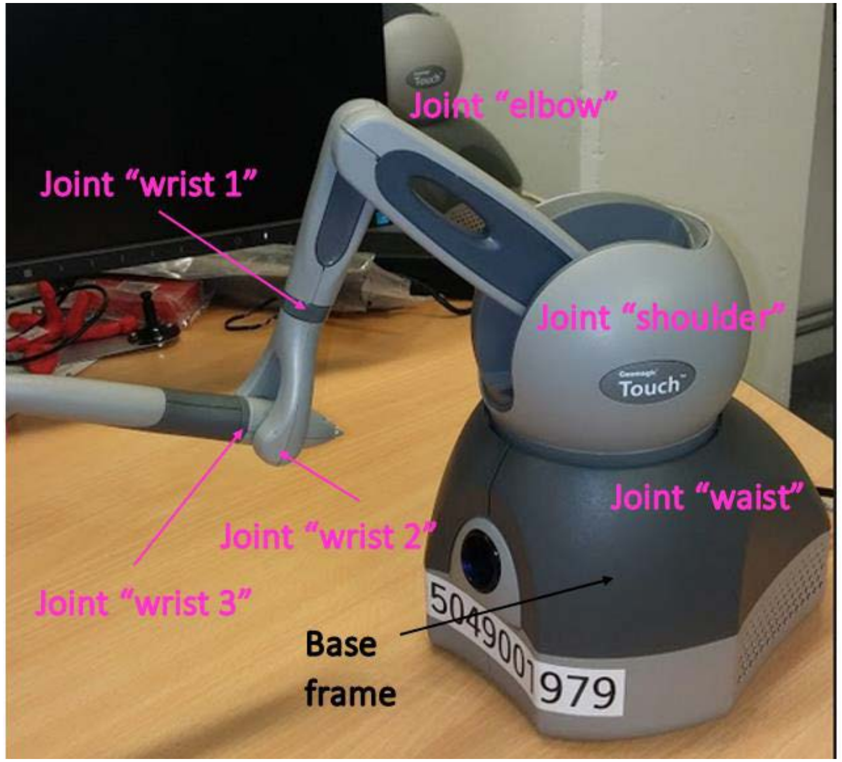

Robotiq Force Torque Sensor FT 150

Geomagic Touch base frame and joints

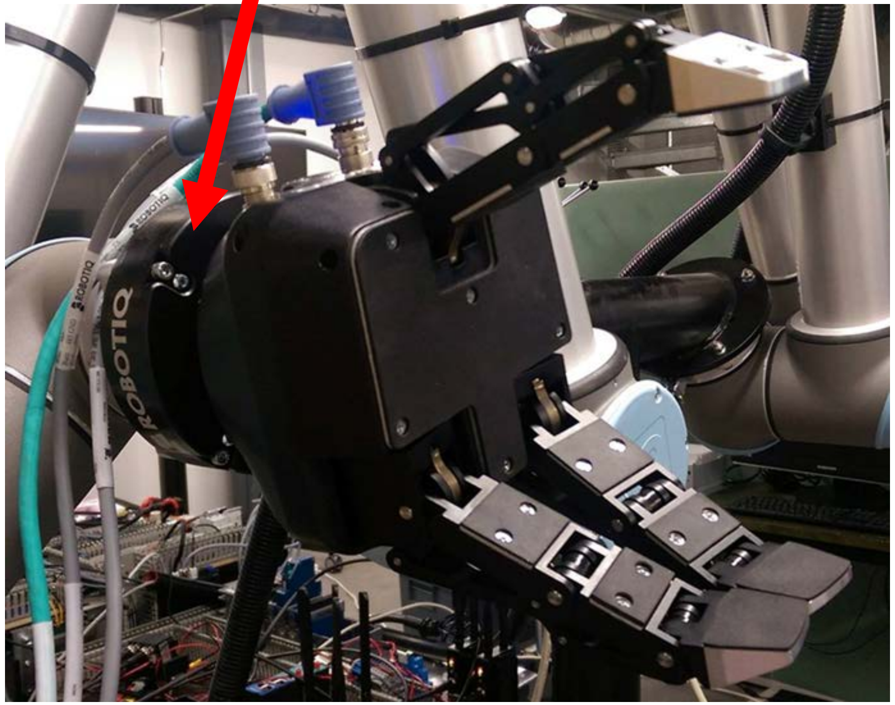

Forward Kinematics and Inverse kinematics

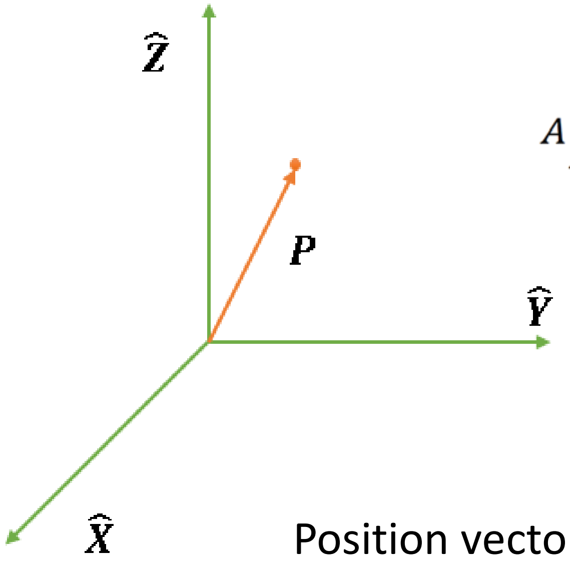

$$^{A}\boldsymbol{P} = \begin{bmatrix} p_x \\ p_y \\ p_z \end{bmatrix}$$

Position vector.

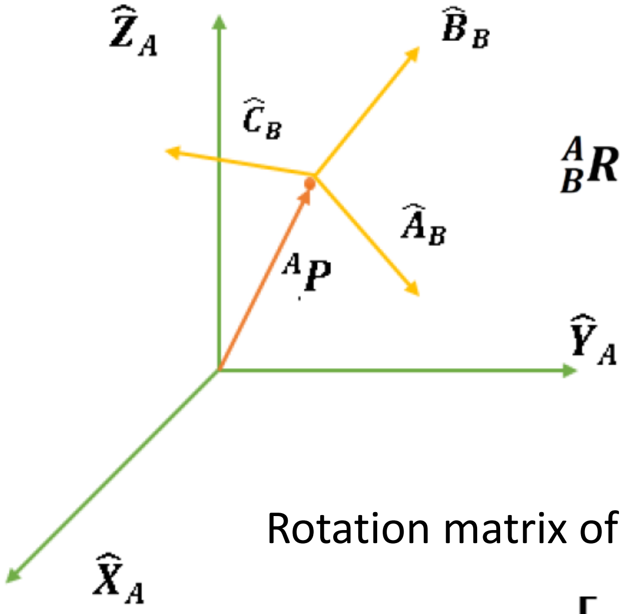

$$^{A}_{B}\boldsymbol{R} = \begin{bmatrix} {}^{A}\hat{A}_B & {}^{A}\hat{B}_B & {}^{A}\hat{C}_B \end{bmatrix} = \begin{bmatrix} a_x & b_x & c_x \\ a_y & b_y & c_y \\ a_z & b_z & c_z \end{bmatrix}$$

Rotation matrix of the end-effector

$$^{A}_{B}\boldsymbol{R} = \begin{bmatrix} a_x & b_x & c_x \\ a_y & b_y & c_y \\ a_z & b_z & c_z \end{bmatrix} = \begin{bmatrix} r_{11} & r_{12} & r_{13} \\ r_{21} & r_{22} & r_{23} \\ r_{31} & r_{32} & r_{33} \end{bmatrix}$$

$$^{A}_{B}\boldsymbol{T} = \begin{bmatrix} a_x & b_x & c_x & p_x \\ a_y & b_y & c_y & p_y \\ a_z & b_z & c_z & p_z \\ 0 & 0 & 0 & 1 \end{bmatrix}$$

$$\alpha = Atan2(r_{32}, r_{33})$$

$$\beta = Atan2\left(-r_{31}, \sqrt{r_{32}{}^2 + r_{33}{}^2}\right)$$

$$\gamma = Atan2(r_{21}, r_{11})$$

Forward Kinematics

$$R_x = \begin{bmatrix} 1 & 0 & 0 \\ 0 & cos\,\theta & sin\,\theta \\ 0 & -sin\,\theta & cos\,\theta \end{bmatrix}$$

$$R_y = \begin{bmatrix} cos\,\theta & 0 & -sin\,\theta \\ 0 & 1 & 0 \\ sin\,\theta & 0 & cos\,\theta \end{bmatrix}$$

$$R_z = \begin{bmatrix} cos\,\theta & -sin\,\theta & 0 \\ sin\,\theta & cos\,\theta & 0 \\ 0 & 0 & 1 \end{bmatrix}$$

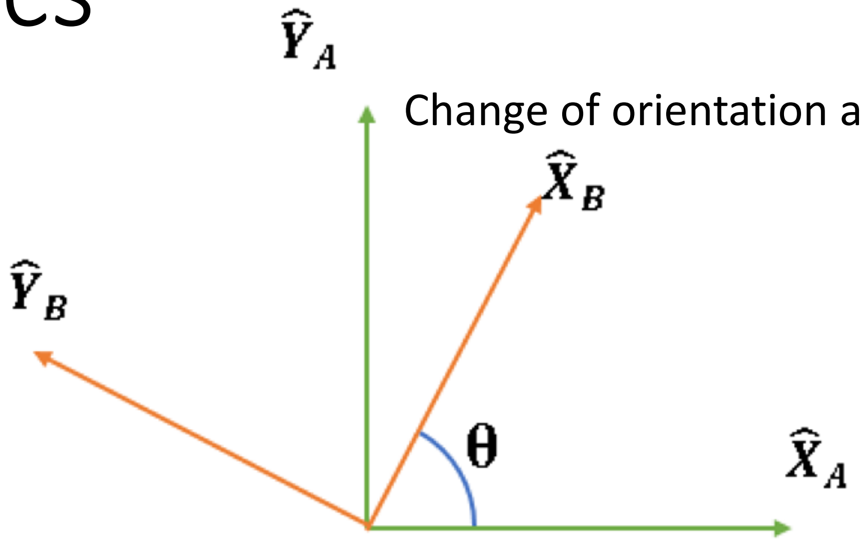

Change of orientation around Z.

$$^{A}\hat{\boldsymbol{X}}_{\boldsymbol{B}} = \begin{bmatrix} \cos\theta \\ \sin\theta \\ 0 \end{bmatrix}$$

$$^{A}\hat{\boldsymbol{Y}}_{\boldsymbol{B}} = \begin{bmatrix} \sin\theta \\ \cos\theta \\ 0 \end{bmatrix}$$

$$^{A}\hat{\boldsymbol{Z}}_{\boldsymbol{B}} = \begin{bmatrix} 0 \\ 0 \\ 1 \end{bmatrix}$$

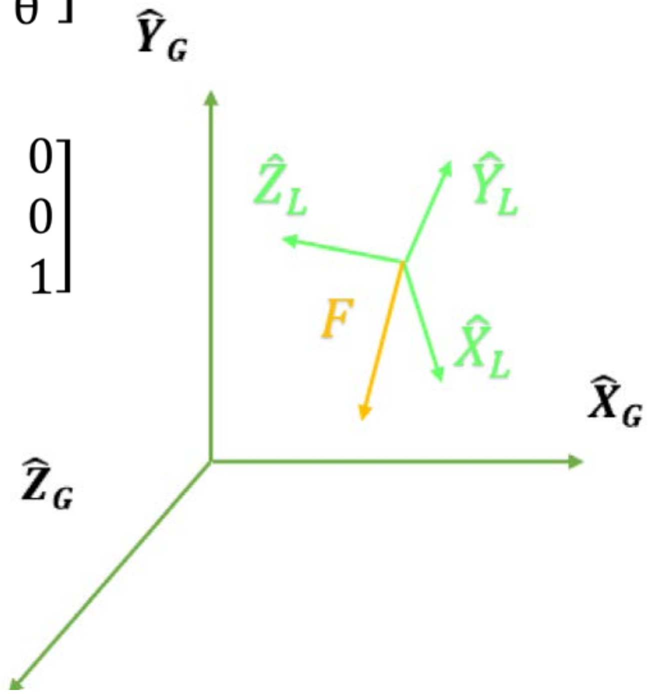

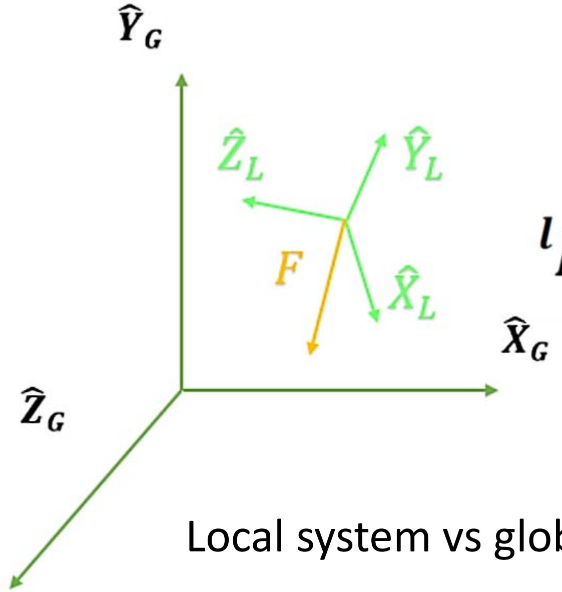

$$^{l}\boldsymbol{F} = f_a\hat{A} + f_b\hat{B} + f_c\hat{C}$$

Local system vs global system

$$^{G}\boldsymbol{F} = (f_a a_x + f_b b_x + f_c c_x)\hat{X} + (f_a a_y + f_b b_y + f_c c_y)\hat{Y} + (f_a a_z + f_b b_z + f_c c_z)\hat{Z}$$

Outline of Haptic Communication

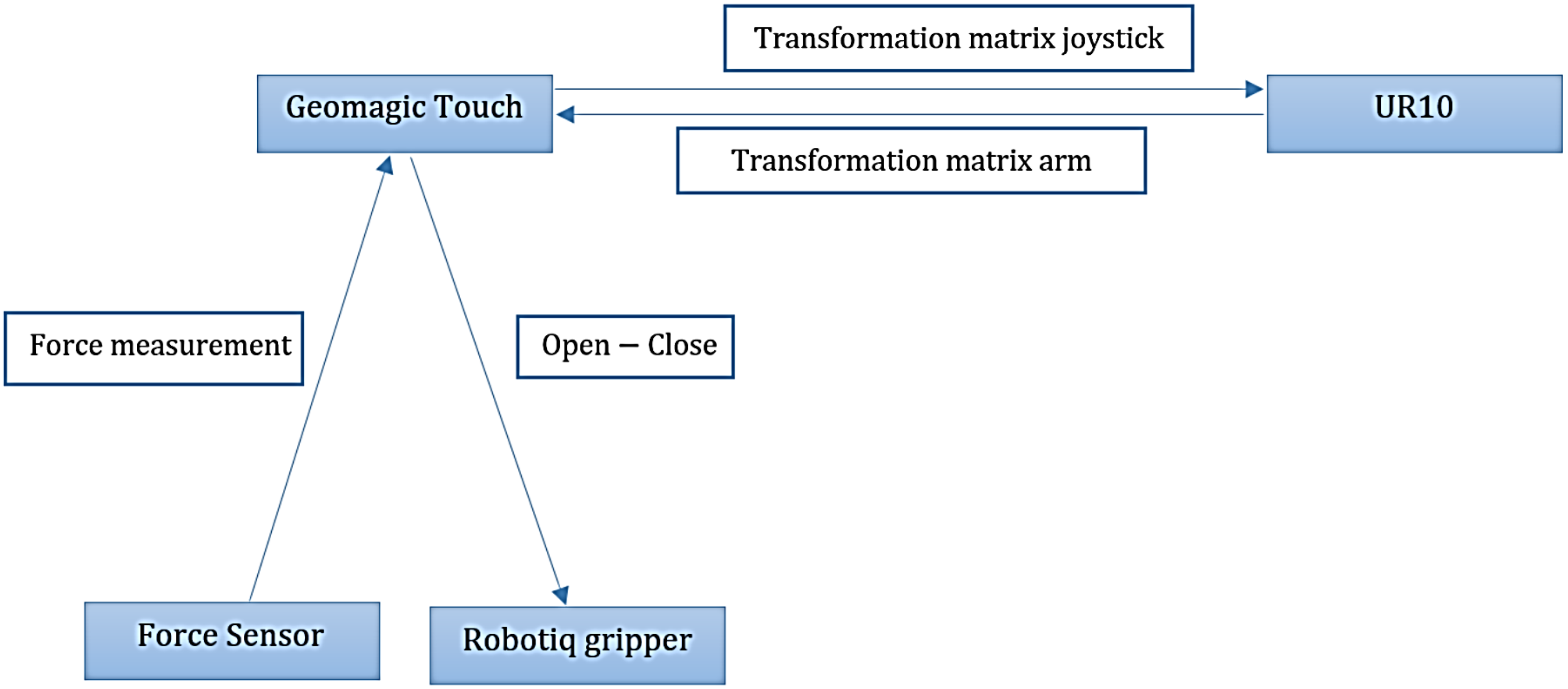

Geomagic Touch controller that is utilized for control of UR10 robotic arms

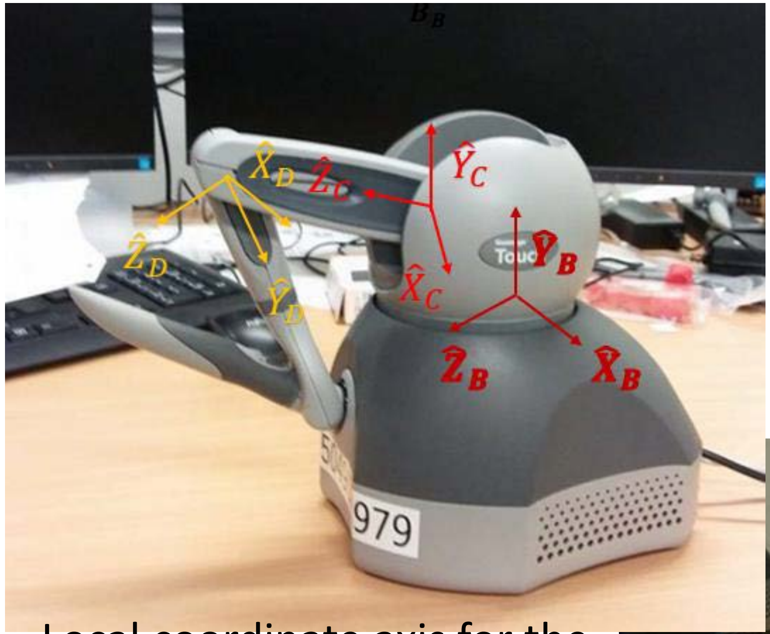

Local coordinate axis for the first three joints

Global coordinate system for the Geomagic Touch

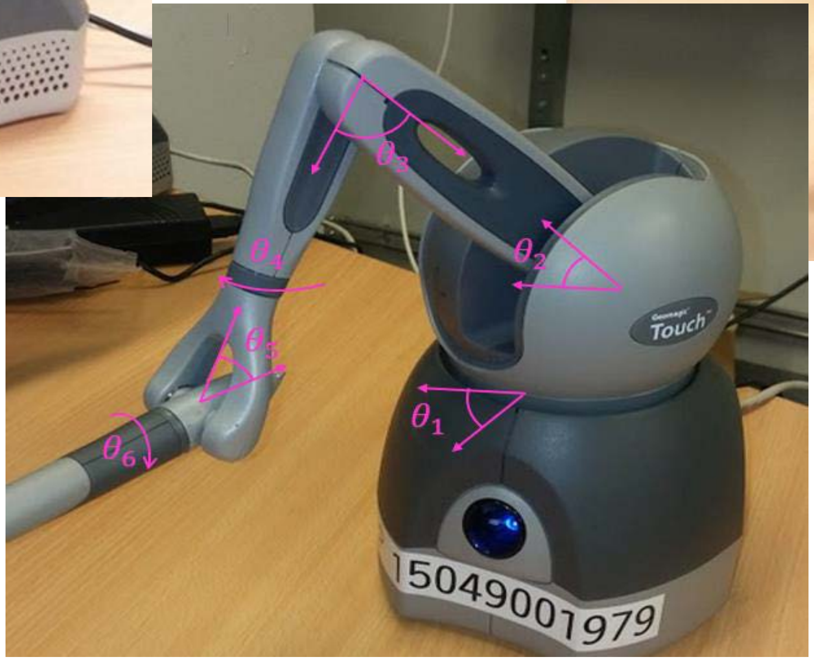

Degrees of freedom of each joint

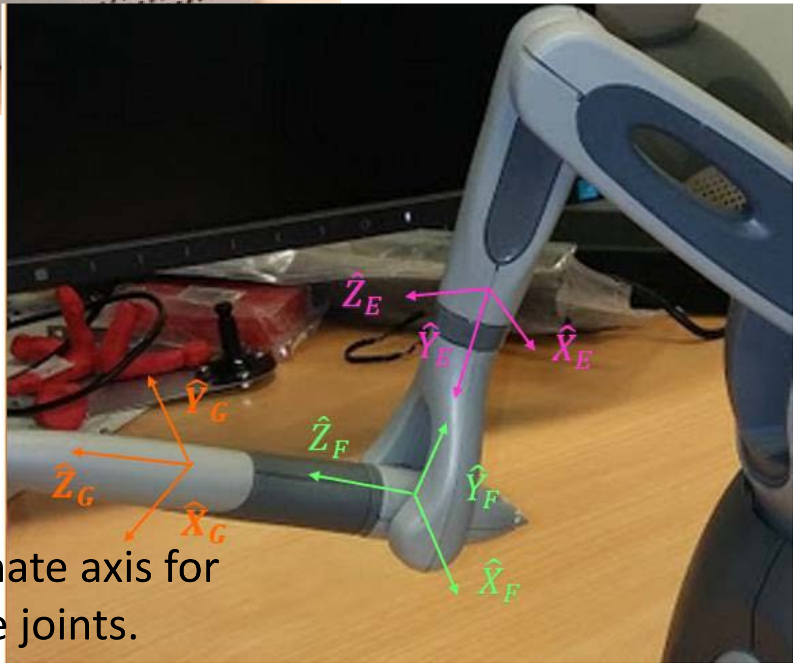

Local coordinate axis for the last three joints.

Rotation matrixes

$$ {}^{A}_{B}\boldsymbol{R} = \begin{bmatrix} \cos\theta_1 & 0 & -\sin\theta_1 \\ 0 & 1 & 0 \\ \sin\theta_1 & 0 & \cos\theta_1 \end{bmatrix} $$

$$ {}^{B}_{C}\boldsymbol{R} = \begin{bmatrix} 1 & 0 & 0 \\ 0 & \cos\theta_2 & \sin\theta_2 \\ 0 & -\sin\theta_2 & \cos\theta_2 \end{bmatrix} $$

$$ {}^{C}_{D}\boldsymbol{R} = \begin{bmatrix} 1 & 0 & 0 \\ 0 & \cos\theta_3 & \sin\theta_3 \\ 0 & -\sin\theta_3 & \cos\theta_3 \end{bmatrix} $$

$$ {}^{D}_{E}\boldsymbol{R} = \begin{bmatrix} \cos\theta_4 & 0 & -\sin\theta_4 \\ 0 & 1 & 0 \\ \sin\theta_4 & 0 & \cos\theta_4 \end{bmatrix} $$

$$ {}^{E}_{F}\boldsymbol{R} = \begin{bmatrix} 1 & 0 & 0 \\ 0 & \cos\theta_5 & \sin\theta_5 \\ 0 & -\sin\theta_5 & \cos\theta_5 \end{bmatrix} $$

$$ {}^{F}_{G}\boldsymbol{R} = \begin{bmatrix} \cos\theta_6 & \sin\theta_6 & 0 \\ \sin\theta_6 & \cos\theta_6 & 0 \\ 0 & 0 & 1 \end{bmatrix} $$

$$ si = \sin\theta_i $$

$$ ci = \cos\theta_i $$

$$ R = \begin{bmatrix} r_{11} & r_{12} & r_{13} \\ r_{21} & r_{22} & r_{23} \\ r_{31} & r_{32} & r_{33} \end{bmatrix} $$

$$ r_{11} = -c5 * (s1 * s4 + c4 * (c1 * s2 * s3 - c1 * c2 * c3)) - s5 * (c1 * c2 * s3 + c1 * c3 * s2) $$

$$ r_{12} = s6 * (c4 * s1 - s4 * (c1 * s2 * s3 - c1 * c2 * c3)) + c6 * (s5 * (s1 * s4 + c4 * (c1 * s2 * s3 - c1 * c2 * c3)) - c5 * (c1 * c2 * s3 + c1 * c3 * s2)) $$

$$ r_{13} = c6 * (c4 * s1 - s4 * (c1 * s2 * s3 - c1 * c2 * c3)) - s6 * (s5 * (s1 * s4 + c4 * (c1 * s2 * s3 - c1 * c2 * c3)) - c5 * (c1 * c2 * s3 + c1 * c3 * s2)) $$

$$ r_{21} = s5 * (c2 * c3 - s2 * s3) + c4 * c5 * (c2 * s3 + c3 * s2) $$

$$ r_{22} = c6 * (c5 * (c2 * c3 - s2 * s3) - c4 * s5 * (c2 * s3 + c3 * s2)) + s4 * s6 * (c2 * s3 + c3 * s2) $$

$$ r_{23} = c6 * s4 * (c2 * s3 + c3 * s2) - s6 * (c5 * (c2 * c3 - s2 * s3) - c4 * s5 * (c2 * s3 + c3 * s2)) $$

$$ r_{31} = s5 * (c2 * s1 * s3 + c3 * s1 * s2) - c5 * (c1 * s4 - c4 * (s1 * s2 * s3 - c2 * c3 * s1)) $$

$$ r_{32} = s6 * (c1 * c4 + s4 * (s1 * s2 * s3 - c2 * c3 * s1)) + c6 * (s5 * (c1 * s4 - c4 * (s1 * s2 * s3 - c2 * c3 * s1)) + c5 * (c2 * s1 * s3 + c3 * s1 * s2)) $$

$$ r_{33} = c6 * (c1 * c4 + s4 * (s1 * s2 * s3 - c2 * c3 * s1)) - s6 * (s5 * (c1 * s4 - c4 * (s1 * s2 * s3 - c2 * c3 * s1)) + c5 * (c2 * s1 * s3 + c3 * s1 * s2)) $$

$$ {}^{A}_{G}\boldsymbol{T} = \begin{bmatrix} r_{11} & r_{12} & r_{13} & p_X \\ r_{21} & r_{22} & r_{23} & p_y \\ r_{31} & r_{32} & r_{33} & p_z \\ 0 & 0 & 0 & 1 \end{bmatrix} = \begin{bmatrix} T_0 & T_1 & T_2 & T_3 \\ T_4 & T_5 & T_6 & T_7 \\ T_8 & T_9 & T_{10} & T_{11} \\ 0 & 0 & 0 & 1 \end{bmatrix} $$

```
state->A_now[0] =- c5*(s1*s4 + c4*(c1*s2*s3 - c1*c2*c3)) - s5*(c1*c2*s3 + c1*c3*s2);
state->A_now[1] = s6*(c4*s1 - s4*(c1*s2*s3 - c1*c2*c3)) + c6*(s5*(s1*s4 + c4*(c1*s2*s3 - c1*c2*c3)) - c5*(c1*c2*s3 + c1*c3*s2));
state->A_now[2] =  c6*(c4*s1 - s4*(c1*s2*s3 - c1*c2*c3)) - s6*(s5*(s1*s4 + c4*(c1*s2*s3 - c1*c2*c3)) - c5*(c1*c2*s3 + c1*c3*s2));
state->A_now[3] =- state->position[0];
state->A_now[4] =  s5*(c2*c3 - s2*s3) + c4*c5*(c2*s3 + c3*s2);
state->A_now[5] = c6*(c5*(c2*c3 - s2*s3) - c4*s5*(c2*s3 + c3*s2)) + s4*s6*(c2*s3 + c3*s2);
state->A_now[6] =c6*s4*(c2*s3 + c3*s2) - s6*(c5*(c2*c3 - s2*s3) - c4*s5*(c2*s3 + c3*s2));
state->A_now[7] = state->position[1];
state->A_now[8] =s5*(c2*s1*s3 + c3*s1*s2) - c5*(c1*s4 - c4*(s1*s2*s3 - c2*c3*s1));
state->A_now[9] =s6*(c1*c4 + s4*(s1*s2*s3 - c2*c3*s1)) + c6*(s5*(c1*s4 - c4*(s1*s2*s3 - c2*c3*s1)) + c5*(c2*s1*s3 + c3*s1*s2));
state->A_now[10] = c6*(c1*c4 + s4*(s1*s2*s3 - c2*c3*s1)) - s6*(s5*(c1*s4 - c4*(s1*s2*s3 - c2*c3*s1)) + c5*(c2*s1*s3 + c3*s1*s2));
state->A_now[11] = state->position[2];
```

UR10 Coordinates

$$x_R = z_A$$

$$y_R = \frac{x_A - y_A}{\sqrt{2}}$$

$$z_R = \frac{x_A + y_A}{\sqrt{2}}$$

$$Distance = \sqrt{x^2 + y^2 + z^2} \leq 1.3\ m$$

$$scale = \frac{1.3}{Distance}$$

$$P_{final} = \begin{bmatrix} \frac{x}{scale} \\ \frac{y}{scale} \\ \frac{z}{scale} \end{bmatrix}$$

Limits of the workspace

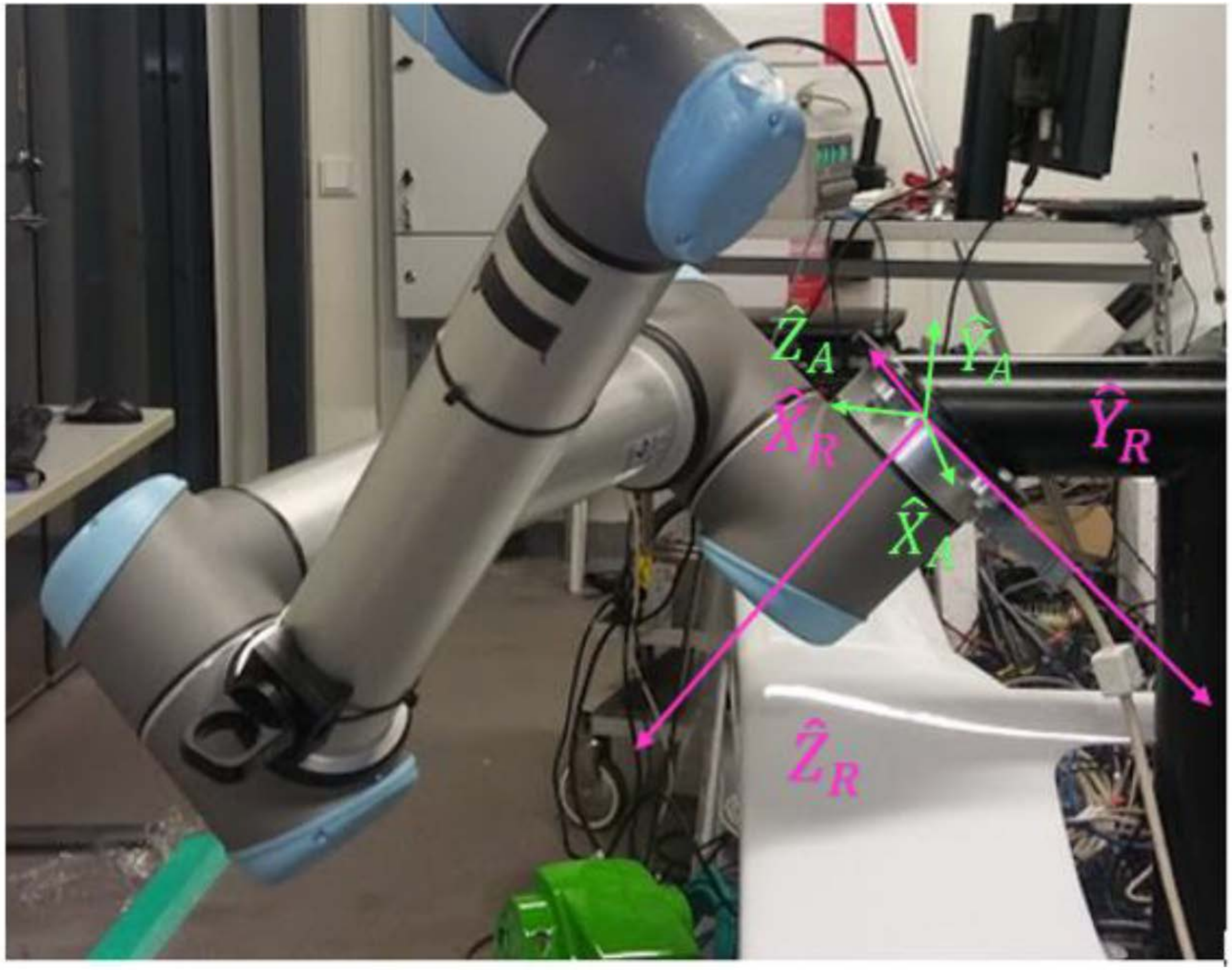

System of coordinates of the right industrial arm {R}, in comparison with the final system of coordinates.

Movement by increments

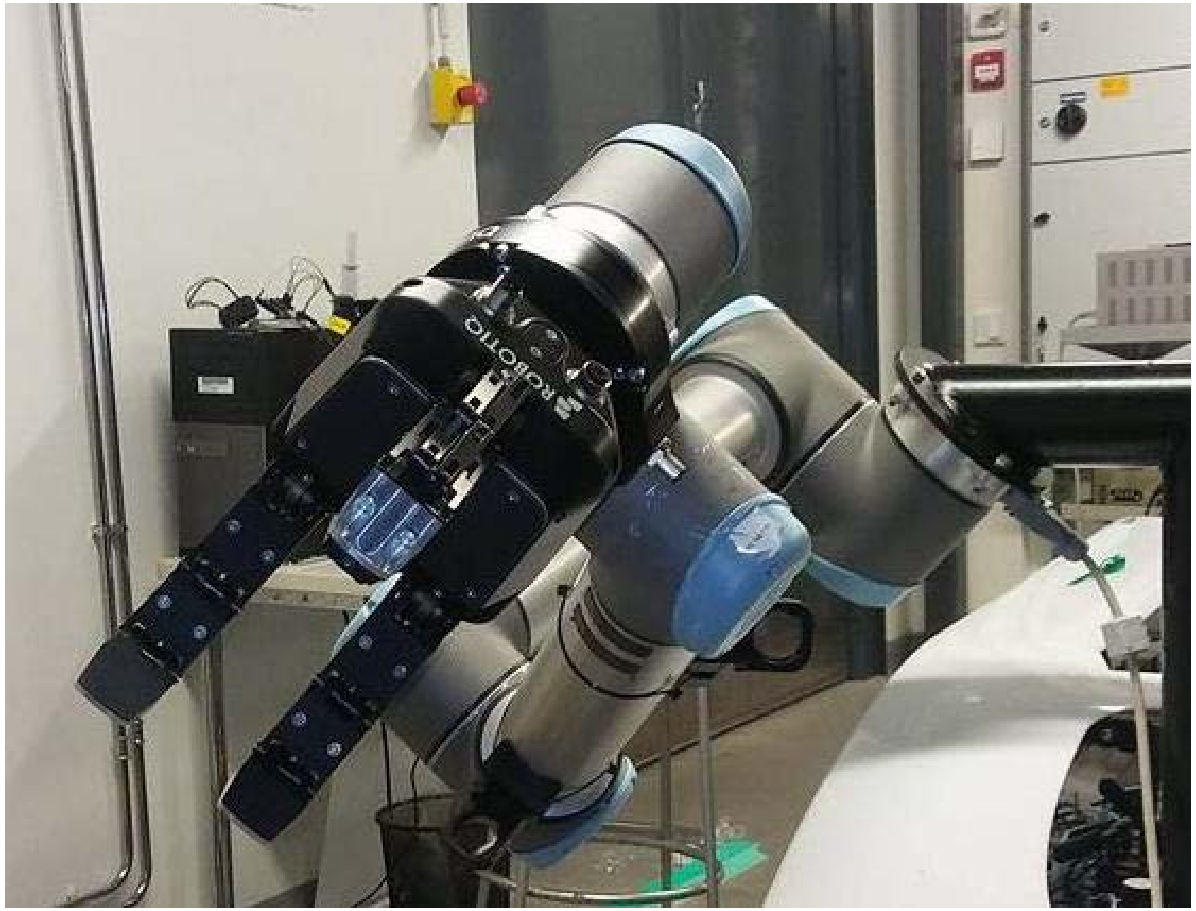

Initial position of the right UR10.

Inkwell, white and grey buttons of Geomagic Touch device

rqt Graph of the system with al connections.

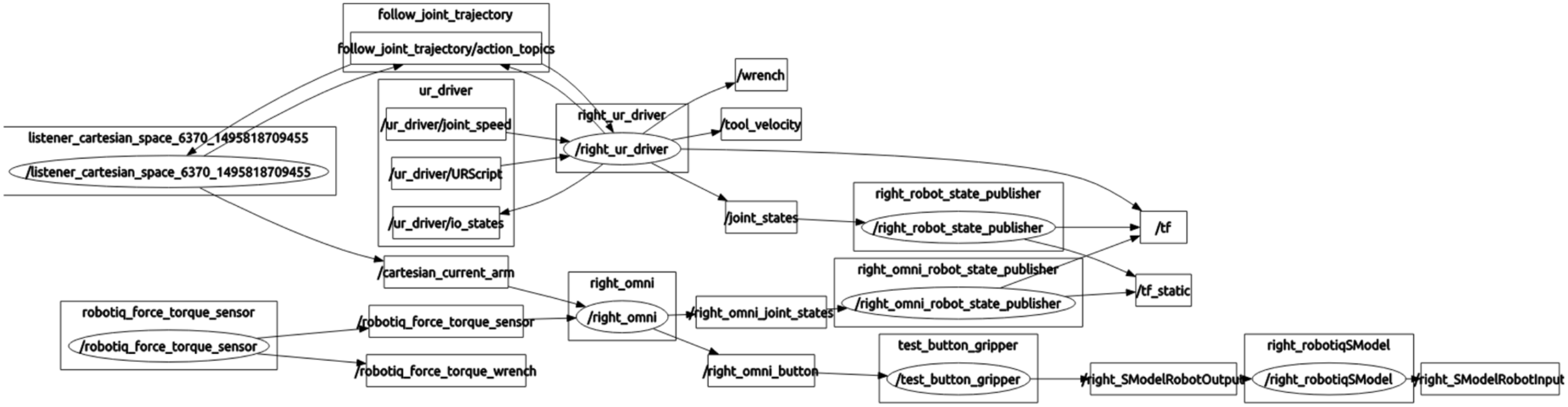

Control of movement .

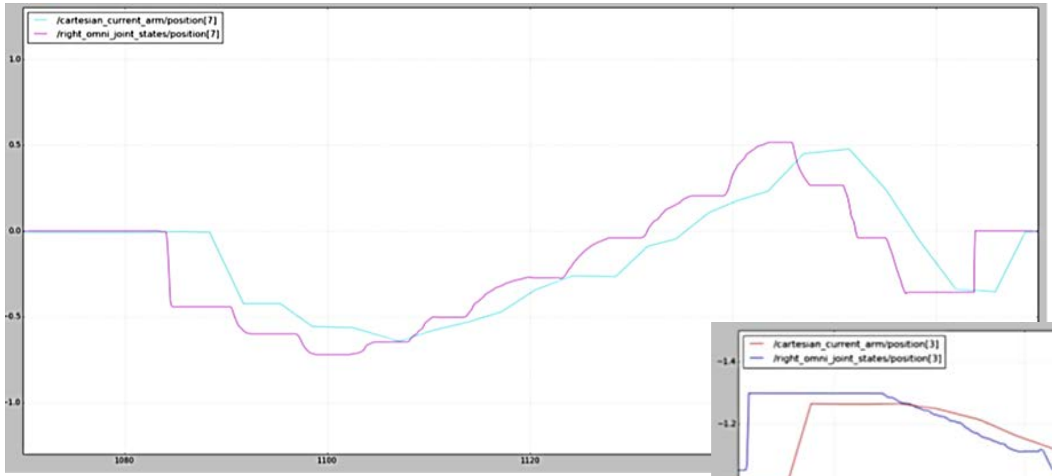

Component X of the movement

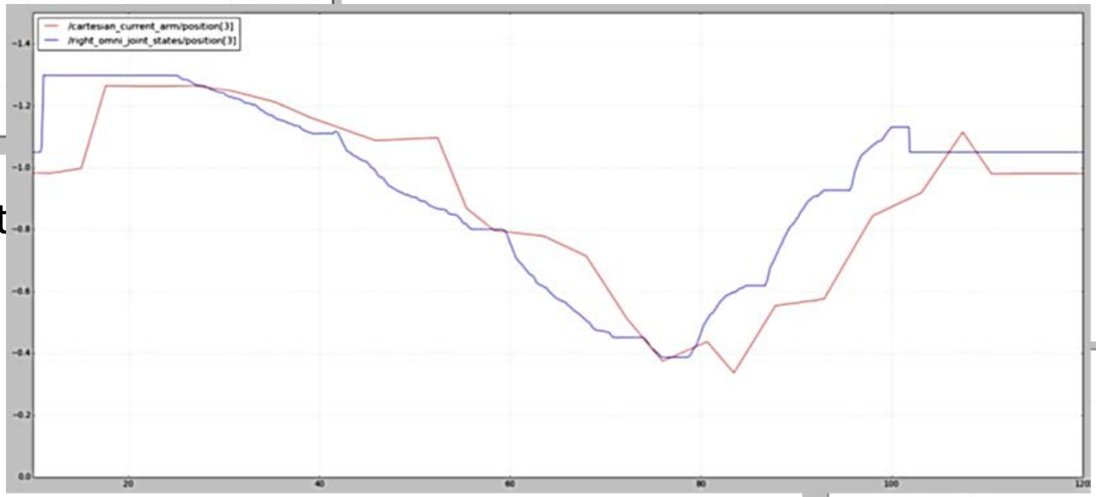

Component Y of the movement

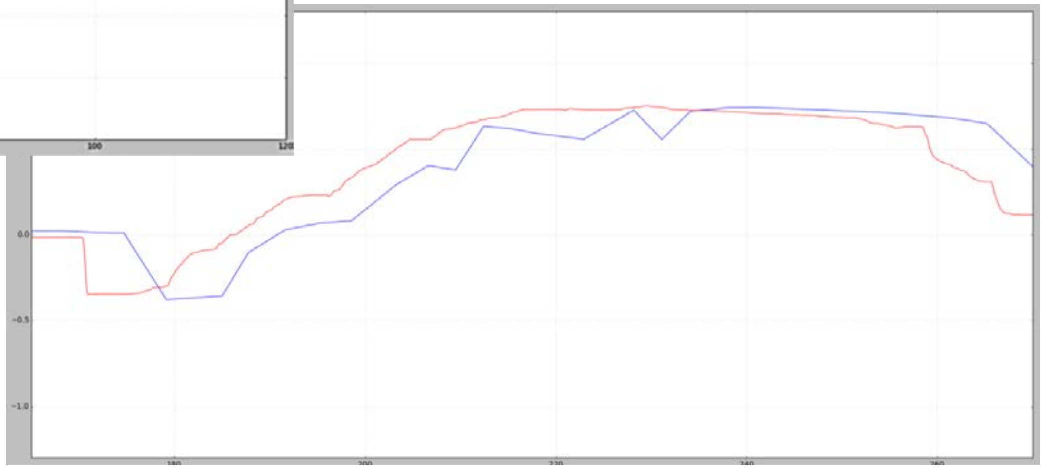

Component Z of the movement

Force and Movement Test in ROS.

```
user@VBubuntu: ~
---
position: [0.9854457808993786, -0.07349832643360651, -0.15327951239181636, -1.15
4948968409345, -0.05901847534102611, 0.6976792263881498, -0.7139751512726852, -0
.25691063204981807, 0.15941591036039865, 0.7126301236110442, 0.6831872908991161,
 -0.18567765958260196, 0.0, 0.0, 0.0, 1.0]
---
```

```
user@VBubuntu: ~
Fx: 12.4899997711
Fy: -10.25
Fz: -55.9399986267
Mx: -0.237000003457
My: 0.282999992371
Mz: 1.76999998093
---
```

```
user@VBubuntu: ~
---
force0: -5.48620720454
force1: -0.851314429905
force2: -0.120893877148
---
```

Vision

Vision

Marshall CV200 MB

Marshall CV500 camera

Swit S-4914 transmitter-receiver set

video switcher

Software in operation (Blackmagic)

Scheme of frame grabber’s operation

Vision

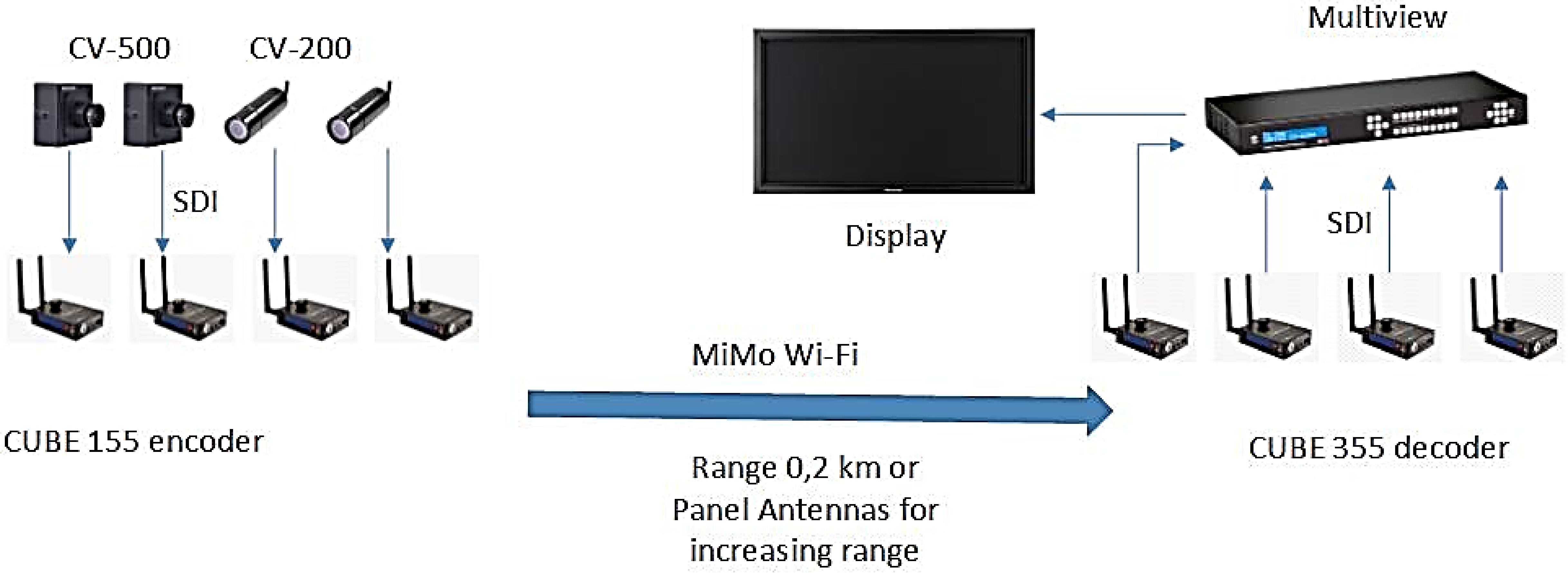

CV-500
CV-200
SDI
Multiview
Display
SDI
MiMo Wi-Fi
CUBE 155 encoder
CUBE 355 decoder
Range 0,2 km or
Panel Antennas for
increasing range

Different signal standards and connectors. .

Different signal standards and connectors.

Signal name	Connector	Type	Max resolution	Used for
DVI	DVI, Mini-DVI, Micro-DVI	Both	2560×1600@60, 3840×2400@33	Recent video cards
HDMI	19 pin HDMI Type A/C	Digital	2560×1600@75, 4096×2160@60	Many A/V systems and video cards (including motherboards with IGP)
GigE	Ethernet	Digital	1280x1024	Computer vision, industrial cameras
CameraLink	MDR26	Digital	1280x1024	Computer vision, industrial cameras
SDI	BNC	Digital	From 143 Mbit/s to 2.970 Gbit/s, depending on variant.480i, 576i, 480p, 576p, 720p, 1080i, 1080p.	Broadcast video. Variants include SD-SDI, HD-SDI, Dual Link HD-SDI, 3G-SDI

HDMI (left) and BNC Connectors (right)

WiFi Communication

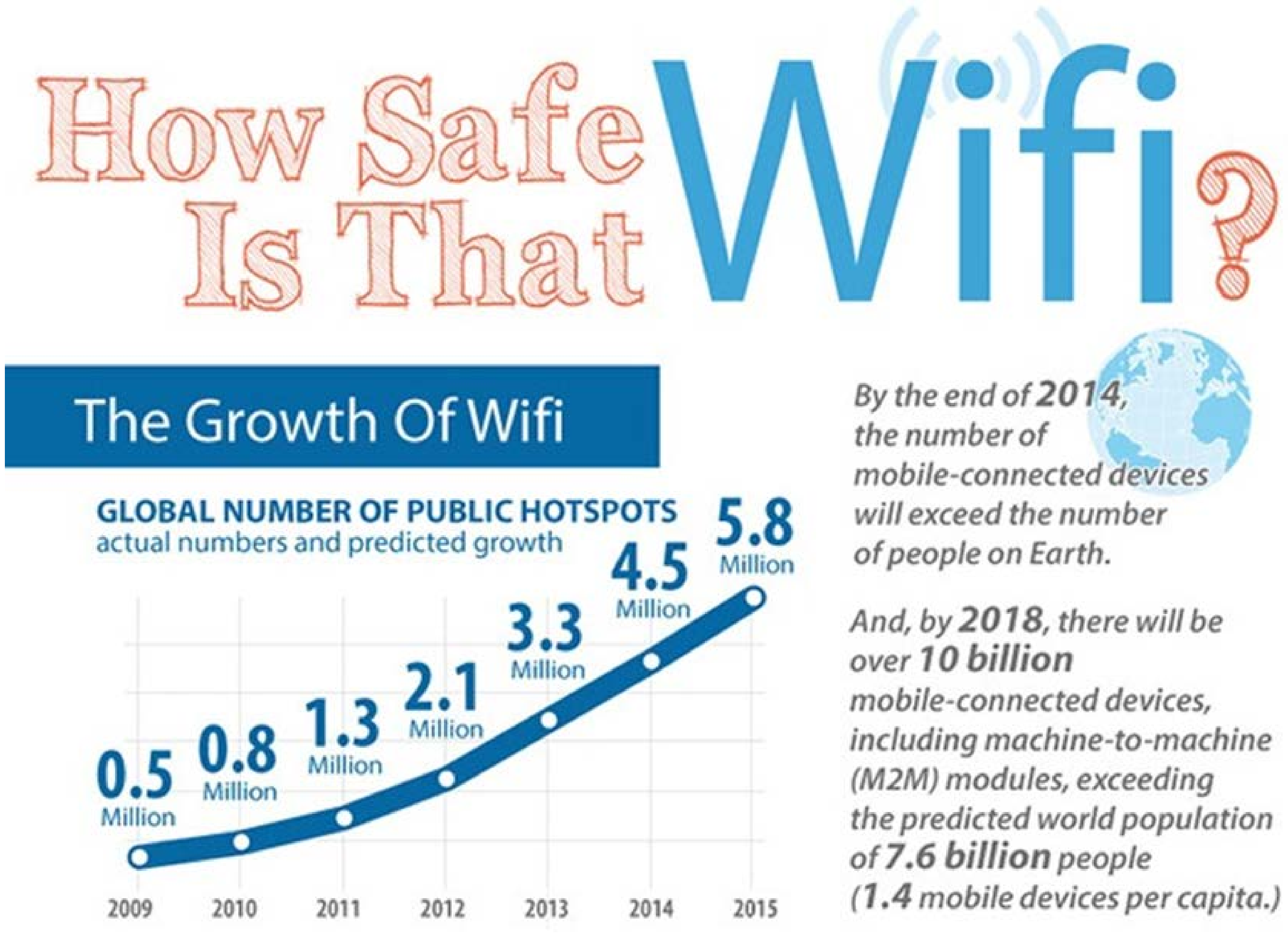

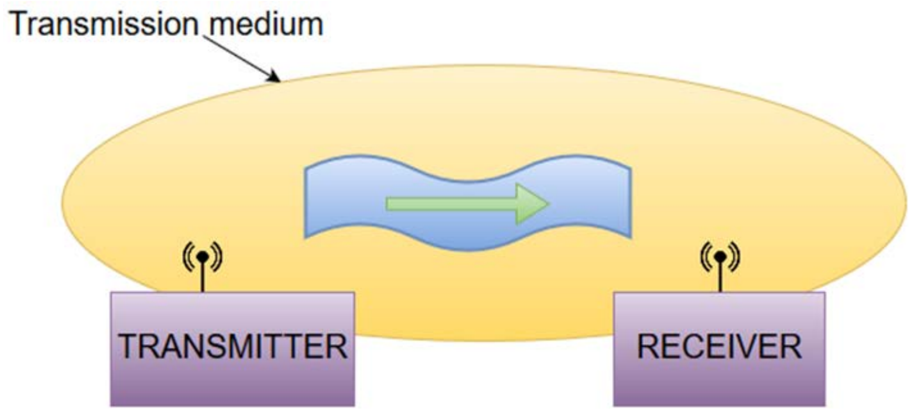

Basic parts of wireless communication link

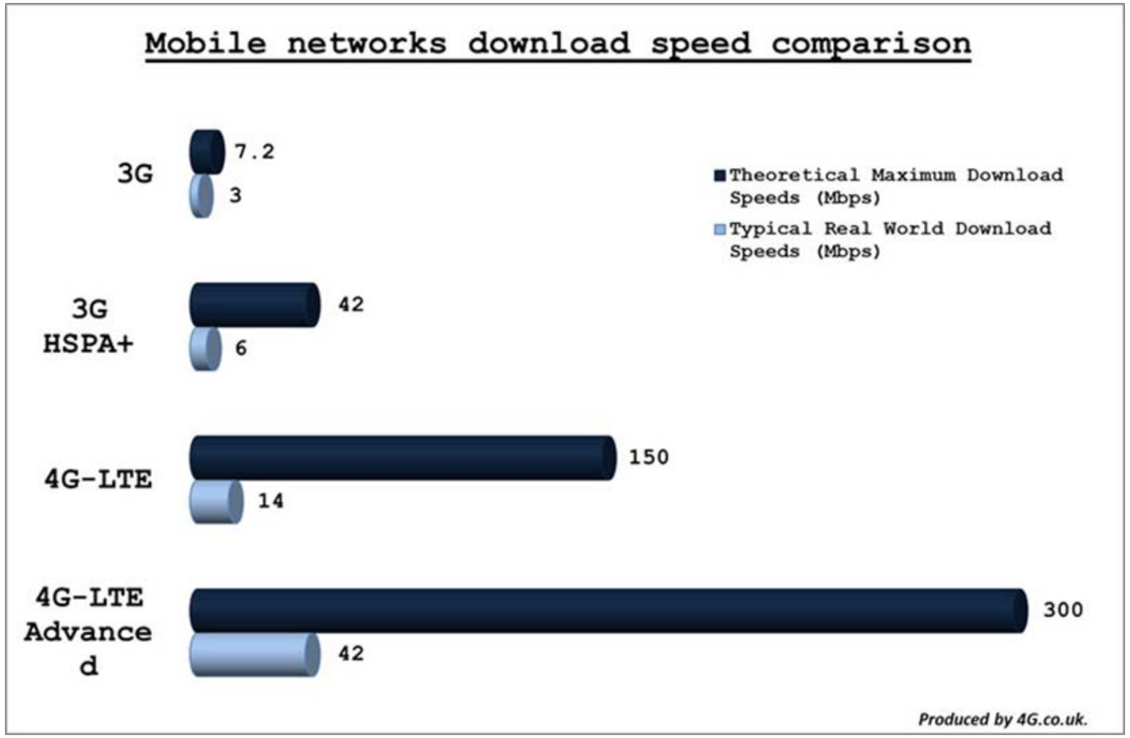

WiFi Communication

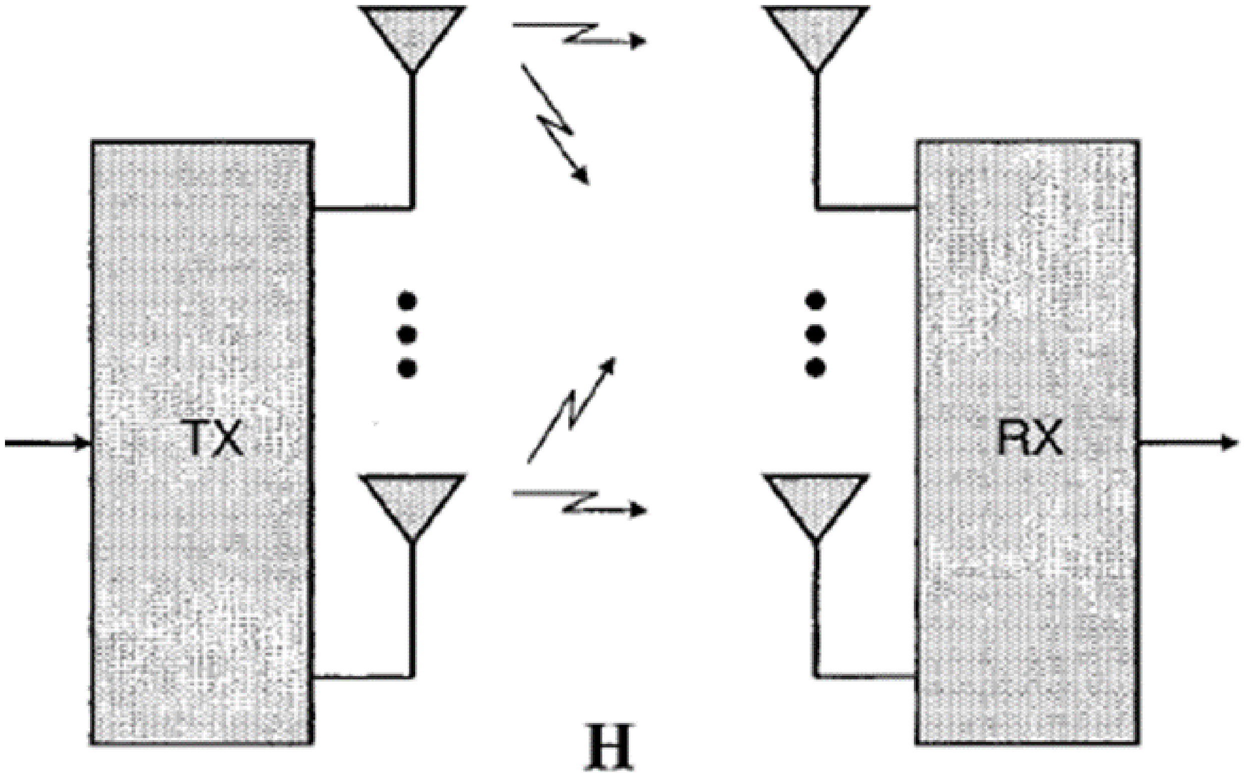

Scheme of transmitting and receiving radio signal with multiple antennas

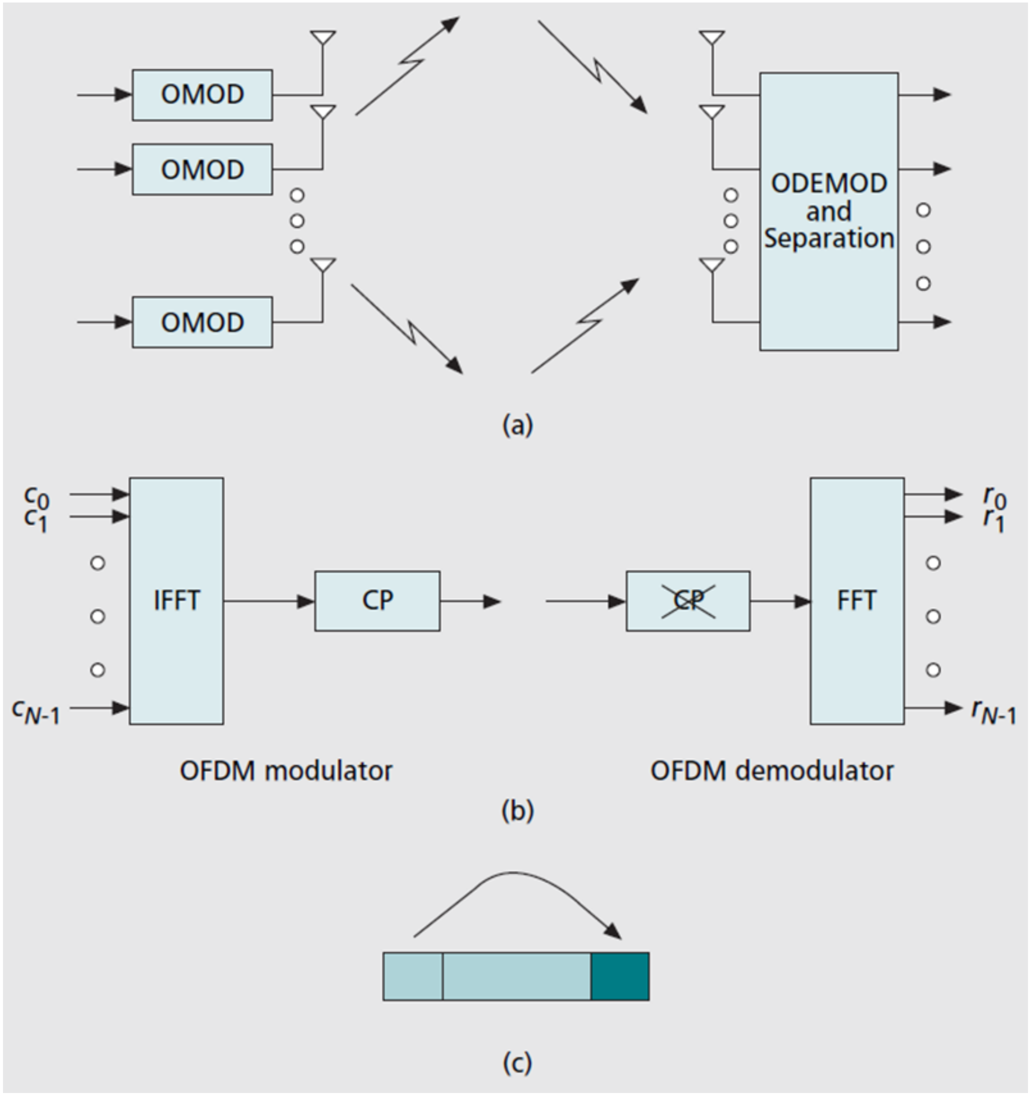

a) Basic principle of MIMO-OFDM system (OMOD is a OFDM modulator, while ODEMOD means demodulator); b) single-antenna OFDM modulator and demodulator; c) adding the CP

WiFi Communication

Various examples of anaglyph glasses

Passive (left) and active (right) shutter glasses.

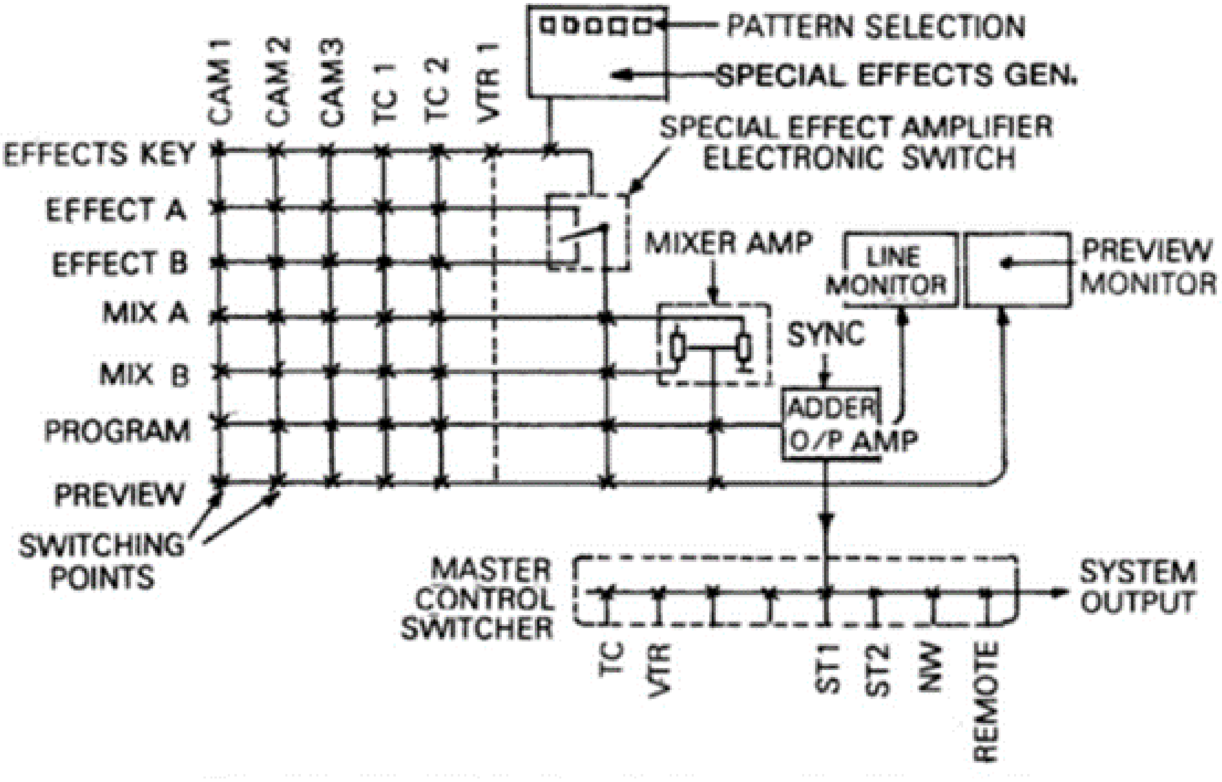

Principle scheme of video switcher

System Integration

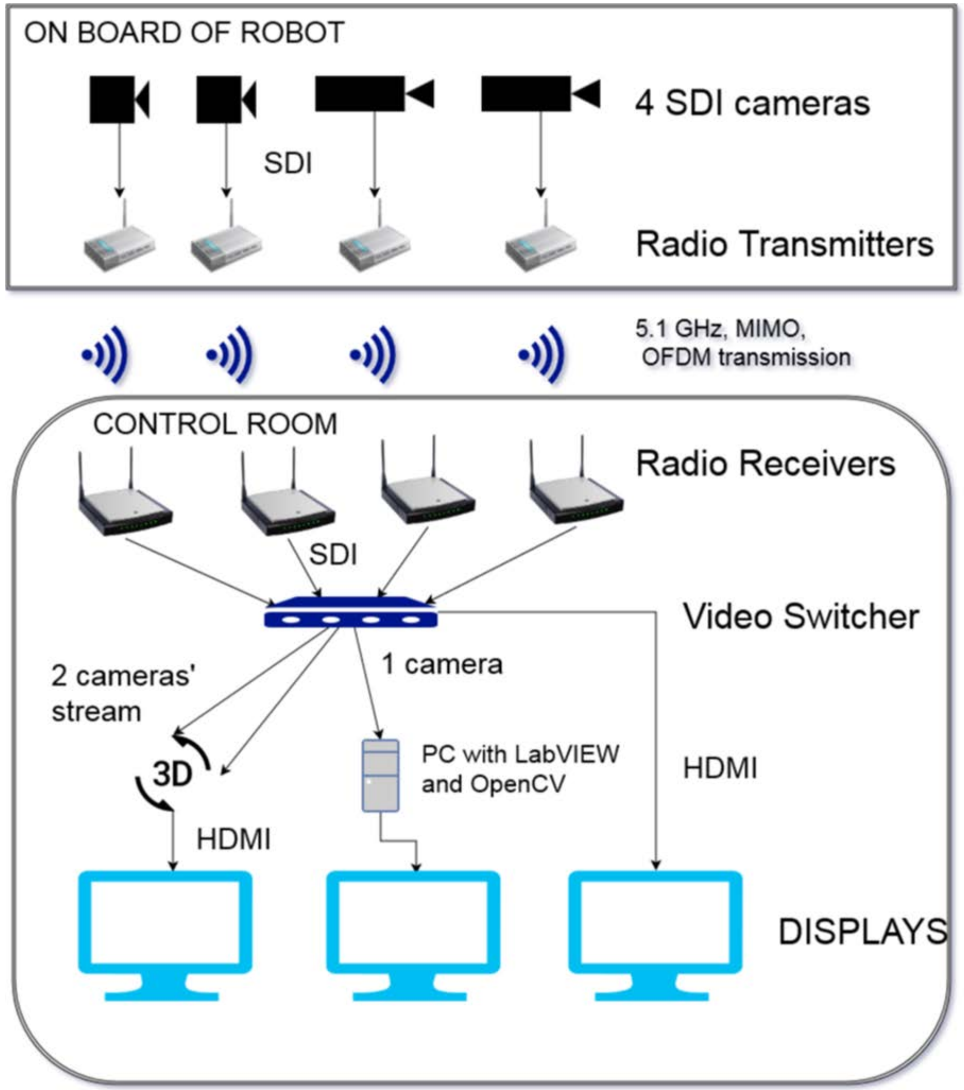

General scheme of the machine vision system

3D Vision

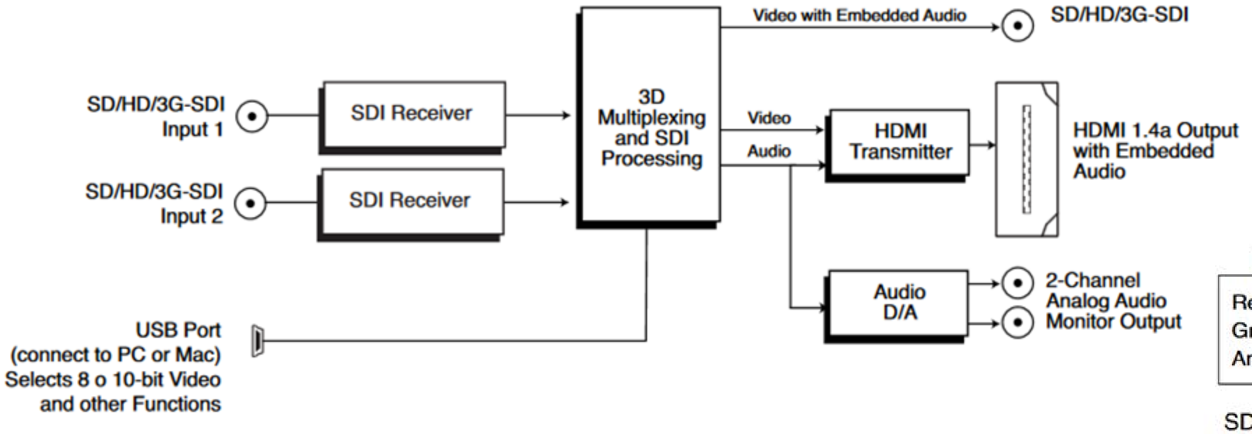

General block scheme of 3D converter

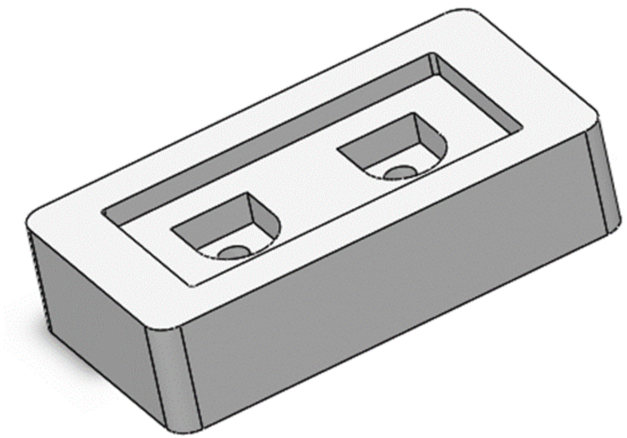

Design of platform for cameras

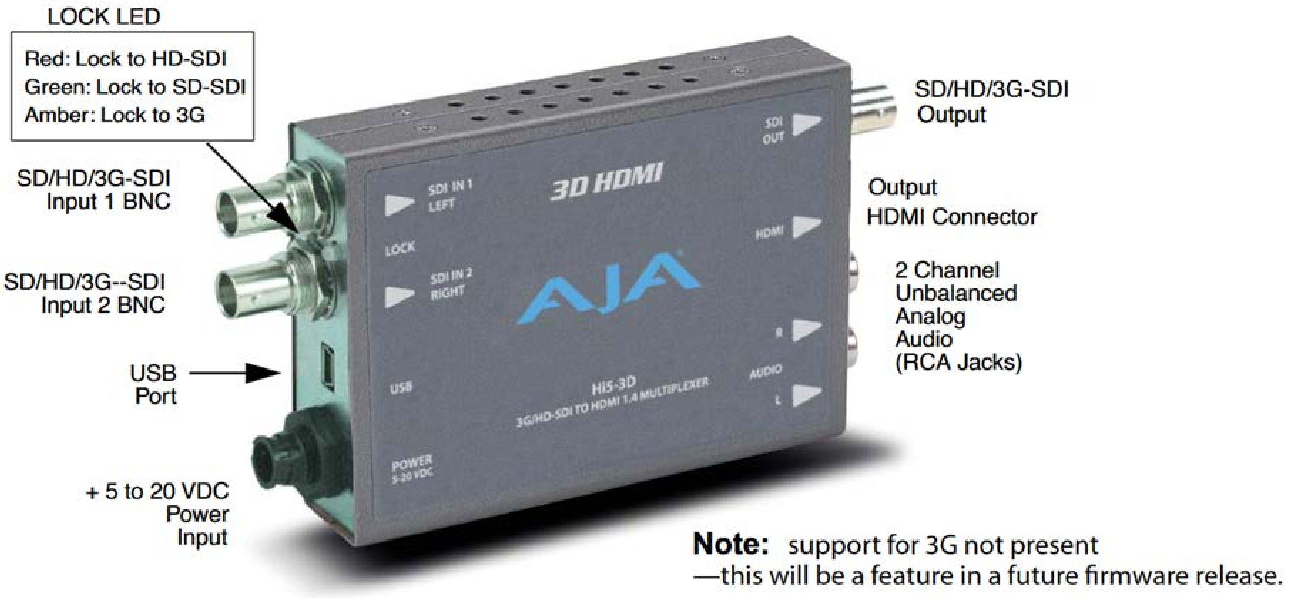

Appearance of AJA Hi5-3D converter

Pattern Recognition & Machine Vision

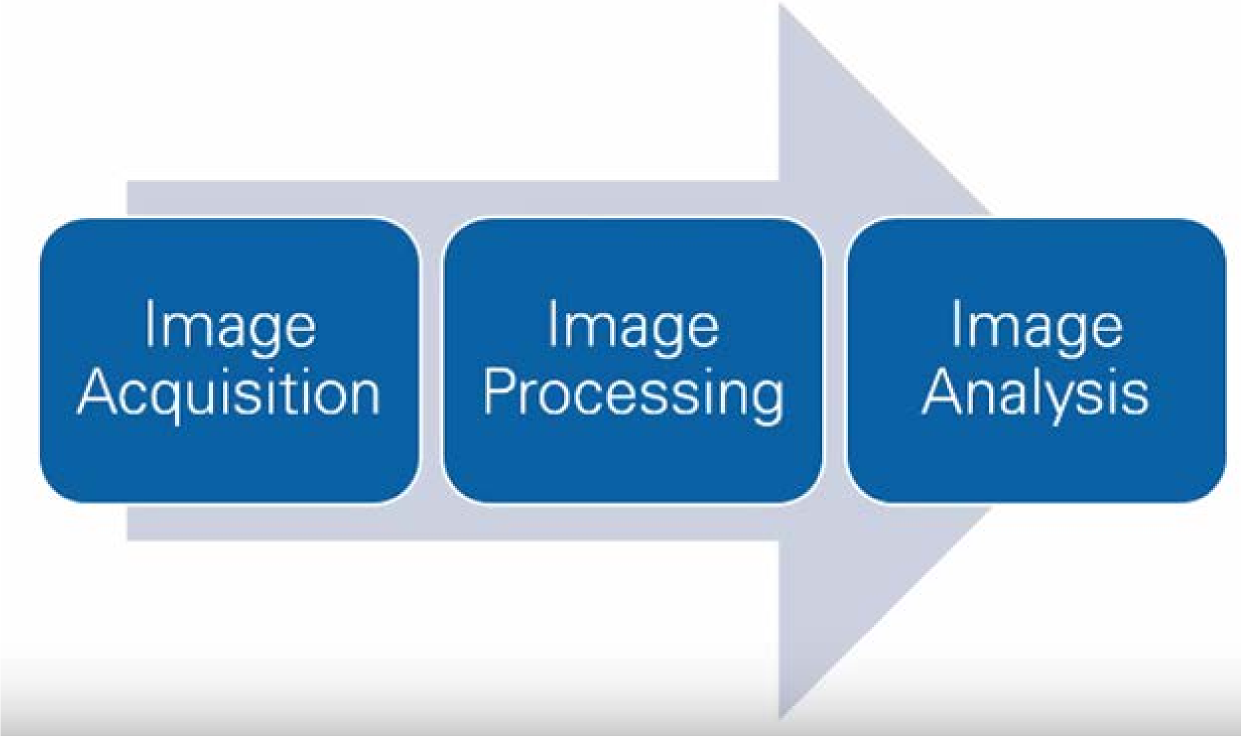

Basic algorithm

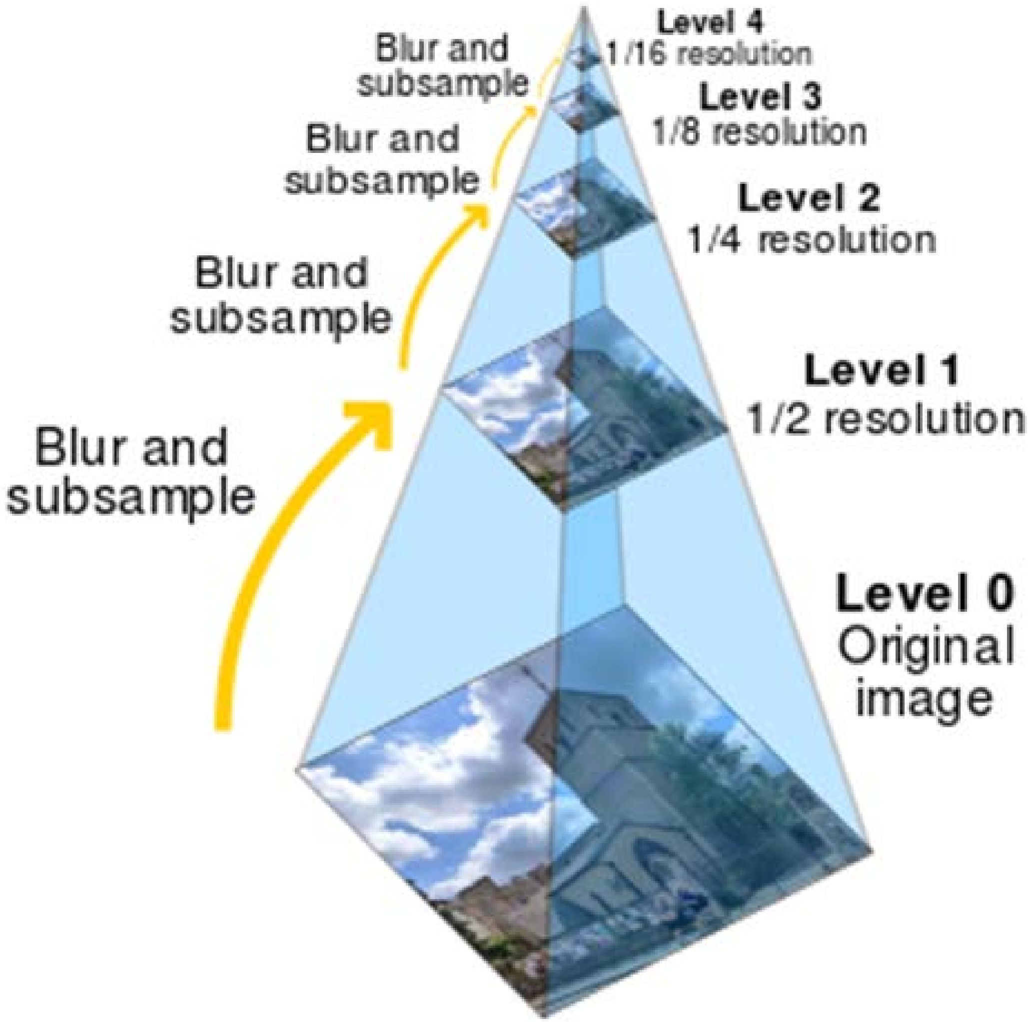

Gaussian pyramid

LabVIEW Interface

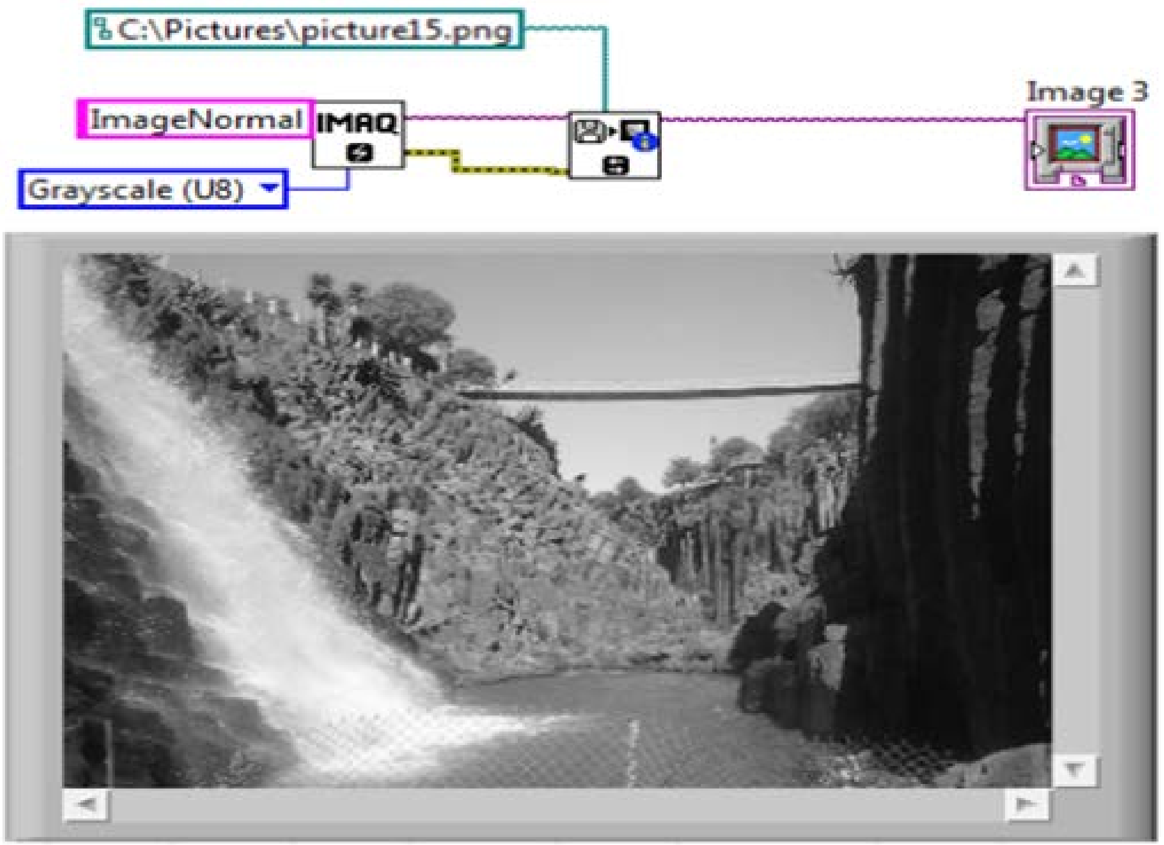

Creation of grayscale image in LabVIEW

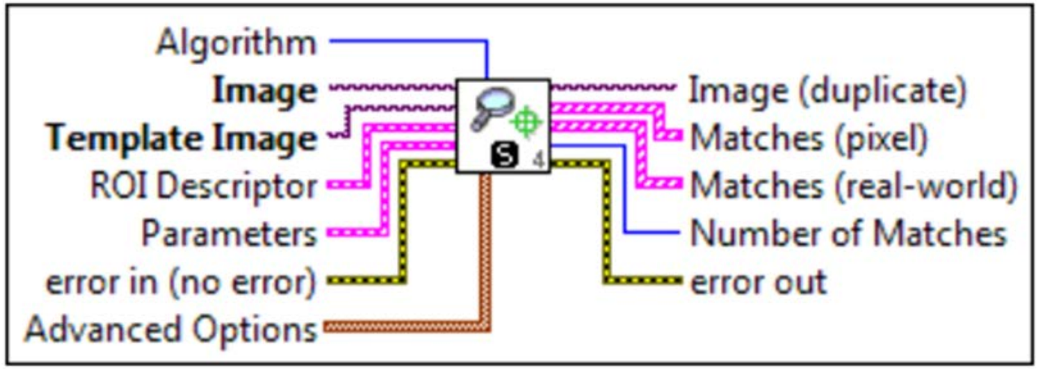

Match pattern block in LabVIEW

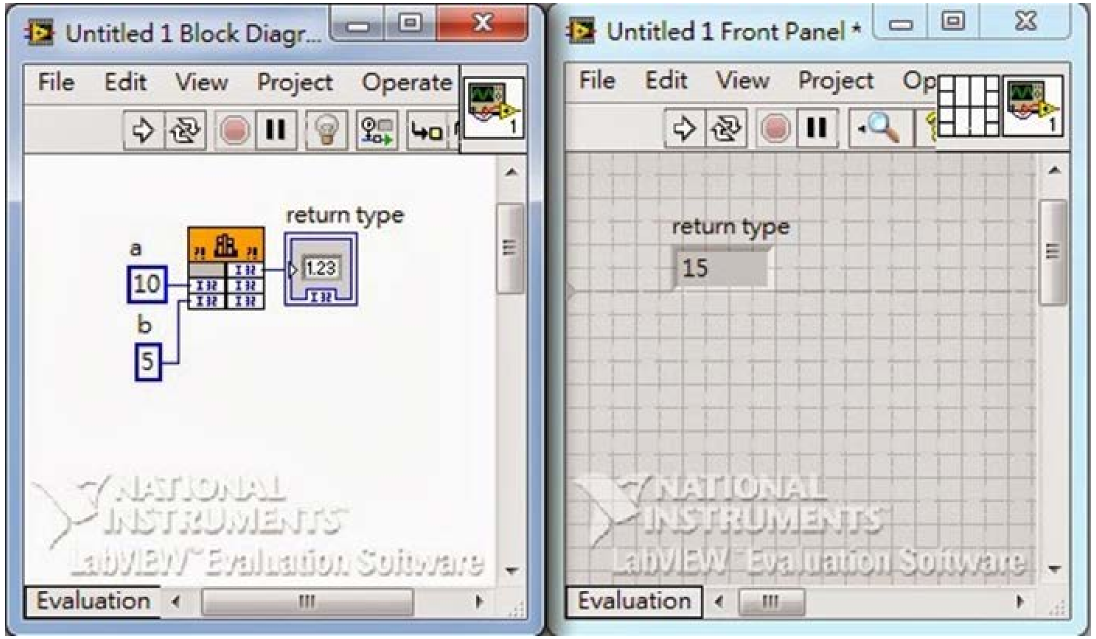

DLL example in LabVIEW

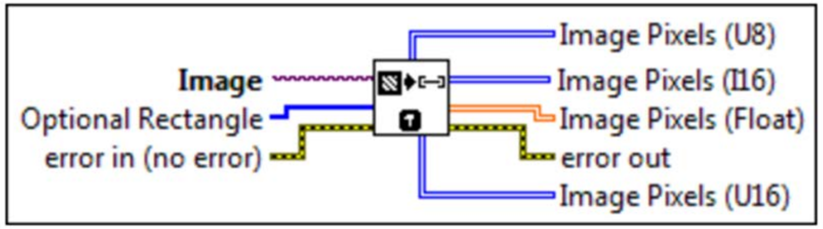

$$I = \begin{pmatrix} a_{11} & \mathrm{K} & a_{1n} \\ \mathrm{M} & \mathrm{O} & \mathrm{M} \\ a_{m1} & \mathrm{L} & a_{mn} \end{pmatrix}$$

Pattern Recognition.

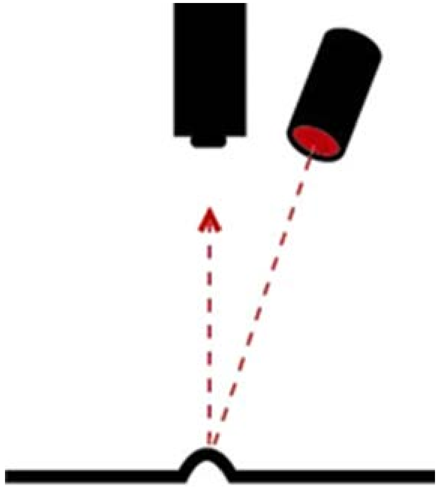

Directional lightning

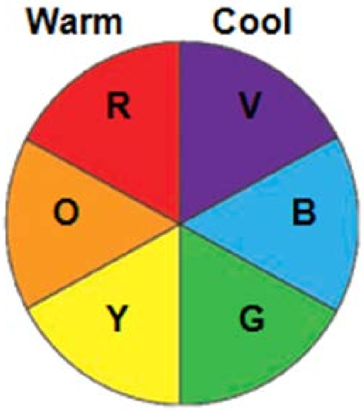

Color wheel with warm and cold colors

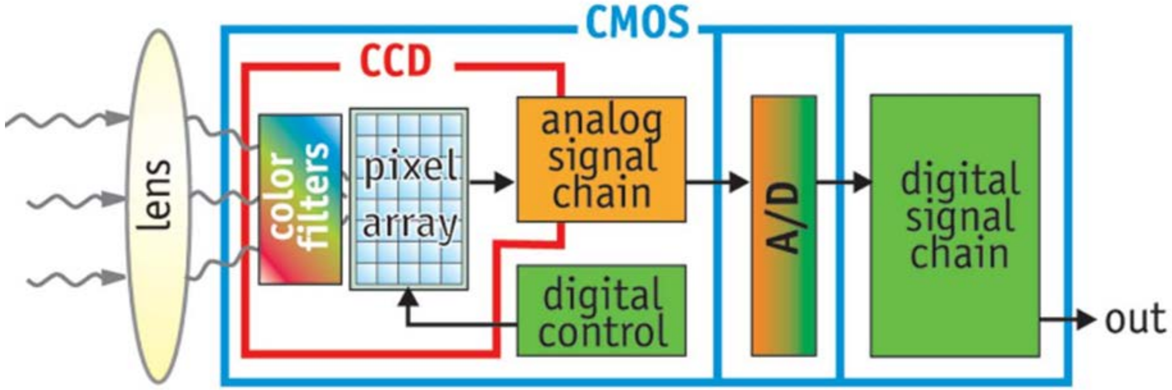

CMOS imager sensor general scheme

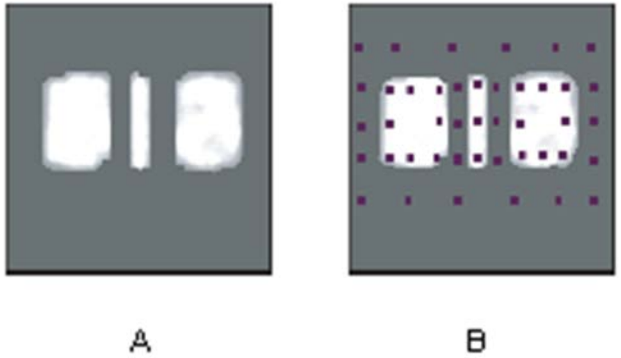

Defining region and edge pixels

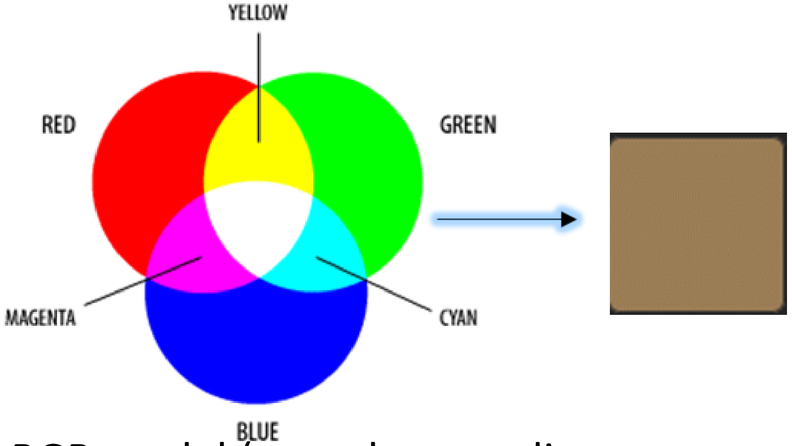

RGB model (a – color coordinate system; b – color, which is got by values)

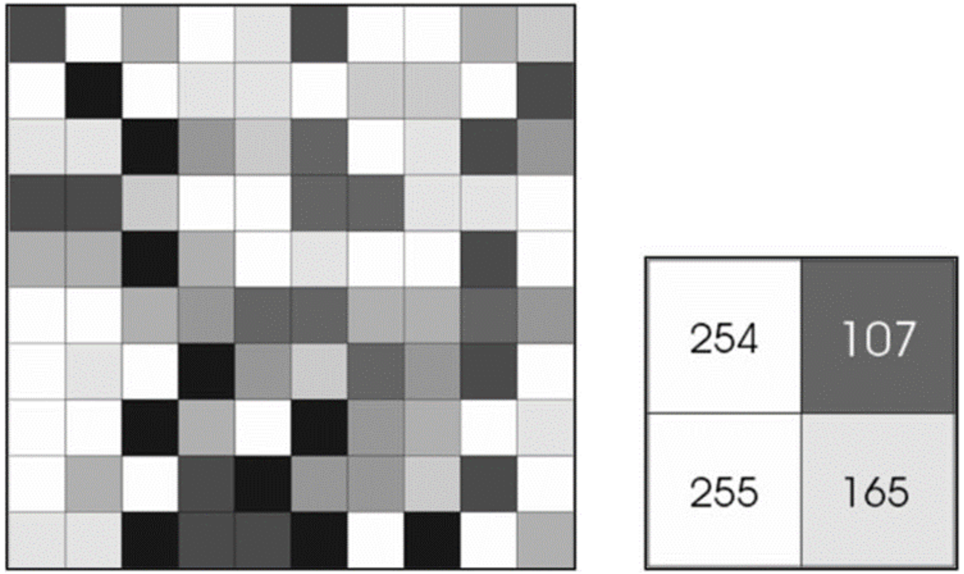

Grayscale (8-bit depth) image representation

Pattern Recognition

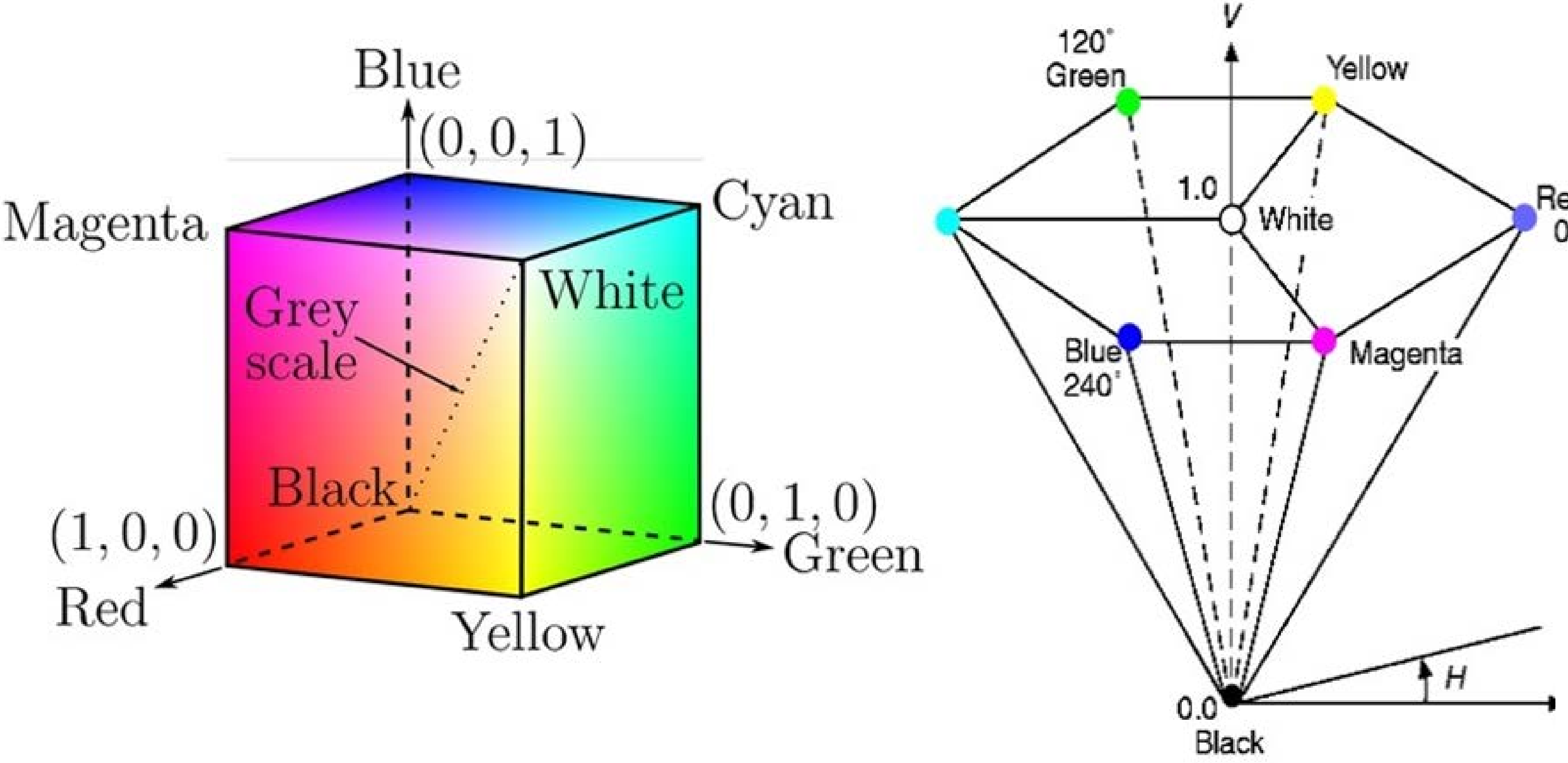

RGB model (left part) and HSV model (right part)

$$V = \max\{R, G, B\}$$

$$S = \frac{\max - \min}{\max}$$

$$H = \begin{cases} \frac{1}{6}\frac{G-B}{\max-\min} & \text{if } R = \max \\ \frac{1}{6}\left(2 + \frac{B-R}{\max-\min}\right) & \text{if } G = \max \\ \frac{1}{6}\left(\frac{R-G}{\max-\min}\right) & \text{if } B = \max \end{cases}$$

Pattern Recognition

Image after finding the exact color range in H, S, V

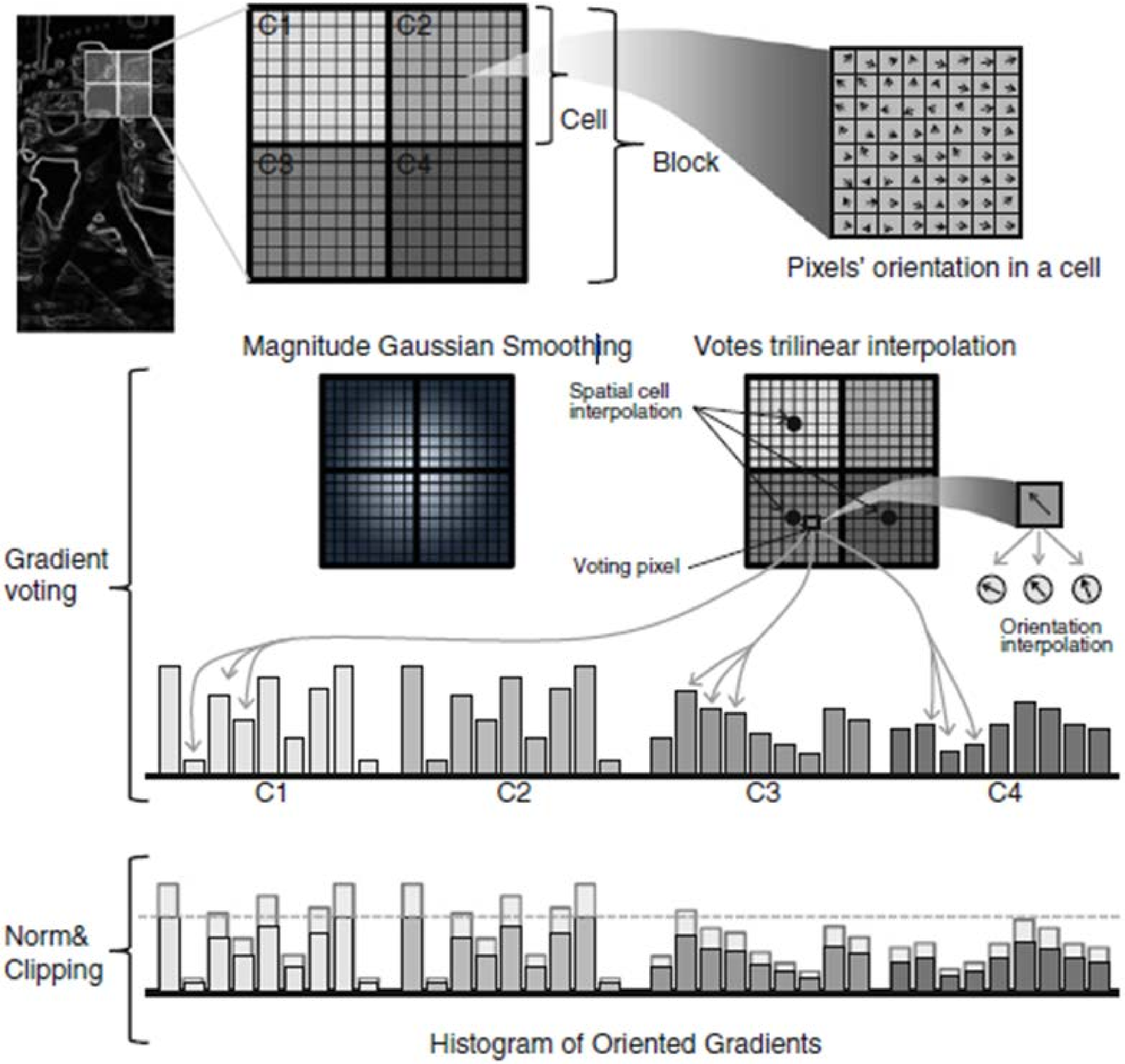

Main steps of HOG

Pattern Recognition & Machine Vision

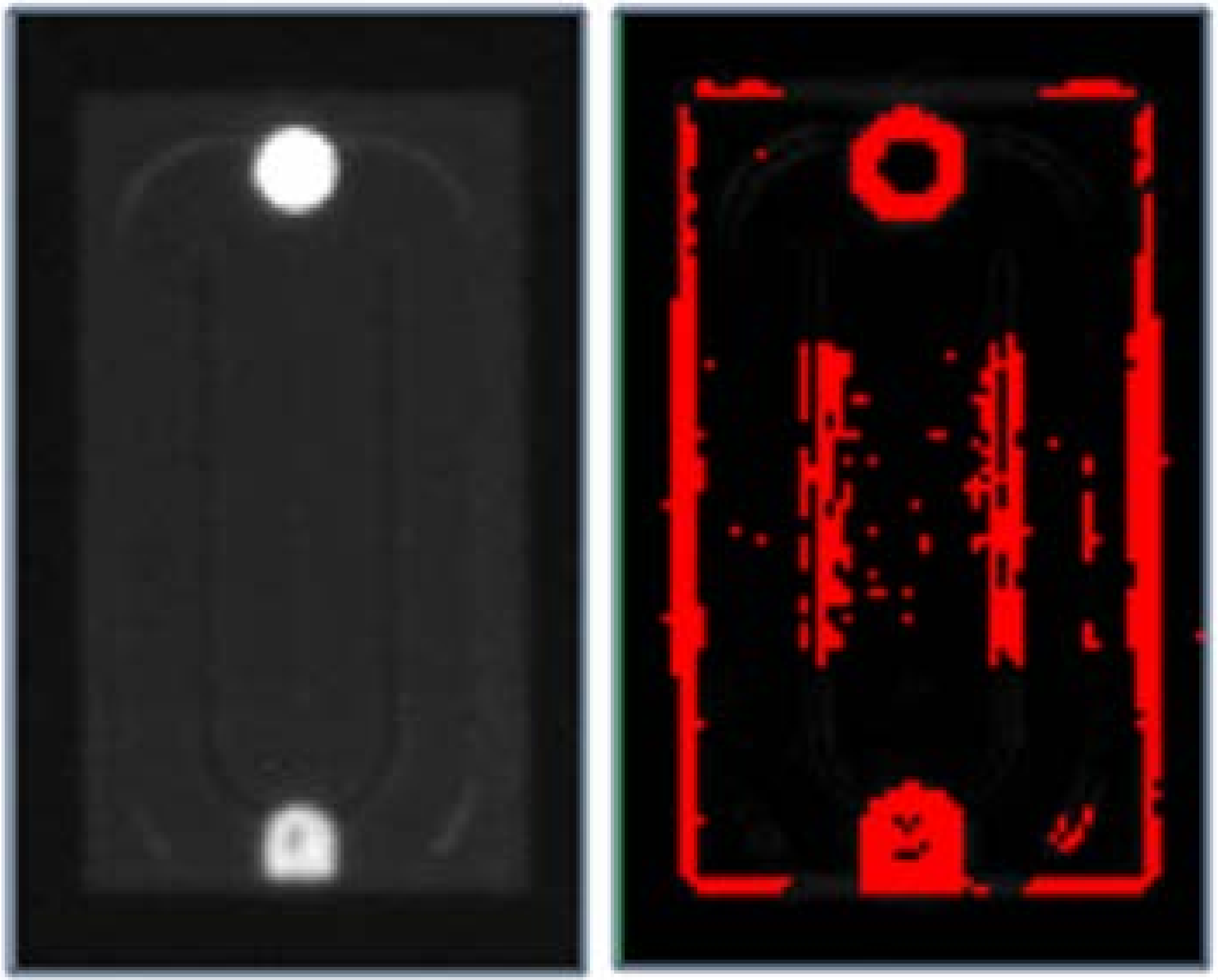

Left – source grayscale image; Right – image with detected edges

Toxic Hazard

Danger!


BE CAREFUL! Attention is needed!
CAUTION
ATTACH
GROUNDING
WIRE CLIPS

Human Recognition

High Voltage!

Neck

Neck


Includes:
• Pan & Tilt Head
• Joystick Control (Proportic
• 25' CAT6 Cable
• 12V Power Supply

Pan and tilt layout

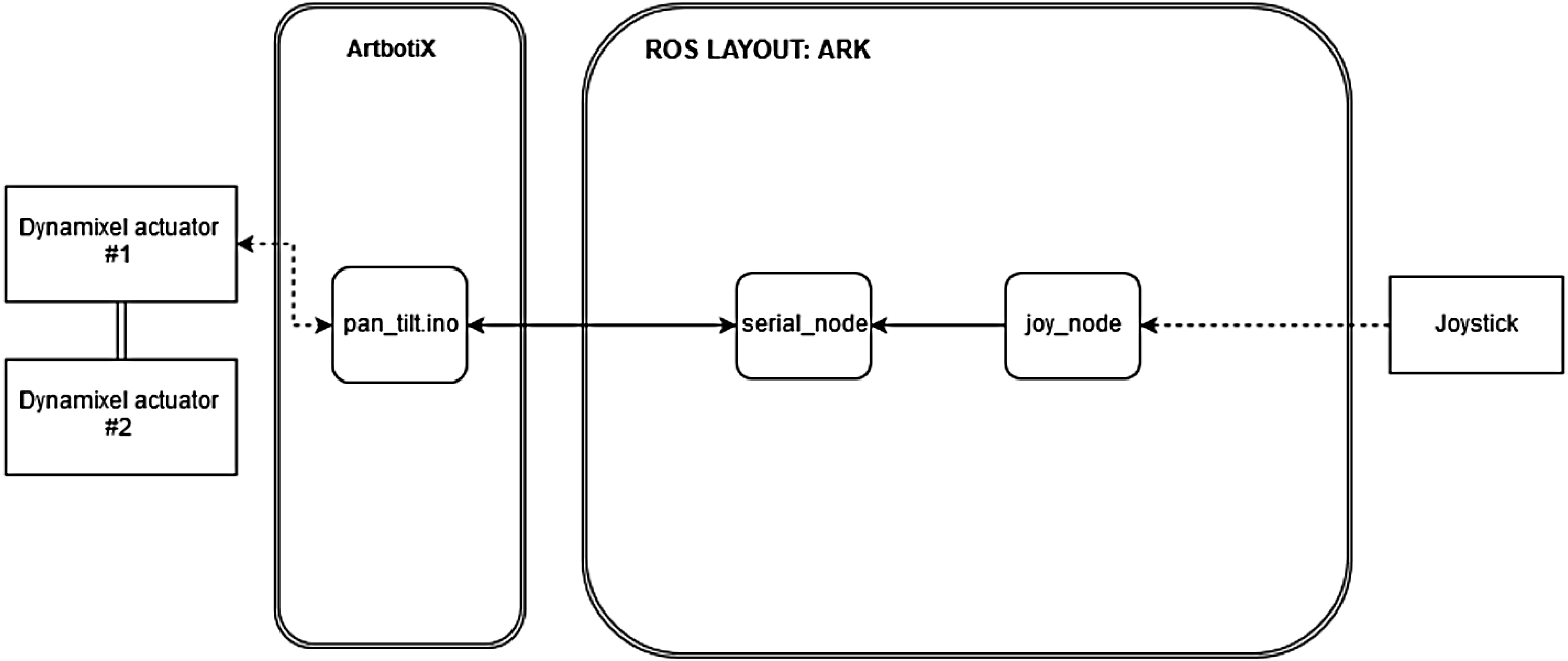

Connections

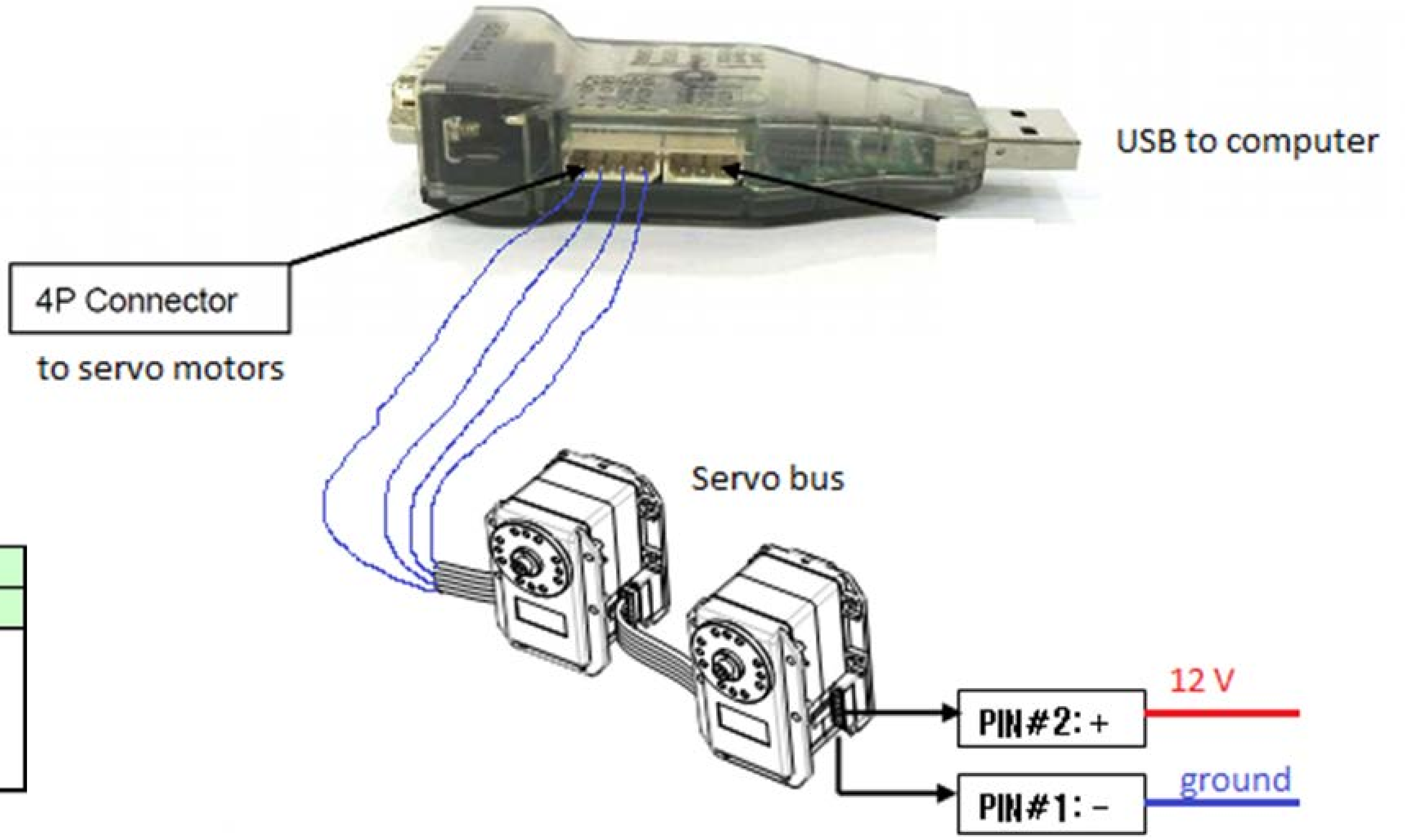

4 Pin Cable		
Pin No.	Signal	Pin Figure
1	GND	
2	12 V	
3	DATA + (RS-485)	
4	DATA - (RS-485)	

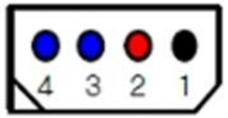

RQT Graph - ROS code

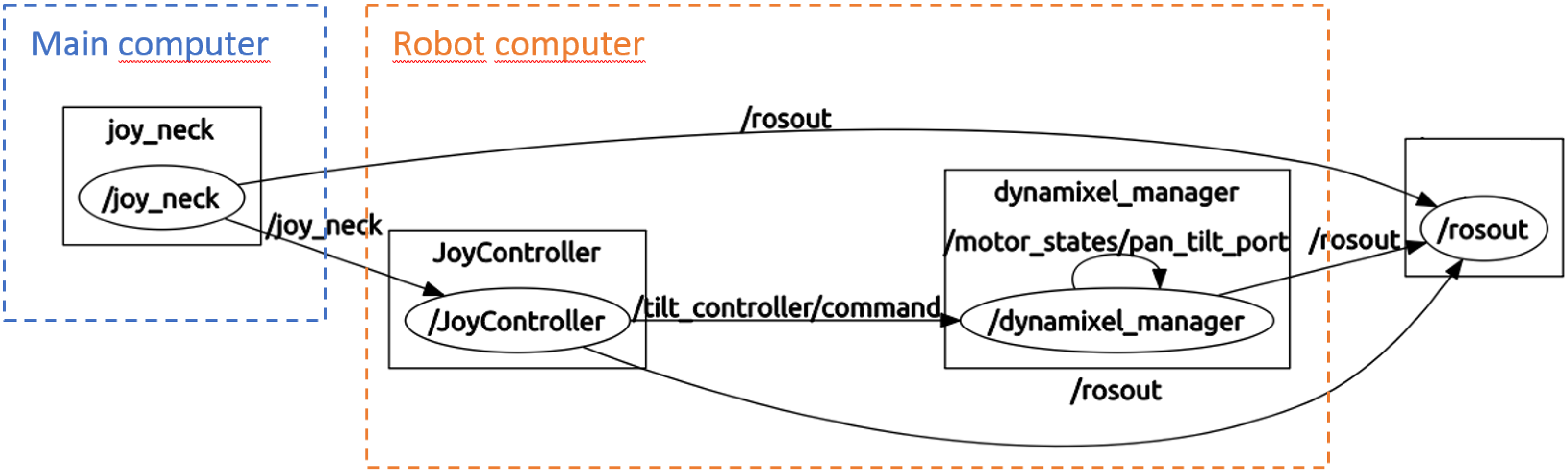

Lidar

Lidar

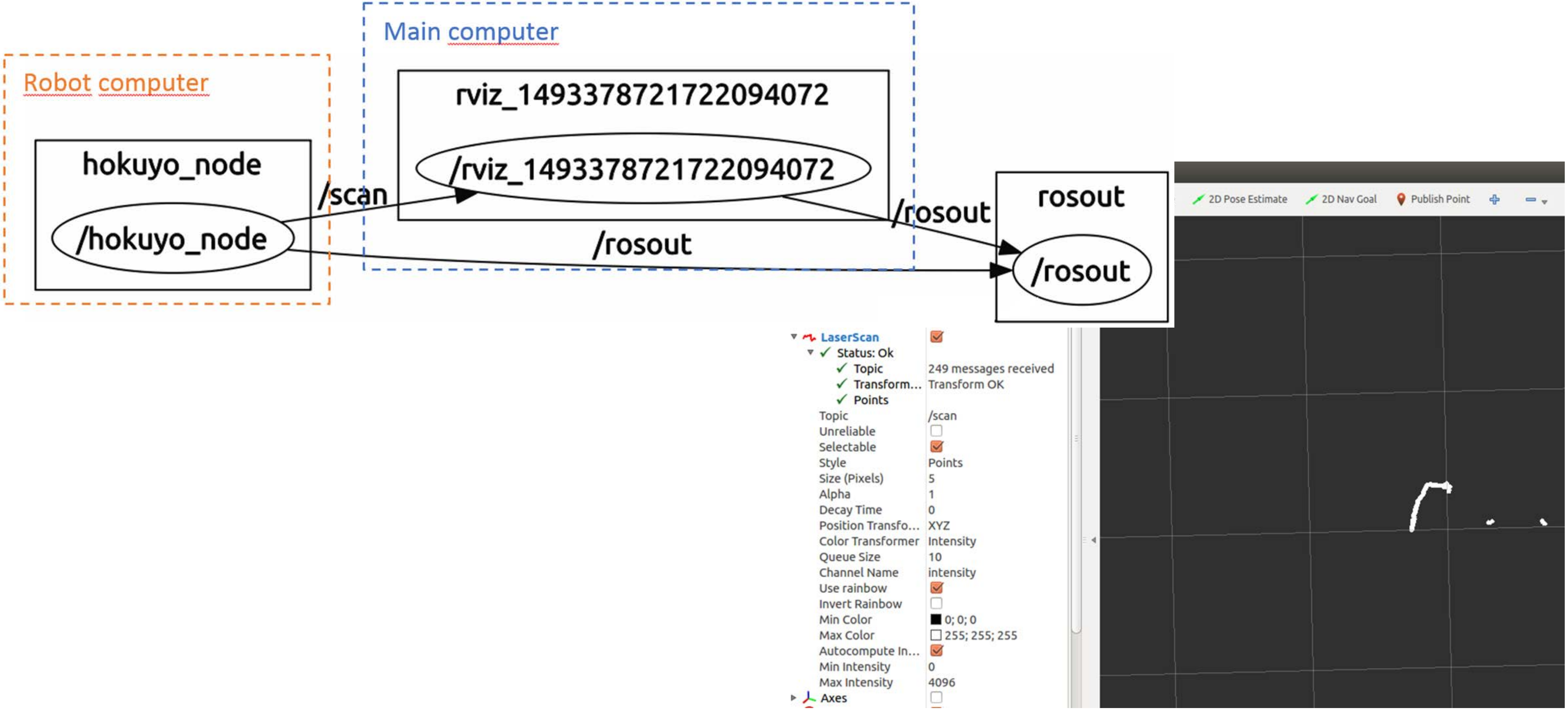

Main computer
Robot computer
rviz_1493378721722094072
/rviz_1493378721722094072
hokuyo_node
/hokuyo_node
/scan
/rosout
/rosout
rosout
/rosout
2D Pose Estimate
2D Nav Goal
Publish Point
LaserScan
Status: Ok
Topic
249 messages received
Transform...
Transform OK
Points
Topic
/scan
Unreliable
Selectable
Style
Points
Size (Pixels)
5
Alpha
1
Decay Time
0
Position Transfo...
XYZ
Color Transformer
Intensity
Queue Size
10
Channel Name
intensity
Use rainbow
Invert Rainbow
Min Color
0; 0; 0
Max Color
255; 255; 255
Autocompute In...
Min Intensity
0
Max Intensity
4096
Axes

Ears and Voice recognition

Ears - Audio stream layout.

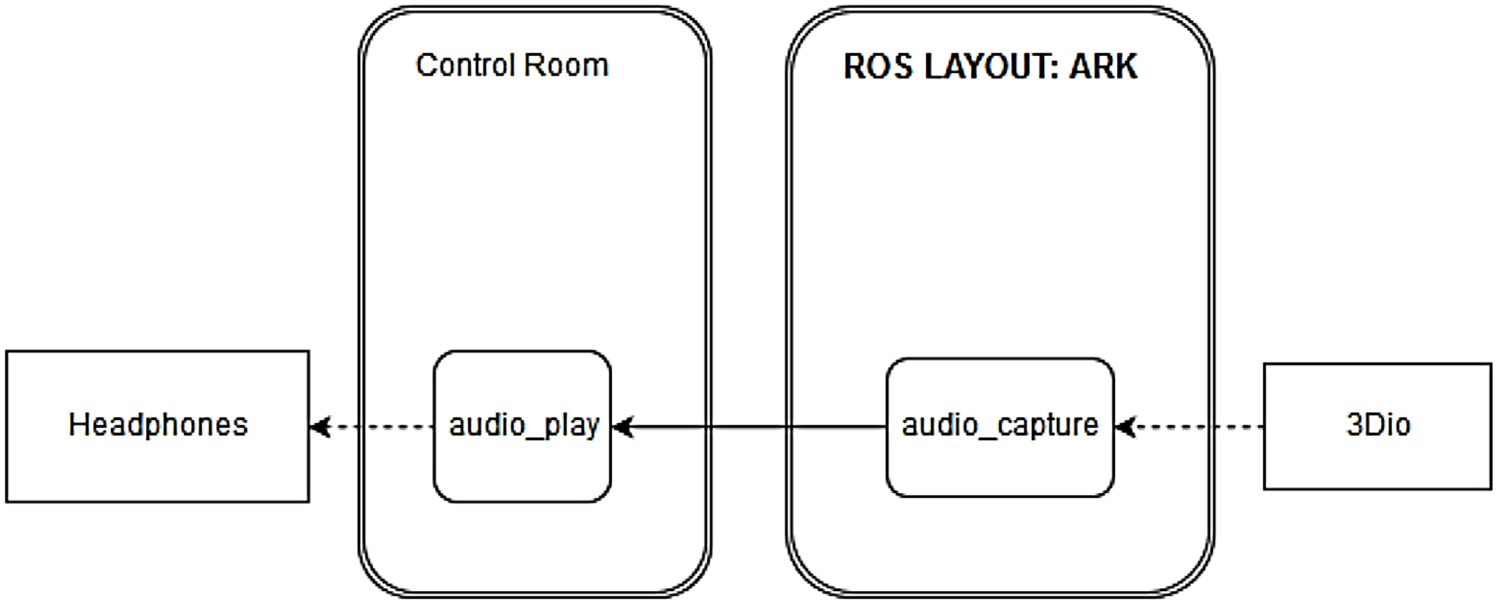

Ears - RQT Graph.

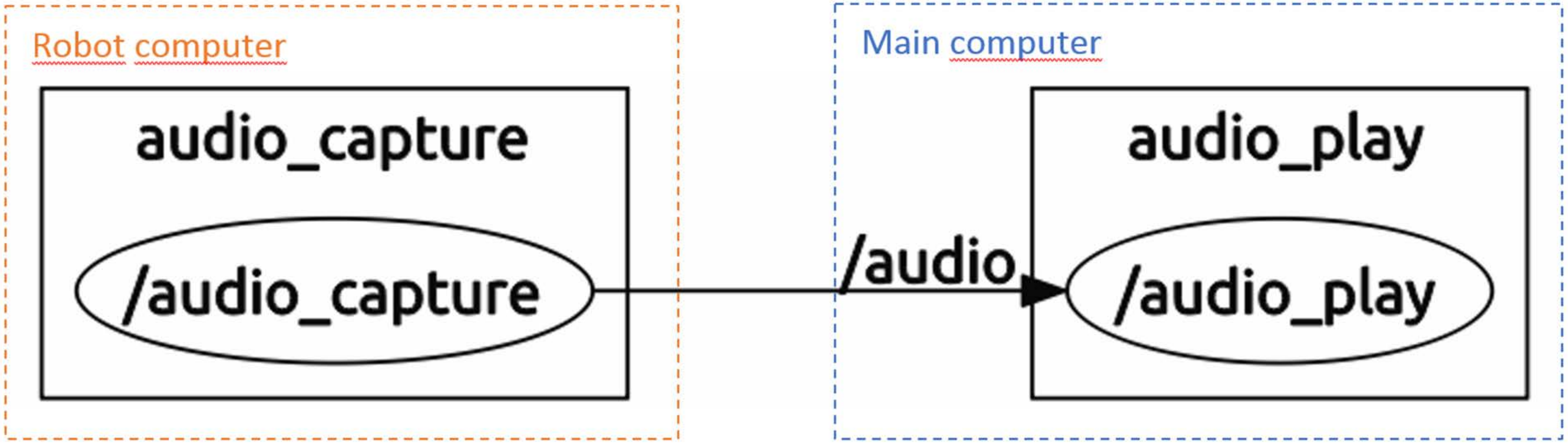

Voice Command RQT Graph.

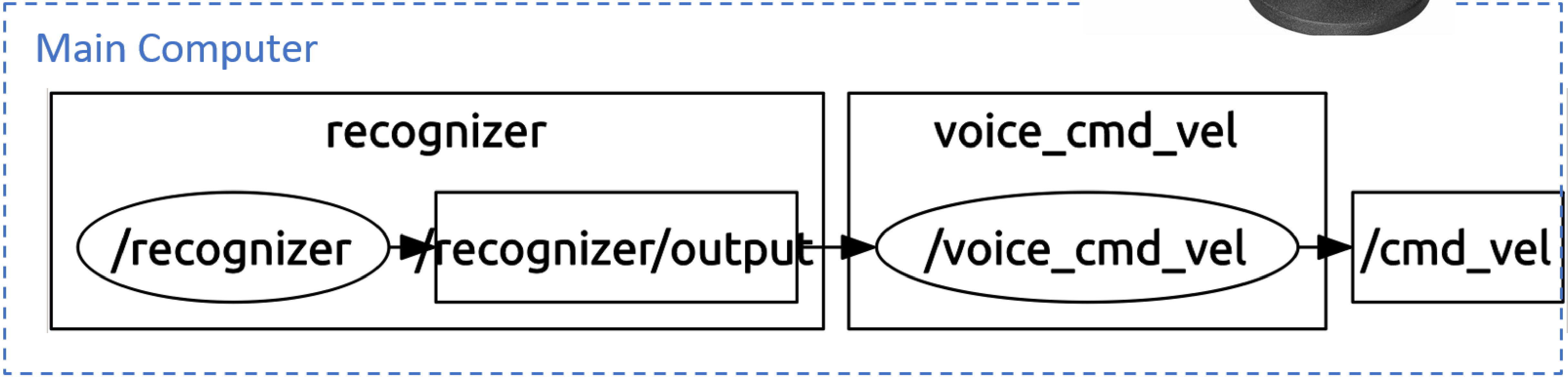

Control Station

Control Station

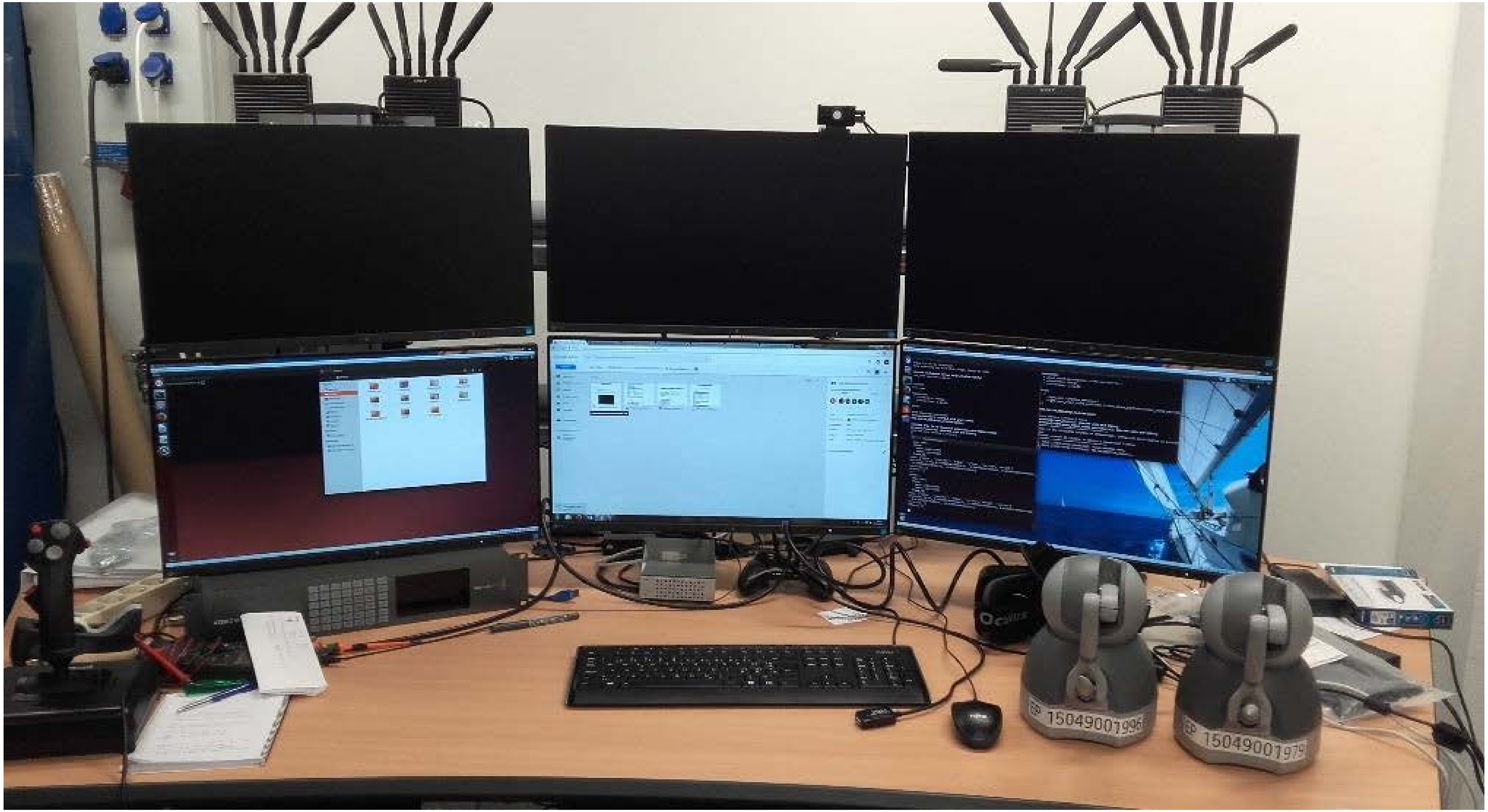

Team







Heikki Handroos


Hamid Roozbahani


Juha Koivisto


Ming Li


Andrija Milojevic


Samrat Gautam


Mikko Rikkonen


Javier Hernandez


LE Weiting


Syed Azad


Andrés Belzunce


Igor Soroka

Contacts:

Lappeenranta University of Technology,
Laboratory of Intelligent Machines,

Hamid Roozbahani,

hamid.roozbahani@lut.fi